

Advances

in Clinical and Experimental Medicine

MONTHLY ISSN 1899-5276 (PRINT) ISSN 2451-2680 (ONLINE)

www.advances.umed.wroc.pl

2021, Vol. 30, No. 1 (January)

Impact Factor (IF) – 1.514
Ministry of Science and Higher Education – 40 pts.
Index Copernicus (ICV) – 152.95 pts



WROCLAW
MEDICAL UNIVERSITY

Advances
in Clinical and Experimental
Medicine



Advances in Clinical and Experimental Medicine

ISSN 1899-5276 (PRINT)

ISSN 2451-2680 (ONLINE)

www.advances.umed.wroc.pl

MONTHLY 2021
Vol. 30, No. 1
(January)

Advances in Clinical and Experimental Medicine (*Adv Clin Exp Med*) publishes high quality original articles, research in progress and reviews of recognized scientists that deal with all clinical and experimental medicine.

Editorial Office

ul. Marcinkowskiego 2–6
50-368 Wrocław, Poland
Tel.: +48 71 784 11 36
E-mail: redakcja@umed.wroc.pl

Publisher

Wrocław Medical University
Wybrzeże L. Pasteura 1
50-367 Wrocław, Poland

© Copyright by Wrocław Medical University,
Wrocław 2021

Online edition is the original version
of the journal

Editor-in-Chief

Prof. Donata Kurpas

Deputy Editor

Prof. Wojciech Kosmala

Managing Editor

Paulina Piątkowska

Statistical Editors

Prof. Dorota Diakowska

Dr. Lesław Rusiecki

Dr. Dominik Marciniak

Dr. Andrzej Dąbrowski

Manuscript editing

Paulina Piątkowska, Marek Misiak

Scientific Committee

Prof. Antonio Cano

Prof. Breno Diniz

Prof. Erwan Donal

Prof. Chris Fox

Prof. Naomi Hachiya

Prof. Carol Holland

Prof. Sabine Bährer-Kohler

Prof. Markku Kurkinen

Prof. Christos Lionis

Prof. Raimundo Mateos

Prof. Zbigniew W. Ras

Prof. Jerzy W. Rozenblit

Prof. Silvina Santana

Prof. James Sharman

Prof. Jamil Shibli

Prof. Michal Toborek

Prof. László Vécsei

Prof. Cristiana Vitale

Section Editors

Basic Sciences

Dr. Mateusz Olbromski

Biochemistry

Prof. Małgorzata Krzystek-Korpacka

Dentistry

Prof. Jamil Shibli

Prof. Marzena Dominiak

Prof. Tomasz Gedrange

Dermatology

Prof. Jacek Szepietowski

Emergency Medicine, Innovative Technologies

Prof. Jacek Smereka

Histology and Embryology

Prof. Marzena Podhorska-Okołów

Intensive Therapy and Anesthesiology

Prof. Waldemar Goździk

Assoc. Prof. Barbara Adamik

Assoc. Prof. Wiesława Duszyńska

Internal Medicine

Angiology

Dr. Angelika Chachaj

Cardiology

Prof. Wojciech Kosmala

Endocrinology

Prof. Marek Bolanowski

Pulmonology

Prof. Elżbieta Radzikowska

Gastroenterology

Assoc. Prof. Katarzyna Neubauer

Hematology

Prof. Dariusz Wołowicz

Microbiology

Prof. Marzenna Bartoszewicz

Assoc. Prof. Adam Junka

Molecular Biology

Dr. Monika Bielecka

Prof. Jolanta Saczko

Dr. Marta Sochocka

Nephrology and Transplantology

Assoc. Prof. Dorota Kamińska

Assoc. Prof. Krzysztof Letachowicz

Neurology

Dr. Masaru Tanaka

Assoc. Prof. Anna Pokryszko-Dragan

Assoc. Prof. Magdalena Koszewicz

Oncology

Prof. Lucyna Kępka

Gynecological Oncology

Dr. Marcin Jędryka

Ophthalmology

Prof. Marta Misiuk-Hojło

Orthopedics

Assoc. Prof. Paweł Reichert

Otolaryngology

Assoc. Prof. Tomasz Zatoński

Pediatrics

Pediatrics, Metabolic Pediatrics, Clinical Genetics, Neonatology, Rare Disorders

Prof. Robert Śmigiel

Pediatric Nephrology

Prof. Katarzyna Kiliś-Pstrusińska

Pediatric Oncology and Hematology

Assoc. Prof. Marek Ussowicz

Pharmaceutical Sciences

Prof. Adam Matkowski

Pharmacoeconomics

Dr. Sylwia Szafraniec-Buryło

Psychiatry

Prof. Istvan Boksay

Prof. Jerzy Leszek

Public Health

Prof. Monika Sawhney

Prof. Izabella Uchmanowicz

Qualitative Studies, Quality of Care

Prof. Ludmiła Marcinowicz

Rehabilitation

Prof. Jakub Taradaj

Surgery

Prof. Renata Taboła

Assoc. Prof. Mariusz Chabowski

Telemedicine, Geriatrics, Multimorbidity

Assoc. Prof. Maria Magdalena

Bujnowska-Fedak

Editorial Policy

Advances in Clinical and Experimental Medicine (Adv Clin Exp Med) is an independent multidisciplinary forum for exchange of scientific and clinical information, publishing original research and news encompassing all aspects of medicine, including molecular biology, biochemistry, genetics, biotechnology and other areas. During the review process, the Editorial Board conforms to the "Uniform Requirements for Manuscripts Submitted to Biomedical Journals: Writing and Editing for Biomedical Publication" approved by the International Committee of Medical Journal Editors (www.ICMJE.org/). The journal publishes (in English only) original papers and reviews. Short works considered original, novel and significant are given priority. Experimental studies must include a statement that the experimental protocol and informed consent procedure were in compliance with the Helsinki Convention and were approved by an ethics committee.

For all subscription-related queries please contact our Editorial Office:
redakcja@umed.wroc.pl

For more information visit the journal's website:
www.advances.umed.wroc.pl

Pursuant to the ordinance No. 134/XV R/2017 of the Rector of Wrocław Medical University (as of December 28, 2017) from January 1, 2018 authors are required to pay a fee amounting to 700 euros for each manuscript accepted for publication in the journal Advances in Clinical and Experimental Medicine.

Indexed in: MEDLINE, Science Citation Index Expanded, Journal Citation Reports/Science Edition, Scopus, EMBASE/Excerpta Medica, Ulrich's™ International Periodicals Directory, Index Copernicus

Typographic design: Monika Kołęda, Piotr Gil

DTP: Wydawnictwo UMW

Cover: Monika Kołęda

Printing and binding: ARGİ SC

Contents

5 **Preface**

Original papers

- 7 Janina Golob Deeb, Lenart Skrijanc, Domen Kanduti, Caroline Carrico, Andrea Marquez Saturno, Kinga Grzech-Leśniak
Evaluation of Er:YAG and Er,Cr:YSGG laser irradiation for the debonding of prefabricated zirconia crowns
- 17 Hanna Danielewicz, Anna Dębińska, Anna Drabik-Chamerska, Danuta Kalita, Andrzej Boznański
IL4RA gene expression in relation to I50V, Q551R and C-3223T polymorphisms
- 23 Jadwiga Radziejewska, Martek Frączkowski, Agnieszka Sławuta, Bernard Panaszek
Can the in-hospital mortality rate in patients with ST-elevation myocardial infarctions be lowered any further?
- 29 Edyta Dziadkowiak, Maciej Guziński, Justyna Chojdak-Łukasiewicz, Małgorzata Wieczorek, Bogusław Paradowski
Predictive factors in post-stroke epilepsy: Retrospective analysis
- 35 Chung-Ze Wu, Chang-Hsun Hsieh, Chieh-Hua Lu, Dee Pei, Jin-Shuen Chen, Yen-Lin Chen
First-phase insulin secretion is positively correlated with alanine aminotransferase in young adults
- 41 Shinsuke Suzuki, Satoshi Toyoma, Yohei Kawasaki, Hiroshi Nanjo, Takechiyo Yamada
CD147 promotes invasion and MMP-9 expression through MEK signaling and predicts poor prognosis in hypopharyngeal squamous cell carcinoma
- 49 Milena Kozera, Joanna Konopińska, Marek Rękas
Mid-term evaluation of the safety and efficacy of the iStent trabecular micro-bypass system combined with phacoemulsification
- 55 Chunfeng Sun, Chen Shen, Yaping Zhang, Chunhong Hu
LncRNA ANRIL negatively regulated chitoooligosaccharide-induced radiosensitivity in colon cancer cells by sponging miR-181a-5p
- 67 Małgorzata Lelonek, Sylwia Wiśniowska-Śmiałek, Paweł Rubiś, Izabela Nowakowska, Agnieszka Pawlak
Sacubitril/valsartan for heart failure with reduced ejection fraction: A first real-life observational study in Poland
- 77 Paweł Hackemer, Bartosz Małkiewicz, Fryderyk Menzel, Aleksandra Drabik, Krzysztof Tupikowski, Romuald Zdrojowy
Determinants of survival in patients with bladder cancer undergoing radical cystectomy: The impact of serum creatinine level
- 83 Iwona Chlebicka, Beata Jastrząb, Aleksandra Stefaniak, Jacek Szepietowski
Basal cell carcinoma secondary to trauma: A 3-year experience of the single center
- 87 Monika Augustynowicz, Krzysztof Kałwak, Danuta Zwolińska, Kinga Musiał
The incidence of acute kidney injury in children undergoing allogeneic hematopoietic stem cell transplantation: A pilot study
- 93 Guoguo Yi, Ruiwen Yi, Xinglu Chen, Ling Peng, Guoqiang Huang, Min Fu, Xiao-he Lu, Hongwei Li
The role of soluble programmed death protein-1 (sPD-1) and soluble programmed death ligand-1 (sPD-L1) in rat corneal transplantation rejection

Reviews

- 101 Burak Erdinc, Sonu Sahni, Vladimir Gotlieb
Hematological manifestations and complications of COVID-19
- 109 Jacek Czubak, Karolina Stolarczyk, Anna Orzeł, Marcin Frączek, Tomasz Zatoński
Comparison of the clinical differences between COVID-19, SARS, influenza, and the common cold: A systematic literature review

PREFACE

Dear Readers, Authors, Reviewers,
Members of the Scientific Committee and Section Editors,

It is my great pleasure to welcome you all to the 30th year of *Advances in Clinical and Experimental Medicine*! I thank you for staying with us as our community continues to expand.

Advances in Clinical and Experimental Medicine has been published by the Wrocław Medical University since 1992. The originator, organizer and first Editor-in-Chief of the journal (1992–1997) was Prof. Bogumił Halawa. The journal was then entitled *Postępy Medycyny Klinicznej i Doświadczalnej* and appeared quarterly. Since 1997 the journal was headed by Prof. Leszek Paradowski who in 1998 introduced changes in the journal's profile and cover design. The title was changed to *Advances in Clinical and Experimental Medicine* to welcome articles in English. Moreover, a number of outstanding representatives of medical science from Poland and abroad were invited to participate in the newly established International Editorial Staff. In years 2000–2005 Prof. Antonina Harłodzińska-Szmyrka was journal's Editor-in-Chief and in years 2006–2007 once again Prof. Leszek Paradowski. Professor Maria Podolak-Dawidziak continued their role in years 2008–2016 and in 2017–2020 the journal's Editor-in-Chief was Prof. Maciej Bałaj. Today, I am honored to continue the journey full of challenges of my venerable predecessors.



2021 has inherited the challenges of 2020. While a global pandemic has been a looming risk for decades, COVID-19 has come as a shock to society, health systems, economies and governments worldwide. In the midst of extraordinary challenges and uncertainty, and countless personal tragedies, leaders are under pressure to make decisions on managing the immediate impact of the pandemic and its consequences, decisions that will shape the state of the world for years to come. The world of science has redirected its interests to the fight against COVID-19 – this is an urgent and important challenge. In this difficult context, we are confronted with the next stages of the journal's development: the need to improve the scientific level of published papers and the internationalization indicators. We would like *Advances in Clinical and Experimental Medicine* to be present not only in databases and among the journals cited by you, but most of all – in your scientific life. Hence the decision to establish the journal as part of scientific conferences and in social media.

The wide range of topics of the journal can be a strength, but also a weakness of our scientific activity – hence the decision to publish Call for Submissions by Section Editors on a regular basis. The topics of the issues published as part of these calls will concern the most current scientific trends.

We started this busy year with the great support of the Rectors' authorities of Wrocław Medical University, our new members of the Scientific Committee and new Section Editors – please accept my sincere thank you for joining the Editorial Board efforts. However, we really count on the support of those without whom no journal can exist: Authors and Reviewers, coming from the farthest scientific institutions of the world. We are all an international community in which the most important value is the development of science to help patients – this mission will guide the term of the Editorial Board in 2021–2024.

On the occasion of this New Year 2021, and on behalf of *Advances in Clinical and Experimental Medicine* Editorial Board, I wish you much fulfilling time spent with your loved ones, perseverance in carrying out the projects of your passion, and success in your research projects which, I hope, will result in publications on the pages of *Advances in Clinical and Experimental Medicine*!

Prof. Donata Kurpas
Editor-in-Chief

Evaluation of Er:YAG and Er,Cr:YSGG laser irradiation for the debonding of prefabricated zirconia crowns

Janina Golob Deeb^{1,A,C-F}, Lenart Skrjanc^{2,B,E}, Domen Kanduti^{2,B,E},
Caroline Carrico^{3,B,C,E}, Andrea Marquez Saturno^{1,B}, Kinga Grzech-Leśniak^{1,4,A,B,D-F}

¹ Department of Periodontics, School of Dentistry, Virginia Commonwealth University, Richmond, USA

² Faculty of Medicine, University of Ljubljana, Slovenia

³ Department of Dental Public Health and Policy, School of Dentistry, Virginia Commonwealth University, Richmond, USA

⁴ Department of Oral Surgery, Wrocław Medical University, Poland

A – research concept and design; B – collection and/or assembly of data; C – data analysis and interpretation;

D – writing the article; E – critical revision of the article; F – final approval of the article

Advances in Clinical and Experimental Medicine, ISSN 1899–5276 (print), ISSN 2451–2680 (online)

Adv Clin Exp Med. 2021;30(1):7–15

Address for correspondence

Kinga Grzech-Leśniak
E-mail: kgl@periocare.pl

Funding sources

None declared

Conflict of interest

None declared

Received on July 19, 2020

Reviewed on August 16, 2020

Accepted on September 20, 2020

Published online on January 30, 2021

Cite as

Golob-Deeb J, Skrjanc L, Kanduti D, Carrico C, Marquez Saturno A, Grzech-Leśniak K. Evaluation of Er:YAG and Er,Cr:YSGG laser irradiation for the debonding of prefabricated zirconia crowns. *Adv Clin Exp Med.* 2021;30(1):7–15. doi:10.17219/acem/127686

DOI

10.17219/acem/127686

Copyright

© 2021 by Wrocław Medical University

This is an article distributed under the terms of the Creative Commons Attribution 3.0 Unported (CC BY 3.0) (<https://creativecommons.org/licenses/by/3.0/>)

Abstract

Background. Reduced tooth structure in the pediatric and adolescent population is frequently restored with prefabricated zirconia crowns. On permanent teeth, these restorations may need to be removed and replaced with permanent restorations.

Objectives. To explore and compare the use of 2 high-powered erbium lasers for removing prefabricated zirconia crowns from molar teeth as a non-invasive alternative to rotary instruments.

Material and methods. Twenty-five permanent molars were prepared to dentin and prefabricated all-ceramic zirconia crowns were fitted and cemented with resin modified glass ionomer (RMGI) cement. The teeth were randomly assigned into one of the 2 retrieval treatment groups: the erbium-doped yttrium, aluminum and garnet (Er:YAG) laser group (G1; n = 12) or the erbium, chromium-doped yttrium, scandium, gallium and garnet laser (Er,Cr:YSGG) laser group (G2; n = 13). The laser operating parameters for the Er:YAG laser were 300 mJ, 15 Hz, 4.5 W, and 50-microsecond pulse duration (SSP mode); for the Er,Cr:YSGG laser, they were 4.5 W, 15 Hz, 20 water/20 air, and 5 W, 15 Hz, 50 water/50 air, and 60-microsecond pulse duration (H mode). The experiment was repeated twice. The surface area and the volume of teeth and crowns were measured and the cement space was calculated. The retrieval time and temperature changes were tested and recorded. The data were analyzed with the t-test. The surfaces of the dentin and the crown from each group were further examined using scanning electron microscopy (SEM).

Results. The average time for crown removal using the Er:YAG laser was 1 min 32.7 s; for the Er,Cr:YSGG laser it was 3 min 13.9 s ($p < 0.0001$). The mean temperature changes were $1.41 \pm 1.36^\circ\text{C}$ for the Er:YAG laser and $2.2 \pm 0.99^\circ\text{C}$ for the Er,Cr:YSGG laser ($p = 0.0321$). The SEM examination showed no damage or major structural changes caused by treatment with either erbium-family laser.

Conclusions. Both lasers are effective, non-invasive tools to remove prefabricated zirconia crowns cemented with resin cement and should be considered as viable alternatives to rotary instrumentation.

Key words: debonding, erbium laser, glass ionomer, prefabricated crown, zirconia

Introduction

Prefabricated crowns are a commonly used, predictable restorative option indicated for severely decayed or damaged teeth in the pediatric population. The goal of using them is to restore masticatory function, preserve healthy tooth structure, facilitate oral hygiene, and offer a durable, cost-effective treatment outcome.¹ With the development of biomaterials and an increased desire for esthetic outcomes, tooth-colored restorations, such as monolithic ceramic crowns, are gradually replacing traditional stainless steel crowns. Zirconia is a biocompatible, high-strength, wear-resistant, and color-stable material combining function and esthetics.¹ In the case of secondary caries, endodontic interventions and demand for a permanent restoration, it can be challenging and unpleasant for a pediatric dental patient to have these high-strength, all-ceramic materials removed using rotary instruments.

Recent studies have demonstrated a predictable way of retrieving ceramic restorations using erbium lasers: an erbium, chromium-doped yttrium, scandium, gallium and garnet laser (Er,Cr:YSGG), or an erbium-doped yttrium, aluminum and garnet laser (Er:YAG). They have emission wavelengths of 2780 nm and 2940 nm, respectively, which correlates with the peak absorption range of water.^{2–4} This results in good absorption into biological tissues and materials containing water, making them suitable for ablation, vaporization, disinfection,^{5–8} treatment of caries and osseous tissue,^{9–11} and other beneficial biological effects.^{9,12} The use of erbium lasers has also been explored in the removal of translucent restorations such as composite restorations, fiber-reinforced composite posts,¹³ veneers,^{14,15} brackets,¹⁶ and ceramic crowns.^{5,17–20} The light emitted by erbium lasers is transmitted through the translucent ceramic materials and is selectively absorbed by water molecules and residual monomers in the resin and glass ionomer cements. This absorption results in the vaporization of the molecules and ablation of the cement and hydrodynamic ejection.^{17,20} The mechanism of action for laser ablation in hard tissue or cement is based on rapid subsurface expansion. The volume of water trapped within the mineral substrate or cement is expanded and causes micro-explosions of the surrounding material or tissue.²¹ Heat generation is inevitable and has to be considered to prevent thermal injury of the pulpal tissues.²² Temperature changes during laser irradiation should remain within a tolerable range so as not to affect the vitality of the pulp and surrounding tissues.

The time required to remove lithium disilicate crowns with high-speed burs is approx. 6 min, while laser-assisted removal is estimated to take 60–90 s.²⁰ Using an Er:YAG laser for crown removal has been shown to be an effective and safe method; however, the parameters have not yet been optimized and iatrogenic damage has been reported in the literature when using higher laser settings.^{20,23,24} Recent studies have suggested that an Er:YAG laser presents

an effective, efficient method for removing lithium disilicate and zirconia crowns from implant abutments without causing damage to either or significantly increasing the temperature in the process.^{17,18} Similar studies have been performed on human teeth using an Er,Cr:YSGG laser, reporting acceptable temperature changes and effective zirconia and lithium disilicate crown removal.⁵ Both Er:YAG and Er,Cr:YSGG lasers have been shown to be effective and safe, although differences do exist in absorption and ablation efficiency between the 2 erbium lasers. The Er:YAG laser has been shown to be more efficient in enamel and in dentin due to a higher absorption compared to the Er,Cr:YSGG laser.^{23–28} Closer study of the absorption peak between the 2 lasers shows three-fold higher absorption coefficients for the Er:YAG laser over the Er,Cr:YSGG one. Consequently, the heat generated by the Er,Cr:YSGG laser has more time to spread deeper into the irradiated tissue or material, resulting in a thicker indirectly heated zone, which thermally affects the tooth or surrounding tissues more. This undesirable heating causes a waste of energy, resulting in reduced ablation efficiency²⁵ and more charring compared to the Er:YAG laser.²⁷

The aim of this *in vitro* study was to assess and compare the time of laser irradiation required to retrieve the cemented prefabricated zirconia crowns, and to assess the temperature changes during irradiation with Er:YAG and Er,Cr:YSGG pulsed lasers using similar operating parameters. An additional aim was to evaluate whether the length of laser irradiation required to debond the crown is related to the abutment or crown surface area.

Material and methods

In this research, we complied with the World Medical Association (WMA) Declaration of Helsinki and the Code of Medical Ethics of Virginia Commonwealth University (VCU).

Twenty five permanent molars were stored in saline after extraction.²⁹ The teeth were evaluated for the amount of remaining non-carious tooth structure and were excluded from the study if they presented with fractured crowns, gross caries or previous restorations.

All teeth were prepared following the manufacturer's instructions with 1–2 mm of occlusal reduction and 20–30% overall clinical crown reduction. The preparation was slightly tapered with a chamfer and feather-edge margin to ensure the passive fit of the selected prefabricated zirconia crowns (NuSmile, Houston, USA). All teeth were numbered and the prepared surfaces were scanned with an intraoral scanner (Planmeca Emerald; Planmeca, Helsinki, Finland) (Fig. 1A). All prefabricated zirconia crowns were air-dried and cemented using BioCem Universal Active Cement resin modified glass ionomer (RMGI) cement (BioCem; NuSmile) according to the manufacturer's instructions. The crowns were carefully seated and stabilized with finger

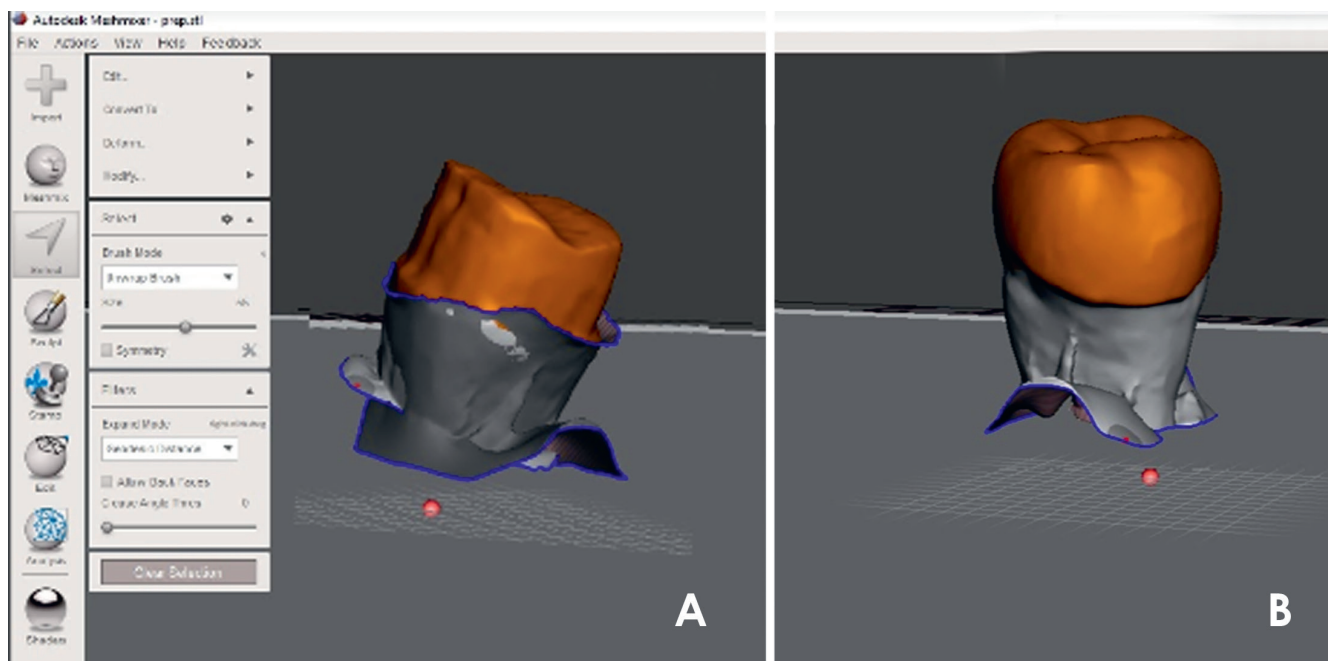


Fig. 1. Prepared surfaces of teeth (A) and cameo surfaces of the crowns (B) were scanned to calculate tooth surface area and the tooth volume

pressure for approx. 20 s. The cement was polymerized for 5–10 s with a curing light (800–1200 mW/cm²) on both the facial and lingual sites. After gently removing any excess cement, the crowns were polymerized for an additional 20 s on the facial, lingual and occlusal surfaces, mimicking the clinical situation where interproximal sites are not accessible. All the teeth were stored in a humidior for 24–48 h before retrieval was initiated. Following cementation, a 2nd scan of each tooth with a cemented crown was made. All stereolithographic files (STL format) were imported into Meshmixer[®] software (MeshMixer[®]; Autodesk, San Rafael, USA) in order to calculate the prepared tooth surface area [mm²] and cement volume [mm³]. Both scans were superimposed and sectioned at the marginal line of the crown to determine the exact margin of the bonding surface area on the prepared teeth. The volume of the bonded tooth preparation and the overall volume of the tooth, cement and crown were measured. The cement volume was then calculated from the difference between the overall volume and sum of the volumes of bonded tooth preparation and prefabricated crown. The prefabricated crown volumes were provided by the manufacturer (Fig. 1B).

The teeth were divided into 2 groups according to the laser used for the debonding procedure.

Group 1 (G1): debonding with Er:YAG laser (LightWalker; Fotona, Ljubljana, Slovenia). The 1st debonding experiment was labeled G1-FL1 (n = 12) and the 2nd debonding experiment was labeled G1-FL2 (n = 10).

Group 2 (G2): debonding with Er,Cr:YSGG laser (Waterlase; Biolase, Irvine, USA). The 1st debonding experiment was labeled G2-BL1 (n = 13) and the 2nd debonding experiment was labeled G2-BL2 (n = 13).

Each crown was debonded twice to determine whether the previous laser debonding process would affect adhesion properties or shorten the time needed to retrieve the crowns.

The laser settings in this study were chosen based on reports from previous studies, manufacturers' recommendations and our observations. The goal was to achieve minimal retrieval time at the lowest possible settings to avoid potentially harmful temperature increases and irreversible damage to the tooth substance. The laser irradiation was combined with light tapping forces and digital manipulation of the crowns for their retrieval.

Experiment 1

The settings used for the Er:YAG laser were the same for both experiments (G1-FL1 or G1-FL2) and were based on our observations from previous studies.^{17,18} The operating parameters of the laser were 300 mJ, 15 Hz, 4.5 W, and 50-microsecond pulse duration (super-short pulse (SSP) mode) with the non-contact H02 tip. The settings for the Er,Cr:YSGG laser were closely matched in the 1st experiment (G2-BL1): 4.5 W, 15 Hz, 20 water/20 air, and 60-microsecond pulse duration with the Turbo MX9 handpiece.

After the 1st debonding, the crowns were cleaned according to the manufacturer's recommendations and checked for cracks and damage. The remaining cement and debris was removed from the tooth using a dental air polishing and the crowns were re-cemented using the same cement and cementation procedure. All teeth were stored in a humidior for 24–48 h before the 2nd retrieval.

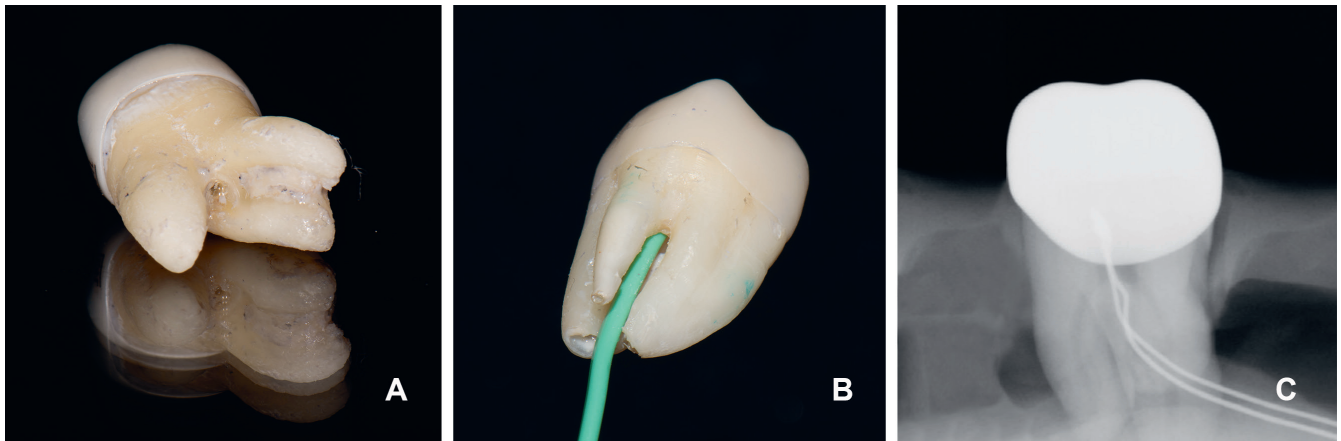


Fig. 2. To measure temperature changes inside the tooth during the laser irradiation, a channel was prepared through the furcation (A) to enable insertion of the temperature probe (B) into the pulpal chamber (C)

Experiment 2

The 2nd experiment was repeated using the same laser parameters for the Er:YAG laser (G1-FL2). Slight modifications were made to the Er,Cr:YSGG laser settings based on the manufacturer's recommendations: 5 W, 15 Hz and 50 water/50 air with the Turbo MX9 handpiece (G2-BL2).

Laser debonding procedure

The crowns were irradiated in a continuous motion of the handpiece on the buccal, occlusal and lingual surfaces, including the crown margins in a back-and-forth motion 2–5 mm from the crown surface for 30 s. The proximal surfaces were not irradiated in order to mimic adjacent teeth being present in the mouth. To test whether the crown could be removed, it was manipulated with digital palpation and a crown tapping instrument applied to the buccal and lingual margins. If the crown could not be successfully removed, additional 30-second intervals of irradiation and tapping followed. These intervals were repeated until the crown could be successfully retrieved.

Surface evaluation

After debonding, each crown and tooth were examined visually and under a microscope using $\times 40$ magnification (Leica M320; Leica Microsystems, Wetzlar, Germany) to analyze the adherence of the cement and any damage to the tooth or the intaglio surface of the crown. The surfaces of the sample teeth and crowns were further examined under a scanning electron microscope (SEM) (JEOL 6610LV; JEOL, Tokyo, Japan) in order to examine the structural integrity and any possible surface damage to the crown and tooth caused by the laser irradiation. The specimens were treated using a low-vacuum mode with an energy range of 20 kV and they were not coated.

Pulpal temperature

Following crown cementation, a channel (3–4 mm in diameter) was drilled through the furcation into the pulpal chamber of each tooth to facilitate the insertion of a microthermal couple probe (Adv. Thermocouple Therm. with RS 232 Output Datalogger Type K-800008; Super Scientific Works Pvt. Ltd., Vadodara, India) into the pulpal chamber (Fig. 2). Before initiating laser irradiation, baseline pulpal temperatures were recorded. The temperature in the pulpal chamber was recorded every 30 s.

Statistical analysis

The data was analyzed using equal and unequal variance t-tests, as appropriate. Associations between crown metrics (inner and outer surface area and spacer volume) were assessed using Pearson's correlation coefficient. The significance level was set at 0.05. SAS EG v. 6.1 software (SAS Institute, Cary, USA) was used for all of the analyses.

Results

Er:YAG laser

The average time for crown removal using the Er:YAG laser in group 1 was 1 min 33.8 s (standard deviation (SD) = 16.8 s) for the 1st experiment (G1-FL1) and 1 min 31.5 s (SD = 16.5 s) for the 2nd experiment (G1-FL2). There was no statistically significant difference between the 2 groups ($p = 0.6480$).

The irradiation time required to debond the crown was positively correlated with the spacer volume ($r = 0.67$; $p = 0.0007$). Debonding time was not significantly associated with inner ($r = -0.21$; $p = 0.34$) or outer ($r = -0.14$; $p = 0.55$) surface area. Table 1 includes correlations for the study groups.

Table 1. Pearson’s correlation coefficients for associations between crown metrics and irradiation time

Type of laser	Group	Outer surface area	Inner surface area	Space volume
Er:YAG	G1-F1 (n = 12)	−0.154	−0.241	0.758*
	G1-F2 (n = 10)	−0.113	−0.176	0.545**
	overall	−0.136	−0.211	0.667*
Er,Cr:YSGG	G2-BL1 (n = 13)	0.506**	0.586*	0.539**
	G2-BL2 (n = 13)	0.711*	0.801*	0.123
	overall	0.515*	0.586*	0.287

*p < 0.05; **0.05 < p < 0.10; Er:YAG – erbium-doped yttrium, aluminum and garnet laser; Er,Cr:YSGG – erbium, chromium-doped yttrium, scandium, gallium and garnet laser.

Table 2. Average temperature changes by group [°C]

Type of laser	Group	n	Mean	SD
Er:YAG	G1-F1 (n = 12)	12	1.7	1.62
	G1-F2 (n = 10)	10	1.0	0.92
	overall change	22	1.4	1.36
Er,Cr:YSGG	G2-BL1 (n = 13)	13	2.2	0.80
	G2-BL2 (n = 13)	13	2.1	1.19
	overall change	26	2.2	0.99

SD – standard deviation; Er:YAG – erbium-doped yttrium, aluminum and garnet laser; Er,Cr:YSGG – erbium, chromium-doped yttrium, scandium, gallium and garnet laser.

Er,Cr:YSGG laser

The average time for crown removal using the Er,Cr:YSGG laser in group 2 was 2 min 34.7 s (SD = 67.9 s) for the 1st experiment (G2-BL1) and 3 min 53.1 s (SD = 63.8 s) for the 2nd experiment (G2-BL2), which indicated a statistically significant difference between the 2 groups (p = 0.0058).

The irradiation time required to debond the crown was positively correlated with both outer surface area (r = 0.52; p = 0.01) and inner surface area (r = 0.59; p = 0.002). Irradiation was not significantly correlated with spacer volume (r = 0.29; p = 0.16). Table 1 includes correlations for the study groups.

Comparison: Er:YAG vs Er,Cr:YSGG

The 1st debonding was, on average, 60.9 s faster (standard error (SE) = 20.2) for the Er:YAG laser than for the Er,Cr:YSGG laser, which was a statistically significant difference (p = 0.0076). For the 2nd debonding, the Er:YAG laser was 2 min 21.6 s faster, on average, than the Er,Cr:YSGG laser, which was also statistically significant (p < 0.0001) (Fig. 3).

Pulpal temperature

The mean temperature changes were 1.40 ±1.36°C for the Er:YAG laser and 2.2 ±0.99°C for the Er,Cr:YSGG laser (p = 0.0321). For both erbium lasers, the differences in temperature change between the 2 debonds were not statistically significant (p = 0.23 and 0.76, respectively).

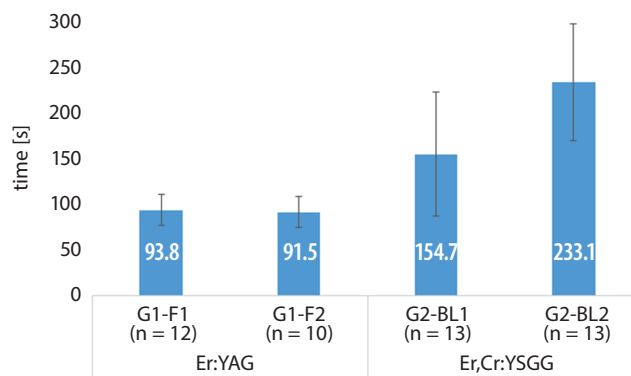


Fig. 3. Debond time for both experiments for Er:YAG and Er,Cr:YSGG lasers

All pulpal temperatures remained within a safe range, with the highest recorded temperature change of 5°C for Er:YAG and 4°C for Er,Cr:YSGG. These temperatures should be interpreted with caution, as they reflect various other factors such as the temperatures of the room and water. The temperature range during the irradiation is shown in Table 2.

Scanning electron microscopy analysis

After irradiation, none of the teeth or crowns appeared damaged on visual inspection or under an optical microscope using a ×40 magnification lens.

The SEM examination did not reveal any damages or major structural changes suggesting photoablation or thermal ablation of the abutment teeth caused by irradiation of either laser (Fig. 4). The decrease in adhesion strength

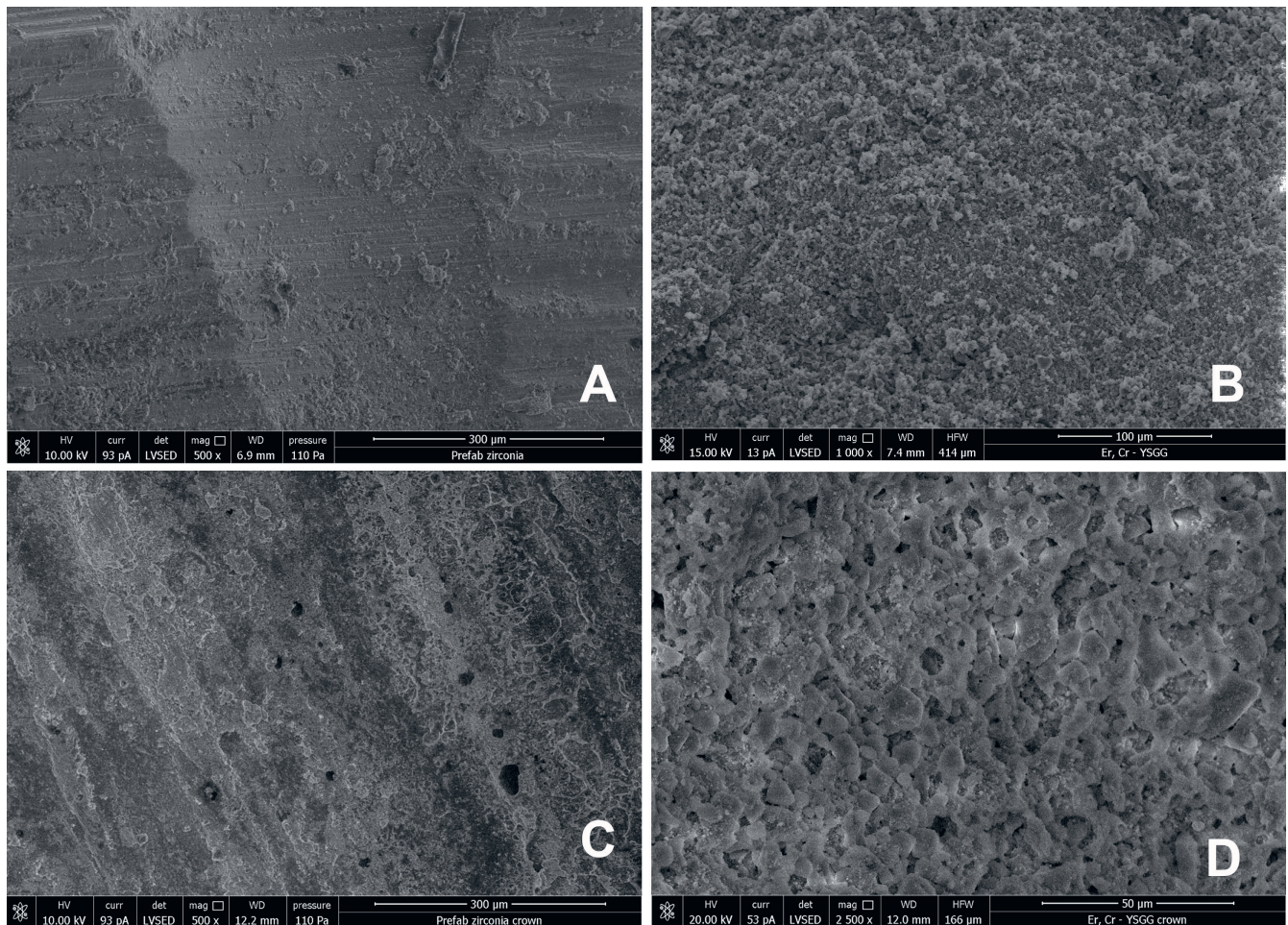


Fig. 4. Residual cement and undamaged surface is observed on SEM images of the teeth following irradiation with Er:YAG laser (A) and Er,Cr:YSGG laser (B) and intaglio surface of the crowns following Er:YAG (C) and Er,Cr:YSGG laser (D) laser

appeared either between the cement and the tooth surface, leaving the cement attached mostly inside the crown, or between the cement and the intaglio surface of the crown, leaving cement attached to the surface of the tooth. No carbonization, cracks or fractures in the macro- or micro-structure were observed on the tooth or on the zirconia prefabricated crown. Slight, partial ablation of the cement caused by Er,Cr:YSGG laser irradiation was occasionally observed. The intaglio surfaces appeared to be similar in roughness for both lasers. The teeth treated with the Er:YAG laser showed less cement remaining on the surfaces than those treated with the Er,Cr:YSGG laser (Fig. 4).

Discussion

The development of prefabricated all-ceramic crowns and modern adhesive systems has improved the restorative options for severely damaged teeth in the pediatric and adolescent population. The removal of these temporary restorations can be challenging and is usually accomplished with rotary instruments. Alternatively, atraumatic removal can be predictably and reproducibly accomplished

using high-powered erbium lasers such as Er:YAG and Er,Cr:YSGG.³⁰ Both erbium lasers are selectively absorbed by water molecules²⁵ and residual monomers of cements, leading to a decrease in adhesion strength between the cement and the crown or a tooth due to photothermal ablation. A dentin–crown interface can be debonded with thermal softening, thermal ablation or photoablation, resulting in cracks in the cement layer and the breakage of material bonds.^{5,17,20}

Closer study of the absorption peak between the 2 lasers shows three-fold higher absorption coefficients for the Er:YAG laser in comparison to the Er,Cr:YSGG laser. The Er,Cr:YSGG laser wavelength thus penetrates deeper into the tissue and requires more time to heat up the irradiated volume to the evaporation temperature, while the substance heated by the Er:YAG laser will reach ablation temperatures faster and progress deeper into the targeted substance.^{25,31} Our findings are in alignment with these observations, since the time required to debond the crowns was shorter for the Er:YAG laser than the Er,Cr:YSGG laser after the 1st debonding using similar settings. Both lasers showed clinically acceptable debonding times, proving them to be an efficient tool for crown debonding.

Heat generated by an Er,Cr:YSGG laser has more time to spread deeper into the tissue, resulting in a thicker indirectly-heated zone exerting greater thermal effects on the tooth. This undesirable heating of the surrounding tissue is also the reason energy is lost, resulting in less efficient ablation.²⁴ To prevent thermal injury of the pulpal tissues, heat generation and accumulation should be minimal. An increase in pulpal temperature of 5.5°C can cause irreversible damage to the pulp tissue³²; a rise in temperature of 10°C for 60 s on the root surfaces can cause irreversible damage to the periodontal ligament and bone that can lead to bone resorption and tooth ankylosis.^{33,34} In this study, temperature changes measured in the pulpal chamber throughout the irradiation were minimal and did not exceed critical temperature changes. No significant temperature increase was observed, even when the slightly higher settings for Er,Cr:YSGG were used in the 2nd experiment.

Both lasers provide continuous water cooling that was in this study effective in regulating temperature during irradiation. Only temperature changes during laser irradiation in relation to the baseline temperature were reported. The initial temperatures were not standardized for all experiments and differed slightly due to variations in room temperature on different days.

The key factors of successful debonding include technique, the duration of laser irradiation, fluency, an adequate

pulse of the mid-infrared wavelength, and continuous, uninterrupted irradiation.³⁵ The working parameters for both lasers used in this study were low and safe, yet provided efficient and reproducible debonding of the restorations.

Laser-assisted ceramic crown removal encompasses several factors that may affect its efficiency: the chemical composition and type of ceramic material, the thickness of the restoration, the type, shade and thickness of the resin cement, the shade and opacity of the ceramic material, and the parameters of the laser (power, pulse duration, frequency, and irradiation time).^{15,36–39} The advantage of retrieving a crown with an erbium laser is to preserve the crown for re-cementation. In this study, all the crowns were re-cemented after the 1st debonding and tested again. The results of this study indirectly showed a predictable bond strength after re-cementation of the crowns as the debonding time did not decrease during the 2nd irradiation; it even increased for the 2nd Er,Cr:YSGG laser group. The slightly higher power (0.5 W) used for the 2nd debonding (G2-BL2) should theoretically result in a shorter irradiation time but resulted in significantly increased debonding time. One possible explanation could be the use of a 50% water spray, causing higher absorption of the laser on the wet surface of the crown, therefore lowering the energy efficiency in the cement layer. Another possible explanation could be a lighter tapping force employed by a different

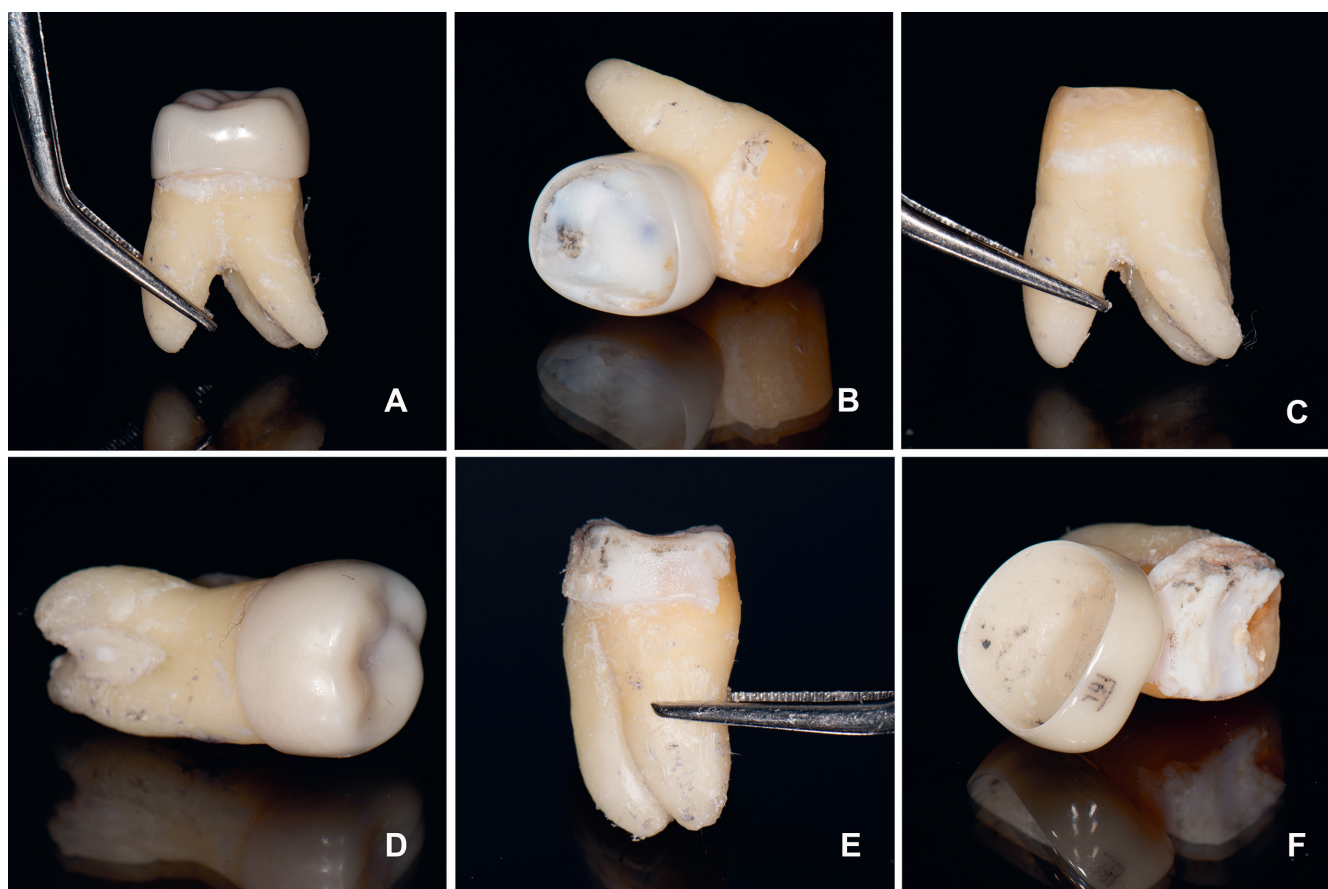


Fig. 5. Following erbium laser irradiation, debonding of the crown resulted in either retention of the cement attached to the intaglio surface of the crown (A–C) or the surface of the tooth (D–F)

operator. This could be an important additional finding, as in many clinical scenarios, the use of tapping instruments with a considerable force may not be feasible. This is also true for younger and more sensitive patients, where parents may object and there is a risk of iatrogenic damage to the tooth and crown. A short burst of additional laser irradiation could therefore be used to minimize or avoid using any kind of tapping instrument, allowing for digital retrieval of the crown from the tooth.

Interestingly, debonding occurred either between the cement and tooth, with the cement remaining inside the crown, or between the cement and inner surface of the crown, with the cement remaining on the tooth surface. The Er,Cr:YSGG laser group, with a longer irradiation time, was associated with less residual cement on the tooth and more residual cement inside the crown. In contrast, most of the remaining cement in the Er:YAG laser group was retained on the tooth surface (Fig. 5).

The laser settings and debonding procedure resulted in minimal structural changes to the crown and tooth surface according to macro- and microscopic examination. No crowns or teeth were fractured or broken during the experiments. Since no thermal effects were exerted by either laser, it can be concluded that this treatment modality with either of the 2 lasers provides safe, efficient and predictable removal of the crown and does not affect future re-cementation.

During the experiment, we encountered some limitations. The force used to tap the crowns off the teeth greatly depends on the clinician and was not measured or standardized in our experiment. With a stronger tapping force, the debonding time was consistently shorter, whereas with the use of a very light tapping force or only digital manipulation, the time required to retrieve the crown increased.

Conclusions

The removal of cemented all-ceramic crowns with the use of an Er:YAG or Er,Cr:YSGG laser is a viable alternative to rotary techniques. Laser-assisted prefabricated zirconia crown debonding is atraumatic, time-efficient, predictable, and reversible with erbium-family lasers.

ORCID iDs

Janina Golob Deeb  <https://orcid.org/0000-0002-3189-0136>
 Lenart Skrjanc  <https://orcid.org/0000-0002-6580-5948>
 Domen Kanduti  <https://orcid.org/0000-0002-0426-3102>
 Caroline Carrico  <https://orcid.org/0000-0001-9521-9854>
 Andrea Marquez Saturno  <https://orcid.org/0000-0001-5129-3091>
 Kinga Grzech-Leśniak  <https://orcid.org/0000-0002-5700-4577>

References

1. Matys J, Swider K, Flieger R, Dominiak M. Assessment of the root analog zirconia implants primary stability designed using cone beam computed tomography software by means of Periotest device: An ex vivo study. Preliminary report. *Adv Clin Exp Med*. 2017;26(5):803–809. doi:10.17219/acem/65069
2. Diener V, Polychronis G, Erb J, Zinelis S, Eliades T. Surface, microstructural, and mechanical characterization of prefabricated pediatric zirconia crowns. *Materials (Basel)*. 2019;12(20):3280. doi:10.3390/ma12203280
3. Iseri U, Oztoprak MO, Ozkurt Z, Kazazoglu E, Arun T. Effect of Er:YAG laser on debonding strength of laminate veneers. *Eur J Dent*. 2014; 8(1):58–62. doi:10.4103/1305-7456.126243
4. Oztoprak MO, Tozlu M, Iseri U, Ulkur F, Arun T. Effects of different application durations of scanning laser method on debonding strength of laminate veneers. *Lasers Med Sci*. 2012;27(4):713–716. doi:10.1007/s10103-011-0959-1
5. Rechmann P, Buu NCH, Rechmann BMTT, Finzen FCF. Laser all-ceramic crown removal and pulpal temperature: A laboratory proof-of-principle study. *Lasers Med Sci*. 2015;30(8):2087–2093. doi:10.1007/s10103-015-1738-1
6. Deeb JG, Smith J, Belvin BR, Grzech-Leśniak K, Lewis J. Er:YAG laser irradiation reduces microbial viability when used in combination with irrigation with sodium hypochlorite, chlorhexidine, and hydrogen peroxide. *Microorganisms*. 2019;7(12):612. doi:10.3390/microorganisms7120612
7. Grzech-Leśniak K, Sculean A, Gašpirc B. Laser reduction of specific microorganisms in the periodontal pocket using Er:YAG and Nd:YAG lasers: A randomized controlled clinical study. *Lasers Med Sci*. 2018;33(7):1461–1470. doi:10.1007/s10103-018-2491-z
8. Grzech-Leśniak K, Matys J, Dominiak M. Comparison of the clinical and microbiological effects of antibiotic therapy in periodontal pockets following laser treatment: An in vivo study. *Adv Clin Exp Med*. 2018;27(9):1263–1270. doi:10.17219/ACEM/70413
9. Matys J, Hadzik J, Dominiak M. Schneiderian membrane perforation rate and increase in bone temperature during maxillary sinus floor elevation by means of Er:YAG laser: An animal study in pigs. *Implant Dent*. 2017;26(2):238–244. doi:10.1097/ID.0000000000000520
10. Matys J, Flieger R, Tenore G, Grzech-Leśniak K, Romeo U, Dominiak M. Er:YAG laser, piezosurgery, and surgical drill for bone decortication during orthodontic mini-implant insertion: Primary stability analysis. An animal study. *Lasers Med Sci*. 2018;33(3):489–495. doi:10.1007/s10103-017-2381-9
11. Pourzarandian A, Watanabe H, Aoki A, et al. Histological and TEM examination of early stages of bone healing after Er:YAG laser irradiation. *Photomed Laser Surg*. 2004;22(4):342–350. doi:10.1089/pho.2004.22.342
12. Grzech-Leśniak K, Matys J, Jurczyszyn K, et al. Histological and thermometric examination of soft tissue de-epithelialization using digitally controlled Er:YAG laser handpiece: An ex vivo study. *Photomed Laser Surg*. 2018;36(6):313–319. doi:10.1089/pho.2017.4413
13. Deeb JG, Grzech-Leśniak K, Weaver C, Matys J, Bencharit S. Retrieval of glass fiber post using Er:YAG laser and conventional endodontic ultrasonic method: An in vitro study. *J Prosthodont*. 2019;28(9):1024–1028. doi:10.1111/jopr.13114
14. Correa-Afonso AM, Palma-Dibb RG, Pécora JD. Composite filling removal with erbium:yttrium-aluminum-garnet laser: Morphological analyses. *Lasers Med Sci*. 2010;25(1):1–7. doi:10.1007/s10103-008-0581-z
15. Rechmann P, Buu NCH, Rechmann BMT, Le CQ, Finzen FC, Featherstone JDB. Laser all-ceramic crown removal: A laboratory proof-of-principle study. Phase 1 – material characteristics. *Lasers Surg Med*. 2014;46(8):628–635. doi:10.1002/lsm.22279
16. Grzech-Leśniak K, Matys J, Zmuda-Stawowiak D, et al. Er:YAG laser for metal and ceramic bracket debonding: An in vitro study on intrapulpal temperature, SEM, and EDS analysis. *Photomed Laser Surg*. 2018;36(11):595–600. doi:10.1089/pho.2017.4412
17. Deeb JG, Bencharit S, Dalal N, Abdulmajeed A, Grzech-Leśniak K. Using Er:YAG laser to remove lithium disilicate crowns from zirconia implant abutments: An in vitro study. *PLoS One*. 2019;14(11):e0223924. doi:10.1371/journal.pone.0223924
18. Grzech-Leśniak K, Bencharit S, Dalal N, Mroccka K, Deeb JG. In vitro examination of the use of Er:YAG laser to retrieve lithium disilicate crowns from titanium implant abutments. *J Prosthodont*. 2019;28(6):672–676. doi:10.1111/jopr.13077
19. Kellesarian SVSSV, Malignaggi V, Aldosary KMK, et al. Laser-assisted removal of all ceramic fixed dental prostheses: A comprehensive review. *J Esthet Restor Dent*. 2018;30(3):216–222. doi:10.1111/jerd.12360

20. Rechmann P, Buu NCHH, Rechmann BMTT, Finzen FC. Laser all-ceramic crown removal: A laboratory proof-of-principle study. Phase 2 – crown debonding time. *Lasers Surg Med*. 2014;46(8):636–643. doi:10.1002/lsm.22280
21. van As G. Erbium lasers in dentistry. *Dent Clin North Am*. 2004;48(4):1017–1059. doi:10.1016/j.cden.2004.06.001
22. Matys J, Grzech-Leśniak K, Flieger R, Dominiak M. Assessment of an impact of a diode laser mode with wavelength of 980 nm on a temperature rise measured by means of k-02 thermocouple: Preliminary results. *Dent Med Probl*. 2016;53(3):345–351.
23. Belikov AV, Skripnik AV, Zholobova EP. Comparative study of human hard tooth tissues removal efficiency by Er-laser pulses with different temporal structure. *Proc SPIE*. 2008;6791:67910U–67910U. doi:10.1117/12.803989
24. Diaci J. Laser profilometry for the characterization of craters produced in hard dental tissues by Er:YAG and Er,Cr:YSGG lasers. *J Laser Health Acad*. 2008;2(1):1–10.
25. Diaci J, Gaspirc B. Review comparison of Er:YAG and Er,Cr:YSGG lasers used in dentistry. *J Laser Health Acad*. 2012;1(1):1–13.
26. Lin S, Liu Q, Peng Q, Lin M, Zhan Z. Ablation threshold of Er:YAG and Er,Cr:YSGG laser in dental dentin. *Sci Res Essays*. 2010;5(16):2128–2135.
27. Perhavec T, Gorkič A, Bračun D, Diaci J. A method for rapid measurement of laser ablation rate of hard dental tissue. *Opt Laser Technol*. 2009;41(4):397–402. doi:10.1016/j.optlastec.2008.08.007
28. Stock K, Hibst R, Keller U. Comparison of Er:YAG and Er:YSGG laser ablation of dental hard tissues: Medical applications of lasers in dermatology, ophthalmology, dentistry, and endoscopy. *Proc SPIE*. 1997;3192:88–95. doi:10.1117/12.297864
29. ISO – ISO/TS 11405:2015. Dentistry: Testing of adhesion to tooth structure. <https://www.iso.org/standard/62898.html>. Accessed April 30, 2020.
30. Tozlu M, Oztoprak MO, Arun T. Comparison of shear bond strengths of ceramic brackets after different time lags between lasing and debonding. *Lasers Med Sci*. 2012;27(6):1151–1155. doi:10.1007/s10103-011-1018-7
31. Mirhashemi A, Chiniforush N, Jadidi H, Sharifi N. Comparative study of the effect of Er:YAG and Er,Cr:YSGG lasers on porcelain: Etching for the bonding of orthodontic brackets. *Lasers Med Sci*. 2018;33(9):1997–2005. doi:10.1007/s10103-018-2573-y
32. Zach L, Cohen G. Pulp response to externally applied heat. *Oral Surg Oral Med Oral Pathol*. 1965;19:515–530. doi:10.1016/0030-4220(65)90015-0
33. Eriksson AR, Albrektsson T. Temperature threshold levels for heat-induced bone tissue injury: A vital-microscopic study in the rabbit. *J Prosthet Dent*. 1983;50(1):101–107. doi:10.1016/0022-3913(83)90174-9
34. Eriksson RA, Albrektsson T, Magnusson B. Assessment of bone viability after heat trauma: A histological, histochemical and vital microscopic study in the rabbit. *Scand J Plast Reconstr Surg Hand Surg*. 1984;18(3):261–268. doi:10.3109/02844318409052849
35. Matys J, Dominiak M, Flieger R. Energy and power density: A key factor in lasers studies. *J Clin Diagn Res*. 2015;9(12):ZL01–ZL02. doi:10.7860/jcdr/2015/15561.6955
36. Corona SAM, De Souza AE, Chinelatti MA, Borsatto MC, Pécora JD, Palma-Dibb RG. Effect of energy and pulse repetition rate of Er:YAG laser on dentin ablation ability and morphological analysis of the laser-irradiated substrate. *Photomed Laser Surg*. 2007;25(1):26–33. doi:10.1089/pho.2006.1075
37. Corona SAM, Souza-Gabriel AE, Chinelatti MA, Pécora JD, Borsatto MC, Palma-Dibb RG. Influence of energy and pulse repetition rate of Er:YAG laser on enamel ablation ability and morphological analysis of the laser-irradiated surface. *J Biomed Mater Res Part A*. 2008;84(3):569–575. doi:10.1002/jbm.a.31335
38. Ekworapoj P, Sidhu SK, McCabe JF. Effect of different power parameters of Er,Cr:YSGG laser on human dentine. *Lasers Med Sci*. 2007;22(3):175–182. doi:10.1007/s10103-006-0426-6
39. Raucchi-Neto W, Chinelatti MA, Palma-Dibb RG. Ablation rate and morphology of superficial and deep dentin irradiated with different Er:YAG laser energy levels. *Photomed Laser Surg*. 2008;26(6):523–529. doi:10.1089/pho.2007.2201

IL4RA gene expression in relation to I50V, Q551R and C-3223T polymorphisms

Hanna Danielewicz^{A–F}, Anna Dębińska^{A–C,E,F}, Anna Drabik-Chamerska^{B,E,F},
Danuta Kalita^{B,E,F}, Andrzej Boznański^{A,C,E,F}

1st Department of Pediatrics, Allergology and Cardiology, Wrocław Medical University, Poland

A – research concept and design; B – collection and/or assembly of data; C – data analysis and interpretation;
D – writing the article; E – critical revision of the article; F – final approval of the article

Advances in Clinical and Experimental Medicine, ISSN 1899–5276 (print), ISSN 2451–2680 (online)

Adv Clin Exp Med. 2021;30(1):17–22

Address for correspondence

Hanna Danielewicz
E-mail: hanna.danielewicz@umed.wroc.pl

Funding sources

This study was supported by statutory funds of the Department of Pediatrics, Allergy and Cardiology, Wrocław Medical University, received from Ministry of Science and Higher Education

Conflict of interest

None declared

Received on July 22, 2019

Reviewed on December 4, 2019

Accepted on August 31, 2020

Published online on January 30, 2021

Abstract

Background. Interleukin 4 (IL-4) and its receptor play important roles in the pathologies of asthma and atopy. The alpha subunit of the IL-4 receptor (IL-4RA) is included in 2 types of receptors which have different modulatory effects on immune responses. This distinct pattern reflects involvement in the immunopathology of both asthma and atopy. A number of studies have proven the association between *IL4RA* gene polymorphisms and asthma and atopy, but it is still an open question whether these variants are functional.

Objectives. To analyze the data from *IL4RA* gene expression in PBMC in relation to specific polymorphisms – the most frequently studied I50V and Q551R and the less known C-3223T.

Material and methods. The analysis was performed for 36 subjects, both atopic and non-atopic. Real-time polymerase chain reaction (PCR) was used with specific primers for the quantification and genotyping. Delta Ct (Δ CT) and delta-delta Ct ($\Delta\Delta$ CT) values were used for the relative quantification of *IL4RA* expression in PBMC.

Results. We observed no significant differences in the *IL4RA* expression profile between the 3 genotypes. A trend toward higher relative expression was observed for homozygous minor I50V and C-3223T genotypes.

Conclusions. We did not find a statistically significant relationship between the genetic polymorphisms and the relative expression of *IL4RA*. The effect of genetic polymorphism on *IL4RA* mRNA expression could interfere with other factors, such as environmental stimuli, and should be evaluated in future studies.

Key words: gene expression, polymorphism, asthma, atopy, *IL4RA*

Cite as

Danielewicz H, Dębińska A, Drabik-Chamerska A, Kalita D, Boznański A. *IL4RA* gene expression in relation to I50V, Q551R and C-3223T polymorphisms. *Adv Clin Exp Med.* 2021;30(1):17–22. doi:10.17219/acem/127031

DOI

10.17219/acem/127031

Copyright

© 2021 by Wrocław Medical University
This is an article distributed under the terms of the
Creative Commons Attribution 3.0 Unported (CC BY 3.0)
(<https://creativecommons.org/licenses/by/3.0/>)

Introduction and objectives

Interleukin 4 (IL-4) and its receptor play important roles in the pathologies of asthma and atopy. The alpha subunit of the IL-4 receptor (IL-4RA) is included in 2 types of receptors, which have different modulatory effects on immune responses. Type I is responsive to IL-4 only, and is mainly expressed on myeloid cells. According to the eQTL database, the highest expression of *IL4RA* (type I) is in whole blood (GeneHopper, <http://genehopper.ifis.cs.tu-bs.de>; GTEXPortal, <https://gtexportal.org>). Type II IL-4R acts as the receptor for both IL-4 and IL-13. It is expressed in bronchial mucosa and a variety of other cells. While type I receptors transmit signals related to immunoglobulin switching and immunoglobulin E (IgE) production, type II plays a role in bronchoconstriction, inflammation and mucus production. This distinct pattern reflects involvement in the immunopathology of both asthma and atopy. Increased *IL4RA* expression has been found in both conditions.^{1–3}

While *IL4RA* is expressed by all subtypes of lymphocytes, the majority are expressed on B and Th2 cells, as reported in the expression profiling database. Changes in the mRNA expression of *IL4RA* mirror changes in the proportion of different T cell subsets.² The regulation of IL-4RA protein production is complex and not yet fully understood. Furthermore, the process differs across different tissue types. T cells react mainly to stimulation by IL-4, but also react to IL-2. Secretion of the IL-2 cytokine occurs as a natural response to microbial infection and autoimmune phenomena, and together with IL-4 can induce and maintain *IL4RA* expression by activating STAT5.⁴ The activation pathway differs for different types of T cells. For instance, naïve CD4⁺ T cells react by upregulating IL-4RA, which is not antigen-specific. The highly activated T cells respond by downregulating IL-4RA, specifically with high amounts of antigen. This mechanism is part of a homeostasis process aimed at “saving” IL-4 for B cells and IgE production.⁵ Also, sIL-4R, which is the soluble form of IL-4R, is known to regulate IL-4. It is formed by alternative splicing or proteolytic shading of the membrane-bound form. The alternation in the concentration of sIL-4R and the expression of *mIL4RA* could reflect immune tolerance, which occurs in situations such as during the course of immunotherapy.²

There are a number of studies in the literature that suggest an association between *IL4RA* polymorphisms and asthma and atopy.^{6–8} Functional changes have been observed for Q551R and I50V, which seem to enhance the response to IL-4 in vitro.⁹ However, only a few experiments have confirmed this phenomenon (OMIM database, <https://www.omim.org>). It has been shown that the presence of Q551R could indicate the degree of responsiveness to IL-4RA-antagonist treatment.¹⁰ This specific polymorphism has also been found to be associated with the IL-4-related Treg differentiation pathway,

a subpopulation of T cells which are crucial for immune tolerance. This dependence is present in the subgroup of asthma patients with the mixed-cellularity Th2/Th17 phenotype.¹¹ Furthermore, upregulation of IL-4RA due to a gain-of-function mutation in the gene with the F709 single nucleotide polymorphism (SNP) results in a failure to produce antigen-specific Treg.¹² Apart from the studies mentioned above, there is still the open question of whether variants within *IL4R* are functional or are only markers for causative variation nearby in the region. Is that specific polymorphism in fact related to the pattern of increased or decreased *IL4R* expression, thus mediating the risk for allergy and asthma?

Our group previously reported *IL4RA* expression in relation to atopy status and place of residence. We did find a trend for atopic subjects to have a higher expression and for those living in the countryside to have lower values, though the differences were not statistically significant.¹³ Herein, we present the results of *IL4RA* expression analysis in relation to specific polymorphisms within the gene – most of them well-known from association studies, I50V and Q551R, and the less-studied C-3223T.

Material and methods

The methods for relative gene expression using real-time quantitative polymerase chain reaction RT-qPCR) and the characteristics of the study group have already been described in detail.¹³ We used the expression data from the subjects enrolled in our previous study and performed genotyping for *IL4RA* polymorphisms. In the current analysis, 36 subjects with available data were enrolled, 18 of whom were atopic. The subjects assigned as controls were otherwise healthy. Atopy was confirmed by the result of a skin prick test (SPT) to common allergens. The SPTs were performed in all atopic and control subjects. Four of the subjects were not assigned to any group due to the lack of conclusive SPT results. Venous blood samples were collected into 2 tubes containing EDTA (Sarstedt AG & Co., Nümbrecht, Germany) for DNA extraction, PBMC isolation and RNA extraction. DNA was extracted from whole-blood samples using the QIAMP kit (Qiagen Inc., Valencia, USA) according to the manufacturer's instructions. The expression data originated in the experiments using a LightCycler 1.5 and specific hybridization probes. *ACTB* (β -actin) was used as reference.¹³ Delta Ct (Δ Ct) and delta-delta mean Ct ($\Delta\Delta$ Ct) values were used for relative quantification of *IL4RA* expression in PBMC, and $2^{-\Delta\Delta$ Ct) was used for fold change (FC) estimation in groups according to genotype. Genotyping for specific SNPs, including rs1805010 (I50V), rs1801275 (Q551R) and rs2057768 (C-3223T), was performed using specific Light SNP primers (TIB Molbiol, Berlin, Germany) and the LightCycler 1.5. The PCR conditions were as follows: denaturation – 1 cycle at 95°C for 10 min; cycling – 45 cycles of 95°C

for 10 s, 60°C for 10 s and 72°C for 15 s; melting – 1 cycle at 95°C for 30 s, 40°C for 2 s and a temperature rise to 75°C; cooling – 1 cycle at 40°C for 30 s.

The Fisher's exact test was performed to compare the frequencies between the specific groups assigned based on their atopic status or genotype. The exact test was used to determine Hardy–Weinberg equilibrium (HWE) in the controls. The Kruskal–Wallis test and the Mann–Whitney U test were used to compare Δ CT between groups in relation to genotype. The analysis was performed in 3 groups: 1) pulled – all subjects with genotype data, 2) atopic and 3) the controls separately. The statistical tests were done with STATISTICA v. 13.2 software (StatSoft Inc., Tulsa, USA).

This study was approved by the ethical committee of the Wrocław Medical University (Poland). All participants signed an informed consent form.

Results

The genotype and allele frequencies are presented in Table 1. For all genotypes, we observed no deviation from the HWE in the control group.

While comparing genotype frequencies in the groups related to atopic status, we observed significant differences

only for I50V for the recessive model. Carriers of 2 minor alleles were more prone to be atopic. Other SNPs were not significantly associated with atopy; however, for SNP C-3223T we observed a trend for the variant allele to be predominant in the atopic group (Table 1).

There were no significant differences in relative *IL4RA* gene expression between the 3 genotypes (I50V, Q551R, and C-3223T; Fig. 1) in any of the 3 analyzed groups, with the use of different models. The most clear trend was observed in the pulled group, where there was a 1.39-fold change ($2^{-\Delta\Delta$ CT) in relative expression for the I50V SNP in the recessive model (GG compared to AA+AG) and a 2.5-fold change for the C-3223T SNP in the recessive model (AA compared to GG+AG). For Q551R, we only included the dominant model, as there was only 1 subject with the GG genotype (AG+GG compared to AA), which showed a 1.09-fold change. The direction of changes in relative gene expression was different in regard to atopy status, which suggests that atopy and the milieu of cytokines associated with it may be an additional determinant of expression (Table 2).

We also analyzed combinations of different genotypes. The most common was the genotype which was homozygous for major alleles of the 3 studied SNPs (25%). There were no significant differences in *IL4RA* gene expression when these combinations of genotypes were analyzed.

Table 1. Genotype frequencies according to genotype for SNPs I50V, Q675R and C-3223T in relation to atopy status and different models. Fisher's exact test for significance; $p < 0.05$ was regarded as statistically significant

Variable	Total n = 36 (%)	Atopic n = 18 (%)	Control n = 14 (%)	HWE in controls, p-value	χ^2 /Fisher, p-value
I50V					
AA	12 (0.33)	4 (0.22)	7 (0.5)	0.75	0.08
AG	14 (0.38)	7 (0.38)	6 (0.42)		
GG	10 (0.27)	7 (0.38)	1 (0.06)		
AA+AG	26 (0.72)	11 (0.61)	13 (0.92)	0.03	0.10
AG+GG	24 (0.67)	14 (0.77)	7 (0.5)		
A	38 (0.53)	15 (0.41)	20 (0.71)	0.02	0.02
G	34 (0.47 – MAF)	21 (0.58)	8 (0.29)		
Q551R					
AA	16 (0.44)	12 (0.66)	5 (0.35)	0.15	0.06
AG	19 (0.53)	5 (0.27)	9 (0.64)		
GG	1 (0.03)	1 (0.05)	0		
AA+AG	35 (0.97)	17 (0.94)	14 (1.0)	0.72	0.12
AG+GG	20 (0.56)	6 (0.33)	9 (0.64)		
A	51 (0.71)	29 (0.8)	19 (0.67)	0.24	0.24
G	21 (0.29 – MAF)	7 (0.19)	9 (0.32)		
C-3223T					
GG	23 (0.64)	10 (0.55)	10 (0.71)	0.6	0.39
AG	10 (0.27)	5 (0.27)	4 (0.28)		
AA	3 (0.08)	3 (0.16)	0		
GG+AG	33 (0.92)	15 (0.83)	14 (1.0)	0.15	0.37
AG+AA	13 (0.36)	8 (0.44)	4 (0.28)		
G	56 (0.78)	25	24	0.11	0.11
A	16 (0.22 – MAF)	11	4		

MAF – minor allele frequency; HWE – Hardy–Weinberg Equilibrium exact test.

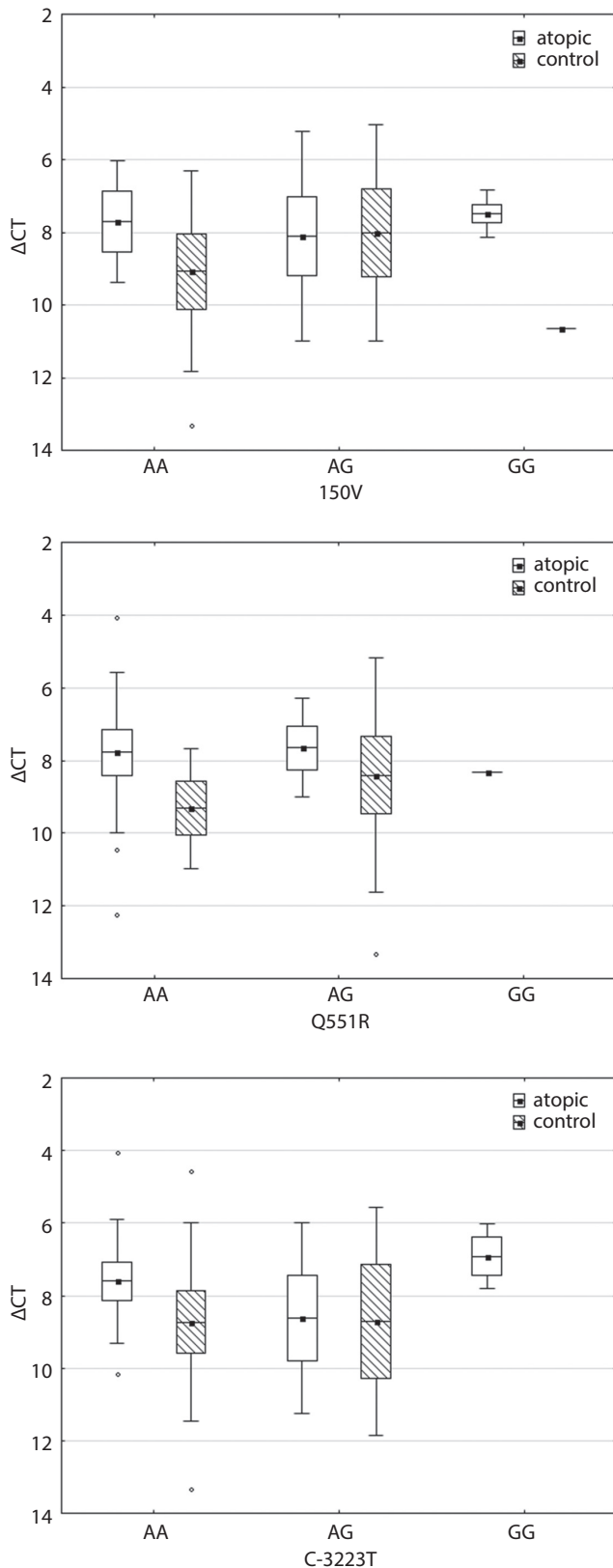


Fig. 1. Relative *IL4RA* gene expression in PBMC in the genotype groups, expressed as ΔCT , where $\Delta\text{CT} = \text{Ct IL-4RA} - \text{Ct ACTB}$ for each sample. The lower the ΔCT values, the higher the gene expression. The Y-axis has been reversed for better illustration. Data is presented as mean \pm standard error (SE) \pm standard deviation (SD). The differences were not statistically significant according to the Kruskal–Wallis rank test ($p > 0.05$)

Discussion

In our previous study, we compared the expression profile of individuals in relation to atopy status and place of residence. Although the results were not statistically significant, they may suggest an environment-related regulatory mechanism connected with rural living.¹³ The aim of the current study was to determine whether the most important and well-studied SNPs within the *IL4RA* gene are responsible for the different patterns of gene expression. We observed no significant differences in expression profile according to genotype within the different models. A trend was observed for I50V and C-3223T. Individuals who were homozygous for minor alleles had a higher gene expression of *IL4RA*. This suggests a pattern where *IL4RA* expression is to some extent related to the presence of the SNPs reported as being associated with allergy.

To our knowledge, there are only 2 studies in the literature to which we can refer our results. As in our study, these researchers found no clear relationship between Q551R and the expression profile of *IL4RA* in their 33 subjects.³ The trend they observed was different to our findings regarding this SNP, though: minor alleles were rather associated with higher, not lower expression. The eQTL database (GTExPortal) revealed a significant eQTL in whole blood related to the C-3223T genotype. The same was present for I50V, but not for Q551R.¹⁴ In both cases homozygous minor alleles showed lower expression, which is contrary to our findings. The small body of evidence in this field is striking in light of the fact that biological treatment with IL-4RA antibody is already in use.^{15,16}

There are also 2 studies suggesting an epigenetic effect of the *IL4RA* polymorphism. In the 1st study, out of the 9 SNPs evaluated (including C-3223T), only 1 (rs3024685) showed an interaction with the methylation status of the gene, which could somehow reflect expression.¹⁷ In the 2nd study, 8 SNPs and 4 CpGs connected to the TH2 pathway were included in the model of interaction with DNA methylation and asthma risk; between them, cg26937798 was revealed to confer such a risk.¹⁸

The polymorphisms we choose for this study were previously explored in various contexts, mainly related to asthma and atopy. Both I50V and Q551R were the first SNPs within *IL4RA* to be described in relation to these conditions. The C-3223T SNP was first described by Hackstein in 2001, and has been subsequently investigated in a few studies.¹⁹ GWA studies (Genome Wide Association Studies) have confirmed the role of all 3 of these polymorphisms.²⁰ Both I50V and Q551R appear to have functional outcomes through enhanced IL-4 signaling, as indicated in the OMIM database. In a meta-analysis including 50 studies, the I50V variant was found to be associated with asthma in the dominant model, and Q551R in the recessive model. In addition, I50V has been associated with asthma in Asian populations, and has also been related to pediatric and atopic asthma.⁷ In other studies,

Table 2. Relative *IL4RA* gene expression in PBMC in the genotype groups. Relative gene expression of *IL4RA* is expressed as ΔCT , where $\Delta CT = Ct\ IL4RA - Ct\ ACTB$ for each sample. The lower the ΔCT values, the higher the gene expression. Data are presented as mean \pm standard error (SE) \pm standard deviation (SD). The differences were not statistically significant according to the Mann–Whitney U test ($p > 0.05$)

Variable	Pulled (n = 36)	p-value	Atopic (n = 18)	p-value	Control (n = 14)	p-value
I50V						
ΔCT AA	8.66 \pm 2.32		7.70 \pm 1.67		9.06 \pm 2.75	
ΔCT AG+GG	7.86 \pm 2.19	0.56	7.79 \pm 2.03	0.87	8.39 \pm 2.89	0.89
ΔCT AA+AG	8.26 \pm 2.53	0.76	7.96 \pm 2.41	1.0	8.58 \pm 2.78	–
ΔCT GG	7.78 \pm 1.19		7.48 \pm 0.65		10.64	
FC dominant	1.74		0.94		1.59	
FC recessive	1.39		1.39		–	
Q551R						
ΔCT AA	8.19 \pm 2.11		7.78 \pm 2.22		9.31 \pm 1.65	
ΔCT AG+GG	8.06 \pm 2.43	0.87	7.76 \pm 1.24	0.81	8.40 \pm 3.23	0.5
ΔCT AA+AG	8.12 \pm 2.27	–	7.74 \pm 1.96	–	8.73 \pm 2.73	–
ΔCT GG	8.31		8.31		–	
FC dominant	1.09		1.01		1.88	
C-3223T						
ΔCT GG	8.07 \pm 2.22		7.60 \pm 1.71		8.73 \pm 2.73	
ΔCT AG+AA	8.22 \pm 2.34	0.89	7.98 \pm 2.23	0.76	8.71 \pm 3.15	1.0
ΔCT GG+AG	8.23 \pm 2.29	0.3	7.94 \pm 2.02	0.28	8.73 \pm 2.73	–
ΔCT AA	6.91 \pm 0.90		6.91 \pm 0.90		–	
FC dominant	0.9		0.77		1.01	
FC recessive	2.5		2.04			

FC – fold change ($2^{\Delta\Delta CT}$).

I50V and C-3223T (homozygous), but not Q551R, were found to be related to early-onset asthma.²¹ In another study that compared eight SNPs of *IL4RA*, including C-3223T, Q551R, and I50V, only I50V showed a significant association with total IgE.²² However, in a study that investigated asthma phenotypes in young infants, none of the abovementioned SNPs demonstrated any significant relationships.²³

Functional experiments were performed for I50V and Q551R. Mice that are homozygous for Q551R present increased inflammation, mucus production, airway hyper-reactivity, eosinophilia, and neutrophilia. The underlying mechanism is possibly associated with redirection of iTreg into Th17. This phenomenon has also been reported in the subgroup of asthma patients who have mixed Th2/Th17 cellularity. This asthma phenotype is characterized by increased severity, steroid resistance and neutrophilia.¹¹ Two other *IL4RA* SNPs, rs8832 and rs1029489, located within the 3' untranslated and proximal regions, have been associated with the response to anti-IL-4/IL-13 treatment (IL-4RA competitive antagonist). Individuals with these variants showed reduced asthma exacerbation and better response to treatment in a dose-dependent manner.¹⁰ Both E400A and Q551R were also associated with a reduction in FEV1 (Forced Expiratory Volume in the first second) and an antigen response during the course of treatment.²⁴

The promoter polymorphism C-3223T has not been widely studied, even though the location suggests a possible impact on transcription. In our previous study, we found an association between this polymorphism and the level of the soluble form of IL-4R.²⁵ Another group reported a similar relationship with *IL4RA* haplotypes. TVR (T-3223, V50, R5 51) subjects were also reported to have lower levels of sIL-4R.²⁶

The limitation of our study is the small sample size. The possible effect and statistical power could be missed because of that. Nevertheless, the results suggest some relationship which could be further investigated.

All of the abovementioned studies suggest a relationship between the genetic polymorphism of *IL4RA* and the pattern of expression, reflecting the link between genotype and phenotype. Some elements of this puzzle are still missing, which may require more comprehensive analysis that includes gene–gene and gene–environment interaction.

Conclusions

We did not find a relationship between these 3 genetic polymorphisms and the relative expression of *IL4RA*. The effect of genetic polymorphism on *IL4RA* mRNA expression could interfere with other factors, such as environmental stimuli, and should be evaluated in future studies.

ORCID iDs

Hanna Danielewicz  <https://orcid.org/0000-0001-7999-8923>
 Anna Dębińska  <https://orcid.org/0000-0002-1136-1974>
 Anna Drabik-Chamerska  <https://orcid.org/0000-0002-5425-6090>
 Danuta Kalita  <https://orcid.org/0000-0003-4335-6376>
 Andrzej Boznański  <https://orcid.org/0000-0002-3447-9326>

References

- Kotsimbos TC, Ghaffar O, Minshall EM, et al. Expression of the IL-4 receptor alpha-subunit is increased in bronchial biopsy specimens from atopic and nonatopic asthmatic subjects. *J Allergy Clin Immunol.* 1998;102(5):859–866.
- Nestor CE, Dadfar E, Ernerudh J, et al. Sublingual immunotherapy alters expression of IL-4 and its soluble and membrane-bound receptors. *Allergy.* 2014;69(11):1564–1566. doi:10.1111/all.12505
- Pascual M, Roa S, García-Sánchez A, et al. Genome-wide expression profiling of B lymphocytes reveals IL4R increase in allergic asthma. *J Allergy Clin Immunol.* 2014;134(4):972–975. doi:10.1016/j.jaci.2014.05.015
- Liao W, Schones DE, Oh J, et al. Priming for T helper type 2 differentiation by interleukin 2-mediated induction of IL-4 receptor α chain expression. *Nat Immunol.* 2009;9(11):1288–1296. doi:10.1038/ni.1656
- Perona-Wright G, Mohrs K, Mayer KD, Mohrs M. Differential regulation of IL-4R α expression by antigen versus cytokine stimulation characterizes Th2 progression in vivo. *J Immunol.* 2010;184(2):615–623. doi:10.4049/jimmunol.0902408
- Hesselmar B, Bergin A-M, Park H, et al. Interleukin-4 receptor polymorphisms in asthma and allergy: Relation to different disease phenotypes. *Acta Paediatr.* 2010;99(3):399–403. doi:10.1111/j.1651-2227.2009.01631.x
- Nie W, Zang Y, Chen J, Xiu Q. Association between interleukin-4 receptor α chain (IL4RA) I50V and Q551R polymorphisms and asthma risk: An update meta-analysis. *PLoS One.* 2013;8(7):e69120. doi:10.1371/journal.pone.0069120
- Sunadome H, Matsumoto H, Petrova G, et al. *IL4Ra* and *ADAM33* as genetic markers in asthma exacerbations and type-2 inflammatory endotype. *Clin Exp Allergy.* 2017;47(8):998–1006. doi:10.1111/cea.12927
- Ford AQ, Heller NM, Stephenson L, Boothby MR, Keegan AD. An atopy-associated polymorphism in the ectodomain of the IL-4R(α) chain (V50) regulates the persistence of STAT6 phosphorylation. *J Immunol.* 2009;183(3):1607–1616. doi:10.4049/jimmunol.0803266
- Slager RE, Otulana BA, Hawkins GA, et al. IL-4 receptor polymorphisms predict reduction in asthma exacerbations during response to an anti-IL-4 receptor α antagonist. *J Allergy Clin Immunol.* 2012;130(2):516–522.e4.
- Massoud AH, Charbonnier L-M, Lopez D, Pellegrini M, Phipatanakul W, Chatila TA. An asthma-associated IL4R variant exacerbates airway inflammation by promoting conversion of regulatory T cells to TH17-like cells. *Nat Med.* 2016;22(9):1013–1022. doi:10.1038/nm.4147
- Rivas MN, Burton OT, Wise P, et al. Regulatory T cell reprogramming towards a Th2 cell-like lineage impairs oral tolerance and promotes food allergy. *Immunity.* 2015;42(3):512–523. doi:10.1016/j.immuni.2015.02.004
- Danielewicz H, Dębińska A, Drabik-Chamerska A, Kalita D, Boznański A. *IL4RA* gene expression in PBMC with regard to place of living and atopy status. *Adv Clin Exp Med.* 2018;27(2):173–177.
- GTEPortal. https://gtexportal.org/home/snp/16_27356203_A_G_b37. Accessed July 13, 2019.
- Chung KF. Dupilumab: A potential new treatment for severe asthma. *Lancet.* 2016;388(10039):3–4. doi:10.1016/S0140-6736(16)30311-7
- Beck LA, Thaçi D, Hamilton JD, et al. Dupilumab treatment in adults with moderate-to-severe atopic dermatitis. *N Engl J Med.* 2014;371(2):130–139. doi:10.1056/NEJMoa1314768
- Soto-Ramírez N, Arshad SH, Holloway JW, et al. The interaction of genetic variants and DNA methylation of the interleukin-4 receptor gene increase the risk of asthma at age 18 years. *Clin Epigenetics.* 2013;5(1):1. doi:10.1186/1868-7083-5-1
- Zhang H, Tong X, Holloway JW, et al. The interplay of DNA methylation over time with Th2 pathway genetic variants on asthma risk and temporal asthma transition. *Clin Epigenetics.* 2014;6(1):8. doi:10.1186/1868-7083-6-8
- Hackstein H, Hecker M, Kruse S, et al. A novel polymorphism in the 5' promoter region of the human interleukin-4 receptor α -chain gene is associated with decreased soluble interleukin-4 receptor protein levels. *Immunogenetics.* 2001;53(4):264–269. doi:10.1007/s002510100324
- Michel S, Liang L, Depner M, et al. Unifying candidate gene and GWAS approaches in asthma. *PLoS One.* 2010;5(11):e13894. doi:10.1371/journal.pone.0013894
- Hesselmar B, Enelund A-C, Eriksson B, Padyukov L, Hanson LÅ, Åberg N. The heterogeneity of asthma phenotypes in children and young adults. *J Allergy.* 2012;2012:163089. doi:10.1155/2012/163089
- Maier LM, Howson JMM, Walker N, et al. Association of IL13 with total IgE: Evidence against an inverse association of atopy and diabetes. *J Allergy Clin Immunol.* 2006;117(6):1306–1313. doi:10.1016/j.jaci.2005.12.1354
- Hoffjan S, Ostrovnaja I, Nicolae D, et al. Genetic variation in immunoregulatory pathways and atopic phenotypes in infancy. *J Allergy Clin Immunol.* 2004;113(3):511–518. doi:10.1016/j.jaci.2003.10.044
- Slager RE, Hawkins GA, Ampleford EJ, et al. IL-4 receptor polymorphisms are predictors of a pharmacogenetic response to a novel IL-4/IL-13 antagonist. *J Allergy Clin Immunol.* 2010;126(4):875–878. doi:10.1016/j.jaci.2010.08.001
- Danielewicz H, Hurkacz M, Boznański A, Wiela-Hojeńska A, Chamerska-Drabik A. Association of soluble IL-4R serum levels and IL-4R α chain gene polymorphisms. *Adv Clin Exp Med.* 2009;18(6):559–565.
- Hytonen A-M, Lowhagen O, Arvidsson M, et al. Haplotypes of the interleukin-4 receptor α chain gene associate with susceptibility to and severity of atopic asthma. *Clin Exp Allergy.* 2004;34(10):1570–1575. doi:10.1111/j.1365-2222.2004.02069.x

Can the in-hospital mortality rate in patients with ST-elevation myocardial infarctions be lowered any further?

Jadwiga Radziejewska^{1,A,B,D–F}, Martek Frączkowski^{2,B,C,E,F}, Agnieszka Sławuta^{3,A–F}, Bernard Panaszek^{4,A,D–F}

¹ Kłodzko County Hospital, Poland

² Department of Gastroenterology and Hepatology, Wrocław Medical University, Poland

³ Department of Cardiology, Kłodzko County Hospital, Poland

⁴ The Witelton State University of Applied Sciences in Legnica, Poland

A – research concept and design; B – collection and/or assembly of data; C – data analysis and interpretation;

D – writing the article; E – critical revision of the article; F – final approval of the article

Advances in Clinical and Experimental Medicine, ISSN 1899–5276 (print), ISSN 2451–2680 (online)

Adv Clin Exp Med. 2021;30(1):23–27

Address for correspondence

Agnieszka Sławuta

E-mail: aslawuta@o2.pl

Funding sources

None declared

Conflict of interest

None declared

Received on May 25, 2020

Reviewed on June 1, 2020

Accepted on October 22, 2020

Published online on December 29, 2020

Cite as

Radziejewska J, Frączkowski M, Sławuta A, Panaszek B.

Can the in-hospital mortality rate in patients with ST-elevation myocardial infarctions be lowered any further?

Adv Clin Exp Med. 2021;30(1):23–27.

doi:10.17219/acem/128746

DOI

10.17219/acem/128746

Copyright

© 2021 by Wrocław Medical University

This is an article distributed under the terms of the Creative Commons Attribution 3.0 Unported (CC BY 3.0)

(<https://creativecommons.org/licenses/by/3.0/>)

Abstract

Background. A myocardial infarction is a specific clinical condition characterized by a relatively high acute mortality rate. Earlier reperfusion results in a smaller infarct size and a lower mortality rate.

Objectives. To assess the in-hospital mortality in patients with ST-elevation myocardial infarction (STEMI) regarding patients' characteristics, and the mechanisms behind the deterioration in hemodynamic and clinical status, in order to assess the possibility of preventing this type of death.

Material and methods. A group of 106 patients aged 64.5 ± 11.3 years was divided into 2 groups: patients who died while hospitalized (group I; $n = 5$) and patients who survived while hospitalized for STEMI (group II; $n = 101$). Primary coronary intervention was performed in all individuals, with direct stent implantation in all but 1 patient. In all patients the standard medication was started or continued, depending on the patient's status. The demographic and selected clinical and biochemical parameters were compared between the study groups.

Results. The patients in group I were significantly older than the survivors (76.2 ± 12.7 compared to 64.0 ± 11.0 years; $p < 0.05$). The group with fatal myocardial infarction had a lower left ventricular ejection fraction (LVEF) ($31.7 \pm 12.8\%$ compared to $60.4 \pm 11.0\%$; $p < 0.05$) and a higher maximal serum troponin level (973.6 ± 1121.8 ng/mL compared to 453.2 ± 924.2 ng/mL; $p < 0.05$). Interestingly, among the patients who died, the pain-to-balloon time was significantly shorter than in the myocardial infarction survivors (84 ± 48 min compared to 342 ± 504 min; $p < 0.05$).

Conclusions. The development of the medical care system has made invasive procedures available, improving outcomes in patients with acute myocardial infarction. This form of treatment is likely optimized to such an extent that any changes in the time before intervention will not substantially improve mortality rates.

Key words: myocardial infarction, in-hospital mortality, ST-elevation myocardial infarction, primary percutaneous coronary intervention

Background

Myocardial infarction is a specific clinical disorder characterized by a relatively high acute mortality rate.¹ Multiple mechanisms contribute to arrhythmia and hemodynamic episodes, leading to cardiomyocyte ischemia and even the relatively sudden death of the individual.² The distinction between ST-elevation and non-ST-elevation made little change in the clinical picture of in-hospital mortality. The most spectacular and fearful type of death is a sudden arrhythmic one in the form of ventricular fibrillation. The other possibility is an acute, high-degree atrioventricular blockage. There are 2 main forms of blockage: in patients with an inferior wall myocardial infarction, the most common type is a transient, proximal atrioventricular block, usually with a relatively rapid, narrow QRS escape rhythm, while in patients with an extensive anterior myocardial infarction, it is caused by interventricular septum ischemia, a typically permanent, distal type with a low, broad QRS escape rhythm. The latter can lead to ventricular asystole and sudden death. The hemodynamic impairment of ischemic ventricular myocardium can also result in low cardiac output with clinical signs of cardiogenic shock. This disorder was historically associated with a very poor prognosis, with mortality rates as high as 90%. An appropriate, timely invasive treatment of the underlying myocardial infarction can of course substantially reduce the burden of ischemia and necrosis.³ However, in some individuals, the changes could be irreversible, which can also lead to in-hospital death.

A report on the care of patients with ST-elevation myocardial infarction (STEMI) in American hospitals showed an improvement in care manifested by an increase in the rate of reperfusion and a shortening of the time from symptom onset to treatment. At the same time, several years of observation did not show a decrease in mortality in the entire study population, but only for patients without cardiac arrest. In the whole population, cardiogenic shock and cardiac arrest steadily increased.¹ When designing our study, we wanted to know the profile of STEMI patients in our center, and the mortality rate and characteristics of the group with the highest risk. The modern cardiac care of patients with STEMI diminished the acute mortality to as low as 4–5%. It is uncertain if this value can be substantially reduced. One of the key obstacles is the numerous comorbidities related to the increasing age of the patients. Various combinations of chronic kidney disease (CKD), diabetes mellitus (DM), chronic atrial fibrillation, chronic obstructive pulmonary disease (COPD), malnutrition, frailty, and cognitive function decline can negatively influence the outcome in myocardial infarction patients even if the infarct-related artery (IRA) is kept open.⁴ Partial or slight insufficiencies of the aforementioned organs and systems in connection with even benign and transient hemodynamic impairment can contribute to a fatal end result – in-hospital death.

The aim of the study was to assess the in-hospital death rate in patients with STEMI in relation to the patients' characteristics, and the mechanisms of deterioration in hemodynamic and clinical status, in order to assess the possibility of preventing this type of death.

Material and methods

The study group comprised all patients hospitalized in 2015 with a diagnosis of STEMI in the regional cardiology ward, featuring a permanently working cardiac catheterization laboratory (Cath Lab). All patients were treated directly in the Cath Lab, undergoing primary coronary angioplasty, usually with a concomitant stent placement. These individuals were divided into 2 subgroups according to in-hospital death. Of the 106 patients included, 5 died during the hospitalization.

The study was approved by the local Bioethics Committee at Wrocław Medical University, Poland.

Statistical analysis

All continuous variables are presented as means and standard deviations (SD). Comparisons were performed with the Mann–Whitney U test for independent groups. All categorical variables are presented as numbers and percentages. The comparisons were performed with the χ^2 test. P-values less than 0.05 were considered significant.

Results

The basic demographic characteristics and selected clinical and biochemical data are presented in Tables 1,2. The difference in ejection fraction between the 2 groups is depicted in Fig. 1.

In the 5 patients who died, the LAD was occluded or subtotally narrowed in 4 cases. The circumflex artery (Cx)

Table 1. The patients' demographic and selected clinical data

Variable	Died (n = 5)	Survived (n = 101)	p-value
Age [years]	76.2 ±12.7	64.0 ±11.0	<0.05
Sex [% female]	20	34	n.s.
Pain-to-balloon time [min]	84 ±48	342 ±504	<0.05
RR syst. [mm Hg]	114.0 ±27.0	137.2 ±28.6	n.s.
Pulse [bpm]	95.3 ±21.7	77.3 ±18.5	n.s.
EF [%]	31.7 ±12.8*	60.4 ±11.0	<0.05
AF [%]	20	4	n.s.
DM/IFG/IGT [%]	40	28	n.s.
Hypertension [%]	60	60	n.s.

*n = 4; EF – ejection fraction; AF – atrial fibrillation; DM – diabetes mellitus; IFG – impaired fasting glucose; IGT – impaired glucose tolerance; RR syst. – systolic blood pressure.

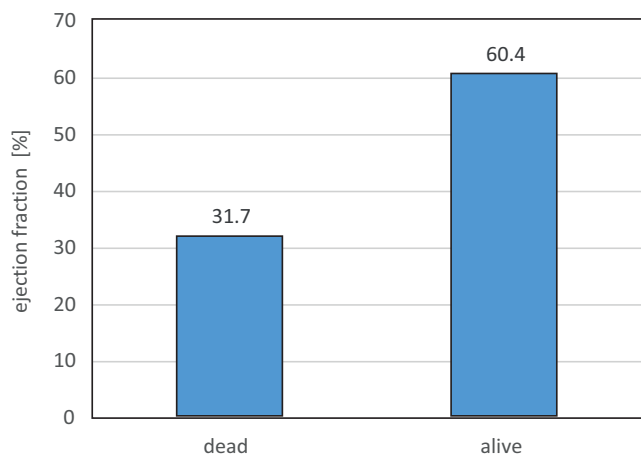


Fig. 1. Comparison between the study groups according to EF

or the right coronary artery (RCA) was occluded or subtotally narrowed in 3 cases. In 4 cases, the primary percutaneous coronary intervention (PCI) was successful; in 1 patient, pulseless electrical activity was observed before the intervention, which was therefore postponed and subsequently not performed.

Selected biochemical parameters in the study groups are presented in Table 2.

Table 2. Patients' biochemical data

Variable	Died (n = 5)	Survived (n = 101)	p-value
Troponin I [ng/mL]	973.6 ± 1121.8	453.2 ± 924.2	<0.05
Creatinine [mg%]	1.1 ± 0.3	1.0 ± 0.3	ns.
Glucose [mg%]	148.2 ± 54.1	160.6 ± 62.2	ns.

ns. – not significant.

Discussion

The implementation of optimal treatment methods in patients with STEMI has led to a significant improvement in the survival rate to the degree that may constitute the limits of medical care. The combination of advanced age, pre-existing myocardial damage, serious co-morbidities, and recent widespread myocardial ischemia can prove fatal despite modern and sophisticated treatment modalities.

In accordance with data from the literature, our study demonstrated that the age of the patients determined their mortality. This parameter is important in all acute coronary syndromes (ACS). Older people usually have more advanced atherosclerosis, and higher rates of co-morbidities and cardiovascular risk factors, which place them at a higher risk of an extensive coronary artery disease (CAD) than younger individuals.^{2–4} The STEMI is the most serious condition of all CAD presentations. Previous studies have suggested that older STEMI patients were at a higher risk of death and other complications regardless of the treatment used.⁵

Our study was conducted among patients with optimal treatment, since they were taken directly to the Cath Lab by emergency medical services. Previous studies have demonstrated that PCI was superior to thrombolysis in terms of re-infarction, stroke and death. If those most appropriate treatments had been offered within the shortest possible time from symptom onset, it would have dramatically improved the clinical outcome compared to conservative treatment strategies. In the present study, all patients had angioplasty of the IRA. The time to the procedure in our group with the fatal outcome was not significantly longer than in the group of survivors. It is likely that the patients with a fatal infarction had a shorter pain-to-balloon time because of the most severe symptoms.

One of possible reasons for death during a STEMI could be concomitant changes in other arteries than the IRA. The prognosis of a patient is related to the extent of ischemia due to the occlusion of the blood vessel. Therefore, the location of the lesion and changes in other vessels are important, as the closure of the artery responsible for collateral circulation may affect a wide area of the myocardium. About 40–65% of the patients presenting with STEMI are found to have a co-existing disease in the non-infarct-related arteries. The 2017 European Society of Cardiology (ESC) guidelines for patients with STEMI recommend PCI of the non-culprit artery at the time of primary PCI as a class IIa (strong) recommendation if the patient is hemodynamically stable.⁶ There are several studies showing that a complete revascularization (immediate and/or staged) is associated with a significant reduction in events, mainly driven by a significant reduction in the rates of repeat revascularization and cardiac death when compared to IRA-only revascularization in patients with STEMI and a concomitant multi-vessel disease.⁷

Our patients who died during hospitalization had a higher heart rate and a lower blood pressure at admission, although these differences were not statistically significant. These findings are consistent with other studies. An observational study on 2,310 STEMI patients treated with primary PCI showed that an elevated heart rate on admission was an independent prognostic factor for in-hospital and long-term mortality.^{8,9} A higher heart rate in combination with a lower blood pressure can predict the development of cardiogenic shock, significantly increasing mortality in ACS.

The extent of ischemia can be expressed by certain biomarkers, including troponin. Troponin level is positively and proportionally related to the extent of myocardium damage. In patients with ACS, the troponin level on admission is an independent predictor of death.^{10,11} However, The prognostic value of troponin level on admission in patients with STEMI is not unambiguous. In a study by Stubbs et al., patients with higher troponin levels on admission had worse outcomes of thrombolytic therapy, but the differences in early mortality were not statistically significant.¹² The same observation was made

in a different study, in a population treated with angioplasty, where higher troponin levels predicted a worse outcome of this treatment as well.¹¹ In the present study, the group with an unfavorable outcome had significantly higher serum troponin levels on admission. This finding is in concordance with the consensus and with previous studies.¹³ The association was proven to be true, not only in the acute phase, but also in the healing phase of myocardial infarction, when the highest troponin levels predicted all-cause death.¹⁴ The correlation appears in ACS as well as in different clinical statuses, where a cardiac troponin level combined with a higher incidence of regional wall motion abnormalities predicts death.¹⁵

As a result of this injury, the authors showed echocardiographic features of worse cardiac muscle performance. Patients who died during hospitalization had a significantly lower ejection fraction of the left ventricle (LVEF), which has been observed in many previous studies. A subsequent cohort study by Vakili et al., which included 304 STEMI patients reperfused with primary PCI, showed that LVEF $\leq 50\%$ was associated with high rates of in-hospital adverse events, including death.¹⁶ Perelshtein Brezinov et al. in their recent study presented LVEF as a very strong predictor of mortality in ACS,¹⁷ which was also the case in our group. The same correlations were shown in previous studies, such as the one by Falcão et al. where the ejection fraction (EF) in patients with STEMI was an independent factor of in-hospital mortality. In a group of 398 patients, the in-hospital mortality was comparable to the one presented in our study, i.e., 5.8%.¹⁸ An interesting analysis of the prognostic value of EF in patients with ACS was presented by Perelshtein Brezinov et al.¹⁷ The patients were categorized according to LVEF at admission, and it was found that the prognosis in those with severe LV dysfunction is mainly related to clinical factors (syncope and STEMI) and clinical instability on admission. In the group with a more preserved EF, the presence of comorbidities predicted a mortality risk.

Anemia is a marker of a poor prognosis in ACS. In a study on a group of 1,111 patients with STEMI who received reperfusion treatment, hemoglobin levels were associated with a better survival rate. The association of hemoglobin with hospital mortality was seen in men and women 65 or older.¹⁹ Our observations were consistent, but not statistically significant. The group with the fatal complication of STEMI was small, but with a larger sample statistical significance of such findings would be possible. The same findings were presented in the recently published STEMI registry (1,498 patients). In this group, anemic and non-anemic patients were compared, as a result of which the in-hospital mortality rate was observed to be significantly higher in the patients with anemia. The population characteristics also revealed a gradual increase in mean age with lower hemoglobin levels.²⁰ The probable explanation for this coexistence is the worse overall health of the elderly population.


Study limitations

The main limitation of the study is the small sample size, especially in the group of patients who died while hospitalized, but this is actually the result of a shift in the management of patients with ACS towards more aggressive, invasive interventions. While in the 1990s, a pre-hospital mortality of 25% was reported, and a risk of in-hospital death was $<10\%$, including a similar risk of cardiogenic shock in these patients, in the 2010s, changes in treatment and organization led to the results presented in this study. Therefore, the question asked in the title – “Can the in-hospital mortality rate in patients with ST-elevation myocardial infarctions be lowered any further?” – is an attempt to assess the profile of patients in the study group. The only potential way to increase the positive impact of our work would be new, non-standard therapies applied in the acute phase of myocardial infarction, using new drugs or a new way to administer them.²¹

Conclusions

It is not possible to significantly reduce the in-hospital mortality of STEMI patients who have been successfully treated with primary PCI, despite all modern treatment modalities. The combination of advanced age and numerous comorbidities – including pre-existing low LV ejection fraction – makes in-hospital death inevitable, despite an early and successful myocardial reperfusion. From the clinical point of view, to lower the mortality in patients with CAD, the atherosclerosis risk factors must be substantially modified in primary and secondary prevention.

ORCID iDs

Jadwiga Radziejewska  <https://orcid.org/0000-0001-9153-9754>
 Martek Frączkowski  <https://orcid.org/0000-0001-8150-3897>
 Agnieszka Sławuta  <https://orcid.org/0000-0001-5671-9864>
 Bernard Panaszek  <https://orcid.org/0000-0002-7950-3393>

References

1. Granger CB, Bates ER, Jollis JG, et al. Improving care of STEMI in the United States: 2008 to 2012. *J Am Heart Assoc.* 2019;8(1):e008096.
2. De Luca G, van 't Hof AW, Ottervanger JP, et al. Ageing, impaired myocardial perfusion, and mortality in patients with ST-segment elevation myocardial treated by primary angioplasty. *Eur Heart J.* 2005;26(7):662–666.
3. Guagliumi G, Stone GW, Cox DA, et al. Outcome in elderly patients undergoing primary coronary intervention for acute myocardial infarction: Results from the Controlled Abciximab and Device Investigation to Lower Late Angioplasty Complications (CADILLAC) trial. *Circulation.* 2004;110(12):1598–1604.
4. Antonsen L, Jensen LO, Terkelsen CJ, et al. Outcomes after primary percutaneous coronary intervention in octogenarians and nonagenarians with ST-segment elevation myocardial infarction: From the Western Denmark heart registry. *Catheter Cardiovasc Interv.* 2013; 81(6):912–919.
5. Nakamura M, Yamashita T, Yajima J, et al. Clinical outcome after acute coronary syndrome in Japanese patients: An observational cohort study. *J Cardiol.* 2010;55(1):69–76.

6. Ibanez B, James S, Agewall S, et al; ESC Scientific Document Group. 2017 ESC Guidelines for the management of acute myocardial infarction in patients presenting with ST-segment elevation: The Task Force for the management of acute myocardial infarction in patients presenting with ST-segment elevation of the European Society of Cardiology (ESC). *Eur Heart J*. 2018;39(2):119–177.
7. Wald DS, Morris JK, Wald NJ, et al; PRAMI Investigators. Randomized trial of preventive angioplasty in myocardial infarction. *N Engl J Med*. 2013;369(12):1115–1123.
8. Noman A, Balasubramaniam K, Das R, et al. Admission heart rate predicts mortality following primary percutaneous coronary intervention for ST-elevation myocardial infarction: An observational study. *Cardiovasc Ther*. 2013;31(6):363–369.
9. Engström AE, Vis MM, Bouma BJ, et al. Mitral regurgitation is an independent predictor of 1-year mortality in ST-elevation myocardial infarction patients presenting in cardiogenic shock on admission. *Acute Card Care*. 2010;12(2):51–57.
10. Antman EM, Tanasijevic MJ, Thomson B, et al. Cardiac-specific troponin levels to predict the risk of mortality in patients with acute coronary syndromes. *N Engl J Med*. 1996;335(18):1342–1349.
11. Matetzky S, Sharir T, Domingo M, et al. Elevated troponin level on admission is associated with adverse outcome of primary angioplasty in acute myocardial infarction. *Circulation*. 2000;102(14):1611–1616.
12. Stubbs P, Collinson P, Moseley D, et al. Prognostic significance of admission troponin T concentrations in patients with myocardial infarction. *Circulation*. 1996;94:1291–1297.
13. Ottani F, Galvani M, Nicolini FA, et al. Elevated cardiac troponin levels predict the risk of adverse outcome in patients with acute coronary syndromes. *Am Heart J*. 2000;140(6):917–927.
14. Shimizu M, Sato H, Sakata Y, et al. Effect on outcome of an increase of serum cardiac troponin T in patients with healing or healed ST-elevation myocardial infarction. *Am J Cardiol*. 2007;100(12):1723–1726.
15. Mehta NJ, Khan JA, Gupta V, Jani K, Gowda RM, Smith PR. Cardiac troponin I predicts myocardial dysfunction and adverse outcome in septic shock. *Int J Cardiol*. 2004;95(1):13–17.
16. Vakili H, Sadeghi R, Rezapoor P, Gachkar L. In-hospital outcomes after primary percutaneous coronary intervention according to left ventricular ejection fraction. *ARYA Atheroscler*. 2014;10(4):211–217.
17. Perelshtein Brezinov O, Klempfner R, Zekry SB, Goldenberg I, Kuperstein R. Prognostic value of ejection fraction in patients admitted with acute coronary syndrome: A real world study. *Medicine (Baltimore)*. 2017;96(9):e6226.
18. Falcão FJ, Alves CM, Barbosa AH, et al. Predictors of in-hospital mortality in patients with ST-segment elevation myocardial infarction undergoing pharmacoinvasive treatment. *Clinics (Sao Paulo)*. 2013;68(12):1516–1520.
19. Velásquez-Rodríguez J, Diez-Delhoyo F, Valero-Masa MJ, et al. Prognostic impact of age and hemoglobin in acute ST-segment elevation myocardial infarction treated with reperfusion therapy. *Am J Cardiol*. 2017;119(12):1909–1916.
20. Jomaa W, Ben Ali I, Hamdi S, et al. Prevalence and prognostic significance of anemia in patients presenting for ST-elevation myocardial infarction in a Tunisian centre. *J Saudi Heart Assoc*. 2017;29(3):153–159.
21. Borak B, Arkowski J, Skrzypiec M, et al. Behavior of silica particles introduced into an isolated rat heart as potential drug carriers. *Biomed Mater*. 2007;2(4):220–223.

Predictive factors in post-stroke epilepsy: Retrospective analysis

Edyta Dziadkowiak^{1,A,D}, Maciej Guziński^{2,C}, Justyna Chojdak-Łukasiewicz^{1,B,D}, Małgorzata Wieczorek^{3,C}, Bogusław Paradowski^{1,F}

¹ Department of Neurology, Wrocław Medical University, Poland

² Department of General Radiology, Interventional Radiology and Neuroradiology, Wrocław Medical University, Poland

³ Department of Geoinformatics and Cartography, University of Wrocław, Poland

A – research concept and design; B – collection and/or assembly of data; C – data analysis and interpretation;

D – writing the article; E – critical revision of the article; F – final approval of the article

Advances in Clinical and Experimental Medicine, ISSN 1899–5276 (print), ISSN 2451–2680 (online)

Adv Clin Exp Med. 2021;30(1):29–34

Address for correspondence

Justyna Chojdak-Łukasiewicz

E-mail: justyna.ch.lukasiewicz@gmail.com

Funding sources

None declared

Conflict of interest

None declared

Received on April 12, 2020

Reviewed on August 8, 2020

Accepted on October 22, 2020

Published online on January 30, 2021

Abstract

Background. Cerebrovascular disease is an important cause of epilepsy. The incidence may significantly vary (from 2.3% to 43%). Post-stroke seizures occur within 2 weeks of stroke onset (as early-onset seizures) or 2 weeks after a stroke (as late-onset seizures).

Objectives. To retrospectively evaluate and differentiate predictive factors for post-stroke seizures.

Material and methods. We retrospectively analyzed the medical histories of 164 adult patients diagnosed with post-stroke seizures but no epilepsy recognized prior to the stroke who were hospitalized at the Neurology Clinic of Wrocław Medical University between 2012 and 2018. The seizures were classified according to the criteria of the International League Against Epilepsy (ILAE) from 2017. The relevant demographic data, type of stroke (ischemic/hemorrhagic), time of occurrence of seizures in relation to the type of stroke, score on the modified Rankin Scale, presence of cardiovascular risk factors, electroencephalography (EEG) recording, and antiepileptic treatment (AED) were collected. In the case of ischemic stroke (IS), the size of the stroke lesion was rated on the ASPECTS scale.

Results. The study involved 164 patients (average age = 68.83 years), including 86 men (average age = 66.2 years). In 20 out of 164 patients, the seizures were associated with hemorrhagic stroke (HS); in 144 out of 164 patients, the post-stroke epilepsy was associated with IS. Generalized tonic-clonic seizures occurred in 101 out of 164 patients, focal aware seizures occurred in 19 out of 164 patients and focal impaired-awareness seizures occurred in 44 out of 164 patients.

Conclusions. Our study has confirmed that generalized seizures occur mostly after an IS and are late complications of it. Early-onset seizures occur mostly after HS associated with severe disability. Seizures are more likely to happen due to the cortical location of the stroke. There is a shift from generalized to focal seizures with an increase in the extent of IS as evaluated using the ASPECTS scale.

Key words: stroke, aspect, post-stroke epilepsy

Cite as

Dziadkowiak E, Guziński M, Chojdak-Łukasiewicz J, Wieczorek M, Paradowski B. Predictive factors in post-stroke epilepsy: Retrospective analysis. *Adv Clin Exp Med.* 2021;30(1):29–34. doi:10.17219/acem/128745

DOI

10.17219/acem/128745

Copyright

© 2021 by Wrocław Medical University

This is an article distributed under the terms of the Creative Commons Attribution 3.0 Unported (CC BY 3.0) (<https://creativecommons.org/licenses/by/3.0/>)

Introduction

Complications after stroke are a growing issue in the ageing population. According to demographic data, in Canada from 2013 to 2018, the number of people suffering stroke-related disabilities will increase by up to 80%.¹

According to the new practical definition of epilepsy by the International League Against Epilepsy (ILAE), the disorder can be diagnosed after a single seizure if other findings suggest a risk of recurrent seizure equivalent to the risk after 2 unprovoked seizures.² Post-stroke epilepsy is defined as recurrent convulsive seizures related to cerebral damage from a stroke, regardless of the time of onset following the stroke.³ Early-onset epileptic seizures often occur within the first 7 days and are defined as acute symptomatic seizures. They occur in 2.5–6% of patients with stroke, more often in the course of hemorrhagic stroke (HS) than ischemic stroke (IS). In 40% of patients, this is a single epileptic seizure, while 60% of patients experience 2 or more seizures. Late-onset epileptic seizure, which affects 10–20% of patients, occurs 7 or more days after stroke symptoms.⁴ The probability of a seizure occurring is estimated at 5–6.1% during the 1st year after stroke, which increases by 1–2% each subsequent year. Post-stroke epilepsy is mostly diagnosed during the first 2 years after a stroke.^{4,5} In patients with acute symptomatic seizures, the risk of developing another unprovoked seizure over the next 10 years is 33%, while in patients whose 1st unprovoked seizure occurred more than 7 days after a stroke, this risk stands at 71.5%.^{4,6,7}

There is high risk of epileptic seizures in HS, subarachnoid hemorrhage and cortical focus in ischemic stroke, especially in patients with high NIHSS score and modified Rankin score of over 3 points.^{7–9} Another risk factor for post-stroke seizures is a patient under 65 years of age.^{10,11} In a literary review on post-stroke epilepsy, patients with late-unprovoked seizure after stroke have a 71.5% risk of another unprovoked seizure.⁶ No previous publications have reported that treatment with antiepileptic drugs (AED) prevents the development of post-stroke epilepsy, and the risk of seizure after stroke is relatively low, so primary prevention does not need to be indicated.¹² According to Zelano, early seizures may be a risk factor for late seizures, at least in intracerebral hemorrhagic stroke (ICH), but the risk is not described as higher than that seen after a single unprovoked seizure, making AED withdrawal reasonable in most cases.¹³

The aim of study was to retrospectively evaluate and differentiate predictive factors for post-stroke seizures.

Material and methods

We retrospectively analyzed the medical histories of 164 adult patients diagnosed with post-stroke seizures but no epilepsy recognized prior to the stroke, who were hospitalized at the Neurology Clinic of Wrocław Medical University (Poland) between January 1, 2012 and December

31, 2018. The following data were assessed: sex, age, type of seizure, type of stroke (IS/HS), time of occurrence of seizures in relation to stroke type, score on the modified Rankin Scale, cardiovascular risk factors (hypertension, diabetes mellitus, atherosclerosis, and dyslipidemia), treatment with recombinant tissue plasminogen activator (rtPA), electroencephalography (EEG) recording, and AED.

The patients were divided into 2 groups. The 1st group consisted of patients with early seizure within 1 week after stroke, with a subgroup of patients whose seizures occurred in the first 24 h. The 2nd group consisted of patients with later-onset post-stroke seizures occurring within 1 year and over 1 year.

Seizures were classified according to the criteria of the International League Against Epilepsy (ILAE) from 2017. The following seizure types were distinguished: focal aware seizure, focal seizure with impaired awareness and generalized tonic–clonic seizure.

The stroke location was assessed based on imaging with the use of 64-slice CT scanners (GE Healthcare, Chicago, USA) with 3D isotropic resolution and a slice thickness of 0.6 mm. In the case of IS, the size of the stroke lesion was rated on the ASPECTS scale. The scale can be divided into 3 ranges: 0–4 for severe stroke; 5–7 for moderate stroke; and 8–10 for mild stroke. Hemorrhagic strokes are classified based on blood volume as mild (<30 mL), moderate (31–60 mL) and severe (>61 mL). The clinical and radiological analyses were performed by a permanent team of neurologists and radiologists with several years of experience.

All statistical analyses were performed with STATISTICA v. 12.0 (StatSoft Inc., Tulsa, USA). All tests were performed at a significance level of $\alpha = 0.05$. The interaction between the type of seizure and other characteristics was analyzed using a contingency table. The significance of the interaction was tested with the χ^2 test and Fisher's exact test (when the number of cases was less than 40).

Results

The study involved 164 patients (average age = 68.83 years), including 86 men (average age = 66.2 years) and 78 women (average age = 78.83 years). The youngest patient was 24 years old; the oldest patient was 93 years old. In 20 out of 164 patients, the seizures were associated with HS, while in the remaining 144 patients, the post-stroke epilepsy was associated with IS. Seizures occurring as the first symptom of IS appeared more often in female patients. Patients with IS were older (average age = 76 ± 10.89 years) than the rest of the group. In 17 patients, a seizure occurred within the first 2 weeks of the stroke. This included 7 patients with seizures appearing as the first symptom and occurring during the first 24 h of the stroke incident. Late-onset seizures occurred in 147 patients (89.6%), including 42 patients with epilepsy in the 1st year following

Table 1. General characteristics of the group

Variable	IS, n = 44	HS, n = 20	All patients, n = 164
Gender (female/male)	69/75	9/11	78/86
Age, mean [years]	76.2 ±10.89	70.5 ±12.4	68.8 ±12.6
Generalized tonic–clonic	94	7	101
Focal aware seizures	14	5	19
Focal impaired-awareness seizures	36	8	44

IS – ischemic stroke; HS – hemorrhagic stroke.

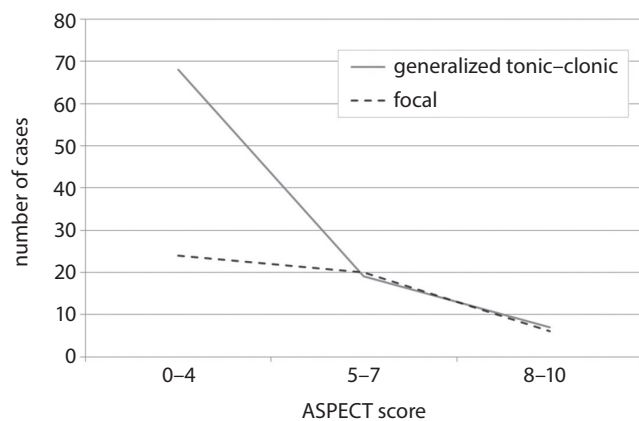


Fig. 1. Correlation between the type of epileptic seizure and the size of IS as assessed using the ASPECTS scale

a stroke. The average time to onset of an epileptic seizure in the study group was 19.5 months. Table 1 presents the characteristics of the study group.

Generalized tonic–clonic seizures occurred in 101 out of 164 patients, focal aware seizures occurred in 19 patients and focal impaired-awareness seizures occurred in 44 patients. The majority of patients with seizures within the first 24 h had the generalized tonic–clonic type (70% of this subgroup). No statistically significant differences were demonstrated between seizure type and the extent of the focus assessed using radiological methods.

Generalized tonic–clonic seizures occurred in 65% (93/144) of the patients with IS. The other types of seizures associated with IS were less common – focal aware seizures occurred in 10% of patients (15/144) and focal impaired-awareness seizures in 25% (36/144). Among the patients with ICH, the distribution of seizure types was different. Focal impaired-awareness seizures were the most common, occurring in 40% (8/20) of patients. Generalized tonic–clonic seizures occurred in 35% (8/20) and focal aware seizures in 25% (4/20) of patients.

There was significant correlation between the type of epileptic seizure and the ASPECTS scores for the 3 ranges. Generalized seizures were most common for severe strokes (0–4 point range) ($p = 0.01430$; Fig. 1). No significant correlation was found between the type of epileptic seizure and HS classified by blood volume.

In 105 patients, IS affected 1 cortical location (in 60%, it was the right hemisphere), and in 50 patients it involved

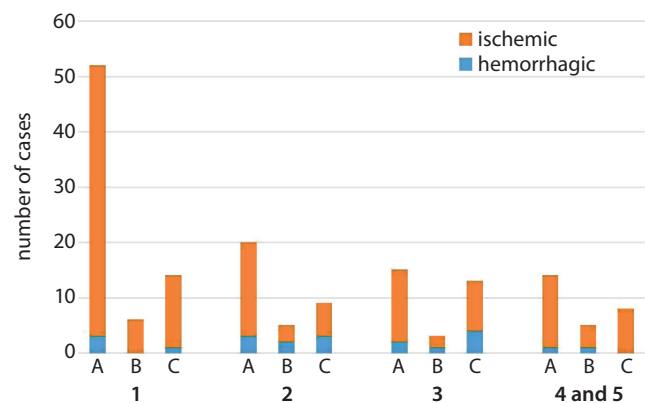


Fig. 2. Radiological range and seizures

Seizures: A – generalized seizure; B – focal aware seizure; C – focal impaired-awareness seizure. Radiological range: 1 – lacunar stroke; 2 – territories of ACA or PCA; 3 – territories of middle cerebral artery (MCA); 4 – territories of MCA and ACA or MCA and PCA; 5 – territories of MCA, ACA and PCA; ACA – anterior cerebral artery; PCA – posterior cerebral artery; IS – ischemic stroke; HS – hemorrhagic stroke.

the fronto-parieto-temporal area; in addition, the focus was in the frontal area in 17 patients, in the parietal area in 6 patients and in the temporal area in 3 patients. The right thalamus was the focus for 1 patient, while 3 patients had epileptic seizures with isolated cerebellar injury. Figure 2 shows radiological range and type of stroke.

Among hemorrhagic lesions, 14 were lobar, 2 were basal gangliar, 2 were thalamic, and 1 was cerebellar. No statistically significant differences were found regarding seizure types or a hemispheric location of the stroke focus (Table 2).

There were also no statistically significant differences in cardiovascular risk factors between the subgroups of patients. Only atrial fibrillation (AF) was statistically more common in early seizures ($p = 0.011$). Patients with diabetes and a history of AF showed a statistically significant higher score on the modified Rankin Scale ($p < 0.05$) (Table 3).

The EEGs showed generalized slowing of the basic activity of both brain hemispheres in 73 of the patients and asymmetrical seizure changes in 89 patients. No correlation was found between EEG results and the extent of radiological changes. The occurrence of seizure changes in EEG and the type of epileptic seizure did not affect the scores on the modified Rankin Scale.

Table 2. Radiological characteristics of the group

Variable	ASPECTS score		
	Mild stroke	Moderate stroke	Severe stroke
Generalized tonic–clonic, n = 94	68	19	7
Focal aware seizures, n = 14	7	5	2
Focal impaired-awareness seizure, n = 36	17	15	4
Variable	Intracerebral hemorrhagic stroke (ICH)		
	Mild ICH <30 mL	Moderate ICH 31–60 mL	Severe ICH >60 mL
Generalized tonic–clonic, n = 7	2	5	0
Focal aware seizures, n = 5	2	1	2
Focal impaired-awareness seizure, n = 8	3	4	1

Table 3. Early seizure compared to late seizures

Variable	Early-onset post-stroke seizures (within 2 weeks), n = 17		Late-onset post-stroke seizures (more than 2 weeks), n = 147		All patients, n = 164
	IS n = 12	HS n = 5	IS n = 132	HS n = 15	
Gender (female/male)	5/7	2/3	64/68	7/8	78/86
Age, mean [years]	69.4 ± 15.7		68.5 ± 12.0		69.8 ± 12.6
	73.2 ± 15.5	62.4 ± 17.6	68.6 ± 12.0	65.3 ± 9.2	F: 73.8 ± 12.0* M: 66.2 ± 12.2
Generalized seizure	5	3	88	5	101
Focal aware seizure	4	0	11	4	19
Focal impaired-awareness seizure	3	2	33	6	44
Hypertension	7	3	101	15	126
Diabetes mellitus	3	2	34	3	42
Atherosclerosis	6	2	78	8	94
Atrial fibrillation	1	1	46	2	50
Smoking	4	2	17	3	26
Deaths	1	2	5	0	8
Modified Rankin Scale	4.1 ± 1.5*		3.0 ± 1.3		2.94 ± 1.48
	3.8 ± 1.4	4.8 ± 1.6	3.1 ± 1.3	2.6 ± 0.9	

* statistical significance.

Carbamazepine was used in 72 patients, valproic acid (VPA) in 38 patients, lamotrigine (LTG) in 23 patients, and levetiracetam (LEV) in 14 patients. In 15 patients, the treatment was based on polypharmacology.

A statistically significantly higher score on the modified Rankin Scale was found in patients with early seizures compared to the group with late seizures ($p < 0.005$). There was no significant correlation between the type of epileptic seizure and the score on the modified Rankin Scale.

Thrombolytic treatment was used in 7.1% of patients (6/84) with IS. These patients had a stroke whose focus was in the areas of vascularization of the right MCA, the left MCA and the left ACA. The focal seizures in these patients manifested as behavioral disturbances. Only 1 patient had a generalized tonic–clonic seizure.

The standardized mortality rate for the study cohort was 5% (8/164).

Discussion

The most frequent cause of epileptic seizures in elderly patients is vascular brain damage. In about 50% of patients over the age of 60 years, epileptic seizure occurs in the course of stroke. According to some authors, post-stroke epilepsy occurs more often in men over the age of 70 years (56%).^{14–17} In 2012, Chen et al. reported post-stroke epilepsy in 38.5% of men with subarachnoid hemorrhage, in 60.7% of men with ICH and in 58% of men with IS.¹⁸ According to the findings of Leung et al., post-stroke epilepsy is more frequent in women (55%).¹⁷ In our analysis, post-stroke epilepsy occurred in over 52% of cases in men. Acute asymptomatic epileptic seizures occur more often in patients with HS than in those with IS. In cases with subarachnoid hemorrhage, seizures are observed in 16.2% of patients. Our study showed that post-stroke

epilepsy was present in 88% of patients who had IS; however, in 12% of patients, epileptic seizures were related to HS. In cases of stroke covering the entire anterior circulation, i.e., the anterior and middle cerebral arteries of the brain (total anterior circulation infarct (TACI)) – most often in the course of internal carotid artery occlusion – the risk of early-onset and late-onset seizures exceeds the risk of epilepsy in the course of HS. Post-stroke epilepsy develops in 15.7% of patients with acute symptomatic seizures.^{14,15}

The pathomechanism of post-stroke epilepsy is not fully understood. According to some hypotheses, the pathomechanism of early-onset seizures is different from the abnormalities that occur during late-onset seizures in the course of cerebrovascular disease.^{19–25} Quoting research by Sung and Chu, Myint et al. observed that “late-onset seizure peaks within 6–12 months after the stroke and has a higher recurrence rate of up to 90% in both ischemic and hemorrhagic stroke”.³ They found significant interaction between the type of seizure and the type of stroke. As many as 93% of patients with generalized seizures had IS. Among the 44 patients with IS, 14 had focal aware seizures and 36 had focal impaired-awareness seizures. Ischemic stroke was associated with generalized seizure (65%) and there was no connection with ICH because a maximum of 40% of patients had focal impaired-awareness seizures.

The factors of early-onset epileptic seizure or post-stroke epilepsy are as follows: embolic etiology, vascular focus within the area of middle cerebral artery circulation, multifocal brain damage, and persistent paresis. In this study, AF occurred statistically more often in cases of early-onset seizures ($p = 0.024$). Kim et al. obtained similar results, i.e., AF was more common in late-onset post-stroke seizure after IS than in early-onset (≤ 1 week) post-stroke seizure after IS ($p < 0.05$).¹⁴ The researchers observed that the association between seizure and cardioembolism is often mentioned in published studies.^{26,27} However, this association remains controversial due to the varying study designs and diagnostic testing. Another important point to be considered is confounding factors and interaction between predictors, such as age with seizure manifestation or survival rate, or AF with cortical involvement, and so on.¹⁴

The occurrence of epileptic seizures also correlates with the size and location of the focus of stroke – an epileptic seizure will more often be a symptom of a stroke in patients with an extensive cortical vascular focus, originating from the anterior circulation area located superficially within the cortical component.^{3,7,19,26} Epileptic seizures were observed more often in patients with stroke in the left hemisphere (2.8%) than in the right hemisphere (1.8%).^{27,28} Subcortical damage and damage in the posterior circulation area increase the risk of more frequent epileptic seizures (recurring seizures). Our study showed that, in most cases, stroke was related to the right frontal and right

temporoparietal regions. In our research, a statistically significant correlation was found between the ASPECTS score and the type of epileptic seizure. Perhaps the correlation between the larger area of ischemic damage and a generalized epileptic seizure is related to the spread of abnormal electrical activity throughout the brain. A similar result was obtained by Kim et al., who stated that seizure recurrence in a group of patients suffering from late post-stroke seizure after IS was more common among patients with large lesions.¹⁴

Also, Reddy et al. indicated 2 predictive factors for developing post-stroke epilepsy – stroke severity and hemorrhagic character – among other related factors. In addition, patients with small-vessel disease were at a significantly higher risk of developing epilepsy.²⁸

According to the new seizure classification, the first step is to separate seizures by how they begin in the brain. Generalized seizures, previously defined as primary generalized seizures, engage or involve networks on both sides of the brain at the onset. By contrast, focal to bilateral seizure describes a seizure that starts in one side or part of the brain and spreads to both sides. Finally, in post-stroke epilepsy, it is sometimes difficult to determine the onset of a seizure. According to the majority of authors, this can be caused by a lack of valid medical history or witnesses of patients suffering from aphasia or disturbances of consciousness.^{10,11,17,29} In the early phase of stroke, there are sporadic status epilepticus events.^{12,30–32} In our group of patients, in 7 cases (41% of patients with early-onset seizure) an epileptic seizure occurred within 24 h of the stroke incident and was accompanied by hemorrhagic focus. Generalized seizures predominantly affected the group of patients who suffered an IS.

Our study has a few limitations. We reviewed the medical records of the patients retrospectively. The small sample in this study may have limited the derivation of adjusted odds ratios (ORs) with multiple predictor variables. However, we tested the distribution of all continuous variables and confirmed that they were normally distributed.

Conclusions

Our study has confirmed that generalized seizures occur mostly after IS and are late complications of it. These seizures are more likely to happen with a cortical locus of the stroke. Early-onset seizures occur mostly after HS and are associated with severe disability. Post-stroke epilepsy occurred more frequently in patients with cardioembolic stroke than in those with strokes of other etiology. There was a significant correlation between the type of epileptic seizure and the ASPECTS score. Generalized tonic–clonic seizures occurred most often after a severe stroke with 0–4 points on the ASPECTS scale.

ORCID iDs

Edyta Dziadkowiak  <https://orcid.org/0000-0002-9618-9308>
 Maciej Guziński  <https://orcid.org/0000-0002-9781-2114>
 Justyna Chojdak-Lukasiewicz  <https://orcid.org/0000-0002-0777-4565>
 Małgorzata Wieczorek  <https://orcid.org/0000-0002-2837-2629>
 Bogusław Paradowski  <https://orcid.org/0000-0003-2940-380X>

References

1. Krueger H, Koot J, Hall RE, O'Callaghan C, Bayley M, Corbett D. Prevalence of individuals experiencing the effects of stroke in Canada: Trends and projections. *Stroke*. 2015;46(8):2226–2231.
2. Fisher R, Cross HJ, D'Souza C, et al. Instruction manual for the ILAE 2017 operational classification of seizure types. *Epilepsia*. 2017;58(4):531–542.
3. Myint PK, Staufenberg EF, Sabanathan K. Post-stroke seizure and post-stroke epilepsy. *Postgrad Med J*. 2006;82(971):568–572.
4. Benninger F, Holtkamp M. Epileptische Anfälle und Epilepsie nach einem Schlaganfall. Inzidenz, Prävention und Behandlung. *Der Nervenarzt*. 2017;88:1197–1207. doi:10.1007/s00115-017-0358-3
5. Roivainen R, Haapaniemi E, Putaala J, Kaste M, Tatlisumak T. Young adult ischaemic stroke related acute symptomatic and late seizures: Risk factors. *Eur J Neurol*. 2013;20(9):1247–1255.
6. Hesdorffer DC, Benn EK, Cascino GD, Hauser WA. Is a first acute symptomatic seizure epilepsy? Mortality and risk for recurrent seizure. *Epilepsia*. 2009;50(5):1102–1108.
7. Alberti A, Paciaroni M, Caso V, Venti M, Palmerini F, Agnelli G. Early seizures in patients with acute stroke: Frequency, predictive factors, and effect on clinical outcome. *Vasc Health Risk Manag*. 2008;4(3):715–720.
8. Biffi A, Rattani A, Anderson CD, et al. Delayed seizures after intracerebral haemorrhage. *Brain*. 2016;139(10):2694–2705.
9. Okuda S, Takano S, Ueno M, Hamaguchi H, Kanda F. Clinical features of late-onset poststroke seizures. *J Stroke Cerebrovasc Dis*. 2012;21(7):583–586.
10. Xu MY. Poststroke seizure: Optimising its management. *Stroke Vasc Neurol*. 2018;4(1):48–56.
11. Tanaka T, Yamagami H, Ihara M, et al. Seizure outcomes and predictors of recurrent post-stroke seizure: A retrospective observational cohort study. *PLoS One*. 2015;10(8):e0136200.
12. Labovitz DL, Hauser WA, Sacco RL. Prevalence and predictors of early seizure and status epilepticus after first stroke. *Neurology*. 2001;57(2):200–206.
13. Zelano J. Poststroke epilepsy: Update and future directions. *Ther Adv Neurol Disord*. 2016;9(5):424–435. doi:10.1177/1756285616654423
14. Kim HJ, Park KD, Choi KG, Lee HW. Clinical predictors of seizure recurrence after the first post-ischemic stroke seizure. *BMC Neurol*. 2016;16(1):212.
15. Neshige S, Kuriyama M, Yoshimoto T, et al. Seizures after intracerebral hemorrhage: Risk factor, recurrence, efficacy of antiepileptic drug. *J Neurol Sci*. 2015;359(1–2):318–322.
16. Conrad J, Pawlowski M, Dogan M, Kovac S, Ritter MA, Evers S. Seizures after cerebrovascular events: Risk factors and clinical features. *Seizure*. 2013;22(4):275–282.
17. Leung T, Leung H, Soo YO, Mok VC, Wong KS. The prognosis of acute symptomatic seizures after ischaemic stroke. *J Neurol Neurosurg Psychiatry*. 2017;88(1):86–94.
18. Chen TC, Chen YY, Cheng PY, Lai CH. The incidence rate of post-stroke epilepsy: A 5-year follow-up study in Taiwan. *Epilepsy Res*. 2012;102(3):188–194.
19. Tanaka T, Ihara M. Post-stroke epilepsy. *Neurochem Int*. 2017;107:219–228.
20. Yang H, Song Z, Yang GP, et al. The ALDH2 rs671 polymorphism affects post-stroke epilepsy susceptibility and plasma 4-HNE levels. *PLoS One*. 2014;9(10):e109634.
21. Pitkänen A, Roivainen R, Lukasiuk K. Development of epilepsy after ischaemic stroke. *Lancet Neurol*. 2016;15(2):185–197.
22. Gibson LM, Hanby MF, Al-Bachari SM, Parkes LM, Allan SM, Emsley HC. Late-onset epilepsy and occult cerebrovascular disease. *J Cereb Blood Flow Metab*. 2014;34(4):564–570.
23. Sarecka-Hujar B, Kopyta I. Poststroke epilepsy: Current perspectives on diagnosis and treatment. *Neuropsychiatr Dis Treat*. 2018;15:95–103.
24. Stefan H, Lopes da Silva FH, Löscher W, et al. Epileptogenesis and rational therapeutic strategies. *Acta Neurol Scand*. 2006;113(3):139–155.
25. Yang H, Rajah G, Guo A, Wang Y, Wang Q. Pathogenesis of epileptic seizures and epilepsy after stroke. *Neurol Res*. 2018;40(6):426–432.
26. Zhang C, Wang X, Wang Y, et al. Risk factors for post-stroke seizures: A systematic review and meta-analysis. *Epilepsy Res*. 2014;108(10):1806–1816.
27. Camilo O, Goldstein LB. Seizures and epilepsy after ischemic stroke. *Stroke*. 2004;35(7):1769–1775. doi:10.1161/01.STR.0000130989.17100.96
28. Reddy DS, Bhimani A, Kuruba R, Park MJ, Sohrabji F. Prospects of modeling poststroke epileptogenesis. *J Neurosci Res*. 2017;95(4):1000–1016. doi:10.1002/jnr.23836
29. Kraus JA, Berlitz P. Cerebral embolism and epileptic seizures: The role of the embolic source. *Acta Neurol Scand*. 1998;97(3):154–159. doi:10.1111/j.1600-0404.1998.tb00629.x
30. Herman ST. Early poststroke seizures. *Neurology*. 2017;77:1–3.
31. Feher G, Gurdan Z, Gombos K, et al. Early seizures after ischaemic stroke: Focus on thrombolysis. *CNS Spectr*. 2020;25(1):101–113.
32. De Reuck J, De Groote L, Van Maele G, Proot P. The cortical involvement of territorial infarcts as a risk factor for stroke-related seizures. *Cerebrovasc Dis*. 2008;25(1–2):100–106.

First-phase insulin secretion is positively correlated with alanine aminotransferase in young adults

Chung-Ze Wu^{1,2,A,C,D,F}, Chang-Hsun Hsieh^{3,B,C,F}, Chieh-Hua Lu^{3,B,C,F}, Dee Pei^{4,5,A,C,E}, Jin-Shuen Chen^{6,7,A–C,E,F}, Yen-Lin Chen^{8,A–C,E,F}

¹ Division of Endocrinology and Metabolism, Department of Internal Medicine, School of Medicine, College of Medicine, Taipei Medical University, Taiwan

² Division of Endocrinology and Metabolism, Department of Internal Medicine, Shuang Ho Hospital, Taipei Medical University, New Taipei City, Taiwan

³ Division of Endocrinology and Metabolism, Department of Internal Medicine, Tri-Service General Hospital, National Defense Medical Center, Taipei, Taiwan

⁴ School of Medicine, College of Medicine, Fu Jen Catholic University, New Taipei City, Taiwan

⁵ Division of Endocrinology and Metabolism, Department of Internal Medicine, Fu Jen Catholic University Hospital, New Taipei City, Taiwan

⁶ Department of Medical Education and Research, Kaohsiung Veterans General Hospital, Taiwan

⁷ Division of Nephrology, Department of Internal Medicine, Tri-Service General Hospital, National Defense Medical Center, Taipei, Taiwan

⁸ Department of Pathology, Cardinal Tien Hospital, Fu Jen Catholic University, School of Medicine, New Taipei City, Taiwan

A – research concept and design; B – collection and/or assembly of data; C – data analysis and interpretation;

D – writing the article; E – critical revision of the article; F – final approval of the article

Advances in Clinical and Experimental Medicine, ISSN 1899–5276 (print), ISSN 2451–2680 (online)

Adv Clin Exp Med. 2021;30(1):35–40

Address for correspondence

Jin-Shuen Chen

E-mail: dgschen@vghks.gov.tw

Funding sources

The study was supported by the Cardinal Tien Hospital (CTH105A-2D06).

Conflict of interest

None declared

Acknowledgements

This manuscript was edited by Wallace Academic Editing. Authors thank all study participants in MJ Health Screening Centers, Taiwan.

Received on April 18, 2020

Reviewed on September 23, 2020

Accepted on October 8, 2020

Cite as

Wu CZ, Hsieh CH, Lu CH, Pei D, Chen JS, Chen YL.

First-phase insulin secretion is positively correlated with alanine aminotransferase in young adults. *Adv Clin Exp Med.* 2021;30(1):35–40. doi:10.17219/acem/128229

DOI

10.17219/acem/128229

Copyright

© 2021 by Wrocław Medical University

This is an article distributed under the terms of the Creative Commons Attribution 3.0 Unported (CC BY 3.0) (<https://creativecommons.org/licenses/by/3.0/>)

Abstract

Background. Type 2 diabetes (T2D) is known to be one of the most prevalent diseases, and its prevalence is significantly associated with age and metabolic syndrome (MetS). Few studies have been conducted on liver function, MetS and insulin secretion among young adults.

Objectives. In the present study, we explored the relationship between the liver function enzyme – alanine aminotransferase (ALT) – and first-phase insulin secretion (FPIS) among young adults.

Material and methods. There were 22,971 men and 28,740 women, aged 18–27 years, assigned to subgroups according to the presence of MetS and quartiles of ALT values. Simple correlation was applied to evaluate their relationship. The difference between the slopes of these relationships and FPIS were statistically analyzed with Chris's calculator.

Results. Most values for metabolic parameters, including ALT and FPIS, were determined to be relatively high in individuals with MetS. By contrast, individuals with MetS had lower high-density-lipoprotein cholesterol (HDL-C) counts and FPIS. Similar results were observed in the quartiles of ALT. Significant positive results were also found in the linear model. Depending on the ALT level, the slope change of FPIS still demonstrated a positive correlation between ALT and FPIS. This correlation was stronger for men than for women.

Conclusions. A positive correlation between ALT and FPIS exists among young adults. Moreover, this correlation was stronger for men than for women. Both the cause and the effect require further investigation.

Key words: metabolic syndrome, alanine aminotransferase, first-phase insulin secretion

Introduction

With the increasing prevalence of obesity, metabolic syndrome (MetS) is also coming to prominence as a serious health problem among adolescents and children worldwide.¹ Following obesity, the prevalence of type 2 diabetes (T2D) has been increasing drastically in Taiwan as well as in many other countries. Moreover, among the factors contributing to the leading causes of mortality in Taiwan, T2D has remained among the top 5 for many years.^{2,3} Accordingly, patients, physicians, and health agencies worldwide have identified childhood obesity as a critical health concern. Children with obesity exhibit a higher risk for developing other diseases – some examples of which are coronary artery disease, fatty liver, polycystic ovary syndrome, and hypertension – not only during childhood, but throughout their lives.⁴ It is well-known that fatty liver is closely and bi-directionally related to MetS and T2D. Currently, the general consensus is that fatty liver is the hepatic manifestation of MetS.⁵

Abnormal liver function is often seen in clinical practice. Among the leading causes of abnormal alanine aminotransferase (ALT), nonalcoholic fatty liver disease is the most common, exhibiting a prevalence of 50–90%.⁶ Viral hepatitis is another disease that is endemic in Taiwan. Hepatitis B viral infection has been reported in the literature to have an estimated prevalence of 15–20%.^{7,8} Patients with hepatitis B also have abnormal liver function. Thus, it is necessary to clarify the relationships between abnormal liver function and T2D.

Three major pathophysiological mechanisms are generally considered to be potential causes of glucose intolerance: reduction of insulin activity (or insulin resistance – IR), insulin secretion and glucose effectiveness.⁹ In addition, there are 2 phases of insulin secretion, namely, first-phase insulin secretion (FPIS) and second-phase insulin secretion.^{10,11} Notably, an impairment of insulin secretion is related to a deterioration of liver function.¹² Consequently, clarifying the underlying causes behind T2D and FPIS is crucial for health providers and future treatment strategy. So far, few studies have evaluated the relationship between ALT and FPIS in young adults. The present study was conducted with the underlying aim of exploring the correlation between FPIS and ALT among young adults.

Methods

Study participants

This study employed random sampling to enroll 22,971 men and 28,740 women aged 18–27 years from private clinics and local hospitals in Taiwan. The MJ Health Screening Centers, which are a chain of private clinics in Taiwan, offer their members regularly

scheduled health examinations. They provided data solely for the purpose of research, and approval was obtained for the protocol of this study from the MJ Health Screening Center Institutional Review Board. All participants in this study remained anonymous and provided informed consent. The definition of obesity in this study was a body mass index (BMI) ≥ 25 kg/m². Participants with obesity were excluded if they took any medications that have been demonstrated to affect blood pressure or glucose and lipid levels. The patients were categorized into 2 groups – without MetS (MetS(–) group) and with MetS (MetS(+) group). The presence of MetS was defined according to World Health Organization (WHO) criteria.¹³ Finally, 768 men and 794 women were included in the MetS(+) group. Furthermore, all participants were divided into quartiles based on their ALT levels for advanced analysis.

On the day of the study, a senior member of the nursing staff recorded the medical history of all participants, including relevant information regarding any medications currently being taken, and conducted a physical examination. Horizontal measurements were performed at the location of the natural waist to record waist circumference (WC). To calculate BMI, the body weight (in kilograms) of participants was divided by the square of their height (in meters). Standard mercury sphygmomanometers were employed to perform measurements of diastolic blood pressure (DBP) and systolic blood pressure (SBP) measured on the right arm of the participants while they were seated.

Laboratory biochemistry measurement

Blood samples were collected for biochemical analysis after 10 h of fasting. Within 1 h of blood collection, the plasma was extracted, after which it was kept at 30°C until the lipid profile and fasting plasma glucose (FPG) assays were performed. A glucose oxidase approach (YSI 203 glucose analyzer; Yellow Springs Instruments, Yellow Springs, USA) was employed for measuring FPG. Measurements of triglyceride (TG) levels and total cholesterol were conducted using a Fuji Dri-Chem 3000 analyzer (Fuji Photo Film, Tokyo, Japan) and a dry, multilayer analytical slide method. Analyses of serum low-density lipoprotein cholesterol (LDL-C) and high-density lipoprotein cholesterol (HDL-C) concentrations were performed after dextran sulfate precipitation through an enzymatic cholesterol assay.

Assessment of FPIS

We used the equation derived from our other groups,¹⁴ which are listed below (international units). To demonstrate the reliability of our equations, a short statement is given here. When performing this study, data of 70% of the participants was used to build the equations and

data the remaining 30% was used for external validation. The accuracy of the equations could therefore be tested.

In total, there were 186 subjects enrolled. The FPIS was measured using a frequently sampled intravenous glucose tolerance test. The R-value between the measured and calculated FPIS was 0.671 ($p < 0.001$).¹⁴ The equation is shown below:

$$FPIS = 10^{(1.477 - 0.119 \times FPG + 0.079 \times BMI - 0.523 \times HDL-C)}$$

Statistical analyses

The IBM SPSS v. 19.0 software (IBM Inc., Armonk, USA) was used in the study to conduct all of the statistical analyses. The resulting data is provided as means ± standard deviation (SD). Levene’s test and the Kolmogorov–Smirnov test were applied to all data to assess the homogeneity of variance and normal distribution, respectively. If an abnormal distribution of data was found, then the data was subjected to log transformation before analysis. To identify differences between groups with and without MetS, a t-test was conducted. The study also used one-way analysis of variance (ANOVA) to assess the difference between the mean values of the 4 groups. Bonferroni post hoc analysis was performed for intergroup comparisons. A simple correlation was adopted in order to assess the correlation between 2 independent variables. Concurrently, the slopes of these relationships could also be obtained. We adopted 0% and 100% as the lowest and highest FPIS values, respectively, with values between these 2 extremes being calculated as the corresponding percentage. To compare the slopes between these 2 lines in order to determine whether they differed significantly, we utilized Chris’s calculator.¹⁵

Results

Table 1 presents the demographics of our study cohort. Regardless of gender, the participants in the MetS(+) group exhibited unfavorable results for MetS-related factors, including BMI, WC, SBP, DBP, TG, FPG, HDL-C, and LDL-C. In addition, the participants in the MetS(+) group were determined to have higher levels of both FPIS and ALT, which constituted the most critical factors. As already mentioned, all participants were subdivided on the basis of the quartiles of ALT results into 4 groups. Notably, for both sexes, participants with higher ALT levels had lower HDL-C levels but higher SBP, WC, FPG, DBP, BMI, TG, and LDL-C levels (Table 2). A scatter plot of the correlation of ALT and log transformation of FPIS is presented in Fig. 1. The correlation coefficient (r) values were 0.349 for men and 0.133 for women. The correlations for both genders were statistically significant ($p < 0.001$). Figure 2 presents the different slopes of log transformation of FPIS in men and women. As described in the Methods section, FPIS was transformed into a percentage of the maximum value (100%). Through a comparison of the genders regarding changes to the FPIS slope according to ALT level, we discovered that men had a higher slope than women.

Discussion

In the current study, our data demonstrated that there is a positive relationship between ALT and FPIS in Chinese young adults. This is the first study, to our knowledge, to present these results for a group of relative healthy, non-obese subjects without any possible confounding effects

Table 1. General characteristics of subjects without and with metabolic syndrome (MetS) according to gender

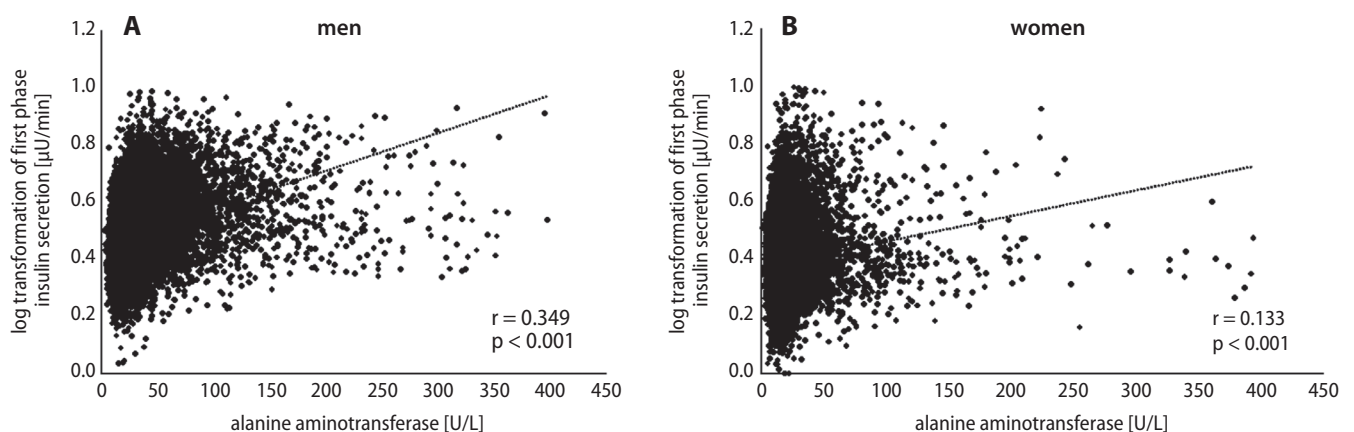
Parameter	Group					
	Men			Women		
	MetS(-)	MetS(+)	p-value	MetS(-)	MetS(+)	p-value
N	21,236	1,735		28,225	515	
Age [years]	24.21 ±2.55	24.58 ±2.54	<0.001	24.23 ±2.42	24.17 ±2.61	0.596
BMI [kg/m ²]	22.4 ±3.3	28.7 ±4.4	<0.001	20.1 ±2.8	28.9 ±5.3	<0.001
WC [cm]	76.3 ±8.1	92.0 ±10.4	<0.001	65.8 ±6.2	84.5 ±10.9	<0.001
SBP [mm Hg]	118.3 ±12.4	133.3 ±12.8	<0.001	106.6 ±11.1	125.6 ±14.1	<0.001
DBP [mm Hg]	68.2 ±8.8	77.1 ±10.3	<0.001	62.8 ±8.1	73.4 ±10.7	<0.001
FPG [mg/dL]	93.51 ±7.38	101.57 ±17.98	<0.001	89.82 ±7.25	101.90 ±23.31	<0.001
TG [mg/dL]	86.30 ±42.12	172.61 ±72.12	<0.001	67.92 ±29.26	146.50 ±66.58	<0.001
HDL-C [mg/dL]	51.81 ±11.54	39.58 ±8.20	<0.001	62.75 ±14.10	43.32 ±7.74	<0.001
LDL-C [mg/dL]	105.02 ±28.37	117.97 ±32.58	<0.001	97.80 ±26.50	112.08 ±30.39	<0.001
ALT [U/L]	27.8 ±25.8	57.6 ±46.0	<0.001	16.0 ±14.7	34.3 ±32.6	<0.001
Log_FPIS [μU/min]	1.928 ±0.327	2.534 ±0.374	<0.001	1.624 ±0.322	2.496 ±0.452	<0.001

Data presented as means ± standard deviation (SD); BMI – body mass index; WC – waist circumference; SBP – systolic blood pressure; DBP – diastolic blood pressure; FPG – fasting plasma glucose; TG – triglyceride; HDL-C – high-density-lipoprotein cholesterol; LDL-C – low-density-lipoprotein cholesterol; ALT – alanine aminotransferase; Log FPIS – log transformation of first-phase insulin secretion.

Table 2. Categorization of alanine aminotransferase levels from low to high

Parameter	ALT1		ALT2		ALT3		ALT4		p-value
Men									
n	5,414		6,230		5,759		5,531		
ALT [U/L]	11.6 ±2.0	^{2,3,4}	17.8 ±2.0	^{1,3,4}	27.0 ±3.7	^{1,2,4}	65.0 ±41.4	^{1,2,3}	<0.001
Age [years]	24.63 ±2.38	^{2,3,4}	24.55 ±2.45	^{1,3,4}	24.15 ±2.57	^{1,2}	25.63 ±2.69	^{1,2}	<0.001
BMI [kg/m ²]	20.8 ±2.4	^{2,3,4}	21.9 ±2.8	^{1,3,4}	23.2 ±3.3	^{1,2,4}	25.6 ±4.4	^{1,2,3}	<0.001
WC [cm]	72.22 ±6.36	^{2,3,4}	75.20 ±7.25	^{1,3,4}	78.42 ±9.30	^{1,2,4}	84.08 ±10.59	^{1,2,3}	<0.001
SBP [mm Hg]	117 ±12	^{2,3,4}	118 ±13	^{1,3,4}	120 ±13	^{1,2,4}	120 ±13	^{1,2,3}	<0.001
DBP [mm Hg]	67 ±9	^{2,3,4}	68 ±9	^{1,3,4}	69 ±9	^{1,2,4}	71 ±10	^{1,2,3}	<0.001
FPG [mg/dL]	93 ±7	^{2,3,4}	94 ±10	^{1,4}	94 ±8	^{1,4}	95 ±9	^{1,2,3}	<0.001
TG [mg/dL]	74 ±31	^{2,3,4}	81 ±39	^{1,3,4}	96 ±48	^{1,2,4}	121 ±65	none	<0.001
HDL-C [mg/dL]	52.3 ±11.3	^{3,4}	52.2 ±11.5	^{3,4}	50.8 ±12.1	^{1,2,4}	48.1 ±11.6	^{1,2,3}	<0.001
LDL-C [mg/dL]	96.4 ±25.7	^{2,3,4}	101.9 ±27.0	^{1,3,4}	108.9 ±28.1	^{1,2,4}	117.1 ±30.6	^{1,2,3}	<0.001
Log_FPIS [μU/min]	1.796 ±0.265	^{2,3,4}	1.885 ±0.300	^{1,3,4}	2.006 ±0.345	^{1,2,4}	2.215 ±0.409	^{1,2,3}	<0.001
Women									
n	7,762		8,070		6,046		6,853		
ALT [U/L]	8.7 ±1.4	^{2,3,4}	11.9 ±0.8	^{1,3,4}	15.2 ±1.1	^{1,2,4}	31.2 ±26.0	^{1,2,3}	<0.001
Age [years]	24.34 ±2.37	^{2,3,4}	24.34 ±2.38	¹	24.22 ±2.43	¹	23.99 ±2.52	¹	<0.001
BMI [kg/m ²]	19.7 ±2.3	^{2,3,4}	19.9 ±2.5	^{1,3,4}	20.3 ±2.9	^{1,2,4}	21.4 ±4.1	^{1,2,3}	<0.001
WC [cm]	65.0 ±5.3	^{2,3,4}	65.5 ±5.7	^{1,3,4}	66.2 ±6.4	^{1,2,4}	68.4 ±8.8	^{1,2,3}	<0.001
SBP [mm Hg]	106 ±11	^{3,4}	107 ±11	⁴	107 ±11	^{1,4}	108 ±12	^{1,2,3}	<0.001
DBP [mm Hg]	63 ±8	⁴	63 ±8	⁴	63 ±8	none	64 ±9	^{1,2}	<0.001
FPG [mg/dL]	90 ±7	⁴	90 ±7	⁴	90 ±7	⁴	91 ±11	^{1,2,3}	<0.001
TG [mg/dL]	65 ±26	^{3,4}	66 ±28	^{3,4}	69 ±32	^{1,2,4}	78 ±40	^{1,2,3}	<0.001
HDL-C [mg/dL]	61 ±13	^{2,3}	63 ±14	^{1,4}	64 ±15	^{1,4}	62 ±15	^{2,3}	<0.001
LDL-C [mg/dL]	95 ±25	^{2,3,4}	97 ±27	^{1,4}	98 ±26	^{1,4}	102 ±28	^{1,2,3}	<0.001
Log_FPIS [μU/min]	1.607 ±0.276	⁴	1.604 ±0.302	⁴	1.625 ±0.343	⁴	1.732 ±0.435	^{1,2,3}	<0.001

Data is presented as means ± standard deviation (SD); ¹ p < 0.05 vs ALT1; ² p < 0.05 vs ALT2; ³ p < 0.05 vs ALT3; ⁴ p < 0.05 vs ALT4; BMI – body mass index; WC – waist circumference; SBP – systolic blood pressure; DBP – diastolic blood pressure; FPG – fasting plasma glucose; TG – triglyceride; HDL-C – high-density-lipoprotein cholesterol; LDL-C – low-density-lipoprotein cholesterol; ALT – alanine aminotransferase; Log FPIS – log transformation of first-phase insulin secretion.

**Fig. 1.** Scatter plot of log-transformed first-phase insulin secretion and alanine aminotransferase levels in (A) men and (B) women

from drugs used for treating hypertension, dyslipidemia or T2D.

Few studies have evaluated the correlation between ALT and FPIS. Therefore, the relative issue is still debated.

By using the homeostasis model assessment, Hsiao et al. reported that both insulin secretion and sensitivity exhibited simultaneously significant impairment with increased ALT levels in 284 Chinese adults.¹² Their findings contrast

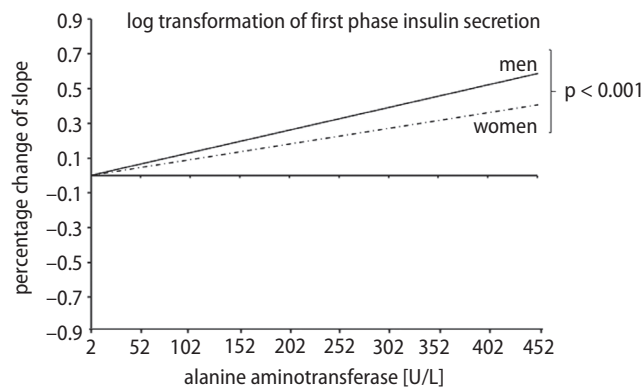


Fig. 2. Comparison of the genders regarding slope changes of first-phase insulin according to ALT levels

with ours. However, their study population was smaller than ours and they evaluated only participants who had FPG levels ranging from 100 mg/dL to 109 mg/dL. In order to explain the discrepancy between these 2 different results, we hypothesize that obesity may be the link between ALT and FPIS. We can observe that individuals with obesity have higher ALT levels as well as elevated insulin secretion. Therefore, it could be postulated that people with higher ALT levels exhibit increased insulin secretion.

It is well-known that insulin secretion consists of 2 phases: FPIS and SPIS.^{10,11} After intravenous glucose infusion, glucose concentration increases rapidly. A biphasic response of insulin secretion is then observed, which comprises a sharp increase that reaches a peak. This stage is followed by a nadir between peaks and subsequently a slower increasing phase. Although the existence of FPIS is still under debate, a great deal of evidence supports it. For instance, Steiner et al. demonstrated that FPIS and SPIS play different roles in insulin secretion.¹⁶ Using a sophisticated method that employed a pancreatic clamp, they discovered that FPIS is crucial for suppressing the acute response of glucose stimulation. Even though this paper was published 30 years ago, it still constitutes a milestone in this topic. Furthermore, Kepner et al. suggested that the cascade involved in SPIS is different from that in FPIS.¹⁷ In SPIS, Cool-1/ β PPIX operates as an exchange factor for guanine nucleotide to regulate insulin secretion, which is not the case in FPIS.

In our study, we discovered that participants with obesity had higher levels of insulin secretion. Kreisberg et al. might be the first group to report this observation.¹⁸ In 1968, Karam et al. further expounded on this relationship.¹⁹ They discovered that after glucose challenge, a more considerable acute insulin increase was noted in obese patients compared with healthy individuals.²⁰ Because studies have indicated no impairment of insulin clearance, they concluded that this increase in insulin response must be due to higher levels of insulin secretion. Many studies conducted since then have also shown that individuals with obesity have superior cell function due to a greater cell mass compared with individuals without obesity.^{21–23}

Recently, our group also validated this result by enrolling individuals with the same age and BMI. Our data suggested that BMI is positively related to FPIS in both men and women (R-value: 0.966 and 0.926, respectively). It should be noted that this is the only reference, to our knowledge, that is directly related to the role of FPIS alone.²⁴

The ALT levels are higher in obese individuals. This finding is the final component needed to clarify the link between BMI and FPIS. Abnormal liver function has an estimated prevalence of 10–21%.²⁵ Among the causes of abnormal ALT, the most common is nonalcoholic fatty liver disease, which accounts for 50–90% of cases.⁶ Fatty liver disease can cause either simple steatosis without inflammation or nonalcoholic steatohepatitis.²⁶ The second most common cause, particularly in Taiwan, is viral hepatitis; this is because Taiwan is one of the most endemic areas for hepatitis.⁸ Research has determined that there is a strong association between obesity and nonalcoholic fatty liver disease, with approx. 80% of obese individuals reported as having nonalcoholic fatty liver disease.^{27,28} Moreover, viral hepatitis C was reported to have a correlation with obesity.²⁹ Such research validates the finding that ALT levels are higher among individuals with obesity.

This study has some limitations worth noting. Firstly, because this is a cross-sectional study, recall and selection bias are inherent limitations. Further research may be required in order to overcome these limitations. Secondly, it may be disputed that our equation is not an accurate method for quantifying FPIS. However, this method has been validated and published with an R-value of 0.6–0.7. Therefore, we still believe that the present study elucidates the relationships between ALT and FPIS by enrolling a large study sample.

Conclusions

In conclusion, our study revealed that there is a positive relationship between FPIS and ALT in Chinese young adults.

ORCID iDs

Chung-Ze Wu <https://orcid.org/0000-0001-6118-6070>
 Chang-Hsun Hsieh <https://orcid.org/0000-0001-8722-3044>
 Chieh-Hua Lu <https://orcid.org/0000-0002-2179-9486>
 Dee Pei <https://orcid.org/0000-0003-3080-4248>
 Jin-Shuen Chen <https://orcid.org/0000-0002-8697-7968>
 Yen-Lin Chen <https://orcid.org/0000-0002-6381-4269>

References

- Poyrazoglu S, Bas F, Darendeliler F. Metabolic syndrome in young people. *Curr Opin Endocrinol Diabetes Obes.* 2014;21(1):56–63.
- Ministry of Health and Welfare. ROC: Annual Statistics Report, 1994–2017. <https://www.mohw.gov.tw/mp-2.html>. Accessed April 4, 2018.
- Tseng CH, Chong CK, Heng LT, Tseng CP, Tai TY. The incidence of type 2 diabetes mellitus in Taiwan. *Diabetes Res Clin Pract.* 2000;50(Suppl 2): S61–S64.

4. Barton M. Childhood obesity: A life-long health risk. *Acta Pharmacol Sin.* 2012;33(2):189–193.
5. Yki-Järvinen H. Non-alcoholic fatty liver disease as a cause and a consequence of metabolic syndrome. *Lancet Diabetes Endocrinol.* 2014; 2(11):901–910.
6. Sanyal AJ, American Gastroenterological Association. AGA technical review on nonalcoholic fatty liver disease. *Gastroenterology.* 2002; 123(5):1705–1725.
7. Chen CJ, Wang LY, Yu MW. Epidemiology of hepatitis B virus infection in the Asia-Pacific region. *J Gastroenterol Hepatol.* 2000;15(Suppl):E3–E6.
8. Chen DS, Kuo GC, Sung JL, et al. Hepatitis C virus infection in an area hyperendemic for hepatitis B and chronic liver disease: The Taiwan experience. *J Infect Dis.* 1990;162(4):817–822.
9. Bergman M. Pathophysiology of prediabetes and treatment implications for the prevention of type 2 diabetes mellitus. *Endocrine.* 2013;43(3):504–513.
10. Caumo A, Luzi L. First-phase insulin secretion: Does it exist in real life? Considerations on shape and function. *Am J Physiol Endocrinol Metab.* 2004;287(3):E371–E385.
11. Polonsky KS, Sturis J, Bell GI. Seminars in Medicine of the Beth Israel Hospital, Boston. Non-insulin-dependent diabetes mellitus: A genetically programmed failure of the beta cell to compensate for insulin resistance. *N Engl J Med.* 1996;334(12):777–783.
12. Hsiao JY, Wang CL, Hsia PJ, et al. Decreased insulin secretion and insulin sensitivity are associated with liver function in subjects with fasting glucose between 100 and 109 mg/dL in Taiwanese population. *Pancreas.* 2007;35(4):343–347.
13. Alberti KG, Zimmet PZ. Definition, diagnosis and classification of diabetes mellitus and its complications. Part 1: Diagnosis and classification of diabetes mellitus provisional report of a WHO consultation. *Diabet Med.* 1998;15(7):539–553.
14. Lin JD, Hsu CH, Liang YJ, et al. The estimation of first-phase insulin secretion by using components of the metabolic syndrome in a Chinese population. *Int J Endocrinol.* 2015;2015:675245.
15. <https://www.surrey.ac.uk/search?query=calculator&op=Search>.
16. Steiner KE, Mouton SM, Bowles CR, Williams PE, Cherrington AD. The relative importance of first- and second-phase insulin secretion in countering the action of glucagon on glucose turnover in the conscious dog. *Diabetes.* 1982;31(11):964–972.
17. Kepner EM, Yoder SM, Oh E, et al. Cool-1/ β PIX functions as a guanine nucleotide exchange factor in the cycling of Cdc42 to regulate insulin secretion. *Am J Physiol Endocrinol Metab.* 2011;301(6):E1072–E1080.
18. Kreisberg RA, Boshell BR, DiPlacido J, Roddam RF. Insulin secretion in obesity. *N Engl J Med.* 1967;276(6):314–319.
19. Karam JH, Grodsky GM, Forsham PH. Insulin secretion in obesity: Pseudodiabetes? *Am J Clin Nutr.* 1968;21(12):1445–1454.
20. Karam JH, Grodsky GM, Forsham PH. Excessive insulin response to glucose in obese subjects as measured by immunochemical assay. *Diabetes.* 1963;12:197–204.
21. Hanley AJ, Wagenknecht LE, D'Agostino RB Jr, Zinman B, Haffner SM. Identification of subjects with insulin resistance and beta-cell dysfunction using alternative definitions of the metabolic syndrome. *Diabetes.* 2003;52(11):2740–2747.
22. Klöppel G, Löhr M, Habich K, Oberholzer M, Heitz PU. Islet pathology and the pathogenesis of type 1 and type 2 diabetes mellitus revisited. *Surv Synth Pathol Res.* 1985;4(2):110–125.
23. van Haeften TW, Dubbeldam S, Zonderland ML, Erkelens DW. Insulin secretion in normal glucose-tolerant relatives of type 2 diabetic subjects: Assessments using hyperglycemic glucose clamps and oral glucose tolerance tests. *Diabetes Care.* 1998;21(2):278–282.
24. Lin JD, Hsu CH, Wu CZ, et al. Effect of body mass index on diabetogenesis factors at a fixed fasting plasma glucose level. *PLoS One.* 2018;13(1):e0189115.
25. Radcke S, Dillon JF, Murray AL. A systematic review of the prevalence of mildly abnormal liver function tests and associated health outcomes. *Eur J Gastroenterol Hepatol.* 2015;27(1):1–7.
26. Agrawal S, Dhiman RK, Limdi JK. Evaluation of abnormal liver function tests. *Postgrad Med J.* 2016;92(1086):223–234.
27. Marchesini G, Moscatiello S, Di Domizio S, Forlani G. Obesity-associated liver disease. *J Clin Endocrinol Metab.* 2008;93(11 Suppl 1):S74–S80.
28. Mota M, Banini BA, Cazanave SC, Sanyal AJ. Molecular mechanisms of lipotoxicity and glucotoxicity in nonalcoholic fatty liver disease. *Metabolism.* 2016;65(8):1049–1061.
29. Hu KQ, Kyulo NL, Esrailian E, et al. Overweight and obesity, hepatic steatosis, and progression of chronic hepatitis C: A retrospective study on a large cohort of patients in the United States. *J Hepatol.* 2004;40(1):147–154.

CD147 promotes invasion and MMP-9 expression through MEK signaling and predicts poor prognosis in hypopharyngeal squamous cell carcinoma

Shinsuke Suzuki^{1,A–F}, Satoshi Toyoma^{1,B,C,F}, Yohei Kawasaki^{1,B,C,F}, Hiroshi Nanjo^{2,C}, Takechiyo Yamada^{1,E,F}

¹ Department of Otorhinolaryngology & Head and Neck Surgery, Akita University Graduate School of Medicine, Japan

² Department of Clinical Pathology, Akita University Graduate School of Medicine, Japan

A – research concept and design; B – collection and/or assembly of data; C – data analysis and interpretation; D – writing the article; E – critical revision of the article; F – final approval of the article

Advances in Clinical and Experimental Medicine, ISSN 1899–5276 (print), ISSN 2451–2680 (online)

Adv Clin Exp Med. 2021;30(1):41–48

Address for correspondence

Shinsuke Suzuki

E-mail: suzukis@med.akita-u.ac.jp

Funding sources

This study was supported by Grant-in-Aid for Scientific Research (No. 18K09337) from the Ministry of Education, Culture, Sports, Science and Technology of Japan.

Conflict of interest

None declared

Received on March 18, 2020

Reviewed on August 24, 2020

Accepted on October 8, 2020

Published online on January 30, 2021

Abstract

Background. Hypopharyngeal cancer is one of the most frequent head and neck cancers and is associated with a poor prognosis because of recurrence and metastases. Therefore, there is a need to improve the prognosis, which requires the identification of prognostic factors and elucidation of the mechanisms involved in tumor progression. Accumulated evidence has demonstrated that cluster of differentiation 147 (CD147) is strongly expressed in malignant tumors, including head and neck squamous cell carcinoma (HNSCC), and contributes to tumor progression.

Objectives. To investigate CD147-induced signaling pathways in HNSCC cells to evaluate the mechanisms of tumor progression mediated by CD147, and the association between CD147 expression in tumors and the survival rate of hypopharyngeal cancer patients.

Material and methods. To determine the downstream signaling of CD147 in HNSCC, expression levels of phosphorylated AKT1, MEK1, p38 MAPK, STAT3, and NF- κ B were evaluated using enzyme-linked immunosorbent assay (ELISA) in FaDu, a hypopharyngeal cell line, exposed to cyclophilin A, a CD147 ligand.

Results. We found that hypopharyngeal cancer patients expressing CD147 showed a poor five-year overall survival (OS) of 11.1% compared with those without CD147 expression (43.0%) ($p = 0.02$). We confirmed that the expression of phosphorylated MEK and matrix metalloproteinase-9 (MMP-9), as well as cell invasion ability, were enhanced in hypopharyngeal cancer cells. In addition, this increased cell infiltration and enhancement of MMP-9 expression induced by CD147 were abolished by a MEK inhibitor.

Conclusions. These results suggest that CD147 can be a predictor of a poor prognosis, and that a CD147-induced MEK-mediated intracellular signaling pathway plays a crucial role in tumor progression in hypopharyngeal carcinoma.

Key words: invasion, MMP, hypopharyngeal cancer, CD147, MEK

Cite as

Suzuki S, Toyoma S, Kawasaki Y, Nanjo H, Yamada T. CD147 promotes invasion and MMP-9 expression through MEK signaling and predicts poor prognosis in hypopharyngeal squamous cell carcinoma. *Adv Clin Exp Med.* 2021;30(1):41–48. doi:10.17219/acem/128228

DOI

10.17219/acem/128228

Copyright

© 2021 by Wrocław Medical University

This is an article distributed under the terms of the Creative Commons Attribution 3.0 Unported (CC BY 3.0) (<https://creativecommons.org/licenses/by/3.0/>)

Introduction

Hypopharyngeal cancer is among the most frequent head and neck cancers. Multidisciplinary treatment is administered according to the stage of the disease, but the prognosis is poor due to recurrence and metastasis.¹ Developing more efficient treatments is essential to improve the prognosis. For this purpose, it is necessary to elucidate the mechanisms of tumor progression.

In recent years, key factors involved in cancer progression have been identified.² The elucidation of the mechanisms involved in tumor progression in head and neck cancer, including hypopharyngeal cancer,³ is a topic of high interest. Furthermore, new therapeutic targets, such as downstream components of receptor signaling cascades, intracellular tyrosine kinases, PI3K, and STAT3, have been identified.⁴

Cluster of differentiation 147 (CD147), also known as extracellular matrix metalloproteinase inducer (EMMPRIN), is a member of the immunoglobulin superfamily that is highly expressed in cancer cells.⁵ CD147 induces the production of matrix metalloproteinases (MMPs), which have many physiological effects, including cell proliferation and extracellular matrix (ECM) degradation. Therefore, CD147 plays an important role in tumorigenesis. CD147 contributes to a variety of malignant phenotypes, including head and neck squamous cell carcinoma (HNSCC).⁶ In addition, it has been reported that CD147 is a predictor of a poor prognosis in HNSCC patients.⁷ We also previously reported that CD147 expression is associated with cervical lymph node metastasis in patients with tongue squamous cell carcinoma (SCC).⁸

Studies have attempted to elucidate the mechanisms underlying CD147-induced tumorigenesis in various types of cancer, and the number of studies on the contribution of CD147 to the progression of HNSCC is increasing.⁹ However, its detailed mechanism has not been fully elucidated yet.

Intracellular signal transduction is an important cell regulatory mechanism.¹⁰ The importance of signal transduction during cancer progression is also widely recognized, and research on this topic is continuously becoming more intensive.^{11,12} In recent years, intracellular signals have been elucidated in many carcinomas, including head and neck cancers, suggesting their potential as therapeutic targets.¹³ In particular, CD147-induced signaling pathways have been investigated in various carcinomas, and the importance of pathways involving Smad, mTOR and STAT3 has been reported.^{14–16}

The involvement of MAPK/ERK signaling in HNSCC has also been reported.¹⁷ However, the role of CD147 in HNSCC tumorigenesis and the underlying mechanisms, including cell signaling pathways, in hypopharyngeal cancer are not fully understood. The purpose of this study was to investigate the mechanisms of tumor progression mediated by CD147 and clinical features of CD147 in hypopharyngeal cancer.

Material and methods

Patients

In this study, we examined 19 patients with pathologically confirmed SCC in their hypopharynx who underwent surgery at the Department of Otorhinolaryngology & Head and Neck Surgery at the Akita University Graduate School of Medicine (Japan) between 2005 and 2014. Patient consent was not deemed necessary because the patient information was obtained from a pathology archive in which patient identification was anonymized and de-identified prior to analysis. All the patients were followed up for at least 60 months or until they died after surgery. The tumors were classified according to the 2002 Union for International Cancer Control staging system (Table 1).¹⁸

Table 1. Patients' characteristics and pathological findings

Variable	Number of patients
Sex	
male	17
female	2
Age [years]	
median	62
range	49–80
Stage	
III	1
IV	18
CD147 index	
0	8
2	2
4	9
Follow-up [months]	
median	68
range	6–91
Prognosis	
survived	6
died from hypopharyngeal cancer	10
died because of factors other than hypopharyngeal cancer	3
Differentiation type	
poor	5
moderate	10
well	4
Vessel invasion	
positive	11
negative	8
Lymph vessel invasion	
positive	12
negative	7
Perineural invasion	
positive	9
negative	10

CD147 – cluster of differentiation 147.

Immunohistochemistry and classification of pathological findings

Excised primary tumor specimens were fixed with 10% neutral-buffered formalin, and consecutive sections were cut every 5 mm; 4- μ m thick tissue sections were obtained. The sections were stained with hematoxylin and eosin (H&E), and the section containing the invasive tumor front was selected for further analysis. The polyclonal anti-CD147 antibody (Santa Cruz Biotechnology, Santa Cruz, USA) was used as the primary antibody for immunohistochemical staining. In brief, 4- μ m thick sections were deparaffinized and initially autoclaved for 15 min at 121°C. Sections were then blocked with 0.3% hydrogen peroxide in methanol for 30 min at room temperature and with 10% normal rabbit serum/Tris (Vector Laboratories Inc., Burlingame, USA) for 30 min at room temperature. All the sections were kept overnight at 4°C in phosphate-buffered saline (PBS) containing the rabbit anti-human CD147 polyclonal antibody (dilution: 1:200), followed by a 1 h incubation with biotinylated anti-rabbit IgG (ready-to-use dilution, cat. No. ab64256; Abcam, Cambridge, UK) at room temperature. The sections were washed with PBS and protein expression was detected with the Vectastain avidin-biotin complex kit (Vector Laboratories Inc.) according to the manufacturer's instructions, and then reacted with diaminobenzidine (Nacalai Tesque Inc., Kyoto, Japan) for 3–5 min at room temperature.

A pathologist and surgeon evaluated the CD147 immunohistochemical staining. CD147 expression in a tumor was scored according to the staining strength and intensity at $\times 200$ magnification using light microscopy. The areas of CD147 staining received scores of 0 if $<10\%$ of cells in the tumor nest were positive; scores of 1 if $\geq 10\%$ but $<50\%$ of cells in the tumor were positive; and scores of 2 if $\geq 50\%$ of cells of the tumor were positive. CD147 staining intensity was also scored from 0 to 2 (negative, weak or strong staining), and a CD147 index (range: 0–4) was calculated as the CD147-positive area score (0–2) \times CD147 intensity score (0–2). An index of 4 was classified as positive.

In addition, H&E-stained samples were examined to determine the SCC differentiation type and the presence or absence of lymphovascular, vascular and perineural invasion. Samples were classified according to the pathological findings as poorly, moderately or well-differentiated, and assessed for the presence or absence of lymphovascular, vascular and/or perineural invasion.

Cells and cell culture

FaDu, a cell line derived from human SCC of the hypopharynx that expresses CD147,¹⁹ was a kind gift from the Department of Cell Biology and Morphology at the Akita University Graduate School of Medicine and

was used for in vitro studies. Cells were maintained in Dulbecco's modified Eagle's medium (DMEM) supplemented with 10% heat-inactivated fetal bovine serum (FBS) and incubated at 37°C in the presence of 5% CO₂. For the stimulation experiments, FaDu cells were pre-incubated with serum-free DMEM and then incubated with serum-free medium containing cyclophilin A (CypA; Sigma-Aldrich, St. Louis, USA). A MEK inhibitor, U0126 (Wako Pure Chemical Industries Ltd., Osaka, Japan), was used for the MEK inhibition studies.

Matrigel invasion assay

We evaluated cell invasiveness in vitro using Matrigel-coated semipermeable-modified Boyden inserts with a pore size of 8 μ m (Becton Dickinson & Co., Franklin Lakes, USA). In addition, FaDu cells were plated at a density of 2.5×10^4 cells/insert in serum-free medium with or without CypA (400 ng/mL). Notably, the lower chamber contained DMEM + 10% FBS and served as a chemoattractant. Meanwhile, we plated cells in 96-well plates to serve as loading controls. After a 48-hour treatment at 37°C in a 5% CO₂ incubator, we removed the cells in the insert by wiping gently with a cotton swab. Next, the cells on the reverse side of the insert were fixed and stained using Diff-Quick (Sysmex, Kobe, Japan) according to the manufacturer's instructions. We counted the invading cells in 4 representative fields using light microscopy at $\times 200$ magnification, and evaluated the mean \pm standard deviation (SD) from 3 independent experiments. Additionally, the cells plated in 96-well plates as loading controls were subjected to 3-(4,5-dimethylthiazol-2-yl)-2,5-diphenyltetrazolium bromide assays, which meant that cell invasion ability was evaluated without the effects of increases in the number of cells across the groups.

Gelatin zymography

FaDu cells were cultured overnight using ordinary serum-containing DMEM, and then washed with serum-free DMEM and further cultured using serum-free DMEM with/without 400 ng/mL of CypA for 48 h. This was followed by detection of gelatinolytic activity in the conditioned media using gelatin zymography. In brief, the conditioned medium was resolved with SDS-PAGE under non-reducing conditions using 7.5% separating gel containing 0.3 mg/mL gelatin. Then, the gels were washed twice in 2.5% (w/v) Triton X-100 for 30 min at room temperature to remove the SDS, then incubated in reaction buffer containing 50 mM Tris-HCl, pH 7.6, 5 mM CaCl₂, and 2.5% Triton X-100 for 24 h at 37°C, followed by staining with 2.5% (w/v) Coomassie brilliant blue R-250 in 30% (v/v) methanol and 10% (v/v) acetic acid. After de-staining with 30% methanol and 10% acetic acid, gelatinolytic activities on the gel were detected as clear bands on a blue background of undigested gelatin.

siRNA and siRNA transfection

CD147 siGENOME siRNA (Dharmacon RNA Technologies, Lafayette, USA) was transfected into FaDu cells for CD147 silencing. We used siGENOME non-targeting siRNA as control. The siRNA transfections were performed using Lipofectamine 2000 (Life Technologies Inc., Carlsbad, USA). In brief, 1.8×10^5 FaDu cells were plated on a six-well plate. After a 24-hour incubation in complete media, the cells were transfected with 200 pmol of CD147 siRNA or non-targeting control siRNA. The transfection medium was replaced with complete media after 4 h of transfection.

Semi-quantitative determination of AKT, Stat3, p38 MAPK, MEK1, and NF- κ B phosphorylation status

PathScan[®] Signaling Nodes Multi-Target Sandwich ELISA Kit No. 7272 was purchased from Cell Signaling Technology, Inc. (Danvers, USA). This solid phase sandwich enzyme-linked immunosorbent assay (ELISA) combines the reagents necessary to detect endogenous levels of AKT1, phospho-AKT1 (Ser473), phospho-MEK1 (Ser217/221), phospho-p38 MAPK (Thr180/Tyr182), phospho-Stat3 (Tyr705), and phospho-NF- κ B p65 (Ser536). FaDu cells (75–80% confluent) were starved overnight and then cultured in the absence or presence of 200 ng/mL of CypA in low-serum (0.1% FBS)-containing culture medium for 48 h. The cells were washed twice with cold PBS and then lysed in buffer (20 mM Tris pH 7.5, 150 mM NaCl, 1 mM EDTA, 1 mM EGTA, 1% Triton[®] X-100, 2.5 mM sodium pyrophosphate, 1 mM β -glycerolphosphate, 1 mM Na₃VO₄, 1 μ g/mL leupeptin, 1 mM phenylmethylsulfonylfluoride), and a complete protease inhibitor cocktail from Sigma-Chemicals (St. Louis, USA), for 30 min on ice. The lysates were cleared by centrifugation in an Eppendorff tube (15 min at $14,000 \times g$, 4°C). The protein content was determined against a standardized control using a commercially available protein assay kit (Pierce Biotechnology Inc., Rockford, USA). Differential phosphorylation of AKT1, phospho-AKT, phosphoMEK1, phospho-p38 MAPK, phospho-Stat3, and phospho-NF- κ B p65 was measured in accordance with the manufacturer's instructions. Briefly, after incubation with cell lysates at a protein concentration of 0.5 mg/mL, the target phospho-protein was captured using the antibody coated onto the microwells. Following extensive washing, a detection antibody was added to detect the captured target phospho-protein. An HRP-linked secondary antibody was then used to recognize the bound detection antibody. The HRP substrate TMB was added to develop color. The magnitude of absorbance (measured at 450 nm) for the developed color is proportional to the quantity of bound target protein.

Statistical analysis

Statistical analyses were performed using Statcel 3 (OMS Publishing, Tokorozawa, Japan). The Wilcoxon–Mann–Whitney two-sided exact test was used to assess the statistical significance of the differences in MMP-9 expression and invasion studies. Fisher's exact test was used to determine the relationship between CD147 expression and the differentiation type, lymphatic invasion, vascular invasion, and perineural invasion. A value of $p < 0.05$ was considered to indicate a statistically significant difference. The difference in survival between patients stratified by CD147 levels was evaluated with a Kaplan–Meier survival analysis.

Results

Patient data and pathological findings

As presented in Table 1, 19 patients (17 men and 2 women) with hypopharyngeal SCC were included in the present study. All the patients presented with stage III or IV (stage III: 1 patient, stage IV: 18 patients). The patients ranged in age from 49 to 80 years (median: 62 years). During the follow-up period (median: 68 months, range: 6–91 months), 10 patients died from hypopharyngeal cancer and 6 survived. Three patients died because of factors other than hypopharyngeal cancer.

When immunohistochemistry was used to measure CD147 levels in tumor tissues, 8 samples were given a score of 0; 2 were given a score of 2; and 9 were given a score of 4. Accordingly, the 9 cases scored as 4 were defined as positive, and the remaining 11 cases were considered negative for CD147 expression.

Regarding the other histopathological findings, 5 cases were poorly differentiated, 10 cases were moderately differentiated and 4 cases were well-differentiated. In addition, 11 exhibited vascular invasion, 12 lymphovascular invasion and 9 perineural invasion.

The patient characteristics and pathological findings are summarized in Table 1.

CD147 expression in primary tumors is an independent post-surgical predictor of a poor prognosis

We then investigated the association between CD147 levels and the survival rate in hypopharyngeal cancer patients using the Kaplan–Meier method. We found that hypopharyngeal cancer patients with positive CD147 expression showed a lower five-year overall survival rate (OS) at 60 months (11.1%) compared with patients with negative CD147 expression (43.0%) ($p = 0.023$; Fig. 1). Therefore, higher CD147 expression is associated with a poor prognosis in hypopharyngeal cancer patients. In contrast, there were no significant differences in the survival rates in terms of SCC

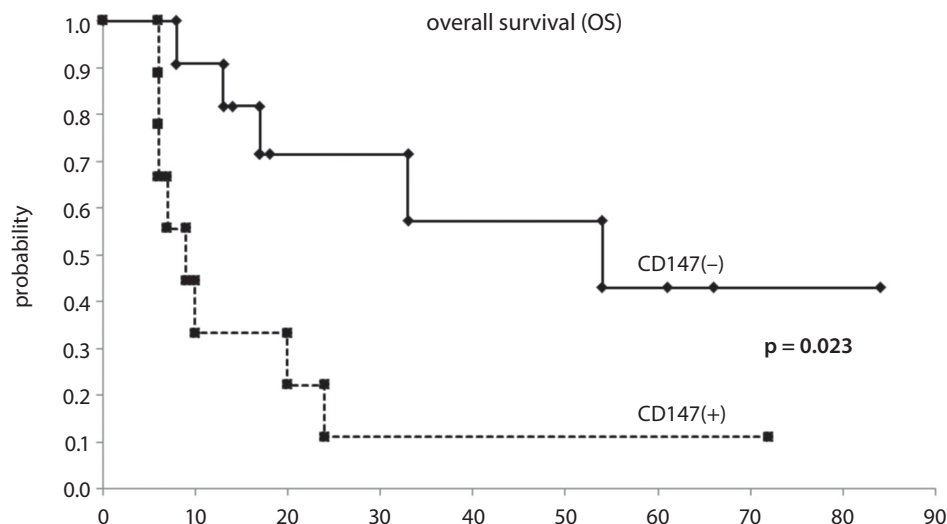


Fig. 1. Overall survival (OS) stratified according to CD147 status among hypopharyngeal cancer patients (log-rank test, $p = 0.023$)

Table 2. The associations between histopathological findings and CD147 expression

Characteristics		CD147		p-value
		positive	negative	
Differentiation type	moderate/poor	7	8	0.667
	well	2	2	
Vascular invasion	positive	7	4	0.115
	negative	2	6	
Lymphovascular invasion	positive	7	5	0.220
	negative	2	5	
Perineural invasion	positive	3	1	0.249
	negative	6	9	

CD147 – cluster of differentiation 147.

differentiation type and the presence or absence of lymphovascular, vascular and perineural invasion (data not shown).

In addition, we investigated the association of CD147 expression and representative pathological findings, including SCC differentiation type and the presence or absence of lymphovascular, vascular and perineural invasion. However, there were no significant correlations between CD147 expression and the pathological findings (Table 2). These results suggest that CD147 may be an independent prognostic factor.

CypA-CD147 interactions upregulate the expression of phosphorylated MEK in FaDu cells

We assessed the activation status of convergence points and key regulatory proteins in several signaling pathways controlling cellular events that contribute to tumor progression. We used the PathScan® Signaling Nodes Multi-Target Sandwich ELISA kit (Cell Signaling Technology, Inc.) to simultaneously assess in a semi-quantitative

manner the endogenous levels of AKT1, phospho-AKT1 (Ser473), phospho-MEK1 (Ser217/221), phospho-p38 MAPK (Thr180/Tyr182), phospho-Stat3 (Tyr705), and phospho-NF- κ B p65 (Ser536) in FaDu cells.

Phosphorylation is the most common mechanism of regulating protein function and transmitting signals throughout the cell.²⁰ Therefore, the observation of a phosphorylated signaling factor implies activation of the pathway in which the factor is involved.

To assess the signaling pathways associated with CD147, FaDu cells were cultured with 400 ng/mL CypA. We previously reported that CypA induces tumorigenicity by interaction with CD147 in FaDu cells.²¹ The findings revealed that among the signaling nodes evaluated, only the protein level of phospho-MEK was upregulated in the presence of CypA.

We then used siRNA to downregulate CD147 before culturing the FaDu cells (Fig. 2A) in the presence or absence of CypA. By silencing CD147, if the protein expression levels of signaling nodes are changed by CypA, it is possible to validate whether CD147 mediates this alteration. We found that CypA induced significant increase in phospho-MEK expression in non-targeting siRNA-treated cells, but this increase was not observed following CD147 knock-down (Fig. 2B). These results suggest that MEK is an important signaling pathway related to CD147 in hypopharyngeal SCC.

MEK mediates CypA-induced cell invasion and MMP-9 expression in FaDu cells

As tumor cell invasion is an important stage in metastasis, several studies have focused on developing methods to control invasion as a target for clinical tumor suppression.²² In addition, it has been reported that MMPs, especially gelatinases MMP-9 and MMP-2, play an important role in tumor invasion and metastasis through degradation of the basement membrane.²³ To evaluate invasion, FaDu

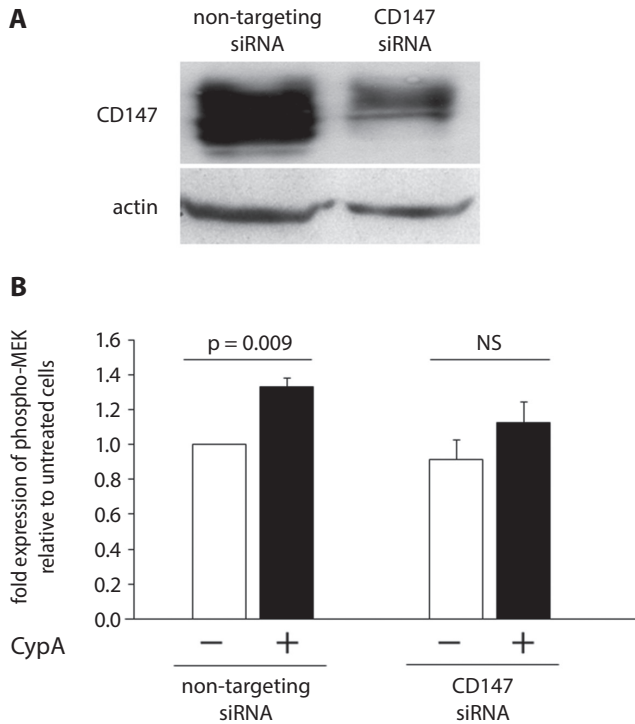


Fig. 2. A. CypA-CD147 interactions upregulate the expression of phosphorylated MEK in hypopharyngeal cancer cells. FaDu cells were transfected with non-targeting siRNA or CD147 siRNA. CD147 expression was analyzed with western blotting. CD147 expression was successfully downregulated 48 h after siRNA transfection; B. FaDu cells were then cultured with or without 200 ng/mL of CypA. The expression of phospho-MEK was examined using ELISA. The experiment was repeated 5 times, and similar results were observed for each replication. The results are expressed as fold change relative to untreated FaDu cells. A significant increase in phospho-MEK induced by CypA was observed during non-targeting siRNA treatment; however, this significance was not observed during CD147 knockdown

NS – not significant ($p > 0.05$); siRNA – small interfering RNA; CypA – cyclophilin A.

cells were seeded into Matrigel-coated invasion chambers and stimulated with CypA. The expression levels of gelatinases were also detected using gelatin zymography in FaDu cells treated with or without CypA. It was revealed that cell invasion was increased in the presence of CypA. In addition, only the expression of MMP-9 was detected, indicating that MMP-9 expression was increased in the presence of CypA.

To determine whether MEK signaling mediates these changes in invasion and MMP expression by CypA, we treated FaDu cells with U0126, a specific MEK inhibitor, in the presence or absence of CypA. We found a significant increase in cell invasion and upregulation of MMP-9 expression by CypA in the absence of U0126. However, these increments were not observed in the presence of U0126 (Fig. 3,4). These results suggest that the MEK signaling pathway mediates CD147 tumorigenesis in hypopharyngeal SCC.

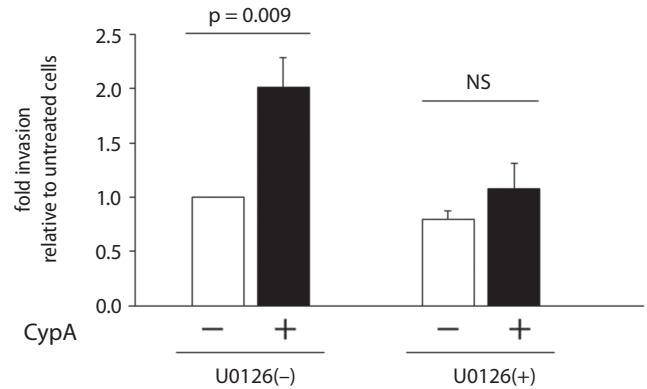


Fig. 3. MEK mediates CypA-induced cell invasion in hypopharyngeal cancer cells. Cell invasiveness was evaluated in vitro using a Matrigel invasion assay. FaDu cells were plated in the inserts in serum-free medium with or without 200 ng/mL of CypA, 10 nM of U0126 (a specific MEK inhibitor), or a combination of CypA and U0126. The number of invading cells in each insert was determined, and means \pm standard error (SE) were calculated from 5 independent experiments. The number of invading cells significantly increased following stimulation with CypA compared with untreated cells, and this increase was attenuated by U0126

NS – not significant ($p > 0.05$); CypA – cyclophilin A.

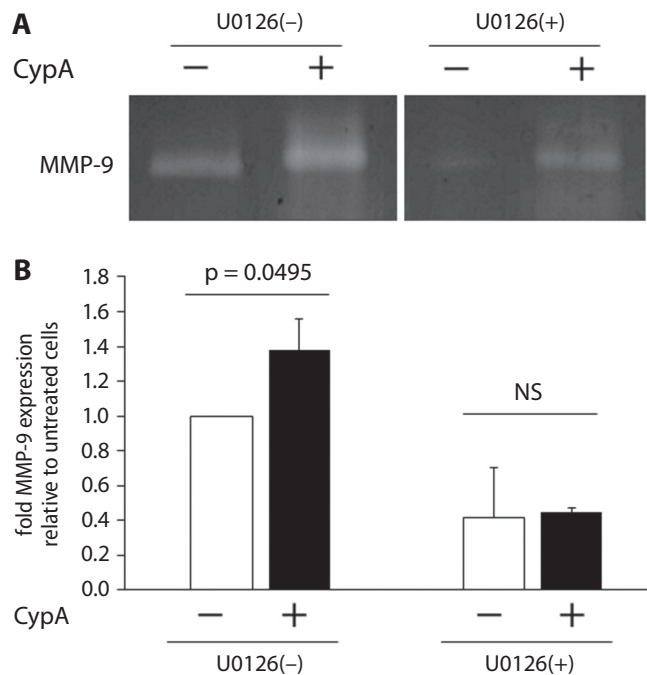


Fig. 4. MEK mediates CypA-induced expression of MMP-9 in hypopharyngeal cancer cells. MMP-9 expression was evaluated using gelatin zymography. FaDu cells were cultured in serum-free medium with or without 200 ng/mL of CypA, 10 nM of U0126 (a specific MEK inhibitor), or a combination of CypA and U0126. A. A representative result of gelatin zymography used to detect MMP-9 in the culture media of FaDu cells; B. Densitometry analysis performed on the gelatin zymography results of MMP-9 levels relative to MMP-9 in untreated FaDu cells. Means \pm standard error (SE) were calculated from 3 independent experiments. The expression of MMP-9 significantly increased following stimulation with CypA compared with untreated cells, and this increase was attenuated by U0126

NS – not significant ($p > 0.05$); CypA – cyclophilin A.

Discussion

It is ideal to improve the effectiveness of cancer treatments while suppressing toxic side effects. For that purpose, it is important to determine the characteristics and identify targets of cancer. To this end, the most important issue is to elucidate the factors involved in the development of each type of cancer.²⁴

Hypopharyngeal cancer is one of the most frequent head and neck cancers and has been shown to have a direct impact on the patients' quality of life, such as causing difficulties with swallowing and phonation. It is associated with a poor prognosis, and there is an essential need to improve therapeutic effects and to reduce unwanted side effects.^{1,25}

To improve the therapeutic effects of treatments for malignant tumors, it is necessary to first understand the characteristics of the carcinoma and to take measures against the factors. Various studies have been conducted on head and neck cancer, and based on the results, attempts have been made to predict the prognosis and select the optimal treatment.²⁶

In head and neck cancers, clinical findings like tumor size and cervical lymph node metastasis have been studied as predictors of the prognosis.²⁷ In addition to these clinical prognostic factors, studies on new biomarkers, like human papillomavirus infection or EGFR expression, have progressed in recent years. Currently, these factors are used to help predict the prognosis and are considered to be actual therapeutic targets.^{13,28}

CD147 is known to be associated with prognosis in various malignant tumors. Targeting CD147 has been shown to be effective, and has great significance in clinical practice.²⁹ In this study, we found that CD147 expression in hypopharyngeal carcinoma was related to the prognosis. These results suggest that CD147 may be an efficient therapeutic target in hypopharyngeal cancer.

While CD147 clearly affects the prognosis, in order to apply these findings to the development of therapeutic methods, it is necessary to elucidate the mechanisms that promote tumor progression. Originally, CD147 was reported as an inducer of MMPs during physiological functions such as wound healing, but this action has also been shown to play an important role in cancer progression.³⁰ In cancer, it is well-established that CD147 is involved in invasion and metastasis mainly by MMP-mediated ECM and basement membrane degradation. It also regulates cell proliferation, drug resistance and epithelial-to-mesenchymal transition in many carcinomas, including head and neck cancer.^{9,21}

The MMPs, a family of zinc-dependent proteinases, are capable of degrading a variety of ECM components and have various physiological functions in normal tissues.³⁰ Furthermore, the degradation of ECM components by MMPs is a determining step in tumor cell invasion and metastasis.³¹ In particular, MMP-2 and -9 (gelatinase A and B) are able to degrade type IV collagen in the basement membrane to promote tumor progression.^{23,32} It has been reported that MMP-9 is involved in the cell invasion

of hypopharyngeal carcinoma.³³ Therefore, the result of the present study showing the involvement of MMP-9 expression in hypopharyngeal cancer cells is important for elucidating the key factors that regulate hypopharyngeal cancer progression.

Intracellular signal transduction is very important for normal cell functions, and understanding these pathways is indispensable for elucidating the behavior of cancer cells.³⁴ To date, key signaling pathways have been identified in various carcinomas,³⁵ and the therapeutic effects of targeting them have been reported.³⁶ Signal transduction pathways in head and neck cancers have also been elucidated, and the therapeutic effects of targeting them have been shown.³⁷ However, there is limited research on hypopharyngeal cancer. In this study, certain signaling pathways, including MEK, were suggested as signals activated by CD147 in a hypopharyngeal cell line.

MEK is a key factor in the Ras/Raf/MEK/ERK (MAPK) signaling pathway. This MAPK cascade forms a complex signaling network that controls a wide variety of cellular processes, such as cell proliferation, growth, differentiation, transformation, and apoptosis.³⁸ Dysregulation of key mediators of the MAPK pathway has been implicated as a driver of tumorigenesis and contributes to the ability of cancer cells to be independent of mitogen signals, produce growth factors, avoid apoptosis, acquire a sensitivity to antiproliferative signals, metastasize, and gain angiogenic potential.³⁹ Much effort has been directed toward the development of inhibitors of this pathway, assuming that mutations in the MAPK pathway contribute to tumor-promoting processes.³⁸ Among them, MEK has been shown to be a potential therapeutic target for some solid cancers, such as prostate cancer, and inhibitors are being developed.⁴⁰

Conclusions

In summary, studies using clinical specimens have shown that CD147 expression in hypopharyngeal carcinoma is a predictor of a poor prognosis. In this study, CD147 expression in hypopharyngeal cancer cells was stimulated using CypA, a CD147 ligand. As a result, it was confirmed that cell invasion ability, MMP-9 expression and phosphorylated MEK levels were enhanced in hypopharyngeal cancer cells. In addition, cell infiltration and the enhancement of MMP-9 expression induced by CD147 were abolished by a MEK inhibitor.

Clinical studies suggest that CD147 may be associated with short OS in hypopharyngeal carcinoma patients. However, the number of patients analyzed in this study was small. Further studies of the prognostic impact of CD147 should be performed with a larger sample size. However, the *in vitro* results indicate that the CD147-induced MEK-mediated intracellular signaling pathway plays an important role in tumor progression in hypopharyngeal carcinoma, and inhibition of these factors may help to control

hypopharyngeal tumor progression and improve the prognosis. Further studies on CD147 and MEK signaling pathways are expected in the future.

ORCID iDs

Shinsuke Suzuki  <https://orcid.org/0000-0001-8555-1722>
 Satoshi Toyoma  <https://orcid.org/0000-0003-0688-8306>
 Yohei Kawasaki  <https://orcid.org/0000-0001-9745-1577>
 Hiroshi Nanjo  <https://orcid.org/0000-0002-0885-7151>
 Takechiyo Yamada  <https://orcid.org/0000-0002-6910-3265>

References

- Carvalho AL, Pintos J, Schlecht NF, et al. Predictive factors for diagnosis of advanced-stage squamous cell carcinoma of the head and neck. *Arch Otolaryngol Head Neck Surg.* 2002;128(3):313–318. doi:10.1001/archotol.128.3.313
- Hamidi H, Ivaska J. Every step of the way: Integrins in cancer progression and metastasis. *Nat Rev Cancer.* 2018;18(9):533–548. doi:10.1038/s41568-018-0038-z
- Peltanova B, Raudenska M, Masarik M. Effect of tumor microenvironment on pathogenesis of the head and neck squamous cell carcinoma: A systematic review. *Mol Cancer.* 2019;18(1):63. doi:10.1186/s12943-019-0983-5
- Santuray RT, Johnson DE, Grandis JR. New therapies in head and neck cancer. *Trends Cancer.* 2018;4(5):385–396. doi:10.1016/j.trecan.2018.03.006
- Riethdorf S, Reimers N, Assmann V, et al. High incidence of EMMPRIN expression in human tumors. *Int J Cancer.* 2006;119(8):1800–1810. doi:10.1002/ijc.22062
- Suzuki S, Sato M, Senoo H, Ishikawa K. Direct cell-cell interaction enhances pro-MMP-2 production and activation in co-culture of laryngeal cancer cells and fibroblasts: Involvement of EMMPRIN and MT1-MMP. *Exp Cell Res.* 2004;293(2):259–266. doi:10.1016/j.yexcr.2003.10.010
- Rosenthal EL, Vidrine DM, Zhang W. Extracellular matrix metalloprotease inducer stimulates fibroblast-mediated tumor growth in vivo. *Laryngoscope.* 2006;116(7):1086–1092.
- Suzuki S, Honda K, Nanjo H, et al. CD147 expression correlates with lymph node metastasis in T1-T2 squamous cell carcinoma of the tongue. *Oncol Lett.* 2017;14(4):4670–4676. doi:10.3892/ol.2017.6808
- Suzuki S, Toyoma S, Tsuji T, Kawasaki Y, Yamada T. CD147 mediates transforming growth factor- β 1-induced epithelial-mesenchymal transition and cell invasion in squamous cell carcinoma of the tongue. *Exp Ther Med.* 2019;17(4):2855–2860. doi:10.3892/etm.2019.7230
- Shah NH, Kuriyan J. Understanding molecular mechanisms in cell signaling through natural and artificial sequence variation. *Nat Struct Mol Biol.* 2019;26(1):25–34. doi:10.1038/s41594-018-0175-9
- Mukherjee TK, Paul K, Mukhopadhyay S. Cell signaling molecules as drug targets in lung cancer: An overview. *Curr Opin Pulm Med.* 2011;17(4):286–291. doi:10.1097/MCP.0b013e328347bda6
- Kim E, Kim JY, Smith MA, Haura EB, Anderson ARA. Cell signaling heterogeneity is modulated by both cell-intrinsic and -extrinsic mechanisms: An integrated approach to understanding targeted therapy. *PLoS Biol.* 2018;16(3):e2002930. doi:10.1371/journal.pbio.2002930
- Schmitz S, Ang KK, Vermorken J, et al. Targeted therapies for squamous cell carcinoma of the head and neck: Current knowledge and future directions. *Cancer Treat Rev.* 2014;40(3):390–404. doi:10.1016/j.ctrv.2013.09.007
- Qin H, Rasul A, Li X, et al. CD147-induced cell proliferation is associated with Smad4 signal inhibition. *Exp Cell Res.* 2017;358(2):279–289. doi:10.1016/j.yexcr.2017.07.003
- Li J, Huang Q, Long X, et al. CD147 reprograms fatty acid metabolism in hepatocellular carcinoma cells through Akt/mTOR/SREBP1c and P38/PPAR α pathways. *J Hepatol.* 2015;63(6):1378–1389. doi:10.1016/j.jhep.2015.07.039
- Xu BQ, Fu ZG, Meng Y, et al. Gemcitabine enhances cell invasion via activating HAb18G/CD147-EGFR-pSTAT3 signaling. *Oncotarget.* 2016;7(38):62177–62193. doi:10.18632/oncotarget.11405
- Ma C, Wang J, Fan L, Guo Y. Inhibition of CD147 expression promotes chemosensitivity in HNSCC cells by deactivating MAPK/ERK signaling pathway. *Exp Mol Pathol.* 2017;102(1):59–64. doi:10.1016/j.yexmp.2017.01.002
- Sobin LH, Wittekind C, Gospodarowicz MK, eds. *TNM Classification of Malignant Tumours*, 6th edition. New York, NY: Wiley-Blackwell; 2002.
- Suzuki S, Sato M, Senoo H, Ishikawa K. Direct cell-cell interaction enhances pro-MMP-2 production and activation in co-culture of laryngeal cancer cells and fibroblasts: Involvement of EMMPRIN and MT1-MMP. *Exp Cell Res.* 2004;293(2):259–266.
- Takahashi M, Suzuki S, Ishikawa K. Cyclophilin A-EMMPRIN interaction induces invasion of head and neck squamous cell carcinoma. *Oncol Rep.* 2012;27(1):198–203. doi:10.3892/or.2011.1474
- Koppikar P, Choi SH, Egloff AM, et al. Combined inhibition of c-Src and epidermal growth factor receptor abrogates growth and invasion of head and neck squamous cell carcinoma. *Clin Cancer Res.* 2008;14(13):4284–4291. doi:10.1158/1078-0432.CCR-07-5226
- Jiang WG, Sanders AJ, Katoh M, et al. Tissue invasion and metastasis: Molecular, biological and clinical perspectives. *Semin Cancer Biol.* 2015;35:S244–S275. doi:10.1016/j.semcancer.2015.03.008
- Jackson SE, Chester JD. Personalised cancer medicine. *Int J Cancer.* 2015;137(2):262–266. doi:10.1002/ijc.28940
- Newman JR, Connolly TM, Illing EA, Kilgore ML, Locher JL, Carroll WR. Survival trends in hypopharyngeal cancer: A population-based review. *Laryngoscope.* 2015;125(3):624–629. doi:10.1002/lary.24915
- Szentkúti G, Dános K, Brauswetter D, et al. Correlations between prognosis and regional biomarker profiles in head and neck squamous cell carcinoma. *Pathol Oncol Res.* 2015;21(3):643–650. doi:10.1007/s12253-014-9869-4
- Talmi YP, Takes RP, Alon EE, et al. Prognostic value of lymph node ratio in head and neck squamous cell carcinoma. *Head Neck.* 2018;40(5):1082–1090. doi:10.1002/hed.25080
- Chera BS, Kumar S, Shen C, et al. Plasma circulating tumor HPV DNA for the surveillance of cancer recurrence in HPV-associated oropharyngeal cancer. *J Clin Oncol.* 2020;38(10):1050–1058. doi:10.1200/jco.19.02444
- Landras A, de Moura CR, Jouenne F, Lebbe C, Menashi S, Mourah S. CD147 is a promising target of tumor progression and a prognostic biomarker. *Cancers (Basel).* 2019;11(11):1803. doi:10.3390/cancers11111803
- Vu TH, Werb Z. Matrix metalloproteinases: Effectors of development and normal physiology. *Genes Dev.* 2000;14(17):2123–2133. doi:10.1101/gad.815400
- Kessenbrock K, Plaks V, Werb Z. Matrix metalloproteinases: Regulators of the tumor microenvironment. *Cell.* 2010;141(1):52–67. doi:10.1016/j.cell.2010.03.015
- Winer A, Adams S, Mignatti P. Matrix metalloproteinase inhibitors in cancer therapy: Turning past failures into future successes. *Mol Cancer Ther.* 2018;17(6):1147–1155. doi:10.1158/1535-7163.MCT-17-0646
- Liu X, Lv Z, Zou J, et al. Elevated AEG-1 expression in macrophages promotes hypopharyngeal cancer invasion through the STAT3-MMP-9 signaling pathway. *Oncotarget.* 2016;7(47):77244–77256. doi:10.18632/oncotarget.12886
- Martin GS. Cell signaling and cancer. *Cancer Cell.* 2003;4(3):167–174. doi:10.1016/S1535-6108(03)00216-2
- Li L, Tang P, Li S, et al. Notch signaling pathway networks in cancer metastasis: A new target for cancer therapy. *Med Oncol.* 2017;34(10):180. doi:10.1007/s12032-017-1039-6
- Tian T, Li X, Zhang J. mTOR signaling in cancer and mTOR inhibitors in solid tumor targeting therapy. *Int J Mol Sci.* 2019;20(3):755. doi:10.3390/ijms20030755
- Aguilar BJ, Zhou H, Lu Q. Cdc42 signaling pathway inhibition as a therapeutic target in Ras-related cancers. *Curr Med Chem.* 2017;24(32):3485–3507. doi:10.2174/0929867324666170602082956
- Horn D, Hess J, Freier K, Hoffmann J, Freudlsperger C. Targeting EGFR-PI3K-AKT-mTOR signaling enhances radiosensitivity in head and neck squamous cell carcinoma. *Expert Opin Ther Targets.* 2015;19(6):795–805. doi:10.1517/14728222.2015.1012157
- Roberts PJ, Der CJ. Targeting the Raf-MEK-ERK mitogen-activated protein kinase cascade for the treatment of cancer. *Oncogene.* 2007;26(22):3291–3310. doi:10.1038/sj.onc.1210422
- Cargnello M, Roux PP. Activation and function of the MAPKs and their substrates, the MAPK-activated protein kinases. *Microbiol Mol Biol Rev.* 2011;75(1):50–83. doi:10.1128/mbr.00031-10
- Nickols NG, Nazarian R, Zhao SG, et al. MEK-ERK signaling is a therapeutic target in metastatic castration resistant prostate cancer. *Prostate Cancer Prostatic Dis.* 2019;22(4):531–538. doi:10.1038/s41391-019-0134-5

Mid-term evaluation of the safety and efficacy of the iStent trabecular micro-bypass system combined with phacoemulsification

Milena Kozera^{1,A–D}, Joanna Konopińska^{2,E}, Marek Rękas^{1,A,F}

¹ Department of Ophthalmology, Military Institute of Medicine, Warszawa, Poland

² Department of Ophthalmology, Medical University of Białystok, Poland

A – research concept and design; B – collection and/or assembly of data; C – data analysis and interpretation;

D – writing the article; E – critical revision of the article; F – final approval of the article

Advances in Clinical and Experimental Medicine, ISSN 1899–5276 (print), ISSN 2451–2680 (online)

Adv Clin Exp Med. 2021;30(1):49–54

Address for correspondence

Milena Kozera

E-mail: m.kozera@onet.eu

Funding sources

None declared

Conflict of interest

None declared

Received on July 16, 2020

Reviewed on August 6, 2020

Accepted on October 29, 2020

Published online on January 30, 2021

Abstract

Background. Micro-invasive glaucoma surgery (MIGS) and MIGS devices have been gaining increasing attention in recent years. One such device is the trabecular micro-bypass stent, or iStent® (Glaukos Corporation, Laguna Hills, USA).

Objectives. To evaluate the safety and efficacy of the minimally invasive ab interno surgical implantation of a trabecular bypass during cataract surgery in reducing intraocular pressure (IOP) in patients with mild and moderate open-angle glaucoma and cataracts.

Material and methods. The study was a prospective, uncontrolled, interventional case series (a prospective study of a case series), including 54 patients with a mean age of 72 years. All subjects underwent ab interno implantation of a single iStent together with cataract surgery. The corrected distance visual acuity (CDVA), IOP, anti-glaucoma medications, visual field, and number and type of complications were investigated after surgery. The patients were followed up at 1, 7, and 30 days, and 3, 6, 12, 24 and 36 months after the operation.

Results. The mean observation time was 20 months. At baseline, CDVA was 0.5 or better in 65% of the eyes; this improved to 0.5 or better in all eyes (0.8 or better in 79%) at the end of the observation. The mean baseline IOP was 17.1 mm Hg, which fell to a mean of 15.1 mm Hg. The mean number of medicinal eye drops prescribed preoperatively was 1.7, which decreased to 0.26 at the end of the observation.

Conclusions. Cataract surgery combined with iStent implantation seems to be an effective procedure in patients with mild to moderate open-angle glaucoma and cataracts. The insertion of 1 stent resulted in a significant decrease in IOP and a reduction in the number of topical anti-glaucoma medications needed. Based on the characteristics of the observed complications, iStent implantation can be considered a safe method.

Key words: open-angle primary glaucoma, micro-invasive glaucoma surgery, iStent®

Cite as

Kozera M, Konopińska J, Rękas M. Mid-term evaluation of the safety and efficacy of the iStent trabecular micro-bypass system combined with phacoemulsification. *Adv Clin Exp Med.* 2021;30(1):49–54. doi:10.17219/acem/129576

DOI

10.17219/acem/129576

Copyright

© 2021 by Wrocław Medical University

This is an article distributed under the terms of the Creative Commons Attribution 3.0 Unported (CC BY 3.0) (<https://creativecommons.org/licenses/by/3.0/>)

Introduction

Glaucoma is the second most common cause of blindness in the world and one of the major causes in Europe. It is a group of diseases that share a common feature: progressive damage to the optic nerve and related visual field defects. The main risk factor for the development of glaucoma neuropathy is elevated intraocular pressure (IOP). Reducing this pressure is still the only proven method of treating glaucoma.¹

A common treatment of newly diagnosed mild to moderate open angle glaucoma (OAG) begins with local antihypertensive therapy, though laser trabeculoplasty is an alternative. The traditional approach to glaucoma treatment to date involves the use of surgical techniques as the ultimate therapeutic method. With the use of filtration procedures, which are the most common methods, obtaining good pressure control is associated with the risk of numerous intra- and postoperative complications. In addition, the use of anti-metabolites increases the risk of complications such as hypotension, leakage, filter bubble infection, and endophthalmitis.²

A better understanding of the pathophysiology of glaucoma, especially aqueous humor outflow pathways, has resulted in newer treatments. Starting from ab externo procedures, such as trabeculectomy or viscocanalostomy, through canoplasty, a group of ab interno treatments has been created, resulting in minimal trauma to the target tissue without affecting the anatomical structures and physiology of the eye, less invasiveness, good efficiency, and a high safety profile.³ A common term for these procedures is micro-invasive glaucoma surgery (MIGS).⁴ The MIGS uses different types of implants. One of the first stents to be placed in the Schlemm's canal was the iStent[®] microstent (Glaukos Corporation, Laguna Hills, USA). This is one of the smallest medical implants ever used in humans. Many prospective multicenter clinical trials have shown that the iStent[®] safely and effectively reduces IOP while reducing or eliminating the need for antihypertensive drugs. The data shows that the implantation of a single iStent in conjunction with a cataract surgery significantly reduces IOP for up to 5 years after surgery in patients with glaucoma and cataracts.^{5–11}

To investigate the potential usefulness of the microstent as a therapy in patients with early and intermediate glaucoma and cataracts, we conducted a prospective case series study assessing the efficacy and safety of a single iStent implant in surgery combined with cataract phacoemulsification.

Material and methods

Patients and study protocol

A prospective single-center study was conducted in which patients with primary open-angle glaucoma and cataracts were enrolled. The study protocol was in line with

the principles of the Declaration of Helsinki and was approved by the Bioethics Committee at the Military Medical Institute (Warszawa, Poland). Prior to recruitment, legally binding, informed consent was obtained from each patient for Glaukos iStent implantation and cataract surgery.

The inclusion criteria were an IOP \leq 31 mm Hg; the use of up to 4 antihypertensive drugs; open angle confirmed with gonioscopy; and mild (mean deviation (MD) from 0 to -6.0 dB) or moderate (MD from -6.0 to -12 dB) defects in the field of view confirmed using the ZEISS Humphrey Field Analyzer (Carl Zeiss AG, Jena, Germany) with the SITA Standard 24-2 program (Ophthalmological Clinic Military Institute of Medicine, Warszawa, Poland). Other inclusion criteria included a pre-operative best-corrected visual acuity (BCVA) of 20/200 or better, and the willingness to attend follow-up appointments for the duration of the study, i.e., 12 months.

The key exclusion criteria were forms of glaucoma other than primary open-angle glaucoma and pseudoexfoliative glaucoma; evidence of serious eye diseases other than glaucoma and senile cataracts, such as proliferative diabetic retinopathy, corneal diseases (e.g., Fuchs dystrophy), age-related macular degeneration – the dry or exudative form; a narrow angle of filtration; previous anti-glaucoma treatment (trabeculoplasty, trabeculectomy, filtration, cycloablation, etc.); previous surgery not caused by glaucoma or cataracts, except for ophthalmic procedures; glaucoma defects in the field of view with an MD < -12 dB, as confirmed with a Humphrey field analyzer; and the use of more than 4 anti-glaucoma drugs.

iStent and surgical technique

An iStent[®] is a one-piece, L-shaped, heparin-coated titanium implant smaller than 1 mm and approx. 0.3 mm high. The iStent microfistula is inserted through a small incision in the transparent part of the cornea. It is used to drain the aqueous humor directly into the Schlemm's canal. The stent is introduced ab interno into the Schlemm's canal using a spring mechanism with a diameter of 27 G. One or more implants can be inserted into the corner on the nasal side. When the fistula is in place, a small blood reflux may occur, usually self-limiting in nature. The iStent implantation does not bypass the physiological outflow pathway, but supports it in the hope of achieving an acceptable IOP level and reducing or eliminating the use of anti-glaucoma drugs.

The surgical procedure was performed under local anesthesia with 2% xylocaine. After cataract removal and the creation of an artificial intraocular posterior chamber with phacoemulsification (faco chop), the implantation of iStent began. The right stent was used in the right eyes and the left stent was used in the left eyes. The patient's eyes were positioned nasally, and the microscope was turned 30° from the surgeon. A viscoelastic agent was administered into the anterior chamber for visibility. Through the existing temple opening in the corneal limbus, the iStent was introduced into the trabecular mesh at an angle of 20° and

moved deeper. A spring injector was used for stent implantation, while a Swan–Jacobs gonioscope was used to visualize the angle of filtration. The “impact” of the stent on the tip of the injector from back to front confirmed the correct placement of the microimplant. After the applicator was withdrawn, the remaining viscoelastic agent was removed by irrigation and aspiration. The anterior chamber was sealed with saline solution and intraocular pressure was controlled to complete the surgery. All procedures were performed by the same surgeon (MR) in the Department of Ophthalmology of the Military Institute of Medicine.

Postoperative management

The patients used antibiotic and anti-inflammatory eye drops for 4 weeks. Postoperative check-ups took place on day 1, 7 and 30, and after 3, 6, 12, 24, and 36 months. At each examination, the BCVA was assessed with Snellen chart, IOP was measured with a Goldmann applanation tonometer, and the anterior segment and the fundus was examined in the slit lamp. The gonioscopic angle was also assessed (except for the 1st day after surgery). At the 12- and 24-month follow-up, the field of view was taken using a Humphrey apparatus with the SITA Standard 24-2 program. An important parameter evaluated in the study was the number of anti-glaucoma drugs used. Additional information collected throughout the study was related to treatment and/or study-related adverse effects.

Statistical analysis

The effectiveness of the procedures used in the study was analyzed on the basis of all available data from IOP measurements and the number of local antihypertensive drugs. A total IOP reduction to ≤15 mm Hg was considered independent of treatment, while a reduction in IOP to ≤18 mm Hg indicated a “partial success.”

For the continuous variables, 2 mock tests were used to assess differences between the groups. Fisher’s exact test was used to compare categorical results between the groups. To assess the effect of time and intervention on the measured parameters, linear mixed models with random constant expression were built for the patient. Model coefficients are reported with a 95% confidence interval (95% CI) and p-value; the level of the latter of 0.05 was considered statistically significant. All analyses were performed using the Statistical Analysis System (SAS) statistical software package v. 9.1.3. (SAS Institute Inc., Cary, USA).

Results

Demographics

The study involved 54 eyes of 52 patients. The study group included 38 women and 14 men with a mean age

Table 1. Demographics and preoperative variables

Variable	Value
Total	54 eyes of 52 patients
Age [years]	72 (8)
Gender (F/M)	38/14
Race – Caucasian	100% (n = 54)
Type of glaucoma	
primary open-angle glaucoma	94% (n = 51)
pseudoexfoliative glaucoma	6% (n = 3)
Preoperative visual field (MD) [dB], mean (SD)	−4.8 (3.9)
Preoperative visual field (PSD) [dB], mean (SD)	3.7 (2.5)
Preoperative S/D ratio, mean (SD)	0.6 (0.2)
Preoperative medicated IOP [mm Hg], mean (SD)	17.1 (3.5)
Preoperative anti-glaucoma medications, mean (SD)	1.7 (0.9)
Preoperative BCVA	
20/25 or better	17% (n = 9)
20/40 or better	65% (n = 35)

BCVA – best-corrected visual acuity; MD – mean deviation; SD – standard deviation.

of 72 years (standard deviation (SD) = 8 years). Most of the eyes (94%; n = 51) had primary open-angle glaucoma; 6% (n = 3) had pseudoexfoliative glaucoma. Two patients had both eyes enrolled in the study. The mean follow-up period was 20 months (SD = 10). A total of 44 eyes were observed for 12 months, observation of 32 eyes was completed within 24 months, and observation of 10 eyes was extended to 36 months. Demographic data and descriptive characteristics are presented in Table 1.

Intraocular pressure and medications

The baseline mean intraocular pressure was 17.1 ±3.5 mm Hg. The last study showed a decrease in IOP to mean values of 15.7 ±2.2 mm Hg; similar results were found after 12 months (Fig. 1).

A reduction in IOP to a value ≤15 mm Hg occurred in 43% of the eyes (compared to 26% before surgery) and ≤18 mm Hg in 94% (compared with 63% before surgery; Fig. 2).

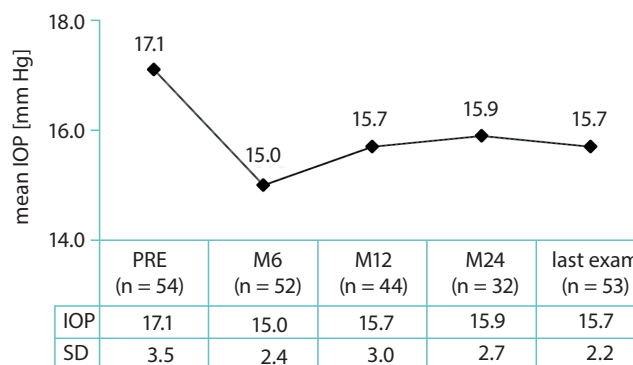


Fig. 1. Mean IOP at time intervals

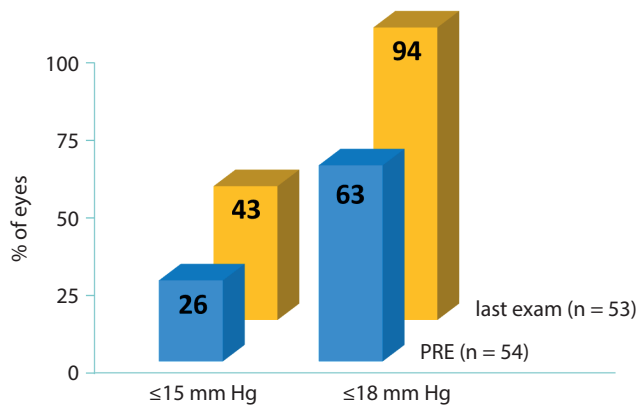


Fig. 2. Proportional analyses of IOP

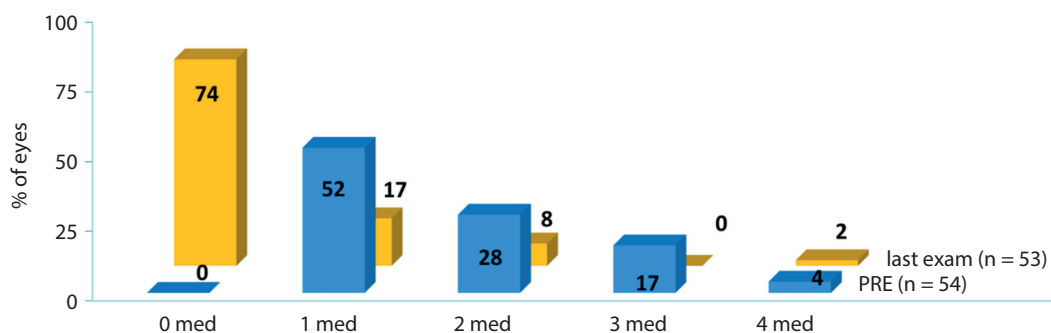


Fig. 3. Proportional analyses of medication use

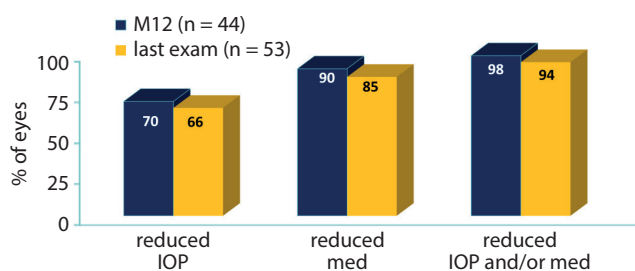


Fig. 4. IOP and medication reduction

The average number of drugs used before surgery was 1.7 ± 0.9 . Drug consumption decreased significantly. In a recent study, 74% of patients were able to eliminate topical medications, compared to 49% of patients on 2 or more drugs in their preoperative examinations (Fig. 3). After 12 months, 70% of patients had achieved a reduction in IOP, 90% had reduced the number of drugs, and 98% had reduced IOP and/or drug use (Fig. 4). At the end of the follow-up period, 66% of patients had lower IOP than before surgery, 85% had reduced their use of anti-hypertensive eye drops, and 94% of patients had achieved a reduction in IOP and/or a reduction in drug use.

Safety

In no case did the visual acuity deteriorate. In the whole study group at the end of observations, BCVA was 20/40; in 79% of cases, BCVA had reached 20/25 (Fig. 5).

There were no significant complications after cataract phacoemulsification surgery with iStent implantation. One patient had a subconjunctival hemorrhage on the 1st day after surgery, in 5 eyes there were erythrocytes in the anterior chamber, and in 1 eye a corneal edema associated with an increase in IOP was revealed. All symptoms resolved completely within 7 days. One patient developed viral keratitis 1 week after surgery. Topical treatment was applied and the condition healed during the 1st month. The final visual acuity in this patient was 20/20. Table 2 presents the postoperative complications. Most complications occurred in the postoperative period and did not differ significantly from those after phacoemulsification of cataracts alone.

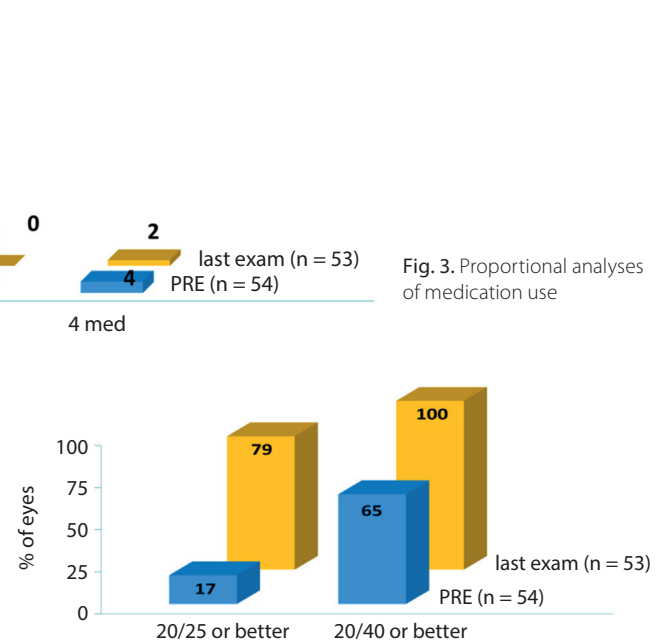


Fig. 5. Preoperative and last reported BCVA

Table 2. Postoperative complications

Complications	n (%)
Conjunctival hemorrhage	1 (1.8)
Temporary increase of IOP	1 (1.8)
Single erythrocytes in anterior chamber	5 (9.2)
Corneal erosion	4 (7.4)
Viral keratitis	1 (1.8)

Discussion

Micro-invasive glaucoma surgery covers 3 anatomical areas: Schlemm's canal, the suprachoroidal and subconjunctival spaces.⁴ Because 80% of the aqueous humor drains through the conventional route, methods have been sought for decades to improve the outflow of aqueous humor using trabecular formulations. Ab externo

trabeculotomy was one such method,^{12,13} used for the first time in adults by Tanihara et al.¹⁴ It was discovered that greater efficiency can be obtained by introducing a non-absorbable thread with prolene into the Schlemm's canal, stretching its walls. The use of microimplants in MIGS implanted into the Schlemm's canal was another step in the quest to develop an effective, less invasive method. Performing surgery with an ab interno approach does not cause damage to eye tissues such as the conjunctiva and the sclera.

Samuelson et al. described the use of a single iStent in a surgery combined with phacoemulsification of cataracts.¹¹ In our report, the patients who had undergone stent implantation had a reduction in IOP of 66% and the average number of antihypertensive drugs decreased. The results of our study are in line with previous reports on the effectiveness of using iStents to reduce IOP and topical drug use, as well as those regarding the high safety profile of the implant.^{5–11} The results show that more than 90% of patients experienced a reduction in IOP, a reduction in the number of drugs used or a reduction in both.

The Early Manifest Glaucoma Trial reported that the risk of glaucoma progression is reduced by 10% with every millimeter of mercury reduced from baseline IOP.¹⁵ Slowing or arresting disease progression is the goal of glaucoma treatment, and as stated in the Early Manifest Glaucoma Trial analysis, even small decreases in IOP are clinically relevant. In our study, the average decrease in IOP was 2 mm Hg 6 months after surgery, with a sustained reduction for 12 months after surgery. Moreover, in about 50% of the eyes (n = 32), the follow-up time was extended to 2 years, and the IOP was <16 mm Hg. Because only 3 patients had pseudoexfoliative glaucoma, we did not further investigate the results by type of glaucoma. This could constitute a topic for further research. In addition, follow-up of all patients is being continued for 3 years to allow future coherent cohort analysis with long-term follow-up.

Our study has several limitations. The study was an open and non-randomized case series study. Baseline IOP without wash-out was analyzed. In their work, Ferguson et al.¹⁶ noticed a correlation between preoperative IOP and the degree of IOP reduction observed 2 years after surgery. Patients with higher preoperative IOP achieved a significantly greater average reduction in IOP; in eyes with a preoperative IOP of 26 mm Hg or more, an average reduction of 11.28 mm Hg was obtained. Our study was a prospective study showing the results in reducing both IOP and the use of anti-glaucoma drugs at each time point. In addition, all the procedures were performed by 1 surgeon (MR) in 1 center.

The use of the iStent reduced the average number of drugs needed to control IOP in patients with open-angle glaucoma. Postoperatively, the average decrease in local anti-glaucoma drugs within the first 2 years after surgery was 1.3 fewer drugs; 74% eliminated the need for antihypertensive agents completely. These data are consistent with

the results of other studies, in which the number of anti-glaucoma eye drops used after cataract surgery with iStent implantation was monitored.^{4,11,17} Non-compliance with medical recommendations and a lack of regularity in taking anti-glaucoma drugs is still a serious problem, which may be responsible for nearly 10% of vision loss.¹⁸ Therefore, the goal of surgical treatment is not only a reduction in IOP, but also the elimination of the need for topical drugs that, when used chronically, have an adverse effect on the surface of the eyeball and reduce the effectiveness of filtration operations.


Micro-invasive procedures using minisents have a high safety profile.^{5–11} There are no complications like those following fistula follicle operations: hypotension, excessive filtration, infection, or early follicular overgrowth. Early undesirable symptoms after cataract surgery with iStent implantation are similar to those after cataract surgery alone. In our study, symptoms such as corneal erosion, conjunctival hemorrhage and erythrocytes in the anterior chamber disappeared within the first week. In addition, the rehabilitation time was significantly shorter compared to filtration procedures and there was no need for additional procedures such as administering subconjunctival metabolites, suture lysis or needling. The surface of the eyeball was not affected during the procedure, thanks to which there is still an unlimited possibility to conduct more invasive anti-glaucoma procedures.


Conclusions

The results of our study of cataract surgery combined with single iStent implantation in patients with primary open-angle glaucoma or pseudoexfoliative glaucoma suggest that this is an effective procedure. The implantation of the minisent caused a permanent decrease in intraocular pressure as well as in the number of topical anti-glaucoma drugs. Based on the types of complications observed within the first 3 years, this surgical technique can be considered a safe method.

ORCID iDs

Milena Kozera  <https://orcid.org/0000-0001-7156-3036>

Joanna Konopińska  <https://orcid.org/0000-0002-9088-6938>

Marek Rekas  <https://orcid.org/0000-0003-0429-6649>

References

- Schmidt W, Kastner C, Sternberg K, et al. New concepts for glaucoma implants: Controlled aqueous humor drainage, encapsulation prevention and local drug delivery. *Curr Pharm Biotechnol*. 2013;14(1):98–111.
- Soltau JB, Rothmann RF, Budenzo DL, et al. Risk factors for glaucoma filtering bleb infections. *Arch Ophthalmol*. 2000;118(3):338–342.
- SooHoo JR, Seibold LK, Radcliffe NM, Kahook MY. Minimally invasive glaucoma surgery: Current implants and future innovations. *Can J Ophthalmol*. 2014;49(6):528–533.
- Saheb H, Ahmed II. Micro-invasive glaucoma surgery: Current perspectives and future directions. *Curr Opin Ophthalmol*. 2012;23(2):96–104.

5. Neuhann TH. Trabecular micro-bypass stent implantation during small-incision cataract surgery for open-angle glaucoma or ocular hypertension: Long-term results. *J Cataract Refract Surg.* 2015;41(12): 2664–2671.
6. Fea AM, Consolandi G, Zola M, et al. Micro-bypass implantation for primary open-angle glaucoma combined with phacoemulsification: 4-year follow-up. *J Ophthalmol.* 2015;2015:795357.
7. Arriola-Villalobos P, Martínez-de-la-Casa J, Díaz-Valle D, Fernández-Pérez C, García-Sánchez J, García-Feijó J. Combined iStent trabecular micro-bypass stent implantation and phacoemulsification for coexistent open-angle glaucoma and cataract: A long-term study. *Br J Ophthalmol.* 2012;96(5):645–649.
8. Belovay GW, Naqi A, Chan BJ, Rateb M, Ahmed IKK. Using multiple trabecular micro-bypass stents in cataract patients to treat open-angle glaucoma. *J Cataract Refract Surg.* 2012;38(11):1911–1917.
9. Craven ER, Katz LJ, Wells JM, Giamporcaro JE; iStent Study Group. Cataract surgery with trabecular micro-bypass stent implantation in patients with mild-to-moderate open-angle glaucoma and cataract: Two-year follow-up. *J Cataract Refract Surg.* 2012;38(8):1339–1345.
10. Fea AM. Phacoemulsification versus phacoemulsification with micro-bypass stent implantation in primary open-angle glaucoma: Randomized double-masked clinical trial. *J Cataract Refract Surg.* 2010;36(3):407–412.
11. Samuelson TW, Katz LJ, Wells JM, Duh YJ, Giamporcaro JE; US iStent Study Group. Randomized evaluation of the trabecular micro-bypass stent with phacoemulsification in patients with glaucoma and cataract. *Ophthalmology.* 2011;118(3):459–467.
12. Burian HM. A case of Marfan's syndrome with bilateral glaucoma. With description of a new type of operation for developmental glaucoma (trabeculotomy ab externo). *Am J Ophthalmol.* 1960;50(6): 1187–1192.
13. Smith R. A new technique for opening the canal of Schlemm: Preliminary report. *Br J Ophthalmol.* 1960;44(6):370–373.
14. Tanihara H, Negi A, Akimoto M, et al. Surgical effects of trabeculotomy ab externo on adult eyes with primary open angle glaucoma and pseudoexfoliation syndrome. *Arch Ophthalmol.* 1993;111(12): 1653–1661.
15. Heijl A, Leske MC, Bengtsson B, Hyman L, Bengtsson B, Hussein M; Early Manifest Glaucoma Trial Group. Reduction of intraocular pressure and glaucoma progression: Results from the early manifest glaucoma trial. *Arch Ophthalmol.* 2002;120(10):1268–1279.
16. Ferguson TJ, Berdahl JP, Schweitzer JA, Sudhagoni RG. Clinical evaluation of a trabecular micro-bypass stent with phacoemulsification in patients with open-angle glaucoma and cataract. *Clin Ophthalmol.* 2016;10:1767–1773.
17. Spiegel D, Wetzel W, Neuhann T, et al. Coexistent primary open-angle glaucoma and cataract: Interim analysis of a trabecular micro-bypass stent and concurrent cataract surgery. *Eur J Ophthalmol.* 2009;19(3): 393–399.
18. European Glaucoma Society. *Terminology and Guidelines for Glaucoma.* 4th ed. Savona, Italy: Dogma; 2014:1–191.

LncRNA ANRIL negatively regulated chito oligosaccharide-induced radiosensitivity in colon cancer cells by sponging miR-181a-5p

Chunfeng Sun^{1,A,D,E}, Chen Shen^{2,B,C}, Yaping Zhang^{3,C,E}, Chunhong Hu^{4,E,F}

¹ Department of Radiology, The First Affiliated Hospital of Soochow University, Affiliated Hospital of Nantong University, Department of Nuclear Medicine, China

² Department of Gastrointestinal Surgery, Affiliated Hospital of Nantong University, China

³ Department of Radiology, The First Affiliated Hospital of Soochow University, Institute of Medicine Imaging, Soochow University, Suzhou, China

⁴ Department of Radiology, The First Affiliated Hospital of Soochow University, Suzhou, China

A – research concept and design; B – collection and/or assembly of data; C – data analysis and interpretation;

D – writing the article; E – critical revision of the article; F – final approval of the article

Advances in Clinical and Experimental Medicine, ISSN 1899–5276 (print), ISSN 2451–2680 (online)

Adv Clin Exp Med. 2021;30(1):55–65

Address for correspondence

Chunhong Hu

E-mail: gyk45663@126.com

Funding sources

Funding or sponsorship was received for this study or publication of this article from: National Key Research and Development Program of China (grant No. 2017YFC0114300), National Natural Science Foundation of China (grant No. 81771885), Nantong Science and Technology Plan Project (grant No. MS12018084), and Nantong Youth Medical Talent Research Fund Project (grant No. WQ2016087).

Conflict of interest

None declared

Received on June 7, 2020

Reviewed on July 11, 2020

Accepted on October 12, 2020

Cite as

Sun C, Shen C, Zhang Y, Hu C. LncRNA ANRIL negatively regulated chito oligosaccharide-induced radiosensitivity in colon cancer cells by sponging miR-181a-5p. *Adv Clin Exp Med.* 2021;30(1):55–65. doi:10.17219/acem/128370

DOI

10.17219/acem/128370

Copyright

© 2021 by Wrocław Medical University

This is an article distributed under the terms of the Creative Commons Attribution 3.0 Unported (CC BY 3.0) (<https://creativecommons.org/licenses/by/3.0/>)

Abstract

Background. The radiosensitivity of colon cancer cells can be regulated by noncoding RNAs.

Objectives. In this study, the lncRNA antisense non-coding RNA in the INK4 locus (ANRIL) was selected to analyze its regulatory role in chito oligosaccharides (COS)-related radiosensitivity in colon cancer cells.

Material and methods. The ANRIL expression in colon cancer cell lines was examined using real-time quantitative polymerase chain reaction (RT-qPCR), based on which we selected the cell line that presented the highest expression of ANRIL for radiosensitivity research. The cells were exposed to X-rays (0 Gy, 2 Gy, 4 Gy, and 6 Gy) and evaluated for changes in ANRIL and miR-181a-5p expression using RT-qPCR. Cell viability was evaluated using the CCK8 method, while apoptosis was detected with flow cytometry assays. Dual luciferase assays validated the binding between ANRIL and miR-181a-5p. The cell survival rates after differential COS treatments (0 mg/mL, 1.0 mg/mL, 2.0 mg/mL, 3.0 mg/mL, 4.0 mg/mL, and 5.0 mg/mL) were rated using CCK8 assay. The cells with the strongest dosage of COS (5.0 mg/mL) were selected to further investigate the role of ANRIL/miR-181a-5p in modulating the radiosensitivity observed with CCK-8 and flow cytometry assays.

Results. The ANRIL was highly expressed in colon cancer cells lines, especially in the SW480 cell line. Irradiation significantly decreased cell viability and ANRIL expression in a dose-dependent manner. The overexpression of ANRIL reduced the cell apoptosis rate after irradiation. MiR-181a-5p directly bound to ANRIL and was upregulated by irradiation in a dose-dependent manner. The suppression of miR-181a-5p decreased cell apoptosis. The COS treatment notably downregulated cell survival and promoted apoptosis in cells exposed to irradiation. The overexpression of ANRIL partially reversed COS-induced apoptosis and the inhibition rate; the upregulation of miR-181a-5p could counteract the impact of ANRIL regulation in cells.

Conclusions. The ANRIL negatively regulated radiosensitivity induced by COS in colon cancer cells by sponging miR-181a-5p.

Key words: colon cancer, lncRNA ANRIL, chito oligosaccharides, miR-181a-5p

Introduction

Colon cancer has been reported as one of the most common malignant tumors of the digestive system, with high morbidity and death rates which account for about 10% of cancer-related deaths.¹ Globally, colon cancer ranks as the 2nd most common cause of death in cancers.² Though the overall incidence rate of colon cancer is falling in many high-income countries, the morbidity of this cancer is increasing in adults under the age of 50 based on analyses in countries like the USA, Australia and Canada.³

In China, colon cancer has already become the 4th leading cause of death among all kinds of malignant tumors, with about 140,000 cases confirmed per year.⁴ Although surgery is the first choice, radiotherapy and chemotherapy are also important methods for blocking the progression of colon cancer. Furthermore, patients with local recurrence are often treated with radiotherapy, which can attack cancer cells by ionizing radiation.⁵ Nevertheless, ionizing radiation results in nearly identical damage to normal cells as cancer cells. In addition, radiotherapy also leads to cell toxicity, cancer cell resistance and immunosuppression.⁶ Hence, the dosage of irradiation should be kept beneath treatment levels in order to protect adjacent healthy tissues.⁷ Therefore, radiation sensitizers are a great help for radiotherapy in cancer patients. Chitoooligosaccharides (COS) have been reported to be an anticancer factor, which can also raise the radiosensitivity of colon cancer.⁸ However, the mechanism of COS in mediating the radiosensitivity of colon cancer is unclear. Therefore, functions of COS at the molecular level were explored in this study.

Recent studies have proven that noncoding RNAs play important roles in regulating the occurrence and progression of tumors. Among these noncoding RNAs, long noncoding RNAs (lncRNAs) have over 200 nucleotides that can encode the expression of genes without protein-coding abilities. miRNAs are endogenous, small noncoding RNAs with 19–22 nucleotides that can negatively regulate target gene expression by binding to mRNAs or suppressing their translation.⁹ According to previous discoveries, the lncRNA antisense non-coding RNA in the INK4 locus (ANRIL), the antisense RNA1 of CDKN2B, is highly expressed in colon cancer tissues and cell lines.^{10,11} Though the radiosensitivity of ANRIL has been mentioned in nasopharyngeal carcinoma,¹² its role in regulating radiosensitivity in colon cancer has seldom been investigated. On the other hand, miR-181a-5p was found to be downregulated in colon cancer and it negatively regulated MMP-14 to inhibit the migration and invasion of cancer cells.¹³ Additionally, miR-181a-5p suppressed tumor growth in vivo and promoted apoptosis of colon cancer by binding to CCAT.¹⁴ Therefore, miR-181a is known as a tumor suppressor. In addition, ANRIL was discovered in previous research to sponge miR-181a, facilitating proliferation and epithelial–mesenchymal transformation in laryngeal squamous cell carcinoma.¹⁵ Therefore, we hypothesized

that ANRIL and miR-181a-5p might play a part in mediating COS-induced radiosensitivity in colon cancer cells. The aim of this study was to explore the roles of ANRIL and miR-181a-5p in regulating the radiosensitivity of colon cancer cells.

Material and methods

Cell culture

Human colonic epithelial cell line NCM460 and colon cancer cell lines SW480, SW620 and HCT116 were all acquired from American Type Culture Collection (ATCC; Manassas, USA). The cells were cultured in Dulbecco's modified Eagle's medium (DMEM) (Gibco, Waltham, USA) containing 10% fetal bovine serum (FBS), 100 U/mL of penicillin and 100 mg/mL of streptomycin at 37°C with 5% CO₂. Cells in the log phase were selected for examination.

Cell transfection

The cell line SW480 was selected for further study because it showed the highest expression of ANRIL among the cell lines. The overexpressed ANRIL plasmid was synthesized with respect to pcDNA 3.1 vector (Invitrogen, Carlsbad, USA). In brief, the ANRIL lncRNA sequence was cloned into a pcDNA 3.1 vector, forming the overexpressed ANRIL plasmid (oeANRIL), while the empty pcDNA3.1 vector (oeNC) served as a negative control (NC). The cells were upregulated through transfection of the oeANRIL plasmid, with oeNC as its control. The upregulation of miR-181a-5p was achieved after the cells were transfected with miR-181a-5p plasmid mimics, while the negative control group was transfected with the NC plasmid mimics (Thermo Fisher Scientific, Waltham, USA). The miR-181a-5p inhibitor and inhibitor NC plasmids were purchased from Thermo Fisher. Lipofectamine™ 3000 Transfection Reagent (Invitrogen) was used during the transfection assays. In addition to the oeNC, oeANRIL, NC mimics, miR-181a-5p mimics, NC inhibitor, and miR-181a-5p inhibitor groups, a combined group was also generated through transfection using Lipofectamine™ 3000 Transfection Reagent (Invitrogen). This combined group was transfected with oeANRIL and miR-181a-5p mimics. To simplify, we named it the oeANRIL+miR-181a-5p mimic in this study. All the groups were examined with real-time quantitative polymerase chain reaction (RT-qPCR) for expression of ANRIL or miR-181a-5p.

RT-qPCR

Beyozol (Beyotime, Shanghai, China) was applied to extract total RNA from the incubated NCM460, SW480, SW620, and HCT116 cells. cDNA was then created through reverse transcription of RNA and utilized as templates for

amplification through PCR. The following conditions were used in the RT-qPCR: pre-denaturation for 5 min at 95°C, followed by 35 cycles of denaturation for 30 s at 95°C, annealing for 30 s at 60°C, and extension for 30 s at 72°C. The sequences of primers were as follows: ANRIL forward, 5'-GGGCCTCAGTGGCACATACC-3' and reverse, 5'-TGCTCTATCCGCCAATCAGG-3'¹⁶; miR-181a-5p, forward, 5'-CCGCGAACATTCAACGCTGTGCG-3' and reverse, 5'-ATCCAGTGCAGGGTCCGAGG-3'¹⁷; GAPDH, forward, 5'-CCACATCGCTCAGACACCAT-3' and reverse, 5'-ACCAGGCGCCCAATACG-3'¹⁶ and U6, forward, 5'-CAAATTCGTGAAGCGTTCCATAT-3' and reverse, 5'-GCTTCACGAATTTGCGTGTTCATCCTTGC-3'.¹⁷ The relative expressions of ANRIL and miR-181a-5p were quantified using the $2^{-\Delta\Delta Ct}$ method, normalized to GAPDH and U6.

CCK-8

Normal SW480 cells and SW480 cells transfected with oeNC, oeANRIL and a mixture of oeANRIL and miR-181a-5p mimics were seeded into a 96-well plate at a density of 1×10^4 cells per well and incubated at 37°C with 5% CO₂. Later, normal SW480 cells were divided into groups and treated with COS (0 mg/mL, 1.0 mg/mL, 2.0 mg/mL, 3.0 mg/mL, 4.0 mg/mL, and 5.0 mg/mL) and SW480 transfected with oeNC, oeANRIL, and compounds of oeANRIL and miR-181a-5p mimics were grouped and treated by COS (5.0 mg/mL). A linear accelerator (Varian, Palo Alto, USA) was then used to irradiate normal SW480, transfected SW480, SW480+COS (5.0 mg/mL) and transfected SW480+COS (5.0 mg/mL) at different dosages (0 Gy, 2 Gy, 4 Gy, and 6 Gy). For cell proliferation detection, 10 µL of CCK-8 was added into wells at 24 h, 48 h and 72 h. After the CCK-8 was added, the cells were kept incubating for another 2 h at 37°C. A Thermo Scientific Varioskan™ LUX Microplate Reader (Thermo Fisher Scientific) then was performed to check the optical density (OD) values at a wavelength of 450 nm. As for toxicity, 10 µL of CCK-8 was mixed after the SW480 cells were treated with COS for 72 h. The cells were also incubated for another 2 h and the OD values were checked at a wavelength of 570 nm with a Varioskan™ LUX Microplate Reader.

Apoptosis

Normal SW480 cells and the cell groups after transfection were seeded into a six-well plate with 1×10^6 cells per well. Then, SW480 cells in normal condition and SW480 cells transfected with oeNC, oeANRIL and oeANRIL with miR-181a-5p mimics were treated with 5.0 mg/mL of COS. Next, different doses of X-rays (0 Gy, 2 Gy, 4 Gy, and 6 Gy) were used to irradiate normal SW480 and transfected SW480 cells. An Annexin V-FITC Apoptosis Detection Kit (Beyotime) was used to check for apoptosis. Cells after irradiation were stained with Annexin V and PI, and

incubated for 15 h without light. The relative apoptosis rate was detected with a BD Biosciences FACSCalibur flow cytometer (Becton Dickinson, Franklin Lakes, USA).

Dual luciferase report assay

The online tool Starbase (<http://starbase.sysu.edu.cn>) was used to predict the potential target genes of ANRIL. Then, wild-type and mutant-type ANRIL containing miR-181a-5p binding sites were inserted into pGLO plasmids (Bio-Rad, Hercules, USA); the recombinant plasmids were named pGLO-ANRIL-wt and pGLO-ANRIL-mut. Then, NC mimics and miR-181a-5p mimics were co-transfected with pGLO-ANRIL-wt or pGLO-ANRIL-mut into the SW480 cells using Lipofectamine™ 3000. A GloMax® Discover Microplate Reader (Promega, Madison, USA) was used to detect luciferase activity.

Statistical analysis

All data is presented as mean ± standard deviation (SD) and was analyzed in GraphPad Prism 7 (GraphPad Software, La Jolla, USA). Each experiment was repeated 3 times. Comparisons among the groups were processed with Student's t-test and one-way analysis of variance (ANOVA).

Results

The ANRIL was highly expressed in the colon cancer cells and upregulating it resulted in less apoptosis.

In order to confirm the role of ANRIL, RT-qPCR was first done to analyze the expression of ANRIL. We found that ANRIL expression was much higher in the colon cancer cell lines than in the normal NCM460 cell line. Moreover, the SW480 cell line displayed the highest ANRIL expression (Fig. 1A). Therefore, the SW480 cell line was selected for subsequent experiments. The cell viability of SW480 cell groups with radiation treatment at different dosages was determined, revealing that cell viability was significantly decreased in a dose-dependent manner after irradiation (Fig. 1B). Meanwhile, ANRIL expression was significantly inhibited as the radiation dosage increased (Fig. 1C). Overexpression of ANRIL was achieved with transfection assay. The RT-qPCR results indicated significantly upregulated expression of ANRIL in the SW480 cells transfected with the oeANRIL plasmid (Fig. 1D). Moreover, the apoptosis rate notably declined in comparison with the negative control group after irradiation when ANRIL was upregulated (Fig. 1E, Supplement 1).

MiR-181a-5p was a target of ANRIL in colon cancer cells and the inhibition of miR-181a-5p suppressed the radiosensitivity of the cells.

Using an online bioinformatics tool, putative binding sites between miR-181a-5p and ANRIL were displayed (Fig. 2A).

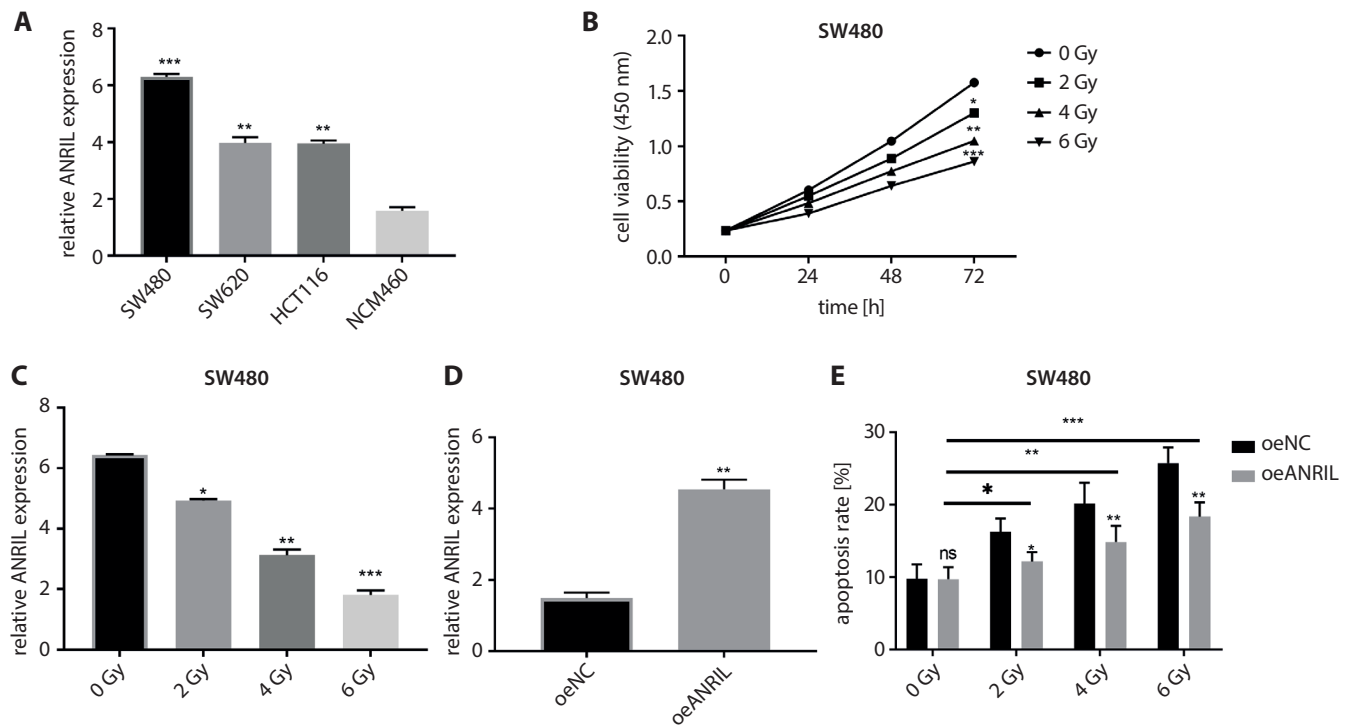


Fig. 1. ANRIL expression was higher in colon cancer cells with downregulating radiosensitivity and apoptosis

A. RNA levels of ANRIL in SW480, SW620, HCT116, and NCM460 were assessed with RT-qPCR, with NCM460 group as a negative control group (* $p < 0.1$, ** $p < 0.05$, *** $p < 0.01$); B. The cell viability of SW480 with X-ray irradiation (0 Gy, 2 Gy, 4 Gy, and 6 Gy) was evaluated using CCK-8, with 0 Gy group as a control group (* $p < 0.1$, ** $p < 0.05$, *** $p < 0.01$); C. The expression of ANRIL at X-ray dosages of 0 Gy, 2 Gy, 4 Gy, and 6 Gy was evaluated using RT-qPCR, with 0 Gy group as a control group (* $p < 0.1$, ** $p < 0.05$, *** $p < 0.01$); D. Overexpressed ANRIL expression was evaluated using RT-qPCR (** $p < 0.05$); E. SW480 cells after transfection with oeNC and oeANRIL plasmids were exposed to radiation (0 Gy, 2 Gy, 4 Gy, and 6 Gy) and then measured using flow cytometry for apoptosis rates. In the same irradiation groups, the oeANRIL group was compared to the oeNC group (* $p < 0.1$, ** $p < 0.05$, *** $p < 0.01$). In addition, the overexpressed groups were compared when they were exposed to different dosages of radiation, with 0 Gy as a negative control (* $p < 0.1$, ** $p < 0.05$, *** $p < 0.01$). Each experiment was run in triplicate.

Dual luciferase reporter assay was used for verification at the binding sites. It was found that the combined group of miR-181a-5p mimics and wild-type ANRIL had significantly low luciferase activity in comparison with the remaining groups, confirming that miR-181a-5p was targeted by ANRIL (Fig. 2B). Then, the expression of miR-181a-5p was examined when the cells were exposed to radiation; the results revealed that miR-181a-5p was significantly up-regulated with increasing X-ray doses (Fig. 2C). Therefore, a transfection assay was conducted to suppress miR-181a-5p in the SW480 cells (Fig. 2D). Apoptosis was also dramatically reduced by inhibiting miR-181a-5p in cells. In general, apoptosis rates were elevated with increasing dosages of X-ray treatment (Fig. 2E, Supplement 2).

The upregulation of ANRIL inhibited COS-induced radiosensitivity in colon cancer cells by targeting miR-181a-5p.

The cell toxicity of COS in the SW480 cells was checked and the results showed that the survival rate significantly decreased as the concentration of COS increased (Fig. 3A). The SW480 cells treated with 5.0 mg/mL of COS were chosen for the following analysis. The cells with or without 5.0 mg/mL COS treatment underwent different irradiation and were then examined using flow cytometry

for apoptosis; it was found that COS treatment induced more apoptosis and led to higher sensitivity to higher dosages of X-ray exposure (Fig. 3B, Supplement 3). The functions of ANRIL and miR-181a-5p in modulating COS were also investigated. Upregulated ANRIL significantly downregulated the cell inhibition rate, while miR-181a-5p mimics partially counteracted this (Fig. 3C). Meanwhile, apoptosis inhibited by ANRIL upregulation was reversed by miR-181a-5p mimics dose-dependently to a certain degree (Fig. 3D, Supplement 4). As Fig. 3B depicts, COS induced apoptosis in cells dose-dependently. Taking the results from Fig. 3D and Fig. 3B together, we decided that ANRIL could inhibit COS-induced apoptosis and deteriorate the radiosensitivity stimulated by COS by targeting and suppressing miR-181a-5p.

Discussion

Though medical technology has developed with the rapid growth of economy, the risks of cancers have not been eliminated. The occurrence rate of colon cancer in China has risen by more than 2 times the international rate.¹⁸ Under such circumstances, it is urgent

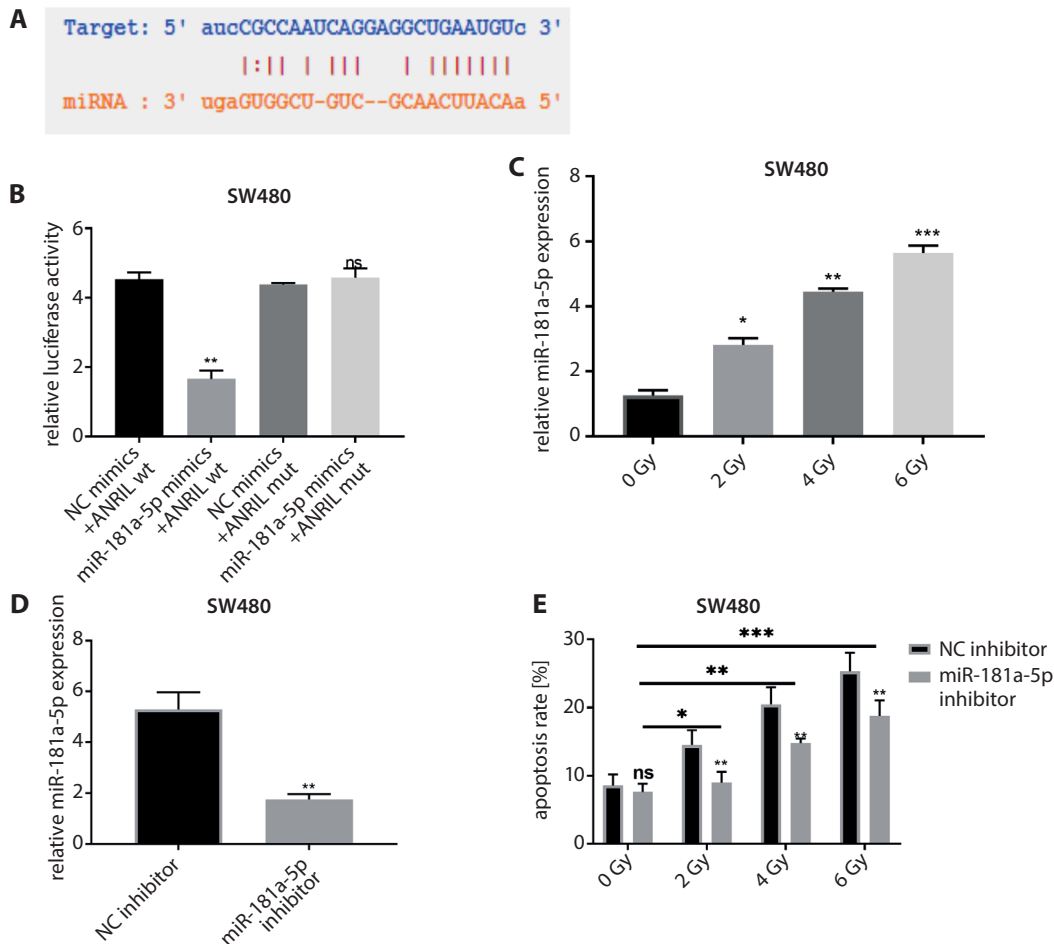


Fig. 2. miR-181a-5p was a target of ANRIL in colon cancer cells and the inhibition of miR-181a-5p suppressed the radiosensitivity of the cells

A. Putative binding sites of miR-181a-5p and ANRIL were predicted using Starbase (<http://starbase.sysu.edu.cn>); B. Luciferase reporter assays were performed to verify the binding between ANRIL and miR-181a-5p (** p < 0.05); C. miR-181a-5p expression was measured using RT-qPCR in SW480 cells exposed to X-rays (0 Gy, 2 Gy, 4 Gy, and 6 Gy), with 0 Gy group as a negative control (* p < 0.1, ** p < 0.05, *** p < 0.01); D. miR-181a-5p expression was detected using RT-qPCR after the cells were transfected with negative control (NC) inhibitor and miR-181a-5p inhibitor plasmids (* p < 0.1, ** p < 0.05, *** p < 0.01); E. Apoptosis rates were validated using flow cytometry (* p < 0.1, ** p < 0.05, *** p < 0.01). In the groups exposed to the same X-ray dosage (NC inhibitor and miR-181a-5p inhibitor), the miR-181a-5p inhibitor group was compared to the NC inhibitor group, while in groups exposed to different dosages, we mainly compared the apoptosis rates in miR-181a-5p inhibitor groups with the 0-Gy treatment group as a control group (* p < 0.1, ** p < 0.05, *** p < 0.01). All experiments were carried out 3 times.

to find efficient treatments for colon cancer. Radiotherapy is widely used in various stages of tumor treatment, which can shrink the tumor before surgery and remove residues after surgery to better prevent recurrence.¹⁹ However, radiotherapy also causes damage to normal cells, which places a burden on patients. Therefore, increasing the radiosensitivity of tumor cells is a key issue in improving the effects of radiotherapy in cancer. This study aimed to explore the regulatory roles of the lncRNA ANRIL and miR-181a-5p in COS-induced radiosensitivity in colon cancer cells. In our study, we first selected the colon cancer cell lines SW480, SW620 and HCT116, and the normal colonic epithelial cell line NCM460 for ANRIL expression. The ANRIL has been found to be abnormally expressed in many kinds of cancers, such as gastric cancer, lung cancer, hepatocellular carcinoma, etc.²⁰ In colon cancer, ANRIL was also reported to be an oncogene that can

accelerate the progression of colon cancer.²¹ Therefore, we studied ANRIL and its regulation of radiosensitivity in colon cancer cells. The ANRIL expression was higher in colon cancer cell lines than in normal NCM460, and was significantly downregulated as radiation dosages increased. The overexpression of ANRIL reduced the rate of apoptosis induced by COS and as the radiation dose increased, the reverse effect was more significant. Therefore, ANRIL was primarily proven to block radiosensitivity in colon cancer cells.

As a potential target gene of ANRIL, miR-181a-5p was widely known as a tumor suppressor, including colon cancer.^{22,23} However, regulation of miR-181a-5p in radiosensitivity in cancers was seldom mentioned before. In this study, miR-181a-5 was confirmed to have binding sites for ANRIL and it directly bound to wild-type ANRIL. Moreover, miR-181a-5p was significantly upregulated

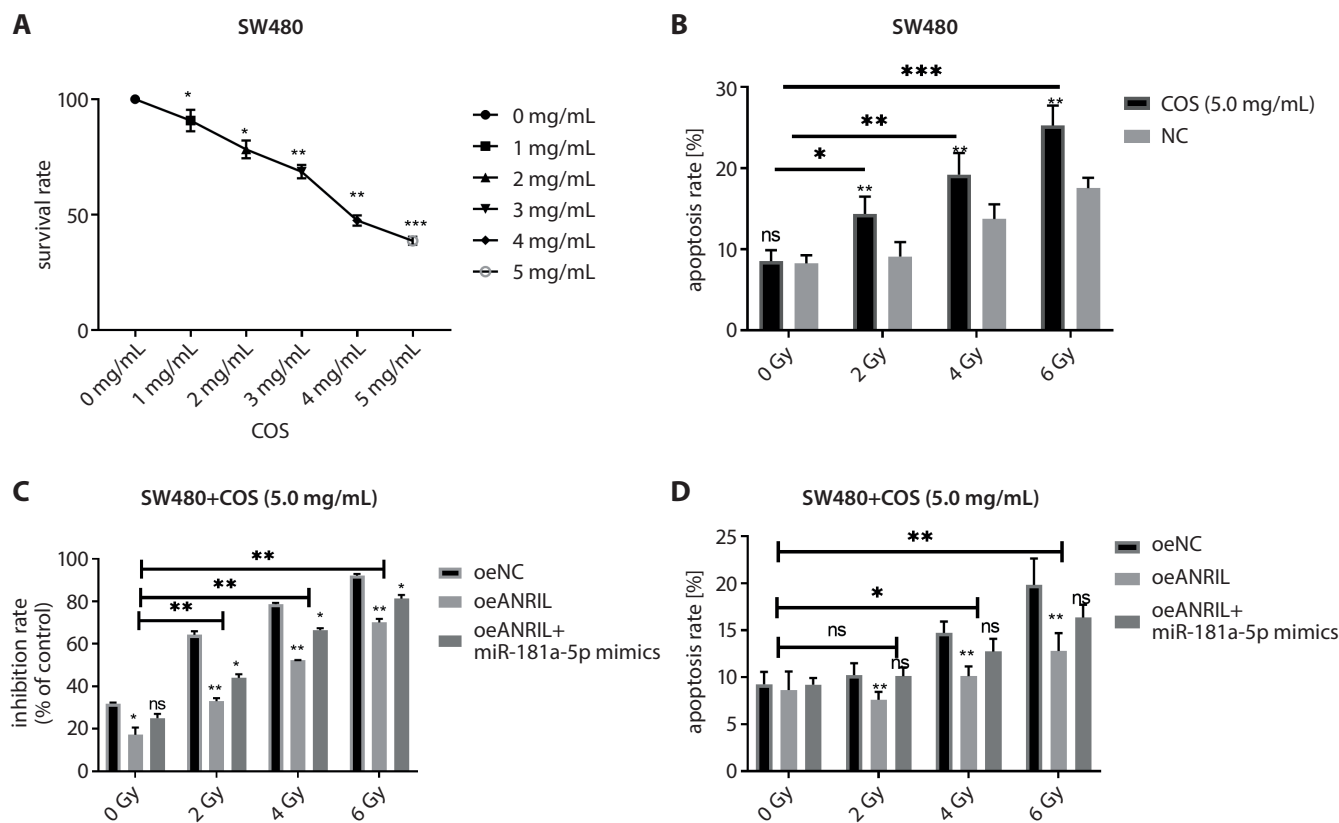


Fig. 3. Overexpressed miR-181a-5p upregulated COS-induced radiosensitivity in colon cancer cells by suppressing ANRIL expression

A. Cell survival rates were evaluated using CCK8 assays when the cells were treated with COS (0 mg/mL, 1.0 mg/mL, 2.0 mg/mL, 3.0 mg/mL, 4.0 mg/mL, and 5.0 mg/mL) (* $p < 0.1$, ** $p < 0.05$, *** $p < 0.01$); B. SW480 cells after COS treatment (5.0 mg/mL) were exposed to X-rays (0 Gy, 2 Gy, 4 Gy, and 6 Gy) and apoptosis was evaluated using flow cytometry, with the 0 Gy treatment group serving as a control group (* $p < 0.1$, ** $p < 0.05$, *** $p < 0.01$); C. SW480 cells transfected with oeNC, oeANRIL and oeANRIL+miR-181a-5p mimics underwent COS treatment (5.0 mg/mL) and were then exposed to X-rays (0 Gy, 2 Gy, 4 Gy, and 6 Gy). The inhibition rates were assessed with CCK-8. Within the same X-ray treatment group, the oeANRIL group was compared to the oeNC group, while the combined group was compared with the oeANRIL group (* $p < 0.1$, ** $p < 0.05$, *** $p < 0.01$). Meanwhile, the general differences when cells were exposed to different dosages of X-rays were compared with 0 Gy group as a control group (* $p < 0.1$, ** $p < 0.05$, *** $p < 0.01$); D. Apoptosis rate was evaluated in each subgroup. Within the same X-ray treatment group, the oeANRIL group was compared to the oeNC group, while the combined group was compared with the oeANRIL group (* $p < 0.1$, ** $p < 0.05$, *** $p < 0.01$). Meanwhile, the general differences between cells exposed to different dosages of X-rays were compared with 0 Gy group as a control group (* $p < 0.1$, ** $p < 0.05$, *** $p < 0.01$). Each experiment was carried out 3 times.

by irradiation and upregulating miR-181a-5p partially alleviated the suppressive function of ANRIL against COS in apoptosis and radiosensitivity in colon cancer cells. Therefore, in this in vitro model, we have proven that miR-181a-5p can serve as a biomarker that might contribute to radiosensitivity by reversing the functions of ANRIL in colon cancer cells.

The COS are of a chitinous substance which is reported to be an anti-tumor factor.²⁴ In various cancers, COS are well-known as a radiation sensitizer which could help to deter cell proliferation.^{25,26} The COS have been proven to promote radiosensitivity by accelerating cell apoptosis in colon cancer.⁸ However, the underlying molecular mechanisms of COS are rarely mentioned. We first measured the toxicity of COS to SW480 cells, revealing that survival rates decreased significantly as concentrations of COS grew. Moreover, SW480 cells with COS treatment promoted apoptosis, compared to untreated cells after irradiation. Additionally, the reduced cell inhibition rate and apoptosis provoked by ANRIL upregulation can be restored by miR-181a-5p

mimics after COS treatment. Taken together, we concluded that ANRIL upregulation could inhibit COS-induced radiosensitivity by targeting miR-181a-5p.

Conclusions

The lncRNA ANRIL was highly expressed in colon cancer cells and suppressed radiosensitivity by binding to miR-181a-5p and reversing the functions of COS, suggesting that those 2 genes might be involved in sensitivity regulation in radiotherapy of colon cancer. However, in vivo and clinical studies are needed to further validate this finding.

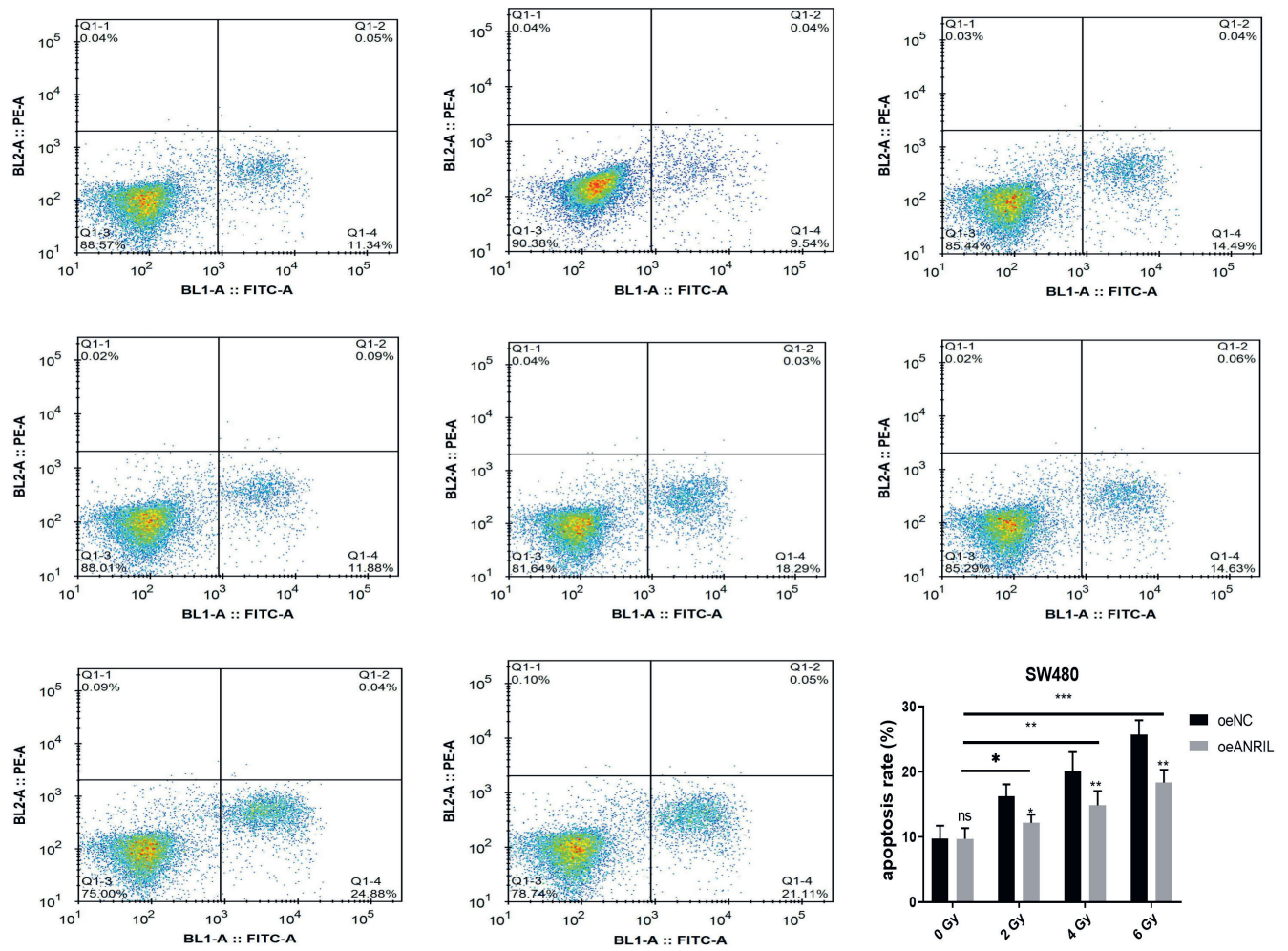
ORCID iDs

Chunfeng Sun <https://orcid.org/0000-0002-4602-7706>
 Chen Shen <https://orcid.org/0000-0002-7854-6877>
 Yaping Zhang <https://orcid.org/0000-0002-0730-5689>
 Chunhong Hu <https://orcid.org/0000-0002-2548-2654>

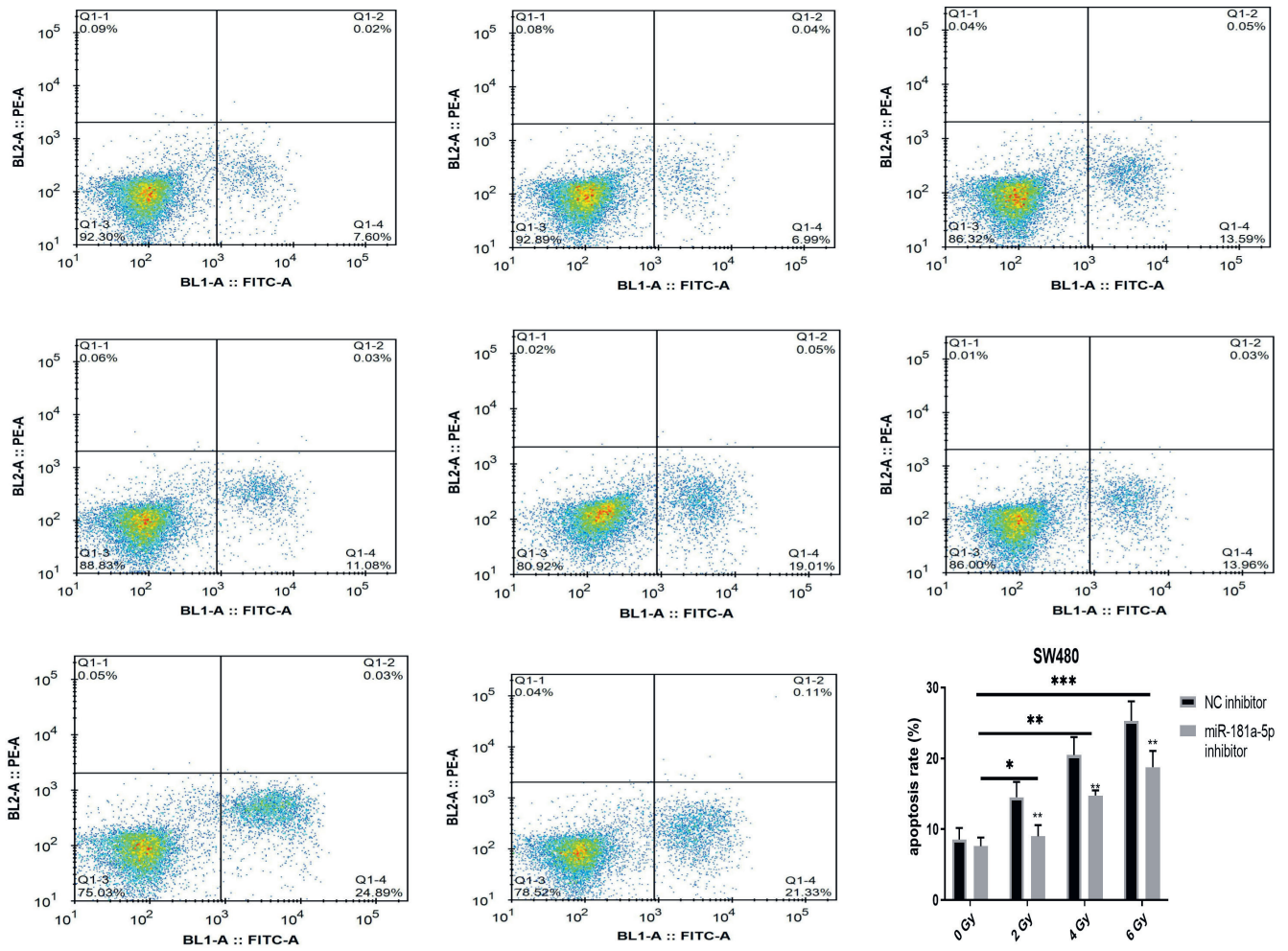
References

1. Siegel R, Desantis C, Jemal A. Colorectal cancer statistics, 2014. *CA Cancer J Clin.* 2014;64(2):104–117.
2. Wu RL, Wang R, Yin R, et al. Epigenetics/epigenomics and prevention by curcumin of early stages of inflammatory-driven colon cancer. *Mol Carcinog.* 2020;59(2):227–236.
3. Araghi MI, Soerjomataram A, Bardot J, et al. Changes in colorectal cancer incidence in seven high-income countries: A population-based study. *Lancet Gastroenterol Hepatol.* 2019;4(7):511–518.
4. Zhai X, Xue Q, Liu Q, Guo Y, Chen Z. Colon cancer recurrence associated genes revealed by WGCNA co expression network analysis. *Mol Med Rep.* 2017;16(5):6499–6505.
5. Yadollahpour AZ, Rezaee V, Bayati V, Tahmasebi Birgani MJ, Negad Dehbashi F. Radiotherapy enhancement with electroporation in human intestinal colon cancer HT-29 cells. *Asian Pac J Cancer Prev.* 2018;19(5):1259–1262.
6. Lettieri-Barbato D, Aquilano K. Pushing the limits of cancer therapy: The nutrient game. *Front Oncol.* 2018;8:148.
7. Hainfeld JF, Dilmanian FA, Slatkin DN, Smilowitz HM. Radiotherapy enhancement with gold nanoparticles. *J Pharm Pharmacol.* 2008;60(8):977–985.
8. Han FS, Yang SJ, Lin MB, Chen YQ, Yang P, Xu JM. Chitooligosaccharides promote radiosensitivity in colon cancer line SW480. *World J Gastroenterol.* 2016;22(22):5193–5200.
9. Hutvagner G, Zamore PD. A microRNA in a multiple-turnover RNAi enzyme complex. *Science.* 2002;297(5589):2056–2060.
10. Gan Y, Ma W, Wang X, et al. Coordinated transcription of ANRIL and P16 genes is silenced by P16 DNA methylation. *Chin J Cancer Res.* 2018;30(1):93–103.
11. Ma W, Qiao J, Zhou J, Gu L, Deng D. Characterization of novel LncRNA P14AS as a protector of ANRIL through AUF1 binding in human cells. *Mol Cancer.* 2020;19(1):42.
12. Hu X, Jiang H, Jiang X. Downregulation of lncRNA ANRIL inhibits proliferation, induces apoptosis, and enhances radio-sensitivity in nasopharyngeal carcinoma cells through regulating miR-125a. *Cancer Biol Ther.* 2017;18(5):331–338.
13. Li Y, Kuscu C, Banach A, et al. miR-181a-5p inhibits cancer cell migration and angiogenesis via downregulation of matrix metalloproteinase-14. *Cancer Res.* 2015;75(13):2674–2685.
14. Shang A, Wang W, Gu C, et al. Long non-coding RNA CCAT1 promotes colorectal cancer progression by regulating miR-181a-5p expression. *Aging (Albany N Y).* 2020;12(9):8301–8320.
15. Hao YR, Zhang DJ, Fu ZM, Guo YY, Guan GF. Long non-coding RNA ANRIL promotes proliferation, clonogenicity, invasion and migration of laryngeal squamous cell carcinoma by regulating miR-181a/Snai2 axis. *Regen Ther.* 2019;11:282–289.
16. Guan H, Mei Y, Mi Y, et al. Downregulation of lncRNA ANRIL suppresses growth and metastasis in human osteosarcoma cells. *Onco Targets Ther.* 2018;11:4893–4899.
17. Mao W, Huang X, Wang L, et al. Circular RNA hsa_circ_0068871 regulates FGFR3 expression and activates STAT3 by targeting miR-181a-5p to promote bladder cancer progression. *J Exp Clin Cancer Res.* 2019;38(1):169.
18. Jia WH, Zhang B, Matsuo K, et al. Genome-wide association analyses in East Asians identify new susceptibility loci for colorectal cancer. *Nat Genet.* 2013;45(2):191–196.
19. Bolla M, van Poppel H, Tombal B, et al. Postoperative radiotherapy after radical prostatectomy for high-risk prostate cancer: Long-term results of a randomised controlled trial (EORTC trial 22911). *Lancet.* 2012;380(9858):2018–2027.
20. Li Z, Yu X, Shen J. ANRIL: A pivotal tumor suppressor long non-coding RNA in human cancers. *Tumour Biol.* 2016;37(5):5657–5661.
21. Wu M, Li W, Huang F, et al. Comprehensive analysis of the expression profiles of long non-coding RNAs with associated ceRNA network involved in the colon cancer staging and progression. *Sci Rep.* 2019;9(1):16910.
22. Han P, Li JW, Zhang BM, et al. The lncRNA CRNDE promotes colorectal cancer cell proliferation and chemoresistance via miR-181a-5p-mediated regulation of Wnt/ β -catenin signaling. *Mol Cancer.* 2017;16(1):9.
23. Wu L, Song WY, Xie Y, et al. miR-181a-5p suppresses invasion and migration of HTR-8/SVneo cells by directly targeting IGF2BP2. *Cell Death Dis.* 2018;9(2):16.
24. Kim EK, Je JY, Lee SJ, et al. Chitooligosaccharides induce apoptosis in human myeloid leukemia HL-60 cells. *Bioorg Med Chem Lett.* 2012;22(19):6136–6138.
25. Han FS, Cui BH, You XF, Xing YF, Sun XW. Anti-proliferation and radiosensitization effects of chitooligosaccharides on human lung cancer line HepG2. *Asian Pac J Trop Med.* 2015;8(9):757–761.
26. Luo Y, Deng L, Deng QJ, Wen L. Comparative study of the chitooligosaccharides effect on the proliferation inhibition and radiosensitization of three types of human gastric cancer cell line. *Asian Pac J Trop Med.* 2016;9(6):601–605.

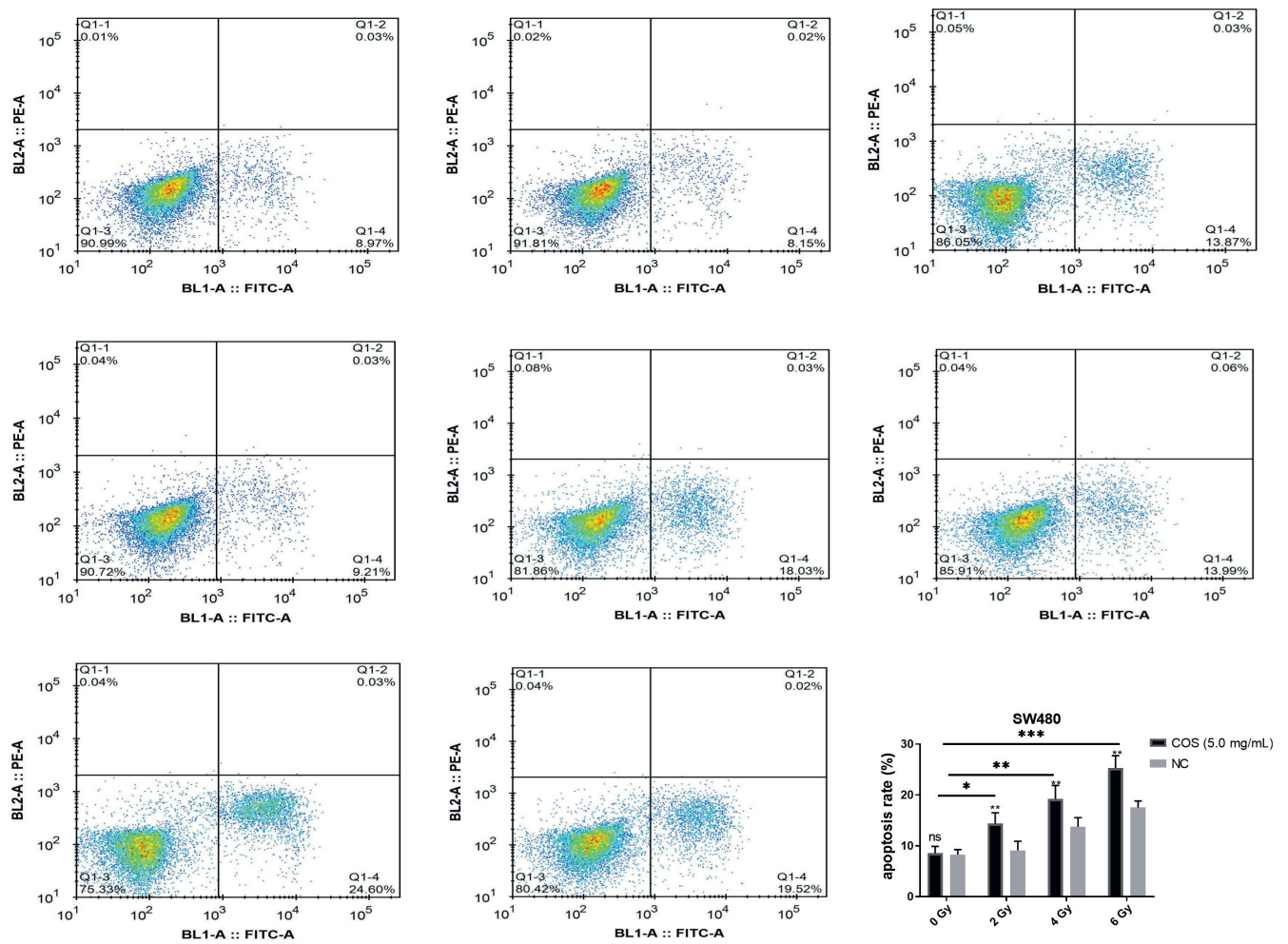
Supplement 1. Flow cytometry images for Fig. 1E. The images (from left to right and up to down) were put in the order of the groups in Fig. 1E



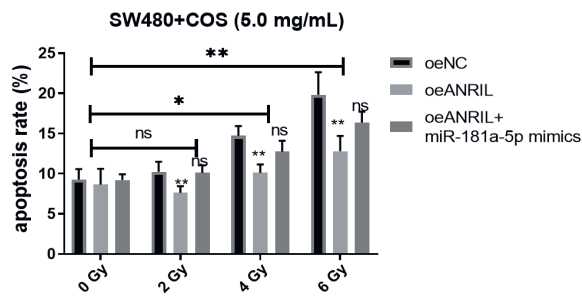
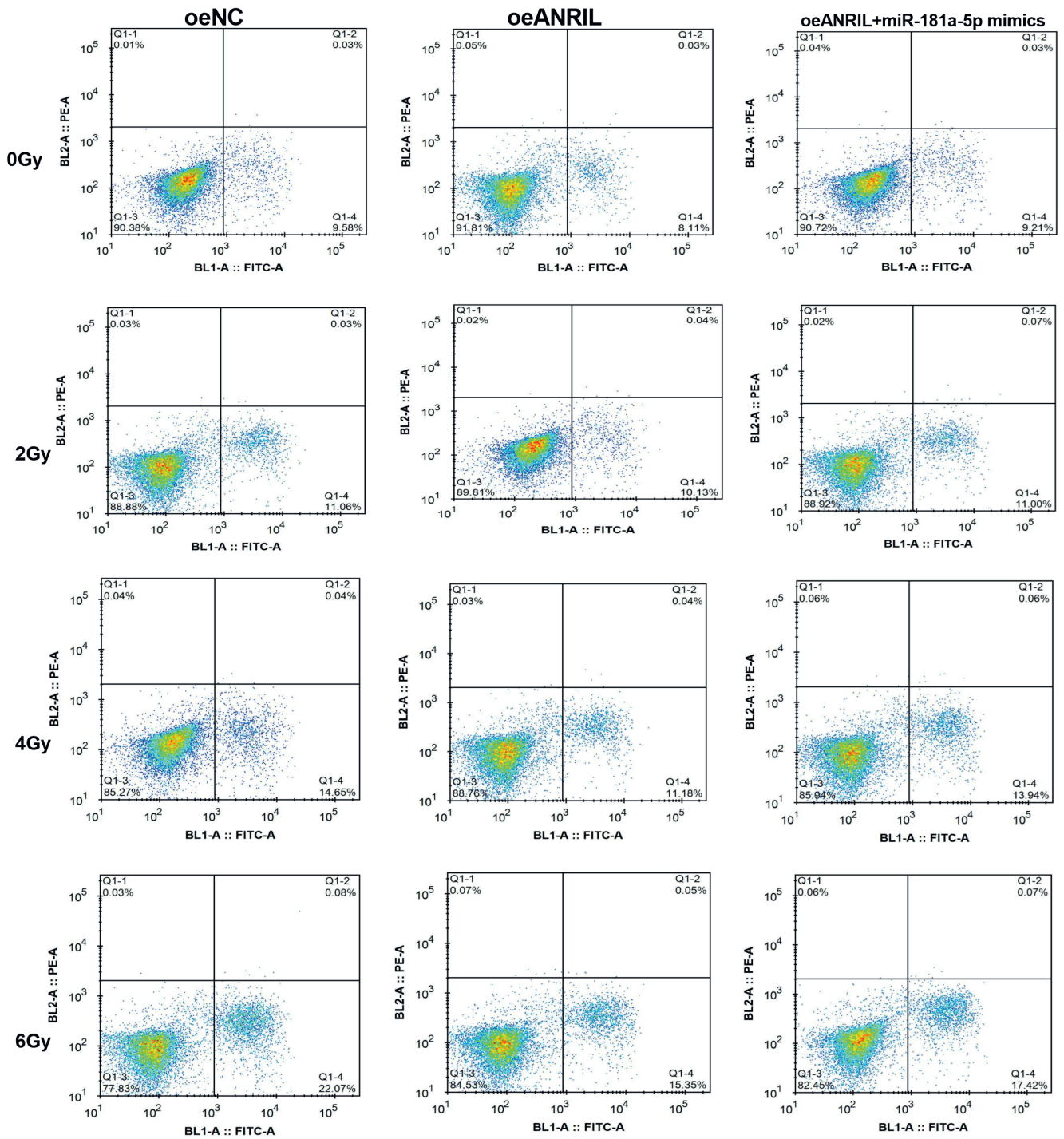
Supplement 2. Flow cytometry images for Fig. 2D. The images (from left to right and up to down) were put in the order of the groups in Fig. 2D



Supplement 3. Flow cytometry images for Fig. 3B. The images (from left to right and up to down) were put in the order of the groups in Fig. 3B



Supplement 4. Flow cytometry images for Fig. 3D. The images were put in the order of the groups in Fig. 3D



Sacubitril/valsartan for heart failure with reduced ejection fraction: A first real-life observational study in Poland

Małgorzata Lelonek^{1,A–F}, Sylwia Wiśniowska-Śmiałek^{2,B–D,F}, Paweł Rubiś^{2,A–F}, Izabela Nowakowska^{3,B,F}, Agnieszka Pawlak^{4,A–F}

¹ Department of Noninvasive Cardiology, Medical University of Lodz, Poland

² Department of Cardiac and Vascular Diseases, Jagiellonian University Medical College, Kraków, Poland

³ Department of Invasive Cardiology, Central Clinical Hospital of the Ministry of the Interior and Administration, Warszawa, Poland

⁴ Department of Invasive Cardiology, Center of Postgraduate Medical Education, Warszawa, Poland

A – research concept and design; B – collection and/or assembly of data; C – data analysis and interpretation;

D – writing the article; E – critical revision of the article; F – final approval of the article

Advances in Clinical and Experimental Medicine, ISSN 1899–5276 (print), ISSN 2451–2680 (online)

Adv Clin Exp Med. 2021;30(1):67–75

Address for correspondence

Małgorzata Lelonek

E-mail: malgorzata.lelonek@umed.lodz.pl

Funding sources

None declared

Conflict of interest

All authors report consultancy and lectures fees from Novartis and also participation in trials with sacubitril/valsartan.

Received on May 25, 2020

Reviewed on September 23, 2020

Accepted on October 8, 2020

Cite as

Lelonek M, Wiśniowska-Śmiałek S, Rubiś P, Nowakowska I, Pawlak A. Sacubitril/valsartan for heart failure with reduced ejection fraction: A first real-life observational study in Poland. *Adv Clin Exp Med.* 2021;30(1):67–75. doi:10.17219/acem/128230

DOI

10.17219/acem/128230

Copyright

© 2021 by Wrocław Medical University

This is an article distributed under the terms of the Creative Commons Attribution 3.0 Unported (CC BY 3.0) (<https://creativecommons.org/licenses/by/3.0/>)

Abstract

Background. Despite the progress in the treatment of heart failure with reduced ejection fraction (HFrEF), the prognosis remains unfavorable.

Objectives. To evaluate the effectiveness, tolerance and safety after one-year follow-up of Polish patients with stable chronic HFrEF treated with sacubitril/valsartan.

Material and methods. This was an observational multicenter study conducted in 3 centers (Kraków, Łódź and Warszawa) specializing in heart failure (HF). We enrolled 89 HFrEF patients (aged 59.3 ± 13.5 years, 82% males) in NYHA class II–IV (ambulatory). Clinical, laboratory and echocardiographic parameters were evaluated at baseline and after a one-year follow-up. The composite endpoint was defined as death or urgent HF hospitalization.

Results. After 1 year, 80% of patients used 50% or more of the target dose of sacubitril/valsartan. After a year of treatment, there were significant improvements of HF symptoms, N-terminal prohormone B-type natriuretic peptide (NT proBNP), ejection fraction (EF), and distance in six-minute walk test (6MWP) (all $p < 0.001$). Patients treated with the highest dose of sacubitril/valsartan exhibited the greatest benefits. The safety profile was favorable and consistent with that previously reported; however, therapy discontinuation due to side effects occurred in 11% of patients. The independent predictors for composite endpoint ($n = 24$, 26.9%) were history of HF hospitalization, tricuspid annular plane systolic excursion (TAPSE) and angiotensin-converting-enzyme inhibitor (ACEI)-naive patients.

Conclusions. Treatment of chronic HFrEF patients with sacubitril/valsartan is safe and is associated with significant clinical and objective improvement. The non-survivors had more advanced HF, so the initiation and uptitration of sacubitril/valsartan should be done early.

Key words: sacubitril/valsartan, heart failure with reduced ejection fraction, ARNI

Introduction

The prevalence of heart failure (HF) rises exponentially and affects approx. 1–2% of the adult population; however, it can be as high as 10% in elderly patients.^{1–3} Patients with HF with reduced ejection fraction (HFrEF) constitute approx. 40–50% of all chronic HF patients and are broadly characterized by younger age, more prevalent coronary artery disease (CAD) and worse survival in comparison to HF with relatively preserved ejection fraction (EF).⁴ On the other hand, the population of HFrEF patients is much better studied, and effective and proven therapies have been successfully introduced over the last couple of decades, which have favorably improved the outcomes.⁴

Among effective therapies, a novel class of agents acting simultaneously on the renin-angiotensin-aldosterone system (RAAS) and the neutral endopeptidase system – angiotensin receptor neprilysin inhibitors (ARNI) – has shown promise for numerous HFrEF patients.⁵ In the landmark PARADIGM-HF study, ARNI was clearly superior to enalapril in improving the symptoms and prognosis for HF patients caused by ischemic or non-ischemic HFrEF.⁶ So far, numerous papers that clearly confirmed the benefits of sacubitril/valsartan (ARNI) in the various subgroups of HFrEF patients from different geographical settings have been published. Unfortunately, so far, sacubitril/valsartan is not reimbursed in Poland (unlike in other European and non-European countries) for HFrEF patients, which results in underutilization of this novel treatment in Polish patients. Consequently, the experience with ARNI is limited in Poland.

Therefore, this study aims to respond to the as-yet unmet clinical need to investigate the subject of clinical experience with sacubitril/valsartan in a mid-sized HFrEF cohort from 3 HF referral centers in central and southern Poland.

Material and methods

This observational multicenter study was conducted in 3 clinical centers in Poland (Kraków, Łódź and Warszawa) specializing in HF. The study included 89 patients suffering from chronic HFrEF. The inclusion criteria were as follows: stable (defined as at least 4 weeks without HF exacerbation) and symptomatic HF categorized as NYHA (New York Heart Association) class II–IV (ambulatory); left ventricular ejection fraction (LVEF) lower than or equal to 40%; and optimal treatment of HFrEF according to the guidelines of the European Society of Cardiology (ESC).⁴ The exclusion criteria were: hypotension (systolic blood pressure (SBP) <100 mm Hg), renal dysfunction with estimated glomerular filtration rate (eGFR) <30 mL/min/1.73 m², hyperkalemia >5.4 mmol/L, history of angioedema, and thyroid dysfunction.

The comprehensive analysis of clinical, laboratory and echocardiographic parameters was performed and included the following:

- age, gender, body mass index (BMI), and systolic (SBP) and diastolic (DBP) arterial blood pressure,
- coincidence of arterial hypertension, diabetes mellitus (DM), CAD, history of myocardial infarction, atrial fibrillation (AF), renal failure, chronic obstructive pulmonary diseases (COPD), cancer, and coronary interventions such as percutaneous coronary intervention (PCI) or coronary artery bypass graft (CABG);
- electrotherapy – cardiac resynchronization therapy (CRT-D, CRT-P) and implantable cardioverter defibrillator (ICD);
- HF etiology (ischemic compared to non-ischemic) and duration of HF;
- basic laboratory results, i.e., N-terminal prohormone B-type natriuretic peptide (NT-proBNP) and high-sensitivity troponin T, creatinine with eGFR, and potassium level;
- electrocardiography (ECG) variables: heart rhythm and heart rate (HR), QRS duration;
- selected echocardiographic results, i.e., LVEF, end-diastolic volume (EDV)/end-systolic volume (ESV) of left ventricle, right ventricular diameter (RVD), tricuspid annular plane systolic excursion (TAPSE), pulmonary artery systolic pressure (PASP), volume of left atrium;
- drugs and doses of standard HFrEF therapy: angiotensin-converting-enzyme inhibitors (ACEI), angiotensin receptor blockers (ARB), β -blockers (BB), mineralocorticoid receptor antagonist (MRA), ivabradine, diuretics, and digoxin;
- results of six-minute walking test (6MWT);
- MAGGIC (Meta-Analysis Global Group in Chronic Heart Failure) score.⁷

During a one-year follow-up, the following factors were analyzed: clinically important variables (NYHA class, arterial blood pressure, HR, QRS duration, LVEF, NT-proBNP, 6MWT, creatinine, and potassium level), and the composite endpoint (death and/or HF hospitalization).

The paper also includes an analysis of the sacubitril/valsartan safety and tolerability profile.

Initial dose of sacubitril/valsartan and increase to the target maintenance dose

Patients enrolled in the study received a starting dose of sacubitril/valsartan as 1 tablet of 24/26 mg twice daily or 49/51 mg twice daily, as recommended.⁸ The sacubitril/valsartan 24/26 mg initial dose was used in patients with SBP \geq 100–110 mm Hg, in patients not currently taking ACE-I or ARB, or taking low doses of these medicinal products, and in patients with moderate renal impairment (eGFR 30–60 mL/min/1.73 m²) or moderate hepatic insufficiency (Child–Pugh class B). Sacubitril/valsartan 49/51 mg was used in patients with SBP > 110 mm Hg, and normal eGFR and serum potassium level. The dose was doubled at 2–4 weeks to the target dose of 1 tablet of 97/103 mg twice daily, as tolerated by the patient with

normal pressure tolerance, normal eGFR and normal serum potassium level.

The dose was temporarily reduced or discontinued in case of symptomatic SBP \leq 90 mm Hg, hyperkalemia >5.4 mmol/L and worsening renal function defined as eGFR < 30 mL/min/1.73 m². Patients received sacubitril/valsartan at least 36 h after discontinuing ACE inhibitor therapy.

Statistical analysis

Quantitative variables are reported as mean and standard deviation (SD) or, for non-normally distributed variables, the median and interquartile range (IQR). Normality of the variables was verified using the Shapiro–Wilk normality test. For categorical variables, the number of observations (N) with the corresponding percentage (%) is given.

To compare 2 independent groups, Student's t-test for quantitative variables with normal distribution or the non-parametric Mann–Whitney U test for non-normally distributed variables were used. To compare more than 2 independent groups, analysis of variance (ANOVA, for normally distributed quantitative variables) or the Kruskal–Wallis test (if the distributions of variables were different from normal) with post hoc multiple comparisons (Tukey's honest significant difference (HSD) test) was used.

For categorical variables, Pearson's χ^2 test, the maximum likelihood (ML) χ^2 test or χ^2 test with Yates's correction was applied (regarding the expected counts in the contingency tables).

The paired sample t-test (for normally distributed quantitative variables) or the nonparametric Wilcoxon signed-rank test (for non-normally distributed quantitative variables) or the McNemar–Bowker test with correction for continuity (for categorical variables) was used to compare 2 dependent groups (before and after the treatment).

Variables significant in univariate comparisons at $p < 0.05$ were included in the multivariable stepwise logistic regression model to determine the independent risk factors of the composite endpoint.

Taking into account the time to event (i.e., the time to death, the composite endpoint), the Kaplan–Meier survival curves were determined. To compare 2 Kaplan–Meier curves, the log-rank test was applied. The Cox proportional hazards model was used to determine the independent risk factors of the composite endpoint.

The results were considered statistically significant at $p < 0.05$. All the calculations were performed using the STATISTICA PL v. 13.3 package (StatSoft Inc., Tulsa, USA). The studied population was analyzed in relation to HF etiology: ischemic compared to non-ischemic and composite endpoint.

The study design was approved by the Bioethics Committee of the Jagiellonian University, Kraków, Poland (approval No. 1072.6120.55.2020).

Results

Table 1 shows the baseline characteristics of the total population and the analyzed groups of patients, divided according to HF etiology into ischemic HF ($n = 42$, 47%) and non-ischemic HF, caused mainly by dilated cardiomyopathy (DCM), arrhythmias or primary valvular heart diseases. Patients with non-ischemic HF were younger, had shorter duration of HF, had more preserved renal function, larger left ventricles and lower EF, but they had higher low-density lipoprotein (LDL) levels. The 2 groups did not differ in terms of baseline blood pressure, HR, NYHA class, number of comorbidities, NT-proBNP levels, or baseline HF medications.

For the total population, the comparison of clinically relevant parameters between baseline and at one-year assessment is presented in Table 2. Overall, NYHA class, distance in the 6MWT, LVEF, and NT-proBNP levels significantly improved after a year of treatment. Further, we observed significant reductions in both SBP and DBP, HR, and QRS complex width. Finally, potassium levels and creatinine remained unchanged.

After a year, 20% ($n = 15$) of patients were treated with 24/26 mg of sacubitril/valsartan twice daily, 28% ($n = 20$) received 49/51 mg twice daily and 52% ($n = 38$) received the maximum dose. An adverse event in the form of hypotension, hyperkalemia or worsening renal function occurred in 17.8% ($n = 16$), 5.6% ($n = 5$) and 4.5% ($n = 4$) of patients, respectively.

In 12% ($n = 11$) of patients, the sacubitril/valsartan dose was reduced during the study. Hypotension was the cause of the dose reduction in 10 patients (11%) and the decrease of eGFR in 1 patient (1%). Sacubitril/valsartan was discontinued in 10% ($n = 9$) and hypotension was the main cause (4.5%, $n = 4$), in 1 patient at dose 49/51 mg twice daily and in 3 patients at 97/103 mg twice daily. One patient (1%) discontinued treatment due to worsening renal function (drug dose 49/51 mg twice daily) and 4 patients (4.5%) due to hyperkalemia – 1 patient at a dose of 49/51 mg twice daily and 3 patients at a dose of 97/103 mg twice daily.

The population that received the highest dose of sacubitril/valsartan compared to patients receiving the lowest or intermediate dose had the shortest history of HF (respectively 70 months vs 157 months vs 81 months; $p = 0.001$), the lowest number of visits to primary care (4 vs 6 vs 4.5; $p = 0.005$), the highest SBP (respectively 123 mm Hg vs 108 mm Hg vs 113 mm Hg; $p = 0.002$) and DBP (75 mm Hg vs 66 mm Hg vs 72 mm Hg; $p = 0.002$), and the lowest initial NT-proBNP (respectively 2620 pg/mL vs 4446 pg/mL vs 4417 pg/mL; $p = 0.003$).

During a one-year follow-up, 8 patients died (8.9%); the mean time to death was 5.88 ± 4.16 months. One of non-survivors discontinued the treatment of sacubitril/valsartan 1 month before death. The MAGGIC score in the whole group was 24 ± 5.4 . This implies one-year probability of death of approx. 14.7%, which is much higher

Table 1. Baseline characteristics and related to etiology. Data is presented as mean \pm standard deviation (SD), median (interquartile range – IQR) or number (percentage) in variables with non-parametric distribution

Parameter	Total population, n = 89	Non-ischemic HF, n = 47	Ischemic HF, n = 42	p-value
Age [years]	62 (56–68)	59 (43–66)	63 (59–72)	0.002
Male sex, n (%)	73 (82)	34 (72.3)	39 (92.9)	0.025
BMI [kg/m ²]	27.34 \pm 4/6	26.95 \pm 4.26	27.79 \pm 4.91	0.39
HF duration [months]	72 (32–133)	50.5 (12–120)	85.5 (42–143)	0.03
SBP [mm Hg]	116.9 \pm 14.1	114.94 \pm 14.51	119.1 \pm 13.5	0.17
DBP [mm Hg]	72.5 \pm 8.5	72.30 \pm 8.19	72.76 \pm 8.94	0.85
NYHA class	3 (3–3)	3 (3–3)	3 (3–3)	0.98
Hospitalization HF, n (%)	48 (54)	23 (48.9)	25 (59.5)	0.32
Atrial fibrillation, n (%)	36 (40)	18 (38.3)	18 (42.9)	0.66
Diabetes, n (%)	36 (40)	19 (40.4)	17 (40.5)	0.99
Hypertension, n (%)	52 (58)	23 (48.9)	29 (69)	0.055
Dyslipidemia, n (%)	49 (55)	22 (46.8)	27 (64.3)	0.09
COPD, n (%)	8 (9)	2 (4.3)	6 (14.3)	0.2
NT-proBNP [pg/mL]	2600 (914–4783)	2858 (1017–4967)	2186 (797–4783)	0.73
Hemoglobin [g/dL]	13.8 \pm 1.88	13.97 \pm 2.13	13.6 \pm 1.6	0.4
Na [mmol/L]	139.9 \pm 2.78	140.1 \pm 2.65	139.7 \pm 2.94	0.5
K [mmol/L]	4.49 \pm 0.39	4.46 \pm 0.37	4.52 \pm 0.41	0.53
Creatinine [μ mol/L]	94.6 (81–113)	91 (77–108)	105.1 (85–129)	0.03
eGFR [mL/min/1.73 m ²]	70.9 \pm 22.7	76.22 \pm 22.36	65.1 \pm 21.9	0.02
BUN [mmol/L]	12.3 (8–17.5)	13.2 (7.95–19.8)	13.4 (6.7–26.0)	0.69
Glucose [mmol/L]	5.7 (5.1–6.8)	5.8 (5–7.1)	5.5 (5.1–6.6)	0.45
LDL [mmol/L]	2.23 \pm 0.88	2.43 \pm 0.97	2.02 \pm 0.72	0.04
Bilirubin [mg/dL]	20.7 (14.3–39.4)	17.3 (13–37.9)	26.7 (17–47.6)	0.17
LVD [mm]	66 (60–72)	68.66 \pm 9.57	63.7 \pm 9.1	0.014
EDV LV [mL]	221.2 \pm 90.3	221.9 \pm 106.1	220.1 \pm 65.1	0.69
ESV LV [mL]	171.2 \pm 81.4	175.55 \pm 96.24	165 \pm 55.1	0.66
RVD prox. [mm]	34.9 \pm 6.02	34.87 \pm 6.5	35.1 \pm 5.6	0.88
LA vol. [mL]	133.6 \pm 51.4	129.25 \pm 45.28	136.7 \pm 56.2	0.8
LVEF [%]	23.6 \pm 6.7	22.25 \pm 6.85	25.05 \pm 6.24	0.02
TAPSE [mm]	16.7 \pm 4.2	16.5 \pm 3.96	16.9 \pm 4.5	0.6
PASP [mm Hg]	43.3 \pm 13.19	42.5 \pm 13.9	44.1 \pm 12.6	0.69
6MWT distance [m]	353.2 \pm 99.6	357.64 \pm 96.23	347.9 \pm 105.6	0.73
HR [bpm]	74.4 \pm 7.4	77.7 \pm 12.9	75.9 \pm 8.5	0.86
QRS duration [ms]	114 (102–140)	110 (100–140)	120 (108–128.5)	0.83
Prior ACEI/ARB, n (%)	87 (98)	45 (95.7)	42 (100)	0.98
β -blockers, n (%)	87 (98)	46 (97.9)	41 (97.6)	0.98
MRA, n (%)	80 (90)	43 (91.5)	37 (88.1)	0.86
Ivabradine, n (%)	16 (18)	7 (15.2)	9 (21.4)	0.45
Loop diuretic, n (%)	73 (85)	37 (87.2)	36 (87.8)	0.67
Digoxin, n (%)	16 (18)	10 (21.3)	6 (14.3)	0.39
MAGGIC score	24 \pm 5.4	23.1 \pm 4.7	25 \pm 6.04	0.1
ICD at baseline, n (%)	36 (40)	14 (40.4)	22 (52.4)	0.26
CRT at baseline, n (%)	15 (17)	6 (12.8)	9 (21.4)	0.28

ACEI – angiotensin-converting-enzyme inhibitors; ARB – angiotensin receptor blockers, BMI – body mass index; BUN – blood urea nitrogen; COPD – chronic obstructive pulmonary disease; CRT – cardiac resynchronization therapy; DBP – diastolic blood pressure; DM – diabetes mellitus; eGFR – estimated glomerular filtration rate; HF – heart failure; HR – heart rate; ICD – implantable cardioverter defibrillator; LDL – low-density lipoprotein; LVD – left ventricle diameter; LVEF – left ventricle ejection fraction; MRA – mineralocorticoid antagonist, NT-proBNP – N-terminal prohormone B-type natriuretic peptide; SBP – systolic blood pressure; EDV LV – end diastolic volume – left ventricle; ESV LV – end systolic volume – left ventricle; RVD – reference vessel diameter; LA vol. – left atrial volume; TAPSE – tricuspid annular plane systolic excursion; PASP – pulmonary artery systolic pressure; 6MWT – six-minute walk test; MAGGIC – Meta-Analysis Global Group in Chronic Heart Failure.

Table 2. Comparison of clinically important variables after 1 year of treatment with sacubitril/valsartan. Data is presented as mean ± standard deviation (SD), median (interquartile range – IQR) or number (percentage) in variables with non-parametric distribution

Parameter	Baseline (n = 73)	After 1 year of treatment (n = 73)	p-value
NYHA class	3 (3–3)	2 (1–2)	<0.001
SBP [mm Hg]	117.2 ±13.9	109.9 ±13.4	<0.001
DBP [mm Hg]	72.7 ±8.3	68.3 ±9.9	<0.001
HR [bpm]	76 (70–80)	75 (68–79)	<0.005
QRS duration [ms]	115 (102–140)	110 (107–135)	<0.01
LVEF [%]	23.8 ±6.5	27 ±6.4	<0.001
K [mmol/L]	4.4 ±0.4	4.5 ±0.38	0.88
Creatinine [µmol/L]	95 (81–113)	101 (86–115)	0.21
NT-proBNP [pg/mL]	2600 (969.2–4542)	1628 (679–3009)	<0.001
6MWT distance [m]	337.3 ±96.9	423.8 ±71.9	<0.001

DBP – diastolic blood pressure; HR – heart rate; LVEF – left ventricle ejection fraction; NT-proBNP – N-terminal prohormone B-type natriuretic peptide; SBP – systolic blood pressure; NYHA – New York Heart Association; 6MWT – six-minute walk test.

than the observed one-year mortality in the studied population. Furthermore, the MAGGIC score was similar in non-survivors and survivors (25.7 ±5.7 vs 23.9 ±5.3; p = 0.37). The Kaplan–Meier curves for death in the total population and related to HF etiology (p > 0.05) is presented in Fig. 1 and Fig. 2.

During a one-year follow-up, in 24 patients (26.9%), the composite endpoint was reported. These patients had a higher level of NT-proBNP (4488.5 [2599–7129.5] pg/mL vs 2049.5 [746–3889.5] pg/mL, p = 0.002), more HF hospitalizations in the last 12 months (median 2 [1–3] vs 0 [0–1]; p = 0.0001) and lower SBP (111.3 ±12.5 mm Hg vs 118.5 ±13.9 mm Hg; p = 0.028), distance in 6MWT (301.6 ±101.3 m vs

367.1 ±95.3 m; p = 0.046) and TAPSE (16.6 ±2.65 mm vs 17.5 ±4.46 mm; p = 0.004). These parameters indicated more advanced HF in these patients. In analysis regarding HF etiology, the composite endpoint occurred in 11 patients with ischemic etiology and in 13 with non-ischemic (p = 0.83). The time to composite endpoint was 3.32 ±2.03 months for ischemic etiology of HF and 4.44 ±3.95 months for non-ischemic etiology. The multivariable analysis revealed 3 independent variables for risk of composite endpoint (Table 3): history of HF hospitalization, TAPSE and ACEI treatment. According to ANOVA analysis, only RVD in ischemic etiology of HF was significant for risk of composite endpoint (p = 0.0452) (Fig. 3).

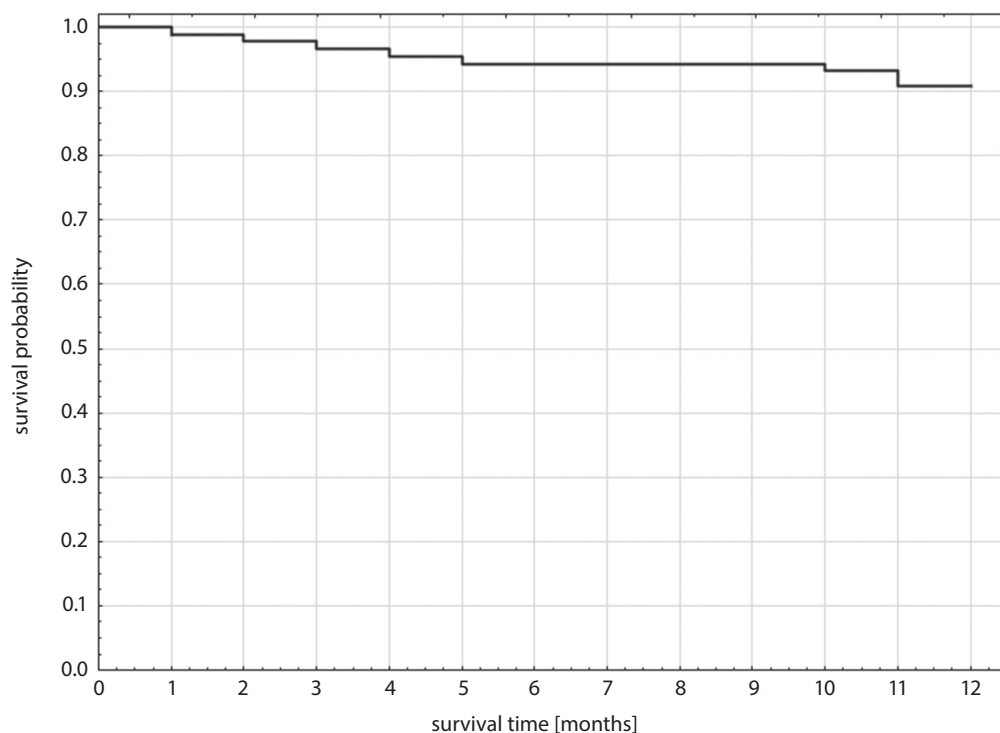


Fig. 1. Kaplan–Meier curve of death during 1 year in the studied population

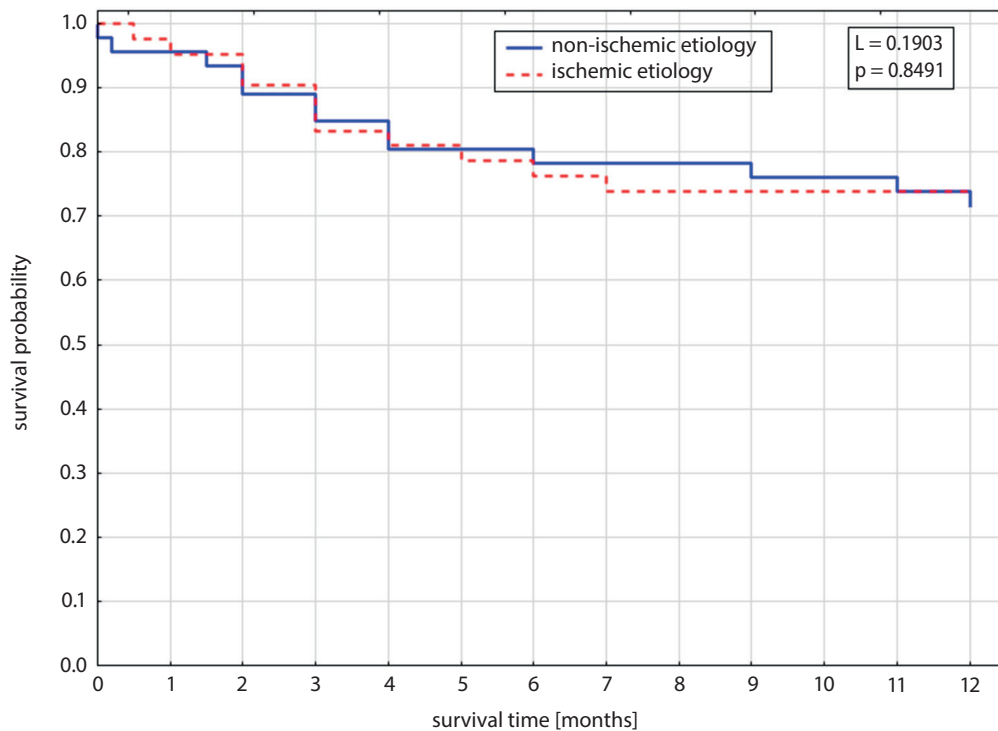


Fig. 2. Kaplan–Meier curve of composite endpoint (death and/or HF hospitalization) during 1 year in the studied population related to etiology of HF

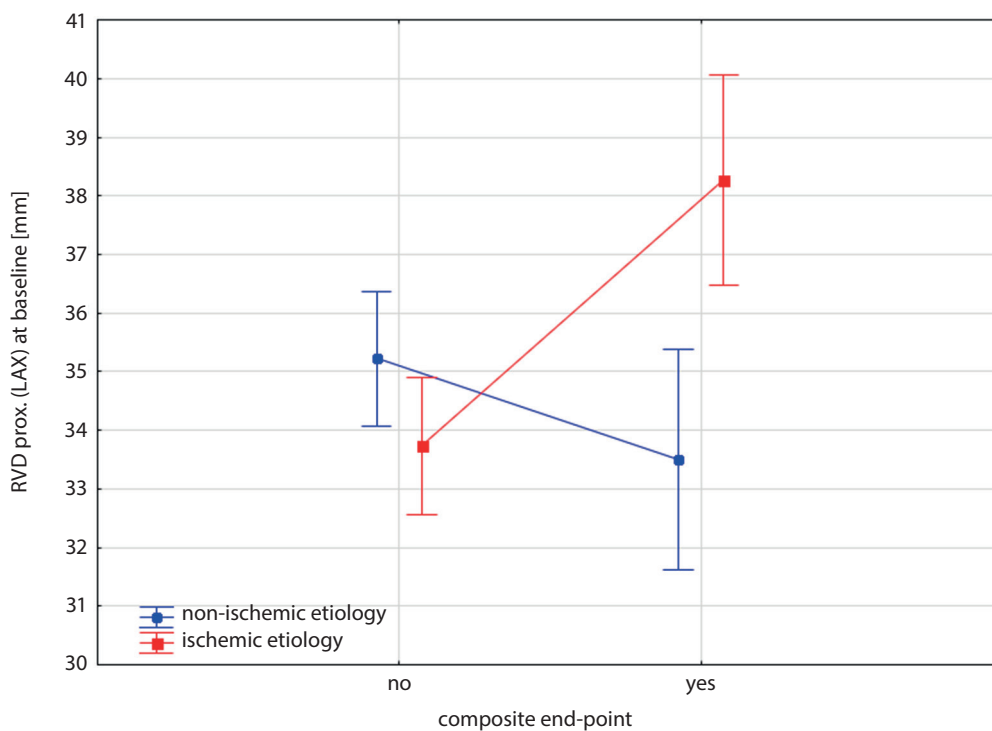


Fig. 3. Two-way ANOVA results for RVD prox. (LAX) at baseline – interaction effect between etiology and composite endpoint (marginal means \pm standard error (SE); $p = 0.0453$)

Discussion

We present the first real-life observation of one-year treatment with sacubitril/valsartan in a Polish HFrEF population. The studied population represents a typical HFrEF cohort. Of note, we report a relatively high proportion of DCM patients (52.5% vs 40% in PARADIGM-HF), lower EF (our population – 23.5 ± 8.9 vs PARADIGM-HF

– $29.6 \pm 6.1\%$ and higher levels of NT-proBNP (ours – 2600 pg/mL vs 1631 pg/mL); such results reflect more advanced HFrEF and probably the fact that our centers serve as regional referral centers for more sophisticated diagnostic work-up (e.g., referrals for heart transplant or mechanical circulatory support in DCM or hemodynamically compromised patients).⁶ More advanced HFrEF in our study as well as in the first report on Polish patients

Table 3. Results of multivariable analysis for the composite endpoint

Variable	p-value	OR	95% CI for OR	
History of HF hospitalization	0.001	2.194	1.397	3.448
TAPSE at baseline	0.035	0.826	0.691	0.987
ACEI before ARNI	0.011	0.176	0.046	0.672
Intercept	0.144	x	x	x

OR – odds ratio; 95% CI – 95% confidence interval; HF – heart failure; TAPSE – tricuspid annular plane systolic excursion; ACEI – angiotensin-converting-enzyme inhibitor; ARNI – angiotensin receptor neprilysin inhibitors.

from 2018⁹ in comparison to the PARADIGM-HF baseline characteristics probably results from the fact that tertiary cardiac centers, with the greatest HF expertise, decided to start ARNI treatment in Poland.

Overall, we observed very favorable outcomes after 1 year of treatment with sacubitril/valsartan, which was consistent in various parameters of clinical interest, such as improvements in NYHA class, EF and distance in 6MWT, as well as substantial reduction of NT-proBNP levels. Reassuringly, and similarly as in other ARNI trials, including PARADIGM-HF, we did not observe safety issues with ARNI, i.e., the substantial reduction of both SBP and DBP was asymptomatic in the great majority of patients, and the much feared worsening of renal function did not occur (stable levels of creatinine and potassium).

Although the study population was relatively small compared to large multi-center randomized controlled trials or ESC-initiated registries, we report here a real-life and probably the largest population of HFrEF patients treated with ARNI in Poland. For the first time we report a one-year follow-up, which reassuringly is similar to other studied populations in real-world studies.^{10–14} This and other studies showed a clear benefit of sacubitril/valsartan treatment of HFrEF patients, which directly translates into improvement in clinical, echocardiographic and laboratory indices. We sincerely hope that the increasing number of papers showing effectiveness of sacubitril/valsartan will pave the way for widespread utilization of this treatment in Polish patients, which currently is limited due to non-medical reasons (unbearable financial cost for the majority of patients).

Sacubitril/valsartan is recommended in the ESC guidelines for further reduction in the risk of hospitalization or death in patients with HFrEF if symptoms continue despite optimal treatment with ACEI/ARB, β -blockers and mineralocorticoid antagonists. At baseline, the studied population was optimally treated in terms of the class of the standard therapy of ACEI/ARB, BB and MRA (Table 1). After 1 year, only ivabradine was more frequently used (from 18% at baseline to 29%, $p = 0.077$). However, the target doses of 50% or more were obtained for BB from 66% at baseline to 63% after a year, for MRA it was stable at 77%, and for ivabradine it varied from 54% at baseline to 69%. It should be emphasized that in comparison to the observational QUALIFY registry for ambulatory Polish patients suffering from chronic HF,¹⁵ both prescription of standard

HFrEF therapy and ivabradine and the proportion of target doses are higher in our study, but still suboptimal.

For ARNI, the TITRATION study indicated that 75.9% of randomized patients achieved ‘treatment success’, defined as achieving and maintaining a dose of sacubitril/valsartan of 97/103 mg twice daily without any dose interruption/down-titration over 12 weeks.¹⁶ In our study, after a year, 80% of patients were on 50% or more of the target dose of sacubitril/valsartan (49/51 mg or 97/103 mg twice daily). In the PROVE-HF study, after a year of treatment, 65% of patients received the maximum dose of sacubitril/valsartan, 21% received a moderate dose and 14% received the lowest dose.¹⁷ In our study, the involvement of individual doses represents 52%, 28% and 20%, respectively, and was comparable in the moderate dose (49/51 mg) to the PROVE-HF study.¹⁷ More frequent use of lower doses in our population in relation to the PROVE-HF populations may have resulted from lower SBP and DBP (116 ± 14 mm Hg and 72 ± 8 mm Hg vs 124.5 ± 16 mm Hg and 76 ± 10.3 mm Hg, respectively) and more advanced HF (NT-proBNP 2600 pg/mL vs 816 pg/mL, respectively).¹⁷

In our study, patients treated with the maximum target dose constituted the least burdened population at baseline (eGFR 75.91 mL/min/1.73 m², SBP 123 mm Hg). It allowed us to use the maximum doses, which further enhanced the therapeutic effects in comparison to the groups at lower doses. Thus, the earlier incorporation of the drug, as well as treatment with higher doses, has a beneficial effect on the prognosis of patients with HFrEF.

Hypotension, hyperkalemia and worsening renal function were the most frequent adverse events in our and the PROVE-HF study. Hypotension was observed with a comparable frequency in the studied population and in the PROVE-HF study (17.8% compared to 17.6%, respectively).¹⁷ It should be emphasized that hyperkalemia and worsening renal function were less frequently observed in our study than in the PROVE-HF study (5.6% and 4.5% compared to 13.2% and 12.3%).¹⁷ Moreover, no statistically significant differences were observed in potassium and creatinine values in our population at the beginning of the study and after 1 year. However, the most common reasons for discontinuation of therapy were hypotension, hyperkalemia and worsening kidney function in both our study and PARADIGM-HF, and at a similar level (11% compared to 11.4%, respectively).⁶

At baseline, a little more than half of the population had devices (ICD or CRT in 57%), and in the one-year follow-up, 14 patients subsequently received an ICD (8) or CRT (6). That is even more than in the QUALIFY population (28.7%); however, there is still a large need for invasive procedures in the HF_rEF population in our country.

In the studied population, AF was highly prevalent (36/89 patients), including 18 (38.3%) out of 47 non-ischemic HF and 18 (42.9%) out of 42 ischemic HF patients. In the AF population, 22 (61%) had severe reduction in LVEF $\leq 25\%$ and 16 (44%) were older than 65. Regardless of HF etiology, there were no differences of the drug therapy, including β -blockers. Digoxin was used in 16 patients (18%). During the one-year observation, no ablation procedure was performed.

The mean HR in the AF group was 81 bpm, while in the sinus rhythm group it was 75 bpm. At baseline, 35 patients with AF (97%) were taking β -blockers and after 1 year – all patients; however, 13 (36%) were treated less than 50% of the target β -blockers. After 1 year of sacubitril/valsartan treatment, a change in β -blockers treatment was observed in 5 patients. Three patients had reduced their β -blockers dose (bradyarrhythmia), 1 discontinued the treatment due to peripheral artery disease (PAD), and 1 patient had increased the dose above 50% of the target dose. During the one-year follow-up, in 13 AF patients (36%), the composite endpoint was reported, including 3 deaths (8%).

In the studied population, patients who died (9.09%) had a higher level of NT-proBNP (3337 [3243–5631] pg/mL vs 1337.5 [653.5–2231.5] pg/mL; $p = 0.002$) and blood urea nitrogen – BUN (27 [21–34] mmol/L vs 10.2 [6.7–21] mmol/L; $p = 0.0056$), lower distance in the 6MWT (273.2 ± 105.1 m vs 431.3 ± 85.5 m; $p = 0.039$), and a larger RVD in echocardiography measured in the parasternal longitudinal axis (40.86 ± 4.71 mm vs 34.3 ± 5.85 mm, $p = 0.0055$). These parameters indicated the more advanced HF in the non-survival population. The integer risk score of approx. 24 locates our population between the 3rd and 4th risk group with estimated one-year probability of death between 13.4% and 16%.⁷ Thus, the MAGGIC score clearly overestimated the one-year probability of death in our population (true one-year mortality in our population – 9.09% compared to estimated one-year mortality – 14.7%).⁷ Apart from numerous factors that may be responsible for this inaccuracy, such as the relatively small population size (which may distort statistical calculations), the majority of patients with non-ischemic HF (with usually worse prognosis in ischemic HF), younger age of our population than the original MAGGIC cohort, etc., the favorable effect of sacubitril/valsartan should also be taken into account.

The composite endpoint (cardiovascular mortality and hospitalization) after a year occurred in 17.3% in the ESC-EORP-HFA Heart Failure Long-Term Registry,¹⁸ and in our study in 27.3%. However, it should be pointed out that the components of the composite endpoint in our study are different (death and HF hospitalization). It should also

be noted that there were differences in hospitalization due to decompensation, in 13% of patients in the abovementioned Registry compared to 27.3% in the present population. It seems that the increased number of hospitalizations in our study is a result of more advanced HF in the studied population and the inadequately organized outpatient care in our country (the routine treatment of patients with decompensation of HF in hospital). Mortality in our population was 9.09% and was higher than in the Registry after a year of treatment of sacubitril/valsartan, which was 8.8%.¹⁸ Ischemic etiology (5.6%, $n = 5$) was a more frequent cause of death in our population than non-ischemic etiology (3.3%, $n = 3$), which is consistent with other studies that indicate a worse prognosis for patients with ischemic HF etiology.

From multivariable analysis independent variables for risk of composite endpoint were revealed (history of HF hospitalization, TAPSE and ACEI treatment at baseline), which indicate more advanced HF and worse prognosis in ACEI-naive patients, and according to ANOVA analysis, in ischemic HF only the RVD was important for risk of composite endpoint. It is well known that the right ventricle dilates in end-stage disease, and is a predictor of poor outcome in HF.^{19,20} However, recently Correale et al. observed in a real-life population with chronic HF_rEF improvement of right ventricular function under sacubitril/valsartan treatment.²¹

Limitations

There are several potential limitations to the present study that should be acknowledged. Firstly, the size of the study population is small; however, ARNI treatment in Poland is not reimbursed, which results in unbearable cost of treatment for the majority of patients in need. Secondly, the fact that patients were recruited in the referral centers may slightly distort the typical HF_rEF patients in Poland, which in fact may be less severe. Thirdly, the observation period of 12 months seems to be relatively short; nevertheless, the composite endpoint occurred in more than a quarter of patients. Fourthly, the mean age of our study population is at least a decade younger than a typical (real-world) HF cohort. Fifthly, a great majority of our patients have long-standing HF. Consequently, new-onset (or de novo) HF patients are under-represented. Also, this was an observational study without a control group. The lack of direct His bundle pacing in our patients with chronic AF, which is more and more widely used in this group of patients,²² may also be considered as a limitation of our work.

Conclusions

In summary, we present the first one-year observation of real-life HF_rEF Polish patients treated with sacubitril/valsartan with clinical improvement and good tolerability.

We confirmed that non-survivors had more advanced HF, so the initiation and uptitration of sacubitril/valsartan should be performed early in HFrEF.

ORCID iDs

Małgorzata Lelonek  <https://orcid.org/0000-0003-0756-5541>
 Sylwia Wiśniowska-Śmiałek  <https://orcid.org/0000-0002-7563-6586>
 Paweł Rubiś  <https://orcid.org/0000-0002-6979-3411>
 Izabela Nowakowska  <https://orcid.org/0000-0002-3729-3359>
 Agnieszka Pawlak  <https://orcid.org/0000-0001-9032-9130>

References

1. Redfield MM, Jacobsen SJ, Burnett JC, Mahoney DW, Bailey KR, Rodeheffer RJ. Burden of systolic and diastolic ventricular dysfunction in the community: Appreciating the scope of the heart failure epidemic. *JAMA*. 2003;289(2):194–202.
2. Bleumink GS, Knetsch AM, Sturkenboom MCJM, et al. Quantifying the heart failure epidemic – prevalence, incidence rate, lifetime risk and prognosis of heart failure: The Rotterdam Study. *Eur Heart J*. 2004;25(18):1614–1619.
3. Seferovic PM, Jankowska E, Coats AJS, et al; Task Force of the HFA Atlas, and the ESC Atlas of Cardiology leadership, developed in collaboration with the National Heart Failure Societies of the ESC member and ESC affiliated member countries. The Heart Failure Association Atlas: Rationale, objectives and methods. *Eur J Heart Fail*. 2020;22(4):638–645. doi:10.1002/ejhf.1768
4. Ponikowski P, Voors AA, Anker SD, et al; ESC Scientific Document Group. 2016 ESC Guidelines for the diagnosis and treatment of acute and chronic heart failure: The Task Force for the diagnosis and treatment of acute and chronic heart failure of the European Society of Cardiology (ESC). Developed with the special contribution of the Heart Failure Association (HFA) of the ESC. *Eur Heart J*. 2016;37(27):2129–2200.
5. Volterrani M, Iellamo F, Senni M, Piepoli MF. Therapeutic options of angiotensin receptor neprilysin inhibitors (ARNis) in chronic heart failure with reduced ejection fraction: Beyond RAAS and sympathetic nervous system inhibition. *Int J Cardiol*. 2017;226:132–135.
6. McMurray JJ, Packer M, Desai AS, et al; PARADIGM-HF Investigators and Committees. Angiotensin-neprilysin inhibition versus enalapril in heart failure. *N Engl J Med*. 2014;371(11):993–1004.
7. Pocock SJ, Ariti CA, McMurray JJ, et al; Meta-Analysis Global Group in Chronic Heart Failure. Predicting survival in heart failure: A risk score based on 39 372 patients from 30 studies. *Eur Heart J*. 2013;34(19):1404–1413.
8. Entresto® Summary of Product Characteristics. https://www.novartis.pl/system/files/product-info/entresto_chpl_2020-09.pdf. Accessed on September 1, 2020.
9. Kałużna-Oleksy M, Kolasa J, Migaj J, et al. Initial clinical experience with the first drug (sacubitril/valsartan) in a new class: Angiotensin receptor neprilysin inhibitors in patients with heart failure with reduced left ventricular ejection fraction in Poland. *Kardiol Pol*. 2018;76(2):381–387.
10. Greene SJ, Butler J, Albert NM, et al. Medical therapy for heart failure with reduced ejection fraction: The CHAMP Registry. *J Am Coll Cardiol*. 2018;72(4):351–366.
11. Martens P, Lambrechts S, Lau CW, Dupont M, Mullens W. Impact of sacubitril/valsartan on heart failure admissions: Insights from real-world patient prescriptions. *Acta Cardiol*. 2019;74(2):115–122. doi:10.1080/00015385.2018.1473825
12. Wachter R, Viriato D, Klebs E, et al. Early insights into the characteristics and evolution of clinical parameters in a cohort of patients prescribed sacubitril/valsartan in Germany. *Postgrad Med*. 2018;130(3):308–316.
13. Moliner-Abos C, Rivas-Lasarte M, Besora JP, et al. Sacubitril/valsartan in real-life practice: Experience in patients with advanced heart failure and systematic review. *Cardiovasc Drug Ther*. 2019;33(3):307–314.
14. Bastien N, Haddad H, Bergeron S, et al. The PARASAIL study: Patient reported outcomes from the Canadian real-world experience use of sacubitril/valsartan in patients with heart failure and reduced ejection fraction. *Can J Cardiol*. 2017;33:S162–S163.
15. Opolski G, Ozierański K, Lelonek M, Balsam P, Wilkins A, Ponikowski P; On Behalf Of The Polish Qualify Investigators. Adherence to systolic heart failure guidelines in ambulatory care in Poland: Data from the international QUALIFY survey. *Pol Arch Med Wewn*. 2017;127(10):657–665. doi:10.20452/pamw.4083
16. Senni M, McMurray JJV, Wachter R, et al. Initiating sacubitril/valsartan (LCZ696) in heart failure: Results of TITRATION, a double-blind, randomized comparison of two uptitration regimens. *Eur J Heart Fail*. 2016;18(9):1193–1202. doi:10.1002/ejhf.548
17. Januzzi JL, Prescott MF, Butler J, et al; PROVE-HF Investigators. Association of change in N-terminal pro-B-type natriuretic peptide following initiation of sacubitril-valsartan treatment with cardiac structure and function in patients with heart failure with reduced ejection fraction. *JAMA*. 2019;322(11):1085–1095. doi:10.1001/jama.2019.12821
18. Kapelios CJ, Lainscak M, Savarese G, et al; Heart Failure Long-Term Registry Investigators. Sacubitril/valsartan eligibility and outcomes in the ESC-EORP-HFA Heart Failure Long-Term Registry: Bridging between European Medicines Agency/Food and Drug Administration label, the PARADIGM-HF trial, ESC guidelines, and real world. *Eur J Heart Fail*. 2019;21(11):1383–1397.
19. Raina A, Meeran T. Right ventricular dysfunction in left-sided heart failure with preserved versus reduced ejection fraction. *Curr Heart Fail Rep*. 2018;15:94–105.
20. Dini FL, Carluccio E, Simioniuc A, et al; Network Labs Ultrasound (NEBULA) in Heart Failure Study Group. Right ventricular recovery during follow-up is associated with improved survival in patients with chronic heart failure with reduced ejection fraction. *Eur J Heart Fail*. 2016;18(12):1462–1471.
21. Correale M, Adriana Mallardi A, Pietro Mazzeo P, et al. Sacubitril/valsartan improves right ventricular function in a real-life population of patients with chronic heart failure: The Daunia Heart Failure Registry. *Int J Cardiol Heart Vasc*. 2020;2(27):100486. doi:10.1016/j.ijcha.2020.100486
22. Sławuta A, Mazur G, Małecka B, Gajek J. Permanent His bundle pacing: An optimal treatment method in heart failure patients with AF and narrow QRS. *Int J Cardiol*. 2016;214:451–452. doi:10.1016/j.ijcard.2016.04.022

Determinants of survival in patients with bladder cancer undergoing radical cystectomy: The impact of serum creatinine level

Paweł Hackemer^{1,A–D}, Bartosz Małkiewicz^{1,A,D,E}, Fryderyk Menzel^{2,B–D}, Aleksandra Drabik^{3,C,D}, Krzysztof Tupikowski^{4,C}, Romuald Zdrojowy^{1,E,F}

¹ Department of Urology and Oncologic Urology, Wrocław Medical University, Poland

² Department of Hygiene, Wrocław Medical University, Poland

³ Department of Endocrinology, Diabetes and Isotope Therapy, Wrocław Medical University, Poland

⁴ Department of Urology, Lower Silesian Oncology Center, Wrocław, Poland

A – research concept and design; B – collection and/or assembly of data; C – data analysis and interpretation;

D – writing the article; E – critical revision of the article; F – final approval of the article

Advances in Clinical and Experimental Medicine, ISSN 1899–5276 (print), ISSN 2451–2680 (online)

Adv Clin Exp Med. 2021;30(1):77–82

Address for correspondence

Bartosz Małkiewicz

E-mail: bartosz.malkiewicz@umed.wroc.pl

Funding sources

None declared

Conflict of interest

None declared

Received on October 19, 2020

Reviewed on October 21, 2020

Accepted on November 18, 2020

Cite as

Hackemer P, Małkiewicz B, Menzel F, Drabik A, Tupikowski K, Zdrojowy R. Determinants of survival in patients with bladder cancer undergoing radical cystectomy: The impact of serum creatinine level. *Adv Clin Exp Med.* 2021;30(1):77–82. doi:10.17219/acem/130597

DOI

DOI: 10.17219/acem/130597

Copyright

© 2021 by Wrocław Medical University

This is an article distributed under the terms of the Creative Commons Attribution 3.0 Unported (CC BY 3.0) (<https://creativecommons.org/licenses/by/3.0/>)

Abstract

Background. Bladder cancer is one of the most common cancers in Europe and is mostly found in men. Cystectomy is the treatment for invasive tumors that infiltrate the muscle of the bladder. This procedure is associated with a large number of complications. Eligibility for surgical treatment is important, because surgery may shorten the patient's life. The main prognostic factor is the severity of the disease, but less specific factors can be very helpful in selecting the form of treatment.

Objectives. To identify and analyze factors affecting significantly the survival in patients undergoing radical cystectomy (RC).

Material and methods. A retrospective analysis of a group of 129 patients treated at the Department of Urology and Urological Oncology of University Hospital in Wrocław (Poland) was carried out. Furthermore, information about the results of laboratory tests from the medical records (blood count, creatinine concentration, etc.) was obtained. The follow-up was performed twice during the postoperative period. The Kaplan–Meier method was used to determine overall survival (OS) curves and statistical significance was assessed using log-rank test.

Results. A statistically significant correlation between preoperative serum creatinine level and OS was found. The OS was significantly shorter in patients with higher serum creatinine levels (log-rank test; $p = 0.002$). The patients were divided into different groups to exclude the relationship between the elevated creatinine concentration and the local disease advancement. The analysis was performed in patients with and without hydronephrosis. In both groups, creatinine levels above the acceptable range were associated with a shorter survival.

Conclusions. Due to the high perioperative mortality, mainly in patients with advanced disease, it is necessary to develop the qualification process for surgical treatment. The awareness of the relationship between elevated creatinine levels and worse prognosis seems to be helpful.

Key words: survival, creatinine, hydronephrosis, cystectomy, urinary bladder neoplasms

Introduction

Bladder cancer is a major health problem in Poland; according to European Association of Urology, it is the 7th most commonly diagnosed cancer in male population worldwide and 5th in Europe. Radical cystectomy (RC) is a standard treatment for muscle-invasive bladder cancer (MIBC); however, it is also recommended for patients with non-muscle-invasive tumor who are at the highest risk of progression – including high risk and recurrent non-muscle-invasive tumours, BCG-refractory, BCG-relapsing and BCG-unresponsive, T1G3 tumours. Although there are number of prognostic factors affecting survival in patients undergoing RC such as tumor grade, tumor stage, preoperative uremia, and lymph node involvement and renal insufficiency, further reliable predictors are needed. Serum creatinine level is one of routine serum biomarkers commonly used in clinical practice associated with renal function. We aimed to determine the impact of serum creatinine levels and hydronephrosis on survival in patients who underwent RC.

Material and methods

Medical records of 143 patients from the Department of Urology and Urological Oncology of University Hospital in Wrocław (Poland), who underwent RC between February 2011 and February 2014, were evaluated retrospectively. Indications for RC in the presented group were MIBC (T2–T4), refractory superficial high-grade tumors as well as palliative reasons. Ten patients who had incomplete medical data were excluded. Four other patients were eliminated from the study since they could not be reached during the postoperative period. The final group consisted of 129 patients.

Table 1 describes the characteristics of 129 patients studied. The mean age was 65.5 years (range: 35–83 years, median: 65 years) and the majority (105; 82%) of patients were male. As for the stage, we observed that 79.8% of the patients presented MIBC (T2–T4); involvement of lymph nodes (N1–N3) was observed in 34.9% of the patients and hydronephrosis in 44 patients (34.1%).

Our regular preoperative blood evaluation included serum creatinine level. Blood samples were drawn on the 1st day of hospitalization, 1–3 days prior to RC. The normal range serum creatinine level in our laboratory was between 0.8 mg/dL and 1.3 mg/dL in men and between 0.7 mg/dL and 1.1 mg/dL in women. Therefore, the value of 1.3 mg/dL in men and 1.1 mg/dL in women was chosen as a cutoff between patients with high and low serum creatinine level.

Hydronephrosis was assessed using the ultrasound scan. In each patient, an ultrasound imaging of urinary tract (including kidneys, ureters and urinary bladder) was performed 1–3 days before the surgery. A visible

Table 1. Characteristics of patients studied

Parameter	n (%)
Age [years]	
Mean/median	65.5 ± 10.4
Variation	35–83
Sex	
Male	105 (81.4)
Female	24 (18.6)
Tumor stage	
T0	4 (3.1)
Ta	1 (0.8)
Tis	14 (10.9)
T1	7 (5.4)
T2	24 (18.6)
T3	35 (27.1)
T4	44 (34.1)
Lymph nodes involvement	
N0	80 (62.0)
N1	11 (8.5)
N2	32 (24.8)
N3	2 (1.6)
Nx	4 (3.1)
Hydronephrosis	
Yes	44 (34.1)
No	85 (65.9)

dilation of the renal pelvis in one or both kidneys, regardless of the stage of advancement, was considered as hydronephrosis.

The follow-up was performed twice during the postoperative period. In June 2014, patients were contacted by telephone. Traditional mail was sent to patients who could not be reached by telephone. For patients who could not be contacted neither by telephone nor by traditional mail, the information whether the person is alive was received from civil registry office in November 2014. In May 2016, a 2nd follow-up was performed by telephone and regular mail. Median follow-up time was 30.3 ± 13.4 months (mean: 30.1 months, min. 5.2 months, max. 60.5 months). In this study, a median follow-up is the time median between a surgery and the time when information about the patient was gathered.

Due to the retrospective nature of the study, it was not possible to assess cancer-specific survival. Information on the cause of death was obtained mainly from relatives.

The data was analyzed using STATISTICA v. 12.5 software (StatSoft Inc., Tulsa, USA). The Kaplan–Meier method was used to determine overall survival (OS) curves and statistical significance was assessed using log-rank test. Univariate analysis was performed using Kaplan–Meier method. Multivariate analysis was performed using

the Cox proportional hazard regression model with a confidence interval of 95% (95% CI). The value of $p < 0.05$ was considered statistically significant.

Results

The mean preoperative serum creatinine level in studied group was 1.29 mg/dL (0.66–2.66 mg/dL). In the univariate analysis using Kaplan–Meier method, a statistically significant correlation between preoperative serum creatinine level and OS was found. The OS was significantly shorter in patients with higher serum creatinine levels (log-rank test; $p = 0.002$; Fig. 1).

Table 2 shows OS time in patients classified by serum creatinine levels. Both 90-day overall survival (89.3% in the high-creatinine group and 94.5% in the low-creatinine group) and one-year overall survival (58.6% and 81.2%, respectively) were significantly shorter in patients with elevated creatinine levels.

The univariate analysis was performed to identify the factors affecting OS (Table 3). In the multivariate

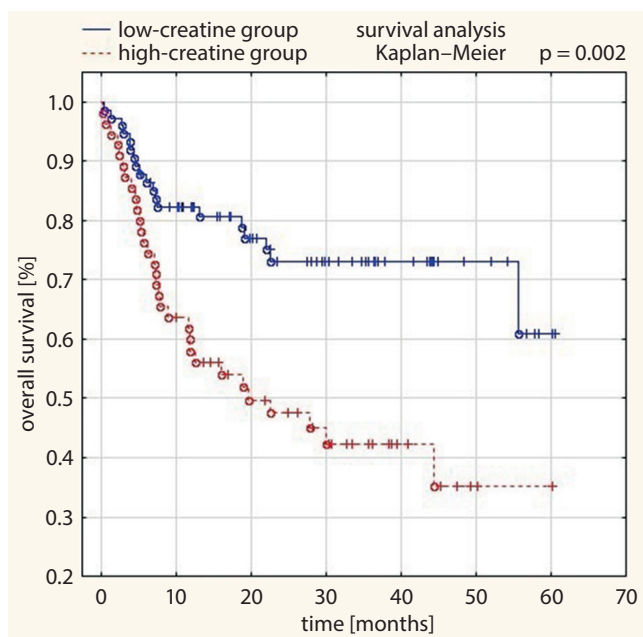


Fig. 1. Comparison of Kaplan–Meier survival curves between low and high creatinine groups

Table 2. Overall survival (OS) in patients classified by serum creatinine level

Survival	Low-creatinine group	High-creatinine group
30-day	98.70%	96.40%
90-day	94.50%	89.30%
One-year	81.20%	58.60%
Two-year	72.30%	48.50%
Three-year	68.50%	45.60%

Table 3. Results of Cox regression to determine the association with overall survival (OS; univariate analysis)

Parameter	HR	95% CI	p-value
Age	1.04	[1.01–1.07]	0.005
RBC	0.29	[0.18–0.47]	0.000
WBC	1.02	[0.97–1.09]	0.399
PLT	1.00	[1.00–1.01]	0.003
HGB	0.63	[0.54–0.74]	0.000
Na+	0.92	[0.83–1.01]	0.092
K+	2.18	[1.06–4.50]	0.035
Blood loss	1.00	[1.00–1.00]	0.008
Creatinine	3.18	[1.80–5.62]	0.000
GFR	0.98	[0.97–0.99]	0.004
T	1.71	[1.22–2.41]	0.002
N	1.41	[1.07–1.85]	0.015
ASA	1.60	[1.00–2.54]	0.048
BMI	1.00	[0.94–1.06]	0.876
Hydronephrosis	1.65	[0.93–2.90]	0.085

HR – hazard ratio; 95% CI – 95% confidence interval; RBC – red blood cells count; WBC – white blood cells count; PLT – platelets; HGB – hemoglobin; GFR – glomerular filtration rate; T – tumor stage, N – lymph nodes involvement, ASA – American Society of Anesthesiologists physical status classification system; BMI – body mass index.

Table 4. Results of Cox regression to determine the association with overall survival (OS; multivariate analysis)

Parameter	HR	95% CI	p-value
Age	1.04	[1.01–1.07]	0.014
Serum creatinine	2.16	[1.19–3.93]	0.012
Serum hemoglobin	0.66	[0.56–0.78]	<0.001

HR – hazard ratio; 95% CI – 95% confidence interval.

Table 5. Overall survival (OS) by T stage

Survival	T2	T3	T4
One-year	83.0%	67.2%	58.6%
Two-year	72.3%	56.8%	44.3%
Three-year	68.0%	51.9%	39.9%
Four-year	60.5%	40.4%	35.9%

analysis (Table 4) performed with the use of Cox proportional hazard regression model, which included selected independent significant variables detected in the univariate analysis (Table 3), it was found that the serum creatinine level was an independent variable significantly associated with OS.

Patients diagnosed with hydronephrosis had significantly higher serum creatinine level (1.43 ± 0.45 mg/dL, $p = 0.003$) compared to patients without hydronephrosis (1.22 ± 0.35 mg/dL; Fig. 2).

Creatinine serum level was also correlated with T score ($p < 0.01$; Fig. 3A). Furthermore, the overall survival was associated with T stage ($p < 0.01$; Fig. 3B, Table 5).

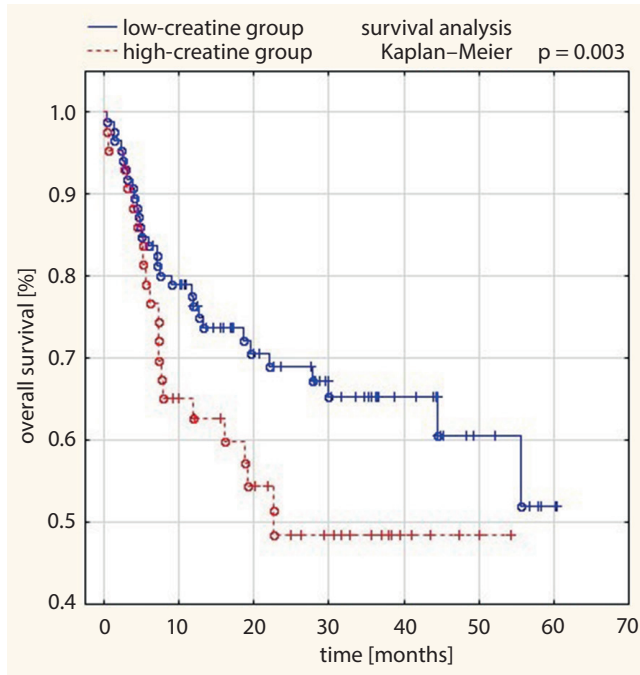


Fig. 2. Comparison of Kaplan–Meier survival curves between patients with or without hydronephrosis

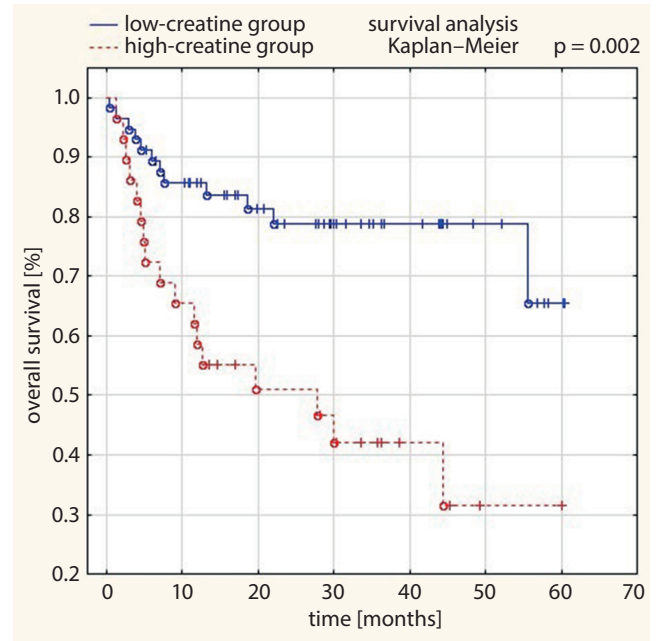


Fig. 4. Comparison of Kaplan–Meier survival curves between low- and high-creatinine groups in patients with hydronephrosis

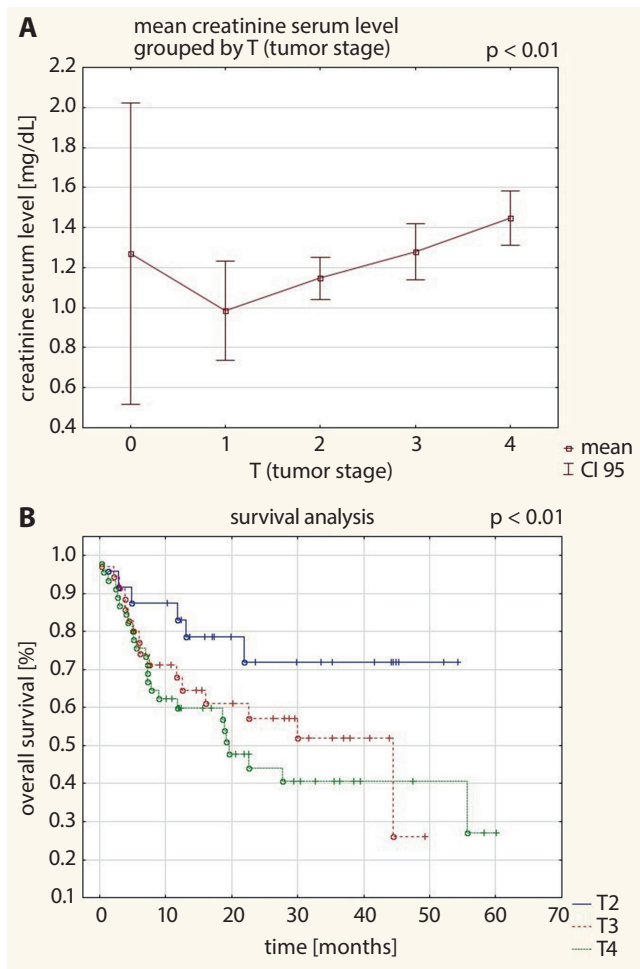


Fig. 3. A. Mean serum creatinine levels grouped by T (tumor stage); B. OS presented as Kaplan–Meier curves grouped by T (tumor stage)

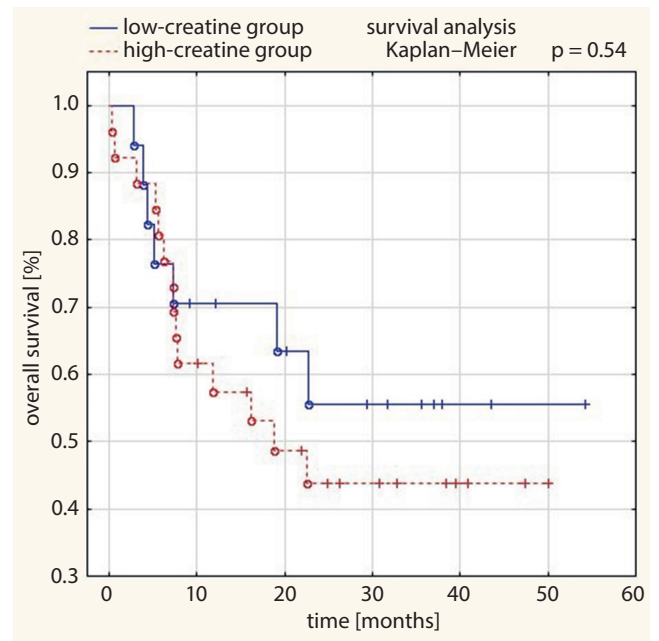


Fig. 5. Comparison of Kaplan–Meier survival curves between low- and high-creatinine groups in patients without hydronephrosis

The OS in patients without hydronephrosis was significantly shorter in those with high serum creatine levels (log-rank test; $p = 0.002$; Fig. 4). There was no statistically significant difference in OS between patient groups of high and low serum creatine level diagnosed with hydronephrosis (Fig. 5; $p = 0.54$).

The presence of hydronephrosis is related to the severity of the disease. In the case of T3 and T4 disease, dilatation of the renal pelvis was observed in almost half of the patients (Fig. 6).

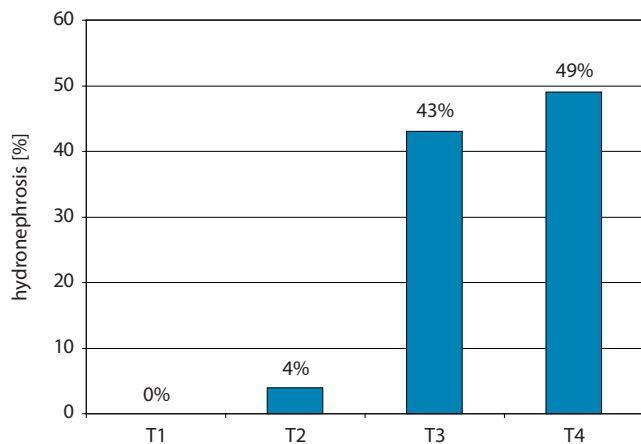


Fig. 6. Percentage of patients with hydronephrosis in different groups of cancer stage

Discussion

While examining a group of patients undergoing cystectomy, the objective was to find prognostic factors that would allow us to estimate the prognosis for patients with MIBC. The most important prognostic factor is the tumor stage.¹ Based on the analysis of survival in the study group, it was found that 60.5% of patients with T2 cancer survived 4 years, compared to 40.4% of T3 patients and 35.9% of T4 patients. Patients with less advanced disease have better results (OS).

It was also shown that preoperative hemoglobin levels are associated with OS after CR, patients with lower hemoglobin levels had a shorter survival time. Anemia reflects the failure of the sick organism.² Advanced bladder cancer often infiltrates the bladder orifices of the ureters, causing hydronephrosis. The obstructed outflow of urine from the kidney leads to a reduction in the filtering capacity of the organ, which results in an increased concentration of creatinine. In the study group, more than 1/3 of patients had hydronephrosis observed during the pre-CR ultrasound examination. Uropathy is a negative prognostic factor, and the probability of four-year survival in a patient with hydronephrosis is lower than in a patient without hydronephrosis (42.3% compared to 60.6%). Hydronephrosis is the result of the advancement of the disease.³

Survival probability analysis was performed for 2 groups: patients with and without hydronephrosis. In both groups, creatinine levels above the acceptable range were associated with a shorter OS. However, in the case of patients without hydronephrosis, the difference was greater and statistically significant (Fig. 4,5).

Creatinine is a product of creatine metabolism, which is produced in the liver. Creatine is transported to the organs that use the most energy, mainly muscles. Creatine occurs mainly in a form of phosphocreatine (75%), a high-energy compound that supplies adenosine triphosphate (ATP). About 2% of the creatine stored in the human body

is converted into creatinine every day. Creatinine is the final product excreted in the urine. Elevated blood creatinine levels indicate renal failure. Creatinine concentration depends on the muscle mass, hence the norm for men is higher than for women. In the elderly, decrease in muscle mass is observed, hence a reduced concentration of creatinine. In the case of musculoskeletal dysfunction, a decreased serum creatinine concentration is also observed.^{4,5} Increased creatinine concentration is also observed during intense exercise (that is, during high energy demand).⁶ The correlation between elevated serum creatinine and increased mortality is unclear. Several hypotheses have emerged.

Elevated creatinine levels indicate renal failure, which has a negative effect on the body.⁷ There is evidence of increased mortality in patients with cardiovascular disease (CVD) and renal failure. There are reports of increased mortality in patients with chronic kidney disease (CKD), suffering from diseases other than cardiovascular.⁸

At the end of 20th century, an association of OS with creatinine levels in patients after CR was observed. The serum concentration of 1.5 mg/dL was adopted as the borderline value. In patients with elevated creatinine levels, the mean OS was 3 years, and in patients with levels below 1.5 mg/dL, it was 8.6 years.⁹

Initially, when looking for a relationship between renal failure and increased mortality, the borderline value of glomerular filtration rate (GFR) was 30 mL/min, then the limit was shifted to 60 mL/min. About 37% of patients are diagnosed with CKD before CR.¹⁰ Cao et al. observed that renal failure is associated with more frequent recurrences of urothelial carcinoma.¹¹ In cancer patients, the presence of CKD may be due to long-term inflammation that leads to oxidative stress. As a result, renal vessels are damaged.¹²

Yang et al. conducted a study on 9,465 patients with newly diagnosed cancer. A significant relationship between renal failure and OS was found in gynecological and hematological neoplasms.¹³

Vulvar cancer is one of the cancers with proven increased mortality in patients with elevated creatinine levels. One of the hypotheses is that the increased energy demand of aggressive tumors leads to energy being obtained from phosphocreatine. Consequently, this increases the concentration of creatinine in the blood serum.¹⁴ Neither of these hypotheses explains unambiguously the mechanism of correlating CKD with mortality in patients after RC.

The main limitation of the work was its retrospective nature. The main problem was inconsistent medical documentation and difficult contact with the patients or their families. For this reason, the study group was significantly reduced. A prospective study would help to standardize the collected data. Due to the number of cystectomies performed in 1 hospital, a multicenter study should be performed to increase the study group and thereby the accuracy of the analysis.

Conclusions

High mortality after cystectomy prompts the search for prognostic factors. According to the results of our study, serum creatinine has a statistically significant correlation with OS. Creatinine level seems to be a promising parameter. The prognostic value of elevated serum creatinine could be implemented in the nomograms to improve its accuracy. A prospective, multicenter, large cohort study should be conducted, which will allow us to assess cancer-specific survival. Patients with elevated serum creatinine level should be treated with caution. Simple urinary diversion should be considered to minimize the trauma associated with the surgery.

ORCID iDs

Paweł Hackemer  <https://orcid.org/0000-0001-7071-2968>
 Bartosz Małkiewicz  <https://orcid.org/0000-0002-5933-3753>
 Fryderyk Menzel  <https://orcid.org/0000-0002-1150-3151>
 Aleksandra Drabik  <https://orcid.org/0000-0001-8525-6387>
 Krzysztof Tupikowski  <https://orcid.org/0000-0001-9728-190X>
 Romuald Zdrojowy  <https://orcid.org/0000-0002-1634-3556>

References

- Nielsen ME, Mallin K, Weaver MA, et al. Association of hospital volume with conditional 90-day mortality after cystectomy: An analysis of the National Cancer Data Base. *BJU Int.* 2014;114(1):46–55. doi:10.1111/bju.12566
- Bhindi B, Hermanns T, Wei Y, et al. Identification of the best complete blood count-based predictors for bladder cancer outcomes in patients undergoing radical cystectomy. *Br J Cancer.* 2016;114(2):207–212. doi:10.1038/bjc.2015.432
- Kim DS, Cho KS, Lee YH, Cho NH, Oh YT, Hong SJ. High-grade hydronephrosis predicts poor outcomes after radical cystectomy in patients with bladder cancer. *J Korean Med Sci.* 2010;25(3):369–373. doi:10.3346/jkms.2010.25.3.369
- Wyss M, Kaddurah-Daouk R. Creatine and creatinine metabolism. *Physiol Rev.* 2000;80(3):1107–1213. doi:10.1152/physrev.2000.80.3.1107
- Odden MC, Shlipak MG, Tager IB. Serum creatinine and functional limitation in elderly persons. *J Gerontol A Biol Sci Med Sci.* 2009;64A(3):370–376. doi:10.1093/gerona/gln037
- Mansour SG, Verma G, Pata RW, Martin TG, Perazella MA, Parikh CR. Kidney injury and repair biomarkers in marathon runners. *Am J Kidney Dis.* 2017;70(2):252–261. doi:10.1053/j.ajkd.2017.01.045
- Liu M, Li X, Lu L, et al. Cardiovascular disease and its relationship with chronic kidney disease. *Eur Rev Med Pharmacol Sci.* 2014;18(19):2918–2926.
- Fried LF, Katz R, Sarnak MJ, et al. Kidney function as a predictor of non-cardiovascular mortality. *J Am Soc Nephrol.* 2005;16(12):3728–3735. doi:10.1681/ASN.2005040384
- Thrasher JB, Frazier HA, Robertson JE, Dodge RK, Paulson DF. Clinical variables which serve as predictors of cancer-specific survival among patients treated with radical cystectomy for transitional cell carcinoma of the bladder and prostate. *Cancer.* 1994;73(6):1708–1715.
- Hamano I, Hatakeyama S, Iwamura H, et al. Preoperative chronic kidney disease predicts poor oncological outcomes after radical cystectomy in patients with muscle-invasive bladder cancer. *Oncotarget.* 2017;8(37):61404–61414. doi:10.18632/oncotarget.18248
- Cao J, Zhao X, Zhong Z, Zhang L, Zhu X, Xu R. Prognostic value of pre-operative renal insufficiency in urothelial carcinoma: A systematic review and meta-analysis. *Sci Rep.* 2016;6:35214. doi:10.1038/srep35214
- Matsumoto A, Nakagawa T, Kanatani A, et al. Preoperative chronic kidney disease is predictive of oncological outcome of radical cystectomy for bladder cancer. *World J Urol.* 2018;36(2):249–256. doi:10.1007/s00345-017-2141-2
- Yang Y, Li HY, Zhou Q, et al. Renal function and all-cause mortality risk among cancer patients. *Medicine (Baltimore).* 2016;95(20):e3728. doi:10.1097/MD.0000000000003728
- Schwameis R, Postl M, Bekos C, et al. Prognostic value of serum creatinine level in patients with vulvar cancer. *Sci Rep.* 2019;9(1):11129. doi:10.1038/s41598-019-47560-3

Basal cell carcinoma secondary to trauma: A 3-year experience of the single center

Iwona Chlebicka^{A–F}, Beata Jastrzab^{B–F}, Aleksandra Stefaniak^{B,D–F}, Jacek Szepietowski^{A,E,F}

Department of Dermatology, Venereology and Allergology, Wrocław Medical University, Poland

A – research concept and design; B – collection and/or assembly of data; C – data analysis and interpretation;
D – writing the article; E – critical revision of the article; F – final approval of the article

Advances in Clinical and Experimental Medicine, ISSN 1899–5276 (print), ISSN 2451–2680 (online)

Adv Clin Exp Med. 2021;30(1):83–86

Address for correspondence

Jacek Szepietowski
E-mail: jacek.szepietowski@umed.wroc.pl

Funding sources

None declared

Conflict of interest

None declared

Received on September 16, 2020

Reviewed on October 11, 2020

Accepted on October 18, 2020

Published online on January 30, 2021

Abstract

Background. Basal cell carcinoma (BCC) is the most frequent cancer worldwide in humans. The risk factors reported in the literature encompass excessive sun exposure, genetic predisposition, irradiation, exposure to arsenic, and trauma. The exact role of trauma in the etiology of BCC remains unexplained.

Objectives. To analyze patients with BCC treated surgically in the Dermatosurgery Unit, looking for possible cases of BCC secondary to trauma.

Material and methods. We performed a retrospective review all of treated BCCs in the Dermatosurgery Unit between January 2017 and June 2020.

Results. Among 1,832 patients with BCC, 5 (0.27%) tumors had a positive history of previous trauma. Many different types of injuries have been associated with oncogenesis in the area of the scar. The clinical presentations of lesions varied between the patients.

Conclusions. It is worth to underline that BCC may be located in the area of post-traumatic scar; however, the incidence seems to be lower comparing to reported previously (7.3–13%). This article illustrates the importance of exclusion malignancy in every non-healing lesion. A neoplasm may be difficult to differentiate from infection or local ischemia in the area of the scar. Prudent management of all clinically unclear lesions should include a biopsy.

Key words: trauma, basal cell carcinoma, SCAR

Cite as

Chlebicka I, Jastrzab B, Stefaniak A, Szepietowski J. Basal cell carcinoma secondary to trauma: A 3-year experience of the single center. *Adv Clin Exp Med.* 2021;30(1):83–86. doi:10.17219/acem/130593

DOI

10.17219/acem/130593

Copyright

© 2021 by Wrocław Medical University
This is an article distributed under the terms of the
Creative Commons Attribution 3.0 Unported (CC BY 3.0)
(<https://creativecommons.org/licenses/by/3.0/>)

Introduction

Basal cell carcinoma (BCC) is the most commonly occurring cancer in humans.¹ It is characterized by a slow growth rate and local malignancy. The etiology of BCC evolution is multifactorial. Both genetic and environmental factors, as well as immunological factors, influence the development of BCC. Excessive ultraviolet (UV) light exposure is the most significant carcinogen.²

It has been suggested that intense sun exposure during childhood and adolescence may be especially important for establishing adult risk for BCC. Additional risk factors for BCC include ionizing radiation, polycyclic aromatic hydrocarbons, arsenic exposure, and chronic immunosuppression.² Previous skin trauma has been also suggested as a predisposing factor.^{2,3} However, the exact underlying mechanism leading to BCC formation within scars still remains unclear.^{1,3} The aim of this study was to analyze patients with BCC treated surgically in the Dermatotomy Unit looking for possible cases of BCC secondary to trauma.

Material and methods

We performed a retrospective review of all excised and histologically confirmed BCCs in the Dermatotomy Unit between January 2017 and June 2020. Medical records of these patients were evaluated for the presence of patients with BCC secondary to injury. The analysis revealed 5 cases of post-traumatic tumor. For each patient, the following

data were extracted through manual search of medical charts: age of patients at the time of treatment, location of each lesion, tumor size, clinical presentation of the lesion, lesion growth, time interval between the trauma and the development of BCC, type of the previous injury, and postsurgical defect reconstruction method.

Results

Among 1,832 treated patients with BCC, 5 (0.27%) tumors had a positive history of previous trauma. Four out of our 5 patients were males and 1 patient was a female (Table 1). Their average age was 61.2 ± 16.8 years. The scars were located on the face, upper limb and foot. Various types of previous injuries in our patients have been observed: physical tearing of the tissue due to a traffic accident, burn, ulceration secondary to venous insufficiency, and even repeated trauma due to blood donation. None of these 5 wounds were originally closed surgically. The period of time from injury to tumor formation ranged between 5 and over 50 years. Different clinical manifestations of BCCs were found in our study group (Fig. 1,2). Two lesions had typical pearl-like borders. The remaining ones presented with sharply demarcated, irregular borders. The time from the onset of the first symptoms noticed by patients until the establishment of proper diagnosis varied from 1 to 4 years (with the median value of 3 years). Concerning the lifestyle habits, all patients were non-smokers, with average sun-exposure during the lifetime. One of the patients had concomitant diseases:

Table 1. Demographic and clinical details of patients with BCC secondary to trauma

Case No.	Age [years]	Sex	Site of BCC	Dimensions of BCC [mm]	Clinical presentation of the lesion	Lesion (BCC) growth [years]	Type of previous injury	Interval between trauma and development of BCC	Type of surgical procedure
1.	59	male	right antecubital fossa	20 × 20	red solid nodule with telangiectasia	4	microinjuries caused by repeated blood donation	15 years of blood donation	cut-and-tape
2.	64	male	forehead	30 × 40	pearly pink lesion with rolled borders, multiple small ulcerations and telangiectasia	3	traffic accident	childhood (50 years)	full thickness graft from the right supraclavicular area
3.	86	male	dorsal surface of left foot	10 × 15	ulcerated lesion with crust on the top	1	previous ulceration due to trauma, diabetes and venous insufficiency	5 years	full thickness graft from the right thigh
4.	58	female	right temple	20 × 20	depressed scariform plaque with sharply demarcated, irregular borders	2	traffic accident	20 years	cut-and-staple
5.	39	male	left arm	94 × 87	brightly erythematous lesion with slightly elevated rolled border, multiple small surface erosions and gentle scaling	3	boiling water burn	childhood (32 years)	cut-and-staple



Fig. 1. Patient No. 3

BCC secondary to trauma presenting as ulcerated lesion with crust on the top.

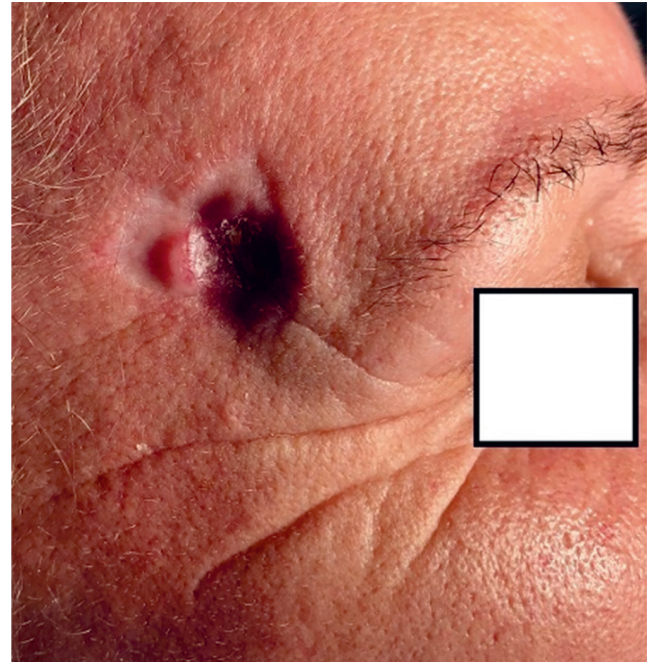


Fig. 2. Patient No. 4

BCC secondary to trauma presenting as depressed plaque with sharply demarcated, irregular borders.

hypertension and type 2 diabetes mellitus. There was no history of long-term usage of the drugs in the analyzed group of patients. The details of all the patients are given in Table 1.

Discussion

Excessive sun exposure is a major factor contributing to the development of BCC. The non-ultraviolet factors reported in the literature include genetic predisposition, irradiation, exposure to arsenic, and trauma.^{1,3} A relationship between BCC and various types of trauma has been reported in analyzed published case reports: surgical incisions, sharp or blunt injuries, deep abrasions, puncture injuries, burns, and those caused by chickenpox or vaccination.^{4–9}

The underlying pathomechanism of BCC secondary to trauma is still unexplained. Nevertheless, several theories have been proposed. Chronic irritation and misplacement of epithelial cells have been suggested to promote tumor growth.^{5,10} Moreover, the imbalance of cytokines and growth factors in initiation of carcinogenesis in scar tissue has been theorized.¹¹

To the best of our knowledge, only 2 retrospective studies of previous trauma as possible etiologic factor in BCC were conducted. Noodleman et al. presented the results of the retrospective analysis of 1,774 BCC patients.³ A history about previous injury was positive in 7.3% of the lesions. Özyazgan et al. analyzed 92 BCC cases and found that 13% of lesions were preceded by an earlier injury.¹ The abovementioned studies suggest that trauma may be

a fairly common risk factor of BCC. However, there are only few publications focused on particular cases of post-traumatic BCC. Our study seems to be one of the largest case series of BCC developed in the area of scar.

Trauma-related BCC was more frequently seen in men and younger patients.³ In our study, the average age was 61.2 ± 16.8 years, while the average age of all our patients with BCC, treated at the same time period (last 3 years) was 70.5 ± 13.7 years (unpublished data). This may suggest the younger age of trauma-related BCC occurrence. Wound healing by secondary intention has been mentioned as the most important etiological factor. In the series of cases reported by Ünverdi et al. each BCC developed from a wound which had healed with secondary intention.⁵ Morpheiform BCC was detected more frequently in patients with a previous injury than in the other patients. It was proven that BCCs arising in scars do not present more aggressive biological behavior.¹

Conclusions


In conclusion, it is worth underlining that BCC may be located in the area of post-traumatic scar. The clinical manifestation of those tumors varies between the patients. Increased surveillance of chronic wounds is very important. Their impaired healing seems to be a major risk factor for trauma-related BCC. Patients may postpone their visit to a specialist if they relate the appearance of the lesion with primary injury. For that reason, they should be alert to any new changes of the scar.

ORCID iDs

Iwona Chlebicka  <https://orcid.org/0000-0001-8120-7270>

Beata Jastrzab  <https://orcid.org/0000-0002-1587-7329>

Aleksandra Stefaniak  <https://orcid.org/0000-0002-3714-8434>

Jacek Szepietowski  <https://orcid.org/0000-0003-0766-6342>

References

1. Özyazgan I, Kontaş O. Previous injuries or scars as risk factors for the development of basal cell carcinoma. *Scand J Plast Reconstr Surg Hand Surg.* 2004;38(1):11–15.
2. Lesiak A, Czuwara J, Kamińska-Winciorek G, et al. Basal cell carcinoma. Diagnostic and therapeutic recommendations of Polish Dermatological Society. *Dermatol Rev.* 2019;106(2):107–126.
3. Noodleman FR, Pollack SV. Trauma as a possible etiologic factor in basal cell carcinoma. *J Dermatol Surg Oncol.* 1986;12(8):841–846.
4. Dolan OM, Lowe L, Orringer MB, Rinek M, Johnson TM. Basal cell carcinoma arising in a sternotomy scar: A report of three cases. *J Am Acad Dermatol.* 1998;38(3):491–493.
5. Ünverdi ÖF, Yücel S. Basal cell carcinomas in trauma-related scar tissue: A rare case series. *Adv Skin Wound Care.* 2020;33(3):1–3.
6. Rustin MHA, Chambers TJ, Munro DD. Post-traumatic basal cell carcinomas. *Clin Exp Dermatol.* 1984;9(4):379–383.
7. Bagazgoitia L, Bea S, Santiago JL, Cuevas J, Juarranz Á, Jaén P. Multiple basal cell carcinomas arising on a thermal-burn scar: Successful treatment with photodynamic therapy. *J Eur Acad Dermatol Venereol.* 2009;23(4):459–461.
8. Hendricks WM. Basal cell carcinoma arising in a chickenpox scar. *Arch Dermatol.* 1980;116(11):1304–1305.
9. Rich JD, Shesol BF, Horne DW. Basal cell carcinoma arising in a smallpox vaccination site. *J Clin Pathol.* 1980;33(2):134–135.
10. Horton CE, Crawford HH, Love HG, Loeffler RA. The malignant potential of burn scar. *Plast Reconstr Surg Transplant Bull.* 1958;22(4):348–353.
11. Wallingford SC, Olsen CM, Plasmeijer E, Green AC. Skin cancer arising in scars: A systematic review. *Dermatol Surg.* 2011;37(9):1239–1244.

The incidence of acute kidney injury in children undergoing allogeneic hematopoietic stem cell transplantation: A pilot study

Monika Augustynowicz^{1,A–D}, Krzysztof Kałwak^{2,A,B}, Danuta Zwolińska^{1,A,E,F}, Kinga Musiał^{1,A,C,D,F}

¹ Department of Pediatric Nephrology, Wrocław Medical University, Poland

² Department of Bone Marrow Transplantation, Pediatric Oncology and Hematology, Wrocław Medical University, Poland

A – research concept and design; B – collection and/or assembly of data; C – data analysis and interpretation; D – writing the article; E – critical revision of the article; F – final approval of the article

Advances in Clinical and Experimental Medicine, ISSN 1899–5276 (print), ISSN 2451–2680 (online)

Adv Clin Exp Med. 2021;30(1):87–92

Address for correspondence

Kinga Musiał
E-mail: kinga_musial@hotmail.com

Funding sources

None declared

Conflict of interest

None declared

Received on September 4, 2020
Reviewed on September 26, 2020
Accepted on November 11, 2020

Published online on January 30, 2021

Abstract

Background. Acute kidney injury (AKI) is a common feature in adults undergoing allogeneic hematopoietic stem cell transplantation (alloHSCT). However, accurate assessment of AKI incidence in the pediatric population still seems a challenge.

Objectives. To evaluate the incidence of AKI according to the pRIFLE criteria in children undergoing alloHSCT, with special focus on differences between patients transplanted due to oncological and non-oncological indications.

Material and methods. A retrospective analysis of data, concerning 135 children undergoing alloHSCT due to oncological (89 patients) or other (46 patients) reasons, was performed. The values of estimated glomerular filtration rate (eGFR) were measured before alloHSCT, 24 h after, 1, 2, 3, 4, 8 weeks, 3 and 6 months after alloHSCT, and the AKI incidence was analyzed.

Results. Acute kidney injury was diagnosed in 54% of all patients. The Risk stage (R) was noticed at least once in 46% of oncological and 37% of non-oncological children. The Injury stage (I) concerned 12% of oncological and 6% of non-oncological patients undergoing alloHSCT. The incidence of AKI in both groups was comparable. The mean eGFR values in oncological children were higher than those in the non-oncological patients even before transplantation and until the 4th week after alloHSCT. The eGFR increased significantly in all patients 24 h after alloHSCT and returned to pre-transplantation records after 2–3 weeks. Then, oncological patients demonstrated a gradual decrement of eGFR. Six months after transplantation, eGFR values in oncological children were significantly lower compared to pre-transplantation records, whereas in non-oncological children, these values were comparable.

Conclusions. Although the type of indication for alloHSCT has no impact on the AKI incidence, children undergoing alloHSCT due to oncological reasons are at greater risk of renal impairment 6 months after transplantation than non-oncological patients.

Key words: acute kidney injury, estimated glomerular filtration rate, hyperfiltration, pRIFLE criteria

Cite as

Augustynowicz M, Kałwak K, Zwolińska D, Musiał K.
The incidence of acute kidney injury in children undergoing
allogeneic hematopoietic stem cell transplantation:
A pilot study. *Adv Clin Exp Med.* 2021;30(1):87–92.
doi:10.17219/acem/130355

DOI

10.17219/acem/130355

Copyright

© 2021 by Wrocław Medical University
This is an article distributed under the terms of the
Creative Commons Attribution 3.0 Unported (CC BY 3.0)
(<https://creativecommons.org/licenses/by/3.0/>)

Introduction

Hematopoietic stem cell transplantation (HSCT) is a recognized treatment method in children, and the indications for it are being constantly expanded.^{1–4} The pediatric population undergoing HSCT is unique in that a substantial number of patients require transplantation as a therapeutic tool against inborn anomalies. Thus, apart from dominating oncological reasons, there is a growing number of non-oncological indications for HSCT in children, such as aplastic anemia, immunodeficiencies or metabolic diseases.^{1,3} Aggressive therapy is associated with the occurrence of numerous side effects and the development of life-threatening complications.^{5–8} In the early post-transplantation period, management of opportunistic infections and symptoms associated with graft-versus-host disease (GVHD) constitute the main issue. Moreover, the majority of the transplantation-related conditions, including GVHD, hypertension, sepsis, or drug nephrotoxicity, compose the list of risk factors for acute kidney injury (AKI).⁹

In the light of these findings, AKI in pediatric patients undergoing HSCT seems to be an underestimated problem. Multicenter analyses, concerning all children hospitalized due to AKI, have shown that HSCT patients constitute the most numerous group among them.¹⁰ World reports also show alarming data on up to 34% of HSCT patients in whom AKI turns into chronic kidney disease.^{11,12}

So far, there have been few publications attempting to assess the scale of kidney damage in children undergoing hematopoietic stem cell allotransplantation (alloHSCT).^{13,14} A systematic review, performed in Australia, has reported the incidence of AKI in children after HSCT as between 11% and 42%, based on changes in absolute serum creatinine values or decrease in diuresis.¹⁵ American data indicate a significantly higher incidence of AKI (up to 84%), based on the pediatric (p)RIFLE criteria defining subsequent stages of acute kidney injury (Risk, Injury, Failure, Loss of function, End stage kidney disease).¹⁶ The latter seem to be a more suitable way of AKI evaluation in children, because they take into account the eGFR variability instead of serum creatinine absolute values, which strongly depend on muscle mass and hydration status.¹⁷

However, none of these reports took into account the pediatric specificity of patients qualified for HSCT, nor compared the subpopulations of patients transplanted due to oncological and non-oncological reasons.

Objectives

Therefore, the objective of the study was to assess the AKI incidence based on the pRIFLE criteria in children undergoing alloHSCT in the early, intermediate and late post-transplantation period, with distinction between children transplanted because of oncological and non-oncological reasons.

Material and methods

A retrospective analysis concerned medical records of 178 patients undergoing first (173 children) or next (5 patients) alloHSCT in the Department of Bone Marrow Transplantation, Pediatric Oncology and Hematology (Wroclaw Medical University, Poland) in the years 2016–2018. The observation period started before introducing conditioning therapy, then control examinations were performed in the early (after 24 h, and then after 1, 2, 3 and 4 weeks), intermediate (after 8 weeks and 3 months) and late (after 6 months) post-transplantation period.

The exclusion criteria for the patients were the age below 2 years and over 18 years. The patients' age varied from 1.5 months to 26 years. One hundred thirty-five out of 178 children (78 boys and 57 girls) met the age criteria (mean age: 8.27 ±5.14 years). They were divided into 2 groups according to the indications for allotransplantation: oncological or other.

The 1st group consisted 89 patients (53 boys, 36 girls; mean age: 9.84 ±4.34 years) qualified for transplantation due to oncological reasons. The detailed indications are given in Fig. 1. Forty-five percent of these patients were classified as a high-risk group according to specific treatment protocols, while 22% experienced recurrence. A total of 17% of children underwent alloHSCT as a standard intervention, consistent with the primary disease protocol; the rest underwent transplantation due to the failure of previous therapy. In 71% of cases, the donor was unrelated, in 23% – related and in 6% – haploidentical.

The 2nd group included 46 patients (25 boys, 21 girls; mean age: 9.16 ±4.78 years) who underwent alloHSCT following non-oncological indications, listed in detail in Fig. 2. A total of 72% of children underwent alloHSCT from an unrelated donor, 24% from a related donor and 4% from a haploidentical donor.

The serum creatinine concentrations were assessed in the fixed time points according to the hematological

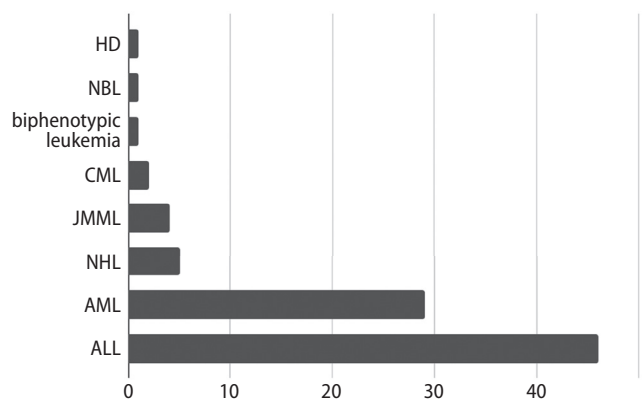


Fig. 1. Quantity of patients with oncological indications for alloHSCT

HD – Hodgkin disease; NBL – neuroblastoma, CML – chronic myeloid leukemia; JMML – juvenile myelomonocytic leukemia; NHL – non-Hodgkin disease; AML – acute myeloblastic leukemia; ALL – acute lymphoblastic leukemia.

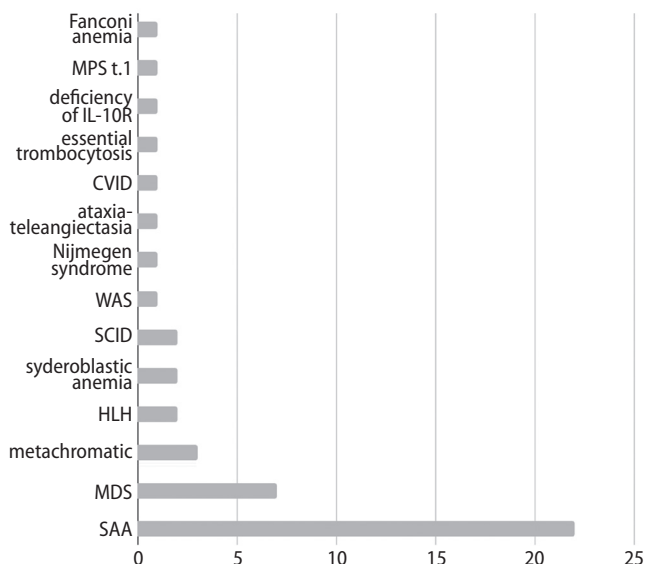


Fig. 2. Quantity of patients with non-oncological indications for alloHSCT

MPS t. 1 – mucopolysaccharidosis type 1; CVID – common variable immunodeficiency; WAS – Wiskott–Aldrich syndrome; SCID – severe variable immunodeficiency; HLH – hemophagocytic lymphohistiocytosis; MDS – myelodysplastic syndrome; SAA – severe aplastic anemia.

protocols: before conditioning, 24 h after allotransplantation, and then 1 week, 2, 3, 4, 8 weeks, and 3 and 6 months after alloHSCT. The creatinine concentration was measured using modified Jaffé method and eGFR was calculated based on the Schwarz formula.¹⁸ The eGFR changes were confronted with the pre-transplantation values.

In the majority of patients, conditioning therapy was myeloablative (busulfan, cyclophosphamide and fludarabine or fludarabine, treosulfan, thiotepa); the minority followed the non-myeloablative (cyclophosphamide, fludarabine) regimen. The protocol of prophylaxis against GVHD contained pre-HSCT ATG, cyclosporine A from 1 day before HSCT and methotrexate given in the 1st, 3rd and 6th day after transplantation. Ninety-eight out of 135 (69% of oncological and 77% of non-oncological) patients developed GVHD.

Acute kidney injury was diagnosed based on the pRI-FLE criteria.¹⁷ Hyperfiltration was defined according to recent pediatric guidelines and meta-analysis as eGFR ≥ 140 mL/min/1.73 m².^{19,20}

Continuous variables were reported as mean \pm standard deviation (SD), and categorical variables as frequencies and percentages. The comparisons of continuous variables were performed with analysis of variance (ANOVA) and Student’s t-test. The relations between categorical variables were tested with χ^2 test or Fisher’s exact test. A value of $p < 0.05$ was considered significant. All calculations were carried out with the use of STATISTICA v. 13.3 (StatSoft Inc., Tulsa, USA).

All procedures were performed in accordance with the 1964 Declaration of Helsinki and its further amendments. The retrospective waiver of consent was obtained from the University Hospital ethical committee.

Results

Patients undergoing alloHSCT due to oncological reasons were more numerous than those transplanted because of non-oncological conditions. The mean eGFR values were above 90 mL/min/1.73 m² in all patients before transplantation, independent of the underlying disease (Fig. 3,4). None of the patients presented with eGFR < 60 mL/min/1.73 m² before alloHSCT. The peak eGFR values were observed 1 day and 1 week after alloHSCT in both groups (Fig. 3,4). Then, they returned to those observed before the treatment after 1 week (non-oncological patients) or after 2 weeks (oncological patients). From that turning point, mean eGFR in oncological children remained lower than before alloHSCT and decreased significantly at each time point from the 4th week until the 6th month of observation

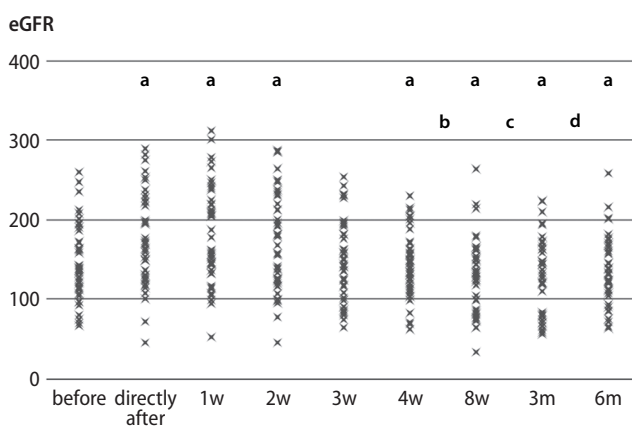


Fig. 3. The values of estimated glomerular filtration rate (eGFR) in oncological patients

before – before alloHSCT; directly after – 24 h after alloHSCT; 1w – 1 week after alloHSCT; 3m – 3 months after alloHSCT; a – $p < 0.05$ any time point compared to before alloHSCT; b – $p < 0.05$ 8 weeks compared to 4 weeks after alloHSCT; c – $p < 0.05$ 3 months compared to 8 weeks after alloHSCT; d – $p < 0.05$ 6 months compared to 3 months after alloHSCT.

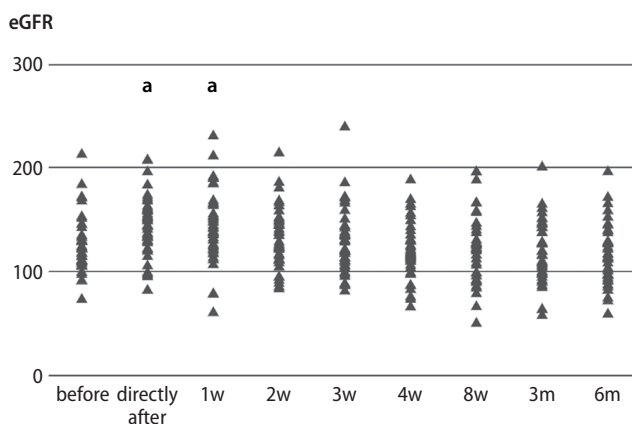


Fig. 4. The values of estimated glomerular filtration rate (eGFR) in non-oncological patients

before – before alloHSCT; directly after – 24 h after alloHSCT; 1w – 1 week after alloHSCT; 3m – 3 months after alloHSCT; a – $p < 0.05$ any time point compared to before alloHSCT.

Table 1. Incidence of acute kidney injury in examined patients

Pediatric(p)RIFLE criteria		1 day after alloHSCT	1 week after alloHSCT	2 weeks after alloHSCT	3 weeks after alloHSCT	4 weeks after alloHSCT	8 weeks after alloHSCT	3 months after alloHSCT	6 months after alloHSCT
Oncological patients	Risk (↓ eGFR > 25%)	1 (1.1%)	0	7 (7.9%)	13 (14.6%)	16 (18.0%)	31 (34.8%)	21 (23.6%)	18 (20.2%)
	Injury (↓ eGFR > 50%)	1 (1.1%)	0	1 (1.1%)	1 (1.1%)	0	2 (2.2%)	6 (6.7%)	0
Non-oncological patients	Risk (↓ eGFR > 25%)	0	1 (2.2%)	4 (8.9%)	3 (6.7%)	9 (20.0%)	8 (17.8%)	8 (17.8%)	5 (11.1%)
	Injury (↓ eGFR > 50%)	1 (2.2%)	0	0	0	0	1 (2.2%)	1 (2.2%)	0

eGFR – estimated glomerular filtration rate; alloHSCT – allogeneic hematopoietic stem cell transplantation.

(Fig. 3). Contrarily, mean eGFR in non-oncological patients remained stable and comparable to pre-transplantation records, from the 3rd week until the 6th month of follow-up (Fig. 4).

The incidence of AKI at subsequent time points before and after alloHSCT varied with time (Table 1). In the entire time interval (0–6 months after transplantation), 54% of patients demonstrated the features of AKI according to the pRIFLE criteria. The risk stage (R) appeared at least once in 58 patients (41 oncological and 17 non-oncological) and the injury stage (I) in 14 patients (11 oncological and 3 non-oncological). The biggest number of AKI episodes was noticed 8 weeks after alloHSCT and the R incidence was then significantly higher in oncological than in non-oncological patients ($\chi^2 = 4.5$; $p = 0.034$). None of the patients experienced the failure stage (F) with eGFR decrease exceeding 75%.

After 6 months, oncological patients demonstrated significantly diminished eGFR values compared to the pre-transplantation records, whereas in non-oncological children these values were comparable (Fig. 3,4). In 12 children, eGFR values varied between 60 mL/min/1.73 m² and 89 mL/min/1.73 m², whereas in 2 patients eGFR dropped below 60 mL/min/1.73 m².

During the observation period, 10 patients died (0.7%). One death was a direct consequence of allotransplantation (20 days after HSCT), while the remaining ones were associated with late, non-nephrological complications. None of the patients, observed for up to 6 months, required renal replacement therapy.

Discussion

The incidence of AKI throughout the 6-month observation period in our study group was as high as 54%. Our data are concordant with the estimations performed by other authors, stressing the importance of renal function follow-up in the post-HSCT period.^{13,15,16}

Indeed, the post-HSCT renal dysfunction is a well-documented phenomenon among adult patients, analyzed from

the perspectives of AKI incidence, other comorbidities, long-term outcome, and mortality.²¹ Recent meta-analysis proved that, despite progress in diagnosing AKI, its incidence in adults remains high and affects more than 50% of patients undergoing HSCT.²² However, analyses in pediatric patients concentrated rather on the impact of AKI on overall mortality or long-term prognosis than on aspects of early renal dysfunction and its consequences.^{13–16}

The higher incidence of AKI among patients after allotransplantation compared to autotransplantation is also well-known and has justified our decision to concentrate on children undergoing alloHSCT.^{22,23} The pediatric specificity gave us a unique opportunity to confront the 2 subpopulations – those with the flagship oncological reason for HSCT with those who had indications like immune deficiencies and inborn metabolic disorders, non-existent in adult patients qualified for HSCT. We have reported the preponderance of children transplanted due to oncological reasons over those treated with HSCT because of non-oncological indications. The evaluation of AKI incidence in the whole group revealed that R was diagnosed over 4 times more often than I. In detail, R concerned 43% of all children after alloHSCT (46% of oncological and 37% of non-oncological patients), whereas I affected 10% of the whole studied group (12% of oncological patients and less than 1% of non-oncological patients). Despite discrepancies in the number and percentage of patients affected by R or I between 2 subgroups, these differences reached statistical significance at only 1 time point. Eight weeks after transplantation, the R incidence was higher among oncological patients compared to non-oncological children.

The pattern of fluctuations in the AKI incidence also seemed similar in both groups. The number of R patients peaked between the 4th and 8th week after alloHSCT (irrespective of the analyzed group), then stabilized (non-oncological) or even diminished (oncological) until the 6th month of observation. Patients classified to I were clinically significant in number only in the oncological population 3 months after alloHSCT. Otherwise, single cases were noticed throughout the whole observation period.

The similar overall AKI incidence and its fluctuations during observation period in both groups may result from the fact that there were no significant differences in treatment regimens or severity of complications between oncological and non-oncological patients. The vast majority of children followed myeloablative protocols and similar GVHD prophylaxis. The incidence of GVHD or infections did not differ between the subgroups.

However, the abovementioned similarity in both subgroups stayed in contrast with the parameters of renal function. The eGFR values and the incidence of hyperfiltration were significantly higher in oncological compared to non-oncological patients. Hyperfiltration is a recognized condition in children with malignancies, increasing in frequency with subsequent cycles of chemotherapy and connected with the patients' hypermetabolic state.²⁴ The routine procedures during first 3 weeks after HSCT, like intravenous nourishment and additional fluid intake at the amount of 3 L/m²/day with subsequent administration of diuretics if needed, may add to already increased eGFR values. Indeed, in our patients a significant elevation of eGFR values was detected 24 h and one week after alloHSCT.

Therefore, the eGFR discrepancy between oncological and non-oncological patients, persisting only until the 4th week after the procedure, was aggravated by iatrogenic interventions. When intravenous supplementation was ceased, the tendency reversed and from the 8th week after alloHSCT eGFR values were similar in both groups. However, an alarming trend appeared from the 4th week after alloHSCT. The eGFR values in oncological patients decreased systematically until the 6th month of observation. Such a result may suggest possible long-term renal function deterioration, but longer observation is needed to confirm this hypothesis.

Our study has limitations. This retrospective report contained data collected according to hematological protocols. Therefore, a few nephrological aspects are missing, such as urine output or cystatin C measurements. Both groups were heterogeneous, especially in the case of non-oncological patients. The majority of patients were followed up regularly only until the 3rd month after alloHSCT; some of them were then transferred to the hematological centers near home. Thus, the analysis longer than 6 months was not possible.

Conclusions

The AKI incidence in children undergoing alloHSCT is independent of indication for this procedure, whereas eGFR values seem conditioned by previous chemotherapy in oncological patients. Children undergoing alloHSCT due to oncological reasons are at a greater risk of renal dysfunction 6 months after transplantation than the population with non-oncological indications for this therapy.

ORCID iDs

Monika Augustynowicz  <https://orcid.org/0000-0002-3229-2832>
 Krzysztof Kałwak  <https://orcid.org/0000-0003-1174-5799>
 Danuta Zwolińska  <https://orcid.org/0000-0002-6714-3992>
 Kinga Musiał  <https://orcid.org/0000-0002-9000-7585>

References

- Slatter MA, Gennery AR. Hematopoietic cell transplantation in primary immunodeficiency: Conventional and emerging indications. *Exp Rev Clin Immunol.* 2008;14(2):103–114.
- Xu L, Chen H, Chen J, et al. The consensus on indications, conditioning regimen and donor selection of allogeneic hematopoietic cell transplantation for hematological diseases in China: Recommendations from the Chinese Society of Hematology. *J Hematol Oncol.* 2018;11(1):33. doi:10.1186/s13045-018-0564-x
- Sureda A, Bader P, Cesaro S, et al. Indications for allo- and auto-HSCT for haematological diseases, solid tumours and immune disorders: Current practice in Europe. *Bone Marrow Transplant.* 2015;50(8):1037–1056.
- Hołowiecki J. Indications for hematopoietic stem cell transplantation. *Pol Arch Med Wewn.* 2008;118(11):658–662.
- Hierlmeier S, Eyrich M, Wölfl M, Schlegel PG, Wiegner V. Early and late complications following hematopoietic stem cell transplantation in pediatric patients: A retrospective analysis over 11 years. *PLoS One.* 2018;13(10):e0204914. doi:10.1371/journal.pone.0204914
- Sahin U, Toprak SK, Atilla PA, Atilla E, Demirel T. An overview of infectious complications after allogeneic hematopoietic stem cell transplantation. *J Infect Chemother.* 2016;22(8):505–514.
- Harris AC, Young R, Devine S, et al. International, multi-center standardization of acute graft versus host disease clinical data collection: A report from the MAGIC consortium. *Biol Blood Marrow Transplant.* 2016;22(1):4–10.
- Ciki K, Dogru D, Kuskonmaz B, et al. Pulmonary complications following hematopoietic stem cell transplantation in children. *Turk J Ped.* 2019;61(1):59–70.
- Wanchoo R, Stotter BR, Bayer RL, Jhaveri KD. Acute kidney injury in hematopoietic stem cell transplantation. *Curr Opin Crit Care.* 2019;25(6):531–538.
- Zeng X, McMahon GM, Brunelli SM, Bates DW, Waikar SW. Incidence, outcomes, and comparisons across definitions of AKI in hospitalized individuals. *Clin J Am Soc Nephrol.* 2014;9(1):12–20.
- Ando M. An overview of kidney disease following hematopoietic cell transplantation. *Int Med.* 2018;57(11):1503–1508.
- Ileri TL, Ertem M, Ozcakar ZB, et al. Prospective evaluation of acute and chronic renal function in children following matched related donor hematopoietic stem cell transplantation. *Pediatr Transplant.* 2010;14(1):138–144.
- Koh KN, Sunkara A, Kang G. Acute kidney injury in pediatric patients receiving allogeneic hematopoietic cell transplantation: Incidence, risk factors and outcomes. *Biol Blood Marrow Transplant.* 2018;24(4):758–764.
- Raina R, Herrera N, Krishnappa V, et al. Hematopoietic stem cell transplantation and acute kidney injury in children: A comprehensive review. *Pediatr Transplant.* 2017;21(4):e12935. doi:10.1111/ptr.12935
- Didsbury MS, Mackie FE, Kennedy SE. A systematic review of acute kidney injury in pediatric allogeneic hematopoietic stem cell recipients. *Pediatr Transplant.* 2015;19(5):460–470.
- Kizilbash SJ, Kashtan CE, Chavers BM, Cao Q, Smith AR. Acute kidney injury and the risk of mortality in children undergoing hematopoietic stem cell transplantation. *Biol Blood Marrow Transplant.* 2016;22(7):1264–1270.
- Sutherland SM, Byrnes JJ, Kothari M, et al. AKI in hospitalized children: Comparing the pRIFLE, AKIN and KDIGO definitions. *Clin J Am Soc Nephrol.* 2015;10(4):554–561.
- Schwartz GJ, Munoz A, Schneider MF, et al. New equations to estimate GFR in children with CKD. *J Am Soc Nephrol.* 2009;20(3):629–637.
- Cachat F, Combesure C, Cauderay M, Girardin E, Chehade H. A systematic review of glomerular hyperfiltration assessment and definition in the medical literature. *Clin J Am Soc Nephrol.* 2015;10(3):382–389.
- Iduoriyekemwen NJ, Ibadin MO, Aikhionbare HA, Idogun SE, Abiodun MT. Glomerular hyperfiltration in excess weight adolescents. *Niger J Clin Pract.* 2019;22(6):842–848.

21. Krishnappa V, Gupta M, Manu G, Kwatra S, Owusu OT, Raina R. Acute kidney injury in hematopoietic stem cell transplantation: A review. *Int J Nephrol*. 2016;2016:5163789. doi:10.1155/2016/5163789
22. Kanduri SR, Cheungpasitporn W, Thongprayoon C, et al. Incidence and mortality of acute kidney injury in patients undergoing hematopoietic stem cell transplantation: A systematic review and meta-analysis. *QJM*. 2020;113(9):621–632. doi:10.1093/qjmed/hcaa072
23. Caliskan Y, Besik SK, Sargin D, Ecder T. Early renal injury after myeloablative allogeneic and autologous hematopoietic cell transplantation. *Bone Marrow Transplant*. 2006;38(2):141–147.
24. Kwatra NS, Meany HJ, Ghelani SJ, Zahavi D, Pandya N, Majd M. Glomerular hyperfiltration in children with cancer: Prevalence and a hypothesis. *Pediatr Radiol*. 2017;47(2):221–226.

The role of soluble programmed death protein-1 (sPD-1) and soluble programmed death ligand-1 (sPD-L1) in rat corneal transplantation rejection

Guoguo Yi^{1,A–F}, Ruiwen Yi^{1,A–D}, Xinglu Chen^{2,B,C}, Ling Peng^{3,A–C}, Guoqiang Huang^{4,B,C}, Min Fu^{1,A,D}, Xiao-he Lu^{1,E,F}, Hongwei Li^{5,E,F}

¹ Zhujiang Hospital of Southern Medical University, Guangzhou, China

² 1st Affiliated Hospital of Guangdong Pharmaceutical University, Kanton, China

³ Women & Children's Health Institute of Futian, Shenzhen, China

⁴ Meizhou People's Hospital, China

⁵ School of Biotechnology, Southern Medical University, Kanton, China

A – research concept and design; B – collection and/or assembly of data; C – data analysis and interpretation;

D – writing the article; E – critical revision of the article; F – final approval of the article

Advances in Clinical and Experimental Medicine, ISSN 1899-5276 (print), ISSN 2451-2680 (online)

Adv Clin Exp Med. 2021;30(1):93–100

Address for correspondence

Xiao-he Lu

E-mail: luxh63@163.com

Funding sources

None declared

Conflict of interest

None declared

Received on December 13, 2017

Reviewed on December 20, 2017

Accepted on April 9, 2018

Published online on January 13, 2021

Cite as

Guoguo Y, Ruiwen Y, Xinglu C, et al. The role of soluble programmed death protein-1 (sPD-1) and soluble programmed death ligand-1 (sPD-L1) in rat corneal transplantation rejection. *Adv Clin Exp Med.* 2021;30(1):93–100. doi:10.17219/acem/89803

DOI

10.17219/acem/89803

Copyright

© 2021 by Wrocław Medical University

This is an article distributed under the terms of the Creative Commons Attribution Non-Commercial License (<http://creativecommons.org/licenses/by-nc-nd/4.0/>)

Abstract

Background. Immunological rejection is one of the problems in corneal transplantation. Recently, some research found out that soluble programmed death protein-1 (sPD-1) and soluble programmed death ligand protein-1 (sPD-L1) play a significant role in immunologic suppression.

Objectives. To explore expression of sPD-1 and sPD-L1 in a penetrative corneal transplantation model and its relationship with transplant rejection.

Material and methods. Autologous corneal transplantation rat models and allogeneic corneal transplantation rat models were used as the control group and the experimental group, respectively. Changes of the transplanted grafts were observed under a slit-lamp microscope. Hematoxylin-eosin (H&E) staining was applied to examine the histopathological features of the corneal grafts. Flow cytometry was used to analyze CD4⁺CD25⁺Treg in the serum and spleen. The sPD-1, sPD-L1, interleukin-10 (IL-10) and interleukin-4 (IL-4) levels in serum and the aqueous humor of the rats were detected using enzyme-linked immunosorbent assay (ELISA).

Results. After the operation, no transplant rejection occurred in the control group. Flow cytometry results showed that expressions of CD4⁺CD25⁺Treg in serum in the experimental group were lower than those in the control group ($p < 0.05$). The ELISA results showed that after the operation, sPD-1 and sPD-L1 expression levels in serum in the experimental group were higher than in the control group (all $p < 0.05$). After the operation, IL-10 and IL-4 content in serum in the experimental group was lower than in the control group (all $p < 0.05$). The sPD-1/sPD-L1 ratio in the experimental group was higher than in the control group.

Conclusions. Increases of sPD-1 content and decreases of CD4⁺CD25⁺Treg, IL-10 and IL-4 levels may be involved in corneal allograft rejection. Dynamic detection of the content of sPD-1 and sPD-L1 in serum and aqueous humor after the operation would help in understanding the local immune response in a clinical setting and predicting the occurrence of corneal graft rejection.

Key words: sPD-1, sPD-L1, CD4⁺CD25⁺Treg, corneal transplantation, immunological rejection

Introduction

Various ocular surface diseases and traumatism can cause irreversible corneal blindness, and corneal transplantation is the most important way of restoring sight. Although the success rate of transplantation operations is high, immunological rejection is still a leading cause of corneal transplantation failure.^{1,2} Immunosuppressors are used in clinical practice and have shown remarkable results. However, the high price and obvious toxicity of immunosuppressors, as well as their side effects, limit the long-term use of immunosuppressors. Hence, in recent years, more attention has been paid to how to suppress corneal transplant rejection and prolong the survival time of corneal grafts by inducing transplant graft tolerance. Much evidence has shown that activating the T lymphocyte requires co-stimulatory signals, which can help successfully induce transplant graft tolerance in transplantation immunity.^{3,4} Programmed death protein-1 (PD-1) and programmed death ligand-1 (PD-L1) are important negative pathways for regulating the T lymphocyte.^{5,6}

CD4⁺CD25⁺Treg has immunosuppressive effects, plays a crucial role in suppressing the immune response, and can enhance immune tolerance by suppressing responding T cells.^{7,8} Research has shown that the PD-1/PD-L1 pathway plays an important part in balancing CD4⁺CD25⁺Treg autoimmunity and negatively regulating transplant rejection.⁹ Programmed death protein-1 and PD-L1 exist in membrane and soluble forms, namely soluble programmed death protein-1 (sPD-1) and soluble programmed death ligand-1 (sPD-L1).¹⁰ Programmed death ligand-1 is a significant factor for corneal immune-privileged status, which can prevent the occurrence of transplant rejection.¹¹ In addition, it has been reported that excessive sPD-1 leads to immunologic injury by blocking the PD-1/PD-L1 pathway.¹² In other words, expression of sPD-1 may increase corneal transplant rejection by restraining the PD-1/PD-L1 signal. Some studies have indicated that the CD4⁺CD25⁺Treg cell is related to successful allotransplantation and expression of Foxp3 on the CD4⁺CD25⁺Treg cell is one of the vital factors for corneal allograft survival.^{13,14} However, research on the functions and relationships of sPD-1/sPD-L1, CD4⁺CD25⁺Treg and correlating factors in corneal transplantation immunity is still rare. This research would establish penetrative corneal transplantation models in rats and primarily explore their functions and relations in transplant rejection after corneal transplantation.

Material and methods

Experimental animals

Thirty healthy female Sprague Dawley (SD) rats were used as donors and 70 female Wistar rats as receptors. All rats were clean, 6–8-weeks old, weighed 180–220 g,

and were provided by the Animal Experiment Center of Southern Medical University (Kanton, China)

The rats were divided into 2 groups. The control group, used 60 Wistar rats as donors and receptors to conduct autologous corneal transplantation. In the experimental group allogeneic corneal transplantations were performed that included 30 SD donor rats and 60 receptor Wistar rats. Another 10 Wistar rats were used to detect preoperative values. This research was examined and approved by the Southern Medical University Ethics Committee. All procedures were performed and animals were cared for and treated in accordance with the policies of the Association for Research in Vision and Ophthalmology Department for the Use of Animals in Ophthalmic and Vision Research.

Reagents

Fluorescent monoclonal antibodies Anti-Rat CD25 per-CP-eFluor[®] 710 and Anti-Rat CD4 FITC were bought from Affymetrix eBioscience (Thermo Fisher Scientific, Waltham, USA). Enzyme-linked immunosorbent assay (ELISA) kits for interleukin-10 (IL-10), interleukin-4 (IL-4), PD-1, and PD-L1 were bought from Sango Biotech (Shanghai, China).

Experimental methods and steps

Establishing allogeneic corneal transplantation models

According to the method described by Williams et al., binocular corneas were taken from all donor rats; receptor rats were operated on their right eyes.¹⁵ Donors and receptors were injected with 10% chloral hydrate (35–42 mg/kg) intraperitoneal injection of anesthesia and received 5% hydrochloric acid, proparacaine eye drops and compound tropicamide eye drops 3 times each 15 min before the operation. The whole operation was conducted aseptically with sterile drapes under a microscope. First, the corneal grafts of donor SD rats were taken with a 3.3-mm trephine and placed into a Petri dish under the protection of viscoelastic sodium hyaluronate. A right-eye implant bed for receptors was made with a 3.0-mm trephine. Viscoelastic sodium hyaluronate was injected during the operation to maintain anterior chamber depth. Grafts were placed on the implant bed and 8 interrupted stitches were sutured with a 10-0 nylon suture without embedding thread residue. After the operation, a proper amount of balanced salt solution was injected into the anterior chamber and levofloxacin eye ointment was applied in the conjunctival sac. The eyelid was sutured with a 5-0 silk thread and the stitches were removed 1 day after the operation.

Establishing autologous corneal transplantation models

Corneal grafts of the Wistar rats were taken with a 3.0-mm trephine and rotated about 180°. Eight interrupted stitches were sutured with a 10-0 nylon suture in situ.

The following steps were the same with allogeneic corneal transplantation models.

Observing immunological rejection after corneal transplantation

The corneal grafts in each group were observed under a slit-lamp microscope and records were made of the transparency, angiogenesis growth condition and rejection response, starting 1 day after the operation. The observation period was 28 days, once a day. Once such ocular complications as graft infection, hyphema, loss of anterior chamber, and anterior synechia occurred because of the operation and other factors, the rat would be removed and replaced. According to the scoring criteria of Larkin et al.,¹⁶ scores would be given considering the opacification, edema and angiogenesis of the corneal grafts. Rejection index (RI) was calculated by adding up the scores of all 3 indexes. The rejection exits were defined when RI > 5 or the opacification of the corneal graft score reached 3.

Histopathological examination

Two receptor rats in each group were killed 3 days, 7 days, 14 days, 4 weeks, and 8 weeks after the operation, respectively. The whole cornea was cut off from the self-limbal grafts and the corneal tissue was fixed in 10% paraformaldehyde solution to receive conventional dehydrating and paraffin embedding. Hematoxylin-eosin (HE) staining and optical microscopy were used in the histopathological examination.

Flow cytometry detection

Four receptor rats in each group were killed 3 days, 7 days, 14 days, 4 weeks, and 8 weeks after the operation, respectively. Anti-clotting serum and spleen cell suspension were detected in sterile conditions with flow cytometry. Anterior chamber aqueous humor was taken for the ELISA detection.

Enzyme-linked immunosorbent assay

Six receptor rats in each group were killed 3 days, 7 days, 14 days, 4 weeks, and 8 weeks after the operation, respectively. Serum and anterior chamber aqueous humor were taken in sterile conditions. The sPD-1, sPD-L1, IL-10, and IL-4 concentration levels were detected in serum and anterior chamber aqueous humor.

Statistical methods

The experimental data was expressed as $\bar{x} \pm s$ and analyzed with SPSS v. 20.0 software (IBM Corp., Armonk, USA). Survival rates of the corneal grafts were analyzed with Kaplan-Meier survival curves. The independent samples t-test was used to compare the detection results in both groups.

A nonparametric rank-sum test was used when non-normal distributions of unequal variances occurred. The data was considered statistical significant when $p < 0.05$.

Results

Postoperative slit-lamp microscope observation and comparison of graft survival time

The comparison of graft survival time is shown in Fig. 1. In the experimental group, 3 days after the operation, there was a slight edema and opacity on the cornea and limbus cornea vessels dilated, while the cornea obviously thickened, and hydrops and opacity increased, with new blood vessels sprouting on day 7. Fourteen days after the operation, corneal graft edema worsened while the grafts thickened and bulged outwards. In addition, opacity of the cornea became apparent with the iris blurred, and new blood corneal vessels developed and embedded into the grafts. Four weeks after the operation, corneal graft edema lightened; grafts thickened and bulged outwards; corneas stayed turbid; new blood corneal vessels grew near the center. Eight weeks after the operation, corneal grafts showed little edema and were overgrown by new blood vessels; pupils could be indistinctly detected; stitches loosened and came off to different extents (Fig. 1A).

In the control group, 3 days after the operation, there was a situation similar to that in the experimental groups and the iris was visible. After 7 days, there was a slight edema in corneal grafts while the iris was visible and the limbus cornea vessels were dilated. After 14 days, corneal graft edema disappeared and the iris vessels were visible. Four weeks after the operation, there was no apparent edema, thickening and opacity of the corneal grafts, and a small number of new blood vessels occurred around the stitches. Eight weeks after the operation, corneal grafts and the iris could be observed. Additionally, a small number of new blood vessels formed around the stitches (Fig. 1B). The survival rates of the grafts are shown in Fig. 2. After the operation, the corneal graft survival rate in the control group remain stable. Unlike the control group, the average survival time between the corneal grafts in the experimental group was 13.1 ± 2.2 days. The difference between the corneal graft survival curves was statistically significant ($t_s = 21.026$, $p = 0.000$).

Histopathological examination

The histopathological features were different between the experimental group and the control group after the operation (Fig. 3). In the experimental group, after the operation, the stroma collagen fiber structure of the corneal grafts was arranged chaotically and proliferated. In addition, not only the new blood vessels appeared over the corneal

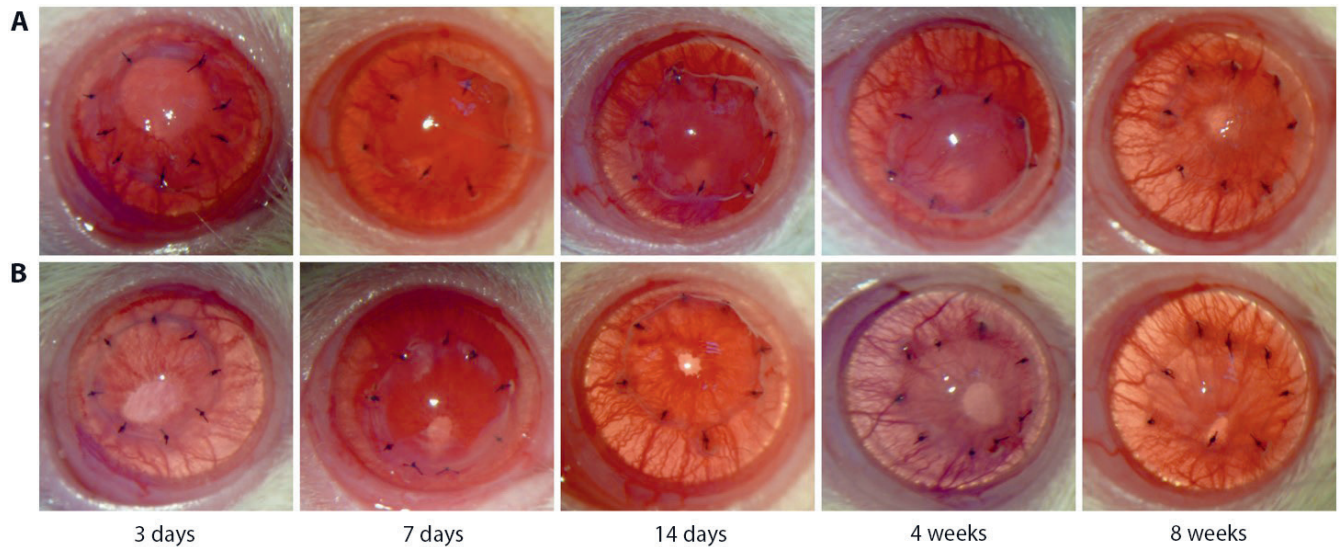


Fig. 1. Postoperative slit-lamp observation results. A. The results showed the change of cornea and limbus cornea vessels in the experimental group within 3 days, 7 days, 14 days, 4 weeks, and 8 weeks after the operation. The corneal graft has slight edema in 3d after the operation and new blood vessels sprouted on the 7th day. Edema worsened in 14 days and in 8 weeks edema was reduced; B. After the operation in the control group, corneal graft edema disappeared within 14 days after the operation. There were few new blood vessels generated. The difference of corneal graft survival curves is statistically significant ($t_s = 21.026$, $p = 0.000$).

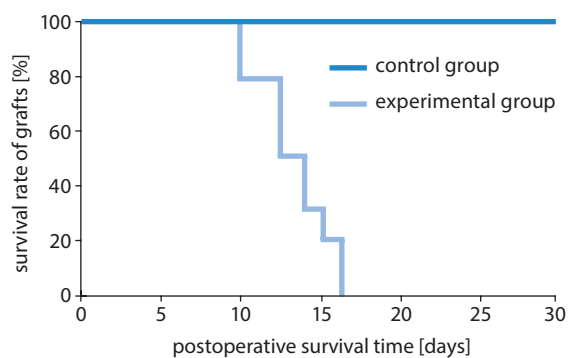


Fig. 2. The results show the comparison of survival rates of the corneal graft between the control group and experimental group

The survival rate of the corneal graft in the experimental group decreased as time increased. The survival rate of the corneal graft in the control group remained unchanged

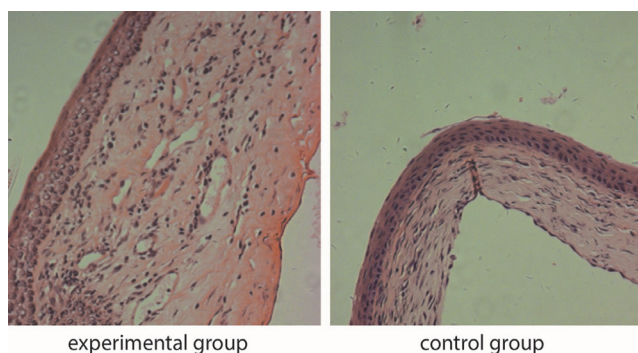


Fig. 3. Comparison of histopathological features between the experimental group and control group

After the operation, the stroma collagen fiber structure of the corneal grafts ranked irregularly in the experimental group while it was arranged orderly in the control group. New blood vessels, spongiform and disintegrating can be observed in the experimental group. There was no significant change in the control group.

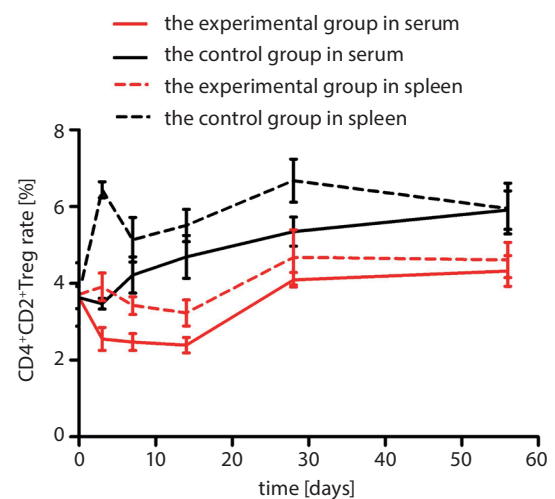


Fig. 4. Expression level of CD4⁺CD25⁺Treg in serum and spleen

The CD4⁺CD25⁺Treg cell expression levels in serum and the spleen in the experimental group were all higher than in the control group (all $p < 0.05$).

periphery, but also spongiform and disintegrating appeared on the epithelial grafts. Additionally, a lot of inflammatory cells were infiltrated after the operation. However, compared to the experimental group, no obvious thickening of the corneal grafts occurred in the control group. Additionally, the stroma collagen fiber structure was basically arranged orderly. Only a small amount of inflammatory cells was infiltrated. No obvious new blood vessels had formed.

Detection results of flow cytometry

The expression level of CD4⁺CD25⁺Treg in the serum and spleen is shown in Fig. 4. The expression level of CD4⁺CD25⁺Treg in serum in the control group decreased

to its lowest point at day 3 and began increasing gradually. It exceeded the preoperative value after 7 days and reached a peak 8 weeks after the operation. In the experimental group, the expression level of CD4⁺CD25⁺Treg in serum started to fall 3 days after the operation, dropping below its preoperative value. It declined to its lowest level after 14 days and then gradually increased to a peak 8 weeks after the operation. CD4⁺CD25⁺Treg content in serum in the experimental group was higher than in the control group at each time point after the operation. The group difference was statistically significant ($t = 5.564, 6.722, 7.667, 5.869, 4.954$; $p = 0.001, 0.001, 0.000, 0.001, 0.003$). In both groups, the expression level of CD4⁺CD25⁺Treg in the spleen immediately increased 3 days after the operation. In the control group, it gradually rose from day 14 and reached a peak 4 weeks after the operation. The expression level of CD4⁺CD25⁺Treg was higher than the preoperative value. In the experimental group, the expression level of CD4⁺CD25⁺Treg started to decrease after 7 days and reached its lowest point 14 days after the operation. The expression level of CD4⁺CD25⁺Treg in the spleen in the experimental group was prominently lower than in the control group. The group difference was statistically significant ($t = 11.885, 5.461, 8.469, 4.407, 3.323$; $p = 0.000, 0.002, 0.000, 0.005, 0.016$).

Expression level of sPD-1

In the experimental group, the expression level of sPD-1 in serum started to increase 3 days after the operation, reached its highest point after 14 days and gradually decreased to its lowest point, reaching 8 weeks after the operation. The sPD-1 content was higher than the preoperative value at each time point after the operation. In the control group, the expression level of sPD-1 in serum was lower than the preoperative value at each time point, except on the 3rd day after the operation, and reached its lowest point 8 weeks after the operation. The expression level of sPD-1 in serum in the experimental group was prominently higher than in the control group. The group difference was statistically significant ($t = 2.399, 3.013, 4.574, 2.921, 2.817$; $p = 0.037, 0.013, 0.001, 0.015, 0.018$). Similarly, the expression level of sPD-1 in the experimental group in aqueous humor immediately increased after 3 days, reached a peak 14 days after the operation and started to decrease afterwards. The expression level of sPD-1 was higher than the preoperative value. In the control group, it reached a peak 3 days after the operation and gradually decreased. The expression level of sPD-1 in the experimental group was prominently higher than in the control group at each time point after the operation. The group difference was statistically significant ($t = 2.409, 2.964, 4.128, 2.375, 2.403$; $p = 0.037, 0.014, 0.002, 0.039, 0.037$) (Fig. 5A).

Expression level of sPD-L1

In both groups, the expression level of sPD-L1 in serum decreased 3 days after the operation, while it began to increase gradually in the control group. In the experimental group,

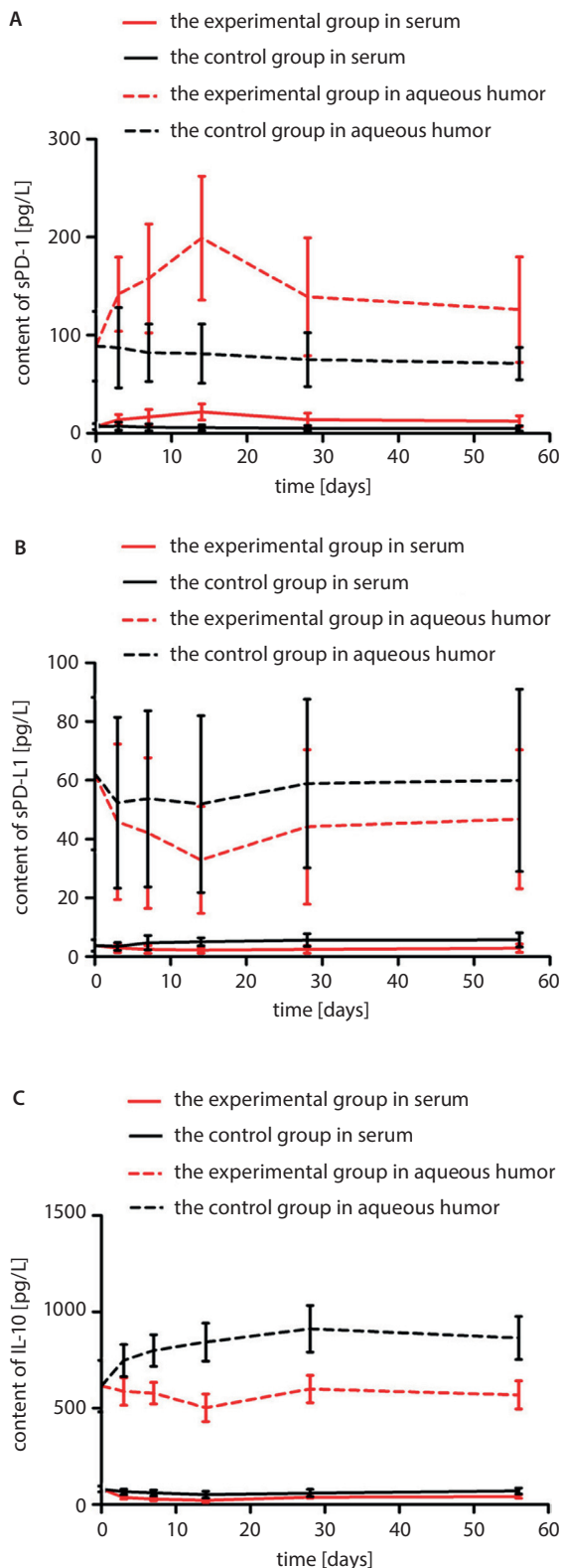
it was gradually reduced to its lowest point, reaching it 14 days after the operation, and then slightly increased. The expression level of sPD-L1 in serum in the experimental group was lower than in the control group at each time point after the operation. Only the group difference 14 days after the operation was statistically significant. In the control group, the expression level of sPD-L1 in aqueous humor immediately decreased on the 3rd day after the operation and gradually increased afterwards. In the experimental group, the expression level of sPD-L1 began to decrease on the 3rd day, reached its lowest point 14 days after the operation and then started to increase gradually. The expression level of sPD-L1 in aqueous humor in the experimental group was lower than in the control group at each time point after the operation; however, the group difference was not statistically significant (Fig. 5B).

Expression level of interleukin-10

In both groups, IL-10 content in serum decreased to its lowest point 14 days after the operation and gradually increased afterwards. The expression level of IL-10 in serum in the experimental group was prominently lower than in the control group. The group difference was statistically significant ($t = 4.515, 4.663, 3.591, 2.673, 3.940$; $p = 0.001, 0.001, 0.005, 0.023, 0.003$). In the control group, the expression level of IL-10 in aqueous humor gradually increased to a peak, which was reached 4 weeks after the operation. In the experimental group, the expression level of IL-10 in aqueous humor started to decrease 3 days after the operation, reaching its lowest point 14 days after the operation, which was lower than the preoperative value. The expression level of IL-10 in aqueous humor in the experimental group was prominently lower than in the control group. The group difference was statistically significant ($t = 3.609, 5.451, 6.868, 5.424, 5.432$; $p = 0.005, 0.000, 0.000, 0.000, 0.000$) (Fig. 5C).

Expression level of interleukin-4

In both groups, IL-4 content in serum decreased 3 days after the operation. In the control group, it gradually increased 7 days after the operation and only the expression level of IL-4 after 3 days was higher than the preoperative value. The expression level of IL-4 in serum in the experimental group was prominently lower than that in the control group. The group difference was statistically significant ($t = 2.338, 2.644, 4.561, 4.896, 6.882$; $p = 0.042, 0.025, 0.001, 0.001, 0.000$). Similarly, IL-4 content in both groups in aqueous humor decreased 3 days after the operation. In the experimental group, it sharply decreased and reached its lowest point 14 days after the operation. In the control group, it gradually increased from the 7th day after the operation. Interleukin-4 content in aqueous humor in the experimental group was prominently lower than in the control group. The group difference was statistically significant ($t = 7.323, 10.639, 11.190, 11.860, 9.327$; $p = 0.000, 0.000, 0.000, 0.000, 0.000$) (Fig. 5D).



Analysis of ratios between sPD-1 and sPD-L1 in control and experimental groups

According to the ELISA results, the expression level of sPD-1 in the experimental group was prominently higher than in the control group while the expression level of sPD-L1 in the experimental group was lower

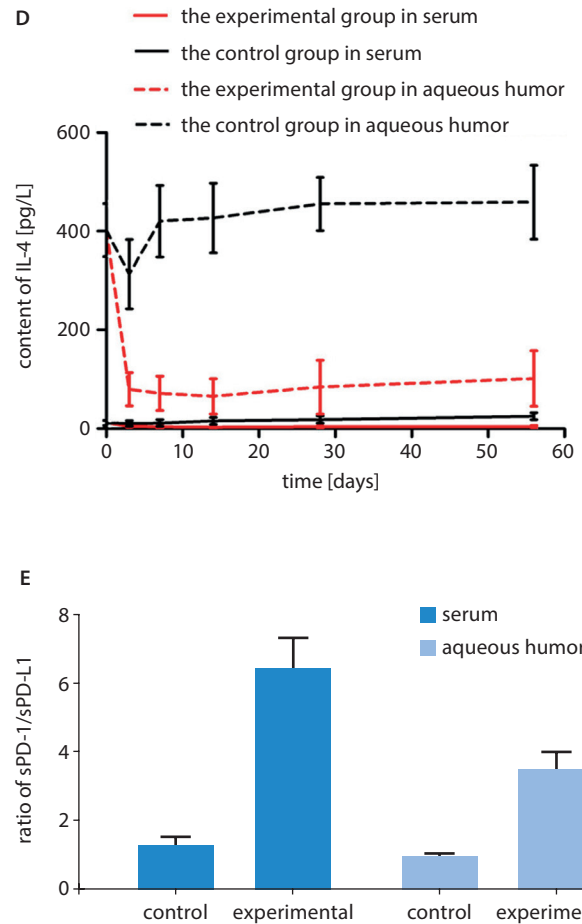


Fig. 5. Expression level of soluble programmed death protein-1 (sPD-1), soluble programmed death ligand protein-1 (sPD-L1), interleukin-10 (IL-10), interleukin-4 (IL-4), and ratios analyzed between sPD-1 and sPD-L1 in serum and aqueous humor

A. The content of sPD-1 in aqueous humor in the experimental group was higher than in the control group (all $p < 0.05$). The expression level of serum sPD-1 in the experimental group was higher than in the control group (all $p < 0.05$); B. In aqueous humor, the content of sPD-L1 in the control group was higher than in the experimental group (all $p < 0.05$). There was no significant difference of the serum sPD-L1 content between the experimental and control groups; C. The expression level of IL-10 in aqueous humor in the control group was lower than in the experimental group (all $p < 0.05$). The expression level of serum IL-10 in the control group was higher than in the experimental group (all $p < 0.05$); D. The expression level of IL-4 in aqueous humor in the control group was higher than in the experimental group (all $p < 0.05$). The expression level of serum IL-4 in the control group was higher than in the experimental group (all $p < 0.05$); E. Both ratios of serum sPD-1/sPD-L1 and aqueous humor in the experimental group were higher than in the control group.

than in the control group. After analysis, it was found that the sPD-1/sPD-L1 ratio in serum in the experimental group was much higher than in the control group. The sPD-1/sPD-L1 ratios in serum in the control group and experimental group were 1.259 ± 0.499 and 6.319 ± 2.317 , respectively, and the difference was statistically significant ($p < 0.05$). Similarly, the ratio of sPD-1/sPD-L1 in aqueous humor in the experimental group was higher than in the control group. The sPD-1/sPD-L1 ratios in aqueous humor in the control group and experimental

group were 1.443 ± 0.204 and 3.749 ± 1.341 , respectively, and the difference was statistically significant ($p < 0.05$) (Fig. 5E).

Discussion

Transplant rejection is a major cause of corneal transplantation failure. Therefore, the core issue of corneal transplantation is how to inhibit transplant rejection. At present, prevention and treatment of transplant rejection after corneal transplantation mainly focuses on the effect phase using eye local and systemic immune inhibitors, angiogenesis inhibitors, etc.,^{17–22} but these drugs can disturb or destroy the normal immune function and environment. Furthermore, the concentration of the drugs will eventually decrease below effective concentration after body metabolism, and transplant rejection may still happen. Thus, if the proliferation and differentiation of immune effector cells can be restrained and prevented from entering the effect phase, the effect of inducing and transplanting immunological tolerance will be achieved, which can effectively and enduringly inhibit transplant rejection and prolong survival time of the grafts. This is one important direction of future study on transplantation immunological tolerance.

In recent years, the co-stimulating signal has become an important issue in immunological research. In transplantation immunity, activating the T lymphocyte needs co-stimulating signals to successfully induce transplantation immunological tolerance. Currently known co-stimulating molecules include the B7 family (immunoglobulin superfamily), tumor necrosis factor (TNF) family and cytokine family negative co-stimulating molecules, while the PD-1/PD-L1 pathway is an important negative regulating pathway of T lymphocytes.^{5–7,23–25} Research shows that in the PD-1/PD-L1 pathway, PD-1 works as an immune inhibitory receptor and is mainly expressed in activated T cells.^{26–28} By interacting with PD-L1, PD-1 can promote immunological suppression and regulation, which can help induce and maintain immunological tolerance.^{29–32} Additionally, studies show that CD4⁺CD25⁺Treg has features of immune incompetence and inhibition, which play a key role of effector T cells in maintaining the body's immune response steady state and the immunological suppression function of immunological tolerance after induction organ transplantation.^{33,34} It was first confirmed by Hall et al. that CD4⁺CD25⁺Treg could induce transplantation immunological tolerance.³⁵ CD4⁺CD25⁺Treg can also secrete cytokines such as IL-10 and IL-4 to suppress the immune response.^{36–38} In this research, the content of serum and aqueous humor increased while the expression level of CD4⁺CD25⁺Treg in serum and the spleen decreased after the operation in the experimental group. In the control group, sPD-1 content in serum and aqueous humor decreased and the expression level

of CD4⁺CD25⁺Treg in serum and the spleen increased. In the experimental group, sPD-1 content was significantly higher than the preoperative value at the beginning of rejection while the expression level of CD4⁺CD25⁺Treg was markedly lower than the preoperative value, indicating that sPD-1 and CD4⁺CD25⁺Treg were related to transplant rejection after corneal transplantation.

In addition, it is worth noting that the rising expression level of sPD-1 was opposite to the increasing tendency of IL-10 and IL-4 content in serum cytokines and aqueous humor. The IL-10 and IL-4 content in aqueous humor were higher than that in serum and the change range was broader. Therefore, we can speculate on the basis of these results that when transplant rejection happens after corneal transplantation, the expression level of sPD-1 will increase. It may be combined with PD-L1 to inhibit the combination of membrane-type PD-1 and PD-L1, and prevent PD-1/PD-L1 from conveying negative stimulation signals after combination, thus inhibiting the function of CD4⁺CD25⁺Treg and indisposing it to conduct immunoregulation. Meanwhile, the decrease of IL-10 and IL-4 secretion may weaken transplant rejection inhibition after corneal transplantation. The group difference of the postoperative expression level of sPD-L1 in serum and aqueous humor is not statistically significant. The changing tendency does not have a clear relationship between transplant rejection and CD4⁺CD25⁺Treg and no regularity was found. Yet in the analysis of sPD-1/sPD-L1 ratios of the 2 groups, it was found that at the same time point, the mean sPD-1/sPD-L1 ratio in serum and aqueous humor in the experimental group was greater than in the control group and it reached its highest level 14 days after the operation. This result showed that the abnormal expression of sPD-1/sPD-L1 may have certain relevance to transplant rejection after corneal transplantation. The content ratio of sPD-1 and sPD-L1 in serum and aqueous humor can work as an important reference index of transplant rejection after corneal transplantation. Monitoring the concentration changes of sPD-1 and sPD-L1 can help to predict and diagnose the occurrence of rejection at an early stage.

Conclusions

To sum up, the experiment preliminarily proved that in transplant rejection after rat corneal transplantation, increased expression level of sPD-1 may inhibit the combination of membrane-type PD-1 and PD-L1, blocking the negative adjustment of PD-1/PD-L1 on CD4⁺CD25⁺Treg after the combination and impeding normal immunological tolerance. The decreasing content of IL-10 and IL-4 secreted in serum and aqueous humor may weaken the protection of the body's immune suppression and increase immune rejection, as well as influence the survival time of corneal grafts.

Two problems are still unclear: whether sPD-1/sPD-L1 work as collaborative or inhibiting regulating factors of PD-1/PD-L1; and the specific mechanism of rejection after corneal transplantation. These issues should be studied further.

References

- Niederhorn JY. The immune privilege of corneal grafts. *J Leukoc Biol.* 2003;74(2):167–171.
- Price MO, Thompson RW Jr, Price FW Jr. Risk factors for various causes of failure in initial corneal grafts. *Arch Ophthalmol.* 2003;121(8):1087–1092.
- Nurieva R, Thomas S, Nguyen T, et al. T-cell tolerance or function is determined by combinatorial costimulatory signals. *EMBO J.* 2006;25(11):2623–2633.
- Snanoudj R, de Preneuf H, Creput C, et al. Costimulation blockade and its possible future use in clinical transplantation. *Transpl Int.* 2006;19(9):693–704.
- Cai G, Karni A, Oliveira EM, Weiner HL, Hafler DA, Freeman GJ. PD-1 ligands, negative regulators for activation of naive, memory and recently activated human CD4⁺ T cells. *Cell Immunol.* 2004;230(2):89–98.
- Latchman YE, Liang SC, Wu Y, et al. PD-L1-deficient mice show that PD-L1 on T cells, antigen-presenting cells, and host tissues negatively regulates T cells. *Proc Natl Acad Sci U S A.* 2004;101(29):10691–10696.
- Taams LS, Vukmanovic-Stejic M, Smith J, et al. Antigen-specific T cell suppression by human CD4⁺CD25⁺ regulatory T cells. *Eur J Immunol.* 2002;32(6):1621–1630.
- Dieckmann D, Plottnner H, Berchtold S, Berger T, Schuler G. Ex vivo isolation and characterization of CD4(+)CD25(+) T cells with regulatory properties from human blood. *J Exp Med.* 2001;193(11):1303–1310.
- Kitazawa Y, Fujino M, Wang Q, et al. Involvement of the programmed death-1/programmed death-1 ligand pathway in CD4⁺CD25⁺ regulatory T-cell activity to suppress alloimmune responses. *Transplantation.* 2007;83(6):774–782.
- Zhang X, Schwartz JC, Guo X, et al. Structural and functional analysis of the costimulatory receptor programmed death-1. *Immunity.* 2004;20(3):337–347.
- Shen L, Jin Y, Freeman GJ, Sharpe AH, Dana MR. The function of donor versus recipient programmed death-ligand 1 in corneal allograft survival. *J Immunol.* 2007;179(6):3672–3679.
- Zhao Y, Jia Y, Li C, Fang Y, Shao R. The risk stratification and prognostic evaluation of soluble programmed death-1 on patients with sepsis in emergency department. *Am J Emerg Med.* 2018;36(1):43–48.
- Guo X, Jie Y, Ren D, et al. In vitro-expanded CD4(+)CD25(high) Foxp3(+) regulatory T cells controls corneal allograft rejection. *Hum Immunol.* 2012;73(11):1061–1067.
- Cunnusamy K, Paunicka K, Reyes N, Yang W, Chen PW, Niederhorn JY. Two different regulatory T cell populations that promote corneal allograft survival. *Invest Ophthalmol Vis Sci.* 2010;51(12):6566–6574.
- Williams KA, Coster DJ. Penetrating corneal transplantation in the inbred rat: A new model. *Invest Ophthalmol Vis Sci.* 1985;26(1):23–30.
- Larkin DF, Calder VL, Lightman SL. Identification and characterization of cells infiltrating the graft and aqueous humor in rat corneal allograft rejection. *Clin Exp Immunol.* 1997;107(2):381–391.
- Xin M, Wang T, Shi W, Wu X. Experimental efficacy of mycophenolate mofetil implant on high-risk corneal allograft rejection and its biocompatibility in the anterior chamber of rabbits. *J Ocul Pharmacol Ther.* 2012;28(6):609–617.
- Fan JC, Chow K, Patel DV, McGhee CN. Corticosteroid-induced intraocular pressure elevation in keratoconus is common following uncomplicated penetrating keratoplasty. *Eye (Lond).* 2009;23(11):2056–2062.
- Reinhard T, Mayweg S, Reis A, Sundmacher R. Topical FK506 as immunoprophylaxis after allogeneic penetrating normal-risk keratoplasty: A randomized clinical pilot study. *Transpl Int.* 2005;18(2):193–197.
- Belin MW, Bouchard CS, Frantz S, Chmielinska J. Topical cyclosporine in high-risk corneal transplants. *Ophthalmology.* 1989;96(8):1144–1150.
- Stevenson W, Cheng SF, Dastjerdi MH, Ferrari G, Dana R. Corneal neovascularization and the utility of topical VEGF inhibition: Ranibizumab (Lucentis) vs bevacizumab (Avastin). *Ocul Surf.* 2012;10(2):67–83.
- Vassileva PI, Hergeldzhieva TG. Avastin use in high risk corneal transplantation. *Graefes Arch Clin Exp Ophthalmol.* 2009;247(12):1701–1706.
- Greenwald RJ, Freeman GJ, Sharpe AH. The B7 family revisited. *Annu Rev Immunol.* 2005;23:515–548.
- Watts TH. TNF/TNFR family members in costimulation of T cell responses. *Annu Rev Immunol.* 2005;23:23–68.
- Chen L. Co-inhibitory molecules of the B7-CD28 family in the control of T-cell immunity. *Nat Rev Immunol.* 2004;4(5):336–347.
- van Dam LS, de Zwart VM, Meyer-Wentrup FA. The role of programmed cell death-1 (PD-1) and its ligands in pediatric cancer. *Pediatr Blood Cancer.* 2015;62(2):190–197.
- Pedoeem A, Azoulay-Alfaguter I, Strazza M, Silverman GJ, Mor A. Programmed death-1 pathway in cancer and autoimmunity. *Clin Immunol.* 2014;153(1):145–152.
- Boussiotis VA, Chatterjee P, Li L. Biochemical signaling of PD-1 on T cells and its functional implications. *Cancer J.* 2014;20(4):265–271.
- Dai S, Jia R, Zhang X, Fang Q, Huang L. The PD-1/PD-Ls pathway and autoimmune diseases. *Cell Immunol.* 2014;290(1):72–79.
- Ott PA, Hodi FS, Robert C. CTLA-4 and PD-1/PD-L1 blockade: New immunotherapeutic modalities with durable clinical benefit in melanoma patients. *Clin Cancer Res.* 2013;19(19):5300–5309.
- Giancchetti E, Delfino DV, Fierabracci A. Recent insights into the role of the PD-1/PD-L1 pathway in immunological tolerance and autoimmunity. *Autoimmun Rev.* 2013;12(11):1091–1100.
- Brusa D, Serra S, Coscia, M, et al. The PD-1/PD-L1 axis contributes to T-cell dysfunction in chronic lymphocytic leukemia. *Haematologica.* 2013;98(6):953–963.
- Suri-Payer E, Amar AZ, Thornton AM, Shevach EM. CD4⁺CD25⁺ T cells inhibit both the induction and effector function of autoreactive T cells and represent a unique lineage of immunoregulatory cells. *J Immunol.* 1998;160(3):1212–1218.
- Stephens LA, Barclay AN, Mason D. Phenotypic characterization of regulatory CD4⁺CD25⁺ T cells in rats. *Int Immunol.* 2004;16(2):365–375.
- Hall BM, Pearce NW, Gurley KE, Dorsch SE. Specific unresponsiveness in rats with prolonged cardiac allograft survival after treatment with cyclosporine. III. Further characterization of the CD4⁺ suppressor cell and its mechanisms of action. *J Exp Med.* 1990;171(1):141–157.
- Schwartz RH. Natural regulatory T cells and self-tolerance. *Nat Immunol.* 2005;6(4):327–330.
- Roncarolo MG, Gregori S, Battaglia M, Bacchetti, R, Fleischhauer K, Levings MK. Interleukin-10-secreting type 1 regulatory T cells in rodents and humans. *Immunol Rev.* 2006;212:28–50.
- Wu K, Bi Y, Sun K, Wang C. IL-10-producing type 1 regulatory T cells and allergy. *Cell Mol Immunol.* 2007;4(4):269–275.

Hematological manifestations and complications of COVID-19

Burak Erdinc^{1,A–D}, Sonu Sahni^{1,E,F}, Vladimir Gotlieb^{2,E,F}

¹ Department of Internal Medicine, Brookdale University Hospital and Medical Center, New York, USA

² Department of Hematology and Oncology, Brookdale University Hospital and Medical Center, New York, USA

A – research concept and design; B – collection and/or assembly of data; C – data analysis and interpretation;

D – writing the article; E – critical revision of the article; F – final approval of the article

Advances in Clinical and Experimental Medicine, ISSN 1899–5276 (print), ISSN 2451–2680 (online)

Adv Clin Exp Med. 2021;30(1):101–107

Address for correspondence

Burak Erdinc

E-mail: berdincmd@gmail.com

Funding sources

None declared

Conflict of interest

None declared

Received on August 31, 2020

Reviewed on October 28, 2020

Accepted on November 18, 2020

Abstract

The virus SARS-CoV-2 commonly causes self-resolving, flu-like illnesses in the majority of patients, but a critical illness can be seen in 5% of cases – especially in the elderly population or in patients with multiple comorbidities. When COVID-19 is severe, it can cause pneumonia and hypoxemic respiratory failure, and can progress to viremia involving multiple organ systems. It causes significant cytopenia, mainly severe lymphopenia, and excessive exhaustion of CD8+ T cells, resulting in an immunocompromised state and cytokine storm. Furthermore, COVID-19 can commonly be complicated with acute thrombotic events, including venous thromboembolism, acute stroke, acute myocardial infarction, clotting of hemodialysis and extracorporeal membrane oxygenation (ECMO) catheters, and acute limb ischemia. This makes SARS-COV-2 a unique virus with an undiscovered pathophysiology. Therefore, patients with COVID-19 need close monitoring of their symptoms and laboratory parameters, and early hospitalization and treatment in severe cases. Early identification of severe cases and the abovementioned complications of COVID-19 could decrease the morbidity and mortality caused by the disease. In the study, we summarize what is currently known about the hematological manifestations and complications of COVID-19.

Key words: COVID-19, lymphopenia, cytokine storm, thromboembolism, hypercoagulable state

Cite as

Erdinc B, Sahni S, Gotlieb V. Hematological manifestations and complications of COVID-19. *Adv Clin Exp Med.* 2021;30(1):101–107. doi:10.17219/acem/130604

DOI

10.17219/acem/130604

Copyright

© 2021 by Wrocław Medical University

This is an article distributed under the terms of the Creative Commons Attribution 3.0 Unported (CC BY 3.0) (<https://creativecommons.org/licenses/by/3.0/>)

Introduction and background

The coronavirus disease from 2019 (COVID-19), which is caused by severe acute respiratory syndrome coronavirus 2 (SARS-CoV-2), has infected more than 16 million people and killed more than 650,000 around the world.^{1,2} It was first identified in Wuhan, China at the end of 2019 and rapidly spread, resulting in a pandemic. Coronaviruses are enveloped RNA viruses which commonly cause cold-like illnesses in immunocompetent hosts.³ It has a similar receptor binding structure to that of the SARS-CoV virus and uses angiotensin-converting enzyme 2 (ACE2) to enter the host cells.⁴ SARS-CoV-2 is mainly transmitted person to person via close contact or droplets with an incubation period – on average 5 days prior to symptoms appearing.⁵ It causes life-threatening disease in 5% of cases, especially in the elderly and in patients with multiple coexisting medical conditions; it has a mortality rate of 2.3%.⁶ Previously detected strains, the severe acute respiratory syndrome coronavirus (SARS-CoV) and Middle East respiratory syndrome coronavirus (MERS-CoV), are zoonotic viruses which caused outbreaks in China and the Middle East, respectively. However, they did not result in a pandemic such as SARS-CoV-2 has.^{7–9} COVID-19 primarily manifests as a respiratory tract infection causing hypoxemic respiratory failure. However, there is an enormous amount of data published almost daily demonstrating that it may involve multiple organ systems, including the nervous, cardiovascular, respiratory, gastrointestinal, renal, hematopoietic, and immune systems. This article summarizes the hematological manifestations and complications of COVID-19.

Alterations in cell counts in COVID-19

One of the first hematological manifestations of COVID-19 to be noticed was alterations in cell lineages, lymphopenia being the most prominent finding. A summary of tables examining cell lineage alterations in COVID-19 is presented in Table 1. A retrospective observation of 7,736 patients in China during the first 2 months of the pandemic outbreak compared the clinical characteristics of patients between severe and non-severe cases.¹⁰ Guan et al. found that the majority of the patients had low blood counts across all lineages, which were more prominent in patients with a severe form of the disease.¹⁰ On admission, lymphopenia was present in 83.2% of the patients, thrombocytopenia in 36.2% and leukopenia in 33.7%. Lymphopenia was the most commonly seen abnormally in blood counts, being present in 96% of the severe cases and 80% of the non-severe cases. The median hemoglobin level was found to be lower in severe cases than in non-severe cases (12.8 g/dL and 13.5 g/dL, respectively). In addition, thrombocytopenia was seen in 57.7% of the severe cases and in 31.6% of the non-severe cases. Other observational studies from China with fewer patients (41, 99, 138, and 201) reported similar results on patients with COVID-19: lymphopenia was evident in all studies and was more commonly seen in severe cases.^{11–13} A retrospective cohort study with 201 patients from Wuhan focused on a comparison of patients with acute respiratory distress syndrome (ARDS) with those without ARDS. They found that the patients with ARDS had significantly lower lymphocyte counts and CD-8 T-cell counts. The study also showed that patients with neutrophilia had an increased risk of mortality.¹³ This might be secondary to the disease course becoming complicated by bacterial superinfection. Further studies from other countries

Table 1. Alterations in cell counts in COVID-19

Study	Patient population	WBC, median [10 ³ /μL]	Leukopenia	ALC, median [10 ³ /μL]	Lymphopenia	Hgb, median [g/dL]	Platelets [10 ³ /μL]	Thrombocytopenia
Guan et al. ¹⁰	1099 hospitalized patients	4700	33.7%	1000	83.2%	13.4	168	36.2%
Wu et al. ¹³	201 hospitalized patients	5940	N/A	910	64%	N/A	180	N/A
Zhou et al. ²⁸	191 hospitalized patients	6200	17%	1000	40%	12.8	206	7%
Wang et al. ²⁷	138 hospitalized patients	4500	N/A	800	70.3%	N/A	163	N/A
Fan et al. ¹⁵	67 hospitalized patients	4700	29.2%	1200	36.9%	14	201	20%
Huang et al. ¹¹	41 hospitalized patients	6200	25%	800	63%	12.6	164	5%
Young et al. ¹⁴	18 hospitalized patients	4600	N/A	1200	39%	13.5	159	N/A

WBC – white blood cell, ALC – absolute lymphocyte count; Hgb – hemoglobin.

that analyzed the effects of SARS-CoV-2 infection on cell counts have shown similar results. A descriptive case series from Singapore on 18 hospitalized patients reported that 39% of the patients had lymphopenia. The majority of their patients had a mild form of the disease and 66% of them did not require supplemental oxygen, which is most likely explained by the low rate of lymphopenia among them.¹⁴ Another retrospective observational study on 69 patients from the National Center for Infectious Diseases (NCID) in Singapore focused on the hematological parameters of COVID-19 patients.¹⁵ They observed that 29% of the patients presented with severe leukopenia ($WBC < 2 \times 10^9/L$); also, 36.9% of the patients presented with lymphopenia and 5 out of 25 had severe lymphopenia ($ALC < 0.5 \times 10^9/L$). Lymphopenia was more profound in intensive care unit (ICU) patients, with 7 out of 9 being lymphopenic, 4 of whom had severe lymphopenia. In addition, 20% of their patients had mild thrombocytopenia (platelet count $100\text{--}150 \times 10^9/L$).

Peripheral blood smears obtained from 69% of the patients showed a few reactive lymphocytes, of which a subset appeared lymphoplasmacytoid. This is contrary to the experience with the SARS-CoV outbreak in 2003, where reactive lymphocytes were not observed in a study from Singapore on hematological parameters and were observed in only 15% of cases in a study from Hong Kong.^{16,17} Lymphopenia is a well-known feature of SARS-CoV, and was described in patients in Hong Kong and Singapore afflicted with the disease in 2003. It was associated with poor prognosis and ICU stay.^{16–18} Monitoring hematological parameters might help physicians to decide which patients need to be admitted to the ICU. Fan et al. recommended that severe lymphopenia $<0.6 \times 10^9/L$ should be considered as one of the indicators for early admission for supportive care in the ICU.¹⁵ Their ICU patients also developed more prominent, statistically significant decreases in their hemoglobin levels, absolute lymphocyte count (ALC) and absolute monocyte count (AMC), and increases in absolute neutrophil count (ANC), as compared to the non-ICU group. Fan et al. also performed flow cytometry (FCM) on the peripheral blood of patients in the ICU who had prominent lymphopenia. They found that the ICU patients had significantly lower CD45+, CD3+, CD4+, CD8+, CD19+, and CD16/56+ counts. Inversion of the CD4/CD8 ratio is commonly seen in viral infections such as the human immunodeficiency virus (HIV) and cytomegalovirus (CMV). However, the CD4/CD8 ratio was not inverted in all groups of patients.

Lymphopenia caused by COVID-19 and its detrimental effects on the immune system have been further analyzed. Zheng et al. studied the immunological characteristics of peripheral blood leukocytes from 16 patients in Kunming, China and found that COVID-19 damages the functioning of CD4+ T cells and promotes the excessive activation and possibly the subsequent exhaustion of CD8+ T cells.¹⁹ A proposed mechanism has been illustrated in Fig. 1. This

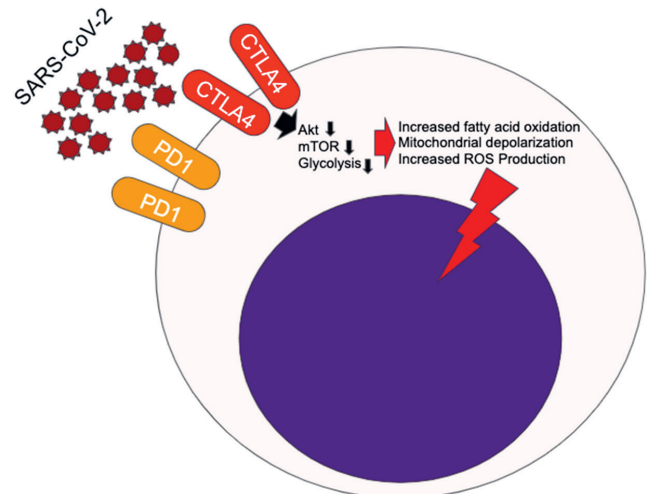


Fig. 1. Exhaustion of CD8+ T cells in SARS-CoV-2 infection.^{19,20} T cells express cytotoxic T-lymphocyte-associated protein-4 (CTLA4) and programmed cell death protein-1 (PD-1) inhibitory receptors which are activated by chronic infections. PD-1 signaling decreases Akt (protein kinase B) and mammalian target of rapamycin (mTOR) activity, which switches T-cell metabolism from glycolysis to fatty acid oxidation, resulting in mitochondrial depolarization, a higher rate of ROS production and functional impairment of T cells

phenomenon was also previously observed in some chronic infections such as HIV, hepatitis B virus (HBV) and hepatitis C virus (HCV), as well as in cancer; it can eventually diminish the host's antiviral immunity.²⁰ Previous studies indicated that multi-functional T cells play an important role in immunity against HIV infection and immunity after vaccination. Therefore, functional damage to CD4+ T cells may have predisposed COVID-19 patients to severe disease.²¹ According to Zheng et al., patients with severe SARS-CoV-2 infection had fewer of the non-exhausted (PD-1-negative, cytotoxic T-lymphocyte-associated protein 4 (CTLA-4)-negative and T-cell immunoreceptor with Ig and ITIM domains (TIGIT)-negative CD8+ T cells than the healthy control and mild disease course groups.¹⁹ For CD8+ T cells, it is beneficial to have a functional blockade of PD-1, CTLA-4 and TIGIT to maintain their antigen-specific immunity and antiviral effects.^{22,23} Therefore, the excessive exhaustion of CD8+ T cells in severe patients may reduce patients' cellular immune response to SARS-CoV-2. A cohort study of 452 patients was performed by Qin et al. in Wuhan, China and showed the dysregulation of immune response in patients with COVID-19.²⁴ They found that severe cases had higher leukocyte and neutrophil counts, lower lymphocyte counts, higher neutrophil-to-lymphocyte ratio, and lower percentages of monocytes, eosinophils and basophils. In addition, a lymphocyte subset analysis in 44 patients with COVID-19 revealed a decreased number of B cells, T cells and natural killer (NK) cells, which was more evident in the severe cases ($743.6/\mu L$ compared to $1020.1/\mu L$; $p = 0.032$) as compared with the non-severe group. The T-cell counts were found to have decreased to nearly half the lower limit of normal, indicating that T cells were more affected by SARS-CoV-2, especially

in severe cases (461.6/ μ L compared to 663.8/ μ L; $p = 0.027$). A subset analysis of T cells showed that both helper T (Th) cells (CD3+ and CD4+) and suppressor T cells (CD3+ and CD8+) were lower in patients with COVID-19. Based on these findings, they suggested that COVID-19 might be damaging lymphocytes directly and causing immune system dysfunction during acute infection.

Lymphopenia has also been commonly reported (67–75%) among critically ill patients with COVID-19 in the USA.^{25,26} Other observational studies from Wuhan with 138 and 191 hospitalized patients showed that patients who died from the disease had more severe lymphopenia than survivors, with their lymphocyte counts continuing to decrease until death.²⁷ Patients who survived the disease had their lowest lymphocyte counts on day 7, followed by improvement of their lymphocyte counts during the hospitalization, whereas the patients who had persistently low lymphocyte counts died from the disease.²⁸ Thus, monitoring lymphocyte counts might help assess disease severity and progression, and outcomes in patients with COVID-19. Tan et al. created a model based on lymphocyte percentage (LYM%) for disease classification and prognosis determination. According to their model, patients who have a LYM% > 20% on days 10–12 after the onset of symptoms have a good prognosis and recover quickly. In contrast, patients with a LYM% < 20 on days 10–12 are classified as severe type. At the second point, 17–19 days after symptom onset, patients with a LYM% > 20% are likely to recover; patients with 5% < LYM% < 20% are still at risk for decompensation, and patients with a LYM% < 5% are considered critically ill and requiring intensive care.²⁹ Even though lymphopenia is the most common alteration seen in cell counts and it has very important prognostic significance in COVID-19, there are studies suggesting the use of thrombocytopenia and platelet–lymphocyte ratio (PLR) as a prognostic factor of severe disease.

Thrombocytopenia is commonly seen in critically ill patients in COVID-19. A meta-analysis with 1,779 COVID-19 patients from 9 different studies showed that platelet count was significantly lower in patients with more severe disease (the weighted mean difference of platelet counts: $-31 \times 10^9/L$; 95% CI = -35 – $-29 \times 10^9/L$).³⁰ It has also been shown that low platelet count is associated with a more than five-fold increased risk of severe SARS-CoV-2 infection (OR = 5.1; 95% CI = 1.8–14.6). Even though its mechanism is not clearly known, it has been suggested that thrombocytopenia might be secondary to endothelial damage from mechanical ventilation and platelet activation, deranged platelet defragmentation from megakaryocytes in the pulmonary vascular bed, and direct bone marrow toxicity as a result of SARS-CoV-2 infection.^{30,31} A single-center case series of 30 hospitalized patients diagnosed with COVID-19 showed that patients with a peak in their platelet counts had worse clinical outcomes.³² In addition, Platelet-lymphocyte ratio (PLR) value at peak platelet count

during treatment was an independent influencing factor for prolonged hospitalization. It was suggested that markedly elevated platelet counts and longer average hospitalization may be related to the cytokine storm.

Hypercoagulable state and acute thrombotic events in COVID-19

COVID-19 is a novel disease with a very broad spectrum of complications involving different organ systems that are mainly caused by a hypercoagulable state. Patients with severe SARS-CoV-2 infection become prone to develop coagulation abnormalities and acute thrombotic events, but the pathogenesis of hypercoagulopathy in COVID-19 is not completely understood. Direct endothelial injury by SARS-CoV-2, immobilization due to severe illness, and a hypercoagulable state caused by increased inflammation and circulating prothrombotic factors are among the reasons why patients with COVID-19 have such a high tendency to develop acute thrombotic events.^{33–36} High d-dimer levels have been reported to be associated with the severe form of disease; as d-dimer is a fibrin degradation product, this indicates thrombin generation and fibrin dissolution. A multicenter retrospective analysis on 1,099 patients from China showed that 46.4% of patients with SARS-CoV-2 infection had elevated d-dimer levels.¹⁰ D-dimer elevation was more prominently seen in patients with severe COVID-19 compared to non-severe cases (59.6% compared with 43.2%). There are additional studies supporting the evidence that an elevated d-dimer level is associated with adverse outcomes and higher mortality.^{11,27}

Panigada et al. studied coagulation parameters and other assays, including von Willebrand factor (VWF) and thromboelastography (TEG), on 24 patients in the ICU who had COVID-19. They also found that the patients were in a hypercoagulable state.³⁵ The patients had normal-to-increased platelet counts, near-normal prothrombin time (PT) and activated partial thromboplastin time (aPTT), increased fibrinogen and dramatically increased d-dimer levels, increased factor VIII and VWF levels, decreased antithrombin levels, and increased protein C levels. There are similar studies supporting these findings.^{36,37}

Severely ill COVID-19 patients might have similar laboratory findings, with patients suffering from disseminated intravascular coagulation (DIC) who meet the criteria for probable DIC in the scoring system published by the International Society on Thrombosis and Hemostasis (ISTH) in 2009.³⁸ However, the majority of acutely ill patients with COVID-19 develop thrombosis rather than bleeding, which later is commonly seen in DIC. As explained previously, patients with COVID-19 have high fibrinogen and factor VIII activity, which suggests that a significant consumption of coagulation factors is not seen as it is in DIC.^{35–37} An observational study

from the Netherlands including 184 ICU patients evaluated the incidence of acute thrombotic events and none of their patients developed overt DIC. The study reported that 38% of their patients had coagulopathy (defined as a spontaneous prolongation of PT by >3 s or of aPTT by >5 s) on admission and the most common thrombotic complication was pulmonary embolism (81% of the thrombotic complications).³⁹ Classically, bleeding is seen in acute decompensated DIC due to the rapid consumption of coagulation factors, while thrombosis predominates in chronic compensated DIC. Even though the hypercoagulable state in COVID-19 is similar to compensated DIC, platelet counts and aPTTs are usually normal in COVID-19.³⁵

Venous thromboembolism is very common, especially in patients with severe COVID-19. Several autopsy studies on patients who died from COVID-19 showed significant incidence of deep vein thrombosis (DVT; 58%), pulmonary embolism (PE; 19–42%) and microthrombi formation in alveolar capillaries (45%).^{40,41} Widespread thrombosis, microangiopathy and capillary microthrombi, and increased angiogenesis were significantly prominent in lung specimens from patients who had died from COVID-19, and severe endothelial injury was deemed to be the main cause of the hypercoagulable state.⁴² Studies with patients in ICUs reported similar findings. A case series of 829 ICU patients with COVID-19 in New York reported PE in 6.2% of cases and DVT in 9.4%.⁴³ Other series with fewer patients reported higher VTE rates of 20–43% even with a prophylaxis dose of anticoagulation, but the rate is as high as 65–69% in studies that perform routine surveillance with bilateral leg ultrasounds.^{39,44,45} Extracorporeal membrane oxygenation (ECMO) is commonly used in patients with severe hypoxemic respiratory failure secondary to COVID-19 pneumonia. Clotting of the circuit was reported in 16% of ICU patients in 1 study.³⁷ Patients receiving continuous renal replacement therapy (CRRT) in the ICU also were reported to have a strikingly high incidence rate of clotting of the extracorporeal circuit – up to 96% of cases.³⁷ Bilaloglu et al. also studied VTE rates in non-ICU patients and found PE in 2.2% and DVT in 2% of 2,505 symptomatic inpatients in New York.⁴³ There is a paucity of data on VTE rates on an outpatient basis, which needs to be studied. Arterial thrombosis (stroke, myocardial infarction and limb ischemia) is less commonly seen than venous thrombosis in patients with COVID-19. Stroke was seen in 1.6% of hospitalized patients and myocardial infarction in 8.9%.⁴³ In an observational cohort of 20 patients with COVID-19 who had acute limb ischemia, it was shown that revascularization was successful in 70% of cases, but patients had a high mortality rate (40%).⁴⁶ Hemorrhagic complications are less commonly seen in patients with COVID-19, being reported in 2.7% of 150 ICU patients, although the bleeding was not spontaneous and it was related to head trauma and anticoagulation.³⁷

Inflammatory markers and cytokine storm in COVID-19

SARS-CoV-2 infection may cause a very broad spectrum of the COVID-19 disease, from asymptomatic (up to 40–45% of all cases), through mild (81% of the symptomatic cases) and severe (14% of the symptomatic cases), to life-threatening infections (5% of the symptomatic cases).^{6,47} Its mean incubation period is 5 days, ranging from 1 to 14 days.⁴⁸ During the incubation period, it can present with fever, malaise, sore throat, diarrhea, and other non-specific symptoms.¹⁰ During this period, peripheral blood leukocytes and lymphocytes are usually not significantly reduced.⁴⁹ In the 2nd phase of the disease, usually occurring 7–14 days after the disease onset, the virus can cause viremia which mainly affects the lungs, gastrointestinal tract and heart by binding to ACE-2 receptors.⁵⁰ In this phase, pneumonia worsens the disease course by causing diffuse bilateral patchy infiltrates in the lungs and potentially causing hypoxemic respiratory failure. As explained previously, lymphocyte counts are significantly lower in severe cases and inflammatory markers (e.g., ferritin, C-reactive protein (CRP), and erythrocyte sedimentation rate), elevated aminotransaminase (ALT/AST) levels and lactate dehydrogenase (LDH) levels can be detected in the blood in high amounts.¹⁰ Patients might also have markedly elevated levels of interleukins (mostly IL-6, IL-2, IL-7, granulocyte colony stimulating factor, interferon- γ inducible protein 10, monocyte chemoattractant protein-1 (MCP-1), and macrophage inflammatory protein 1-a (MIP1-a) and tumor necrosis factor α (TNF- α) if they go into a state of “cytokine storm,” which may induce lymphocyte apoptosis.^{51,52} Cytokine release syndrome (CRS) or cytokine storm is a type of acute systemic inflammatory reaction classically presenting with fever and multiple organ dysfunction. It commonly occurs secondary to immunotherapies (chimeric antigen receptor T-cell therapy or therapeutic antibodies) and haploidentical allogeneic transplantation. However, severe viral infections such as influenza or SARS-CoV-2 can also cause severe inflammatory response and cytokine storm.^{53–58} Mild cases of CRS are treated with antihistamines, antipyretics and intravenous fluids. Intravenous steroids and tocilizumab (an IL-6 receptor antagonist) can be used for severe cases.⁵⁵

Conclusions


SARS-CoV-2 is a novel virus which can cause significant changes in blood counts, mainly causing severe lymphopenia and excessive exhaustion of CD8+ T cells in severe cases, which may reduce patients' cellular immune response. When COVID-19 results in viremia in the later course of the disease, it can cause severe inflammatory reactions similar to cytokine storm, which might require ICU admission. In addition, acute thrombotic events are

commonly seen in patients with severe COVID-19, which makes SARS-CoV-2 a unique virus with undiscovered pathophysiology. Patients who are infected with the virus should be evaluated carefully by checking complete blood counts and inflammatory markers as well as further studies to diagnose acute thrombotic events in high-risk or symptomatic cases, both at baseline and during the disease course. Early identification of severe cases and the complications of COVID-19 could decrease the morbidity and mortality rates associated with this disease.

ORCID iDs

Burak Erdinc  <https://orcid.org/0000-0003-1065-545X>

Sonu Sahni  <https://orcid.org/0000-0001-8766-0703>

Vladimir Gotlieb  <https://orcid.org/0000-0003-2907-3476>

References

- Zhu N, Zhang D, Wang W, et al. A novel coronavirus from patients with pneumonia in China, 2019. *N Engl J Med*. 2020;382(8):727–733. doi:10.1056/NEJMoa2001017
- Johns Hopkins Coronavirus Resource Center. COVID-19 Map. <https://coronavirus.jhu.edu/map.html>. Baltimore, MD; John Hopkins University; 2020. Accessed June 28, 2020.
- Su S, Wong G, Shi W, et al. Epidemiology, genetic recombination, and pathogenesis of coronaviruses. *Trends Microbiol*. 2016;24(6):490–502. doi:10.1016/j.tim.2016.03.003
- Zhou P, Yang X Lou, Wang XG, et al. A pneumonia outbreak associated with a new coronavirus of probable bat origin. *Nature*. 2020; 579(7798):270–273. doi:10.1038/s41586-020-2012-7
- He X, Lau EHY, Wu P, et al. Temporal dynamics in viral shedding and transmissibility of COVID-19. *Nat Med*. 2020;26(5):672–675. doi:10.1038/s41591-020-0869-5
- Wu Z, McGoogan JM. Characteristics of and important lessons from the coronavirus disease 2019 (COVID-19) outbreak in China: Summary of a report of 72314 cases from the Chinese Center for Disease Control and Prevention. *JAMA*. 2020;323(13):1239–1242. doi:10.1001/jama.2020.2648
- Drosten C, Günther S, Preiser W, et al. Identification of a novel coronavirus in patients with severe acute respiratory syndrome. *N Engl J Med*. 2003;348(20):1967–1976. doi:10.1056/NEJMoa030747
- Zhong NS, Zheng BJ, Li YM, et al. Epidemiology and cause of severe acute respiratory syndrome (SARS) in Guangdong, People's Republic of China, in February, 2003. *Lancet*. 2003;362(9393):1353–1358. doi:10.1016/S0140-6736(03)14630-2
- Cui J, Li F, Shi ZL. Origin and evolution of pathogenic coronaviruses. *Nat Rev Microbiol*. 2019;17(3):181–192. doi:10.1038/s41579-018-0118-9
- Guan W, Ni Z, Hu Y, et al. Clinical characteristics of coronavirus disease 2019 in China. *N Engl J Med*. 2020;382(18):1708–1720. doi:10.1056/NEJMoa2002032
- Huang C, Wang Y, Li X, et al. Clinical features of patients infected with 2019 novel coronavirus in Wuhan, China. *Lancet*. 2020;395(10223):497–506. doi:10.1016/S0140-6736(20)30183-5
- Chen N, Zhou M, Dong X, et al. Epidemiological and clinical characteristics of 99 cases of 2019 novel coronavirus pneumonia in Wuhan, China: A descriptive study. *Lancet*. 2020;395(10223):507–513. doi:10.1016/S0140-6736(20)30211-7
- Wu C, Chen X, Cai Y, et al. Risk factors associated with acute respiratory distress syndrome and death in patients with coronavirus disease 2019 pneumonia in Wuhan, China. *JAMA Intern Med*. 2020;180(7):1–11. doi:10.1001/jamainternmed.2020.0994
- Young BE, Ong SWX, Kalimuddin S, et al. Epidemiologic features and clinical course of patients infected with SARS-CoV-2 in Singapore. *JAMA*. 2020;323(15):1488–1494. doi:10.1001/jama.2020.3204
- Fan BE, Chong VCL, Chan SSW, et al. Hematologic parameters in patients with COVID-19 infection. *Am J Hematol*. 2020;95(6):E131–E134. doi:10.1002/ajh.25774
- Chng WJ, Lai HC, Earnest A, Kuperan P. Hematological parameters in severe acute respiratory syndrome. *Clin Lab Haematol*. 2005;27(1): 15–20. doi:10.1111/j.1365-2257.2004.00652.x
- Lee N, Hui D, Wu A, et al. A major outbreak of severe acute respiratory syndrome in Hong Kong. *N Engl J Med*. 2003;348(20):1986–1994. doi:10.1056/NEJMoa030685
- Wong RSM, Wu A, To KF, et al. Haematological manifestations in patients with severe acute respiratory syndrome: Retrospective analysis. *Br Med J*. 2003;326(7403):1358–1362. doi:10.1136/bmj.326.7403.1358
- Zheng HY, Zhang M, Yang CX, et al. Elevated exhaustion levels and reduced functional diversity of T cells in peripheral blood may predict severe progression in COVID-19 patients. *Cell Mol Immunol*. 2020; 17(5):541–543. doi:10.1038/s41423-020-0401-3
- Saeidi A, Zandi K, Cheok YY, et al. T-cell exhaustion in chronic infections: Reversing the state of exhaustion and reinvigorating optimal protective immune responses. *Front Immunol*. 2018;9:2569. doi:10.3389/fimmu.2018.02569
- Van Braeckel E, Desombere I, Clement F, et al. Polyfunctional CD4+ T-cell responses in HIV-1-infected viral controllers compared with those in healthy recipients of an adjuvanted polyprotein HIV-1 vaccine. *Vaccine*. 2013;31(36):3739–3746. doi:10.1016/j.vaccine.2013.05.021
- Johnston RJ, Comps-Agrar L, Hackney J, et al. The immunoreceptor TIGIT regulates antitumor and antiviral CD8+ T-cell effector function. *Cancer Cell*. 2014;26(6):923–937. doi:10.1016/j.ccell.2014.10.018
- Engeland CE, Grossardt C, Veinalde R, et al. CTLA-4 and PD-L1 checkpoint blockade enhances oncolytic measles virus therapy. *Mol Ther*. 2014;22(11):1949–1959. doi:10.1038/mt.2014.160
- Qin C, Zhou L, Hu Z, et al. Dysregulation of immune response in patients with COVID-19 in Wuhan, China. *Clin Infect Dis*. 2020;71(15): 762–768. doi:10.1093/cid/ciaa248
- Bhatraju PK, Ghassemieh BJ, Nichols M, et al. COVID-19 in critically ill patients in the Seattle region: Case series. *N Engl J Med*. 2020;382(21): 2012–2022. doi:10.1056/NEJMoa2004500
- Arentz M, Yim E, Klaff L, et al. Characteristics and outcomes of 21 critically ill patients with COVID-19 in Washington state. *JAMA*. 2020; 323(16):1612–1614. doi:10.1001/jama.2020.4326
- Wang D, Hu B, Hu C, et al. Clinical characteristics of 138 hospitalized patients with 2019 novel coronavirus-infected pneumonia in Wuhan, China. *JAMA*. 2020;323(11):1061–1069. doi:10.1001/jama.2020.1585
- Zhou F, Yu T, Du R, et al. Clinical course and risk factors for mortality of adult inpatients with COVID-19 in Wuhan, China: A retrospective cohort study. *Lancet*. 2020;395(10229):1054–1062. doi:10.1016/S0140-6736(20)30566-3
- Tan L, Wang Q, Zhang D, et al. Lymphopenia predicts disease severity of COVID-19: A descriptive and predictive study. *Signal Transduct Target Ther*. 2020;5(1):33. doi:10.1038/s41392-020-0148-4
- Lippi G, Plebani M, Henry BM. Thrombocytopenia is associated with severe coronavirus disease 2019 (COVID-19) infections: A meta-analysis. *Clin Chim Acta*. 2020;506:145–148. doi:10.1016/j.cca.2020.03.022
- Yang M, Ng MHL, Chi KL. Thrombocytopenia in patients with severe acute respiratory syndrome (review). *Hematology*. 2005;10(2):101–105. doi:10.1080/10245330400026170
- Qu R, Ling Y, Zhang Y, et al. Platelet-to-lymphocyte ratio is associated with prognosis in patients with coronavirus disease-19. *J Med Virol*. 2020;92(9):1533–1541. doi:10.1002/jmv.25767
- Teuwen LA, Geldhof V, Pasut A, Carmeliet P. COVID-19: The vasculature unleashed. *Nat Rev Immunol*. 2020;20(7):389–391. doi:10.1038/s41577-020-0343-0
- Magro C, Mulvey JJ, Berlin D, et al. Complement associated microvascular injury and thrombosis in the pathogenesis of severe COVID-19 infection: A report of five cases. *Transl Res*. 2020;220:1–13. doi:10.1016/j.trsl.2020.04.007
- Panigada M, Bottino N, Tagliabue P, et al. Hypercoagulability of COVID-19 patients in intensive care unit: A report of thromboelastography findings and other parameters of hemostasis. *J Thromb Haemost*. 2020;18(7):1738–1742. doi:10.1111/jth.14850
- Ranucci M, Ballotta A, Di Dedda U, et al. The procoagulant pattern of patients with COVID-19 acute respiratory distress syndrome. *J Thromb Haemost*. 2020;18(7):1747–1751. doi:10.1111/jth.14854
- Helms J, Tacquard C, Severac F, et al. High risk of thrombosis in patients with severe SARS-CoV-2 infection: A multicenter prospective cohort study. *Intensive Care Med*. 2020;46(6):1089–1098. doi:10.1007/s00134-020-06062-x
- Levi M, Toh CH, Thachil J, Watson HG. Guidelines for the diagnosis and management of disseminated intravascular coagulation. *Br J Haematol*. 2009;145(1):24–33. doi:10.1111/j.1365-2141.2009.07600.x

39. Klok FA, Kruip MJHA, van der Meer NJM, et al. Incidence of thrombotic complications in critically ill ICU patients with COVID-19. *Thromb Res.* 2020;191:145–147. doi:10.1016/j.thromres.2020.04.013
40. Menter T, Haslbauer JD, Nienhold R, et al. Post-mortem examination of COVID-19 patients reveals diffuse alveolar damage with severe capillary congestion and variegated findings of lungs and other organs suggesting vascular dysfunction. *Histopathology.* 2020;77(2):198–209. doi:10.1111/his.14134
41. Wichmann D, Sperhake JP, Lütgehetmann M, et al. Autopsy findings and venous thromboembolism in patients with COVID-19. *Ann Intern Med.* 2020;May 6:M20-2003. doi:10.7326/m20-2003
42. Ackermann M, Verleden SE, Kuehnel M, et al. Pulmonary vascular endothelialitis, thrombosis, and angiogenesis in Covid-19. *N Engl J Med.* 2020;383(2):120–128. doi:10.1056/nejmoa2015432
43. Bilaloglu S, Aphinyanaphongs Y, Jones S, Iturrate E, Hochman J, Berger JS. Thrombosis in hospitalized patients with COVID-19 in a New York city health system. *JAMA.* 2020;324(8):799–801. doi:10.1001/jama.2020.13372
44. Nahum J, Morichau-Beauchant T, Daviaud F, et al. Venous thrombosis among critically ill patients with coronavirus disease 2019 (COVID-19). *JAMA Netw Open.* 2020;3(5):e2010478. doi:10.1001/jamanetworkopen.2020.10478
45. Llitjos JF, Leclerc M, Chochois C, et al. High incidence of venous thromboembolic events in anticoagulated severe COVID-19 patients. *J Thromb Haemost.* 2020;18(7):1743–1746. doi:10.1111/jth.14869
46. Bellostta R, Luzzani L, Natalini G, et al. Acute limb ischemia in patients with COVID-19 pneumonia. *J Vasc Surg.* 2020;72(6):1864–1872. doi:10.1016/j.jvs.2020.04.483
47. Oran DP, Topol EJ. Prevalence of asymptomatic SARS-CoV-2 infection. *Ann Intern Med.* 2020;Jun 3:M20-3012. doi:10.7326/m20-3012
48. Li Q, Guan X, Wu P, et al. Early transmission dynamics in Wuhan, China, of novel coronavirus-infected pneumonia. *N Engl J Med.* 2020;382(13):1199–1207. doi:10.1056/NEJMoa2001316
49. Li T, Lu H, Zhang W. Clinical observation and management of COVID-19 patients. *Emerg Microbes Infect.* 2020;9(1):687–690. doi:10.1080/22221751.2020.1741327
50. Xu H, Zhong L, Deng J, et al. High expression of ACE2 receptor of 2019-nCoV on the epithelial cells of oral mucosa. *Int J Oral Sci.* 2020;12(1):1–5. doi:10.1038/s41368-020-0074-x
51. Aggarwal S, Gollapudi S, Yel L, Gupta AS, Gupta S. TNF- α -induced apoptosis in neonatal lymphocytes: TNFRp55 expression and downstream pathways of apoptosis. *Genes Immun.* 2000;1(4):271–279. doi:10.1038/sj.gene.6363674
52. Liao YC, Liang WG, Chen FW, Hsu JH, Yang JJ, Chang MS. IL-19 induces production of IL-6 and TNF- α and results in cell apoptosis through TNF- α . *J Immunol.* 2002;169(8):4288–4297. doi:10.4049/jimmunol.169.8.4288
53. Frey N, Porter D. Cytokine release syndrome with chimeric antigen receptor T-cell therapy. *Biol Blood Marrow Transplant.* 2019;25(4):e123–e127. doi:10.1016/j.bbmt.2018.12.756
54. Frey NV, Porter DL. Cytokine release syndrome with novel therapeutics for acute lymphoblastic leukemia. *Hematology.* 2016;2016(1):567–572. doi:10.1182/asheducation-2016.1.567
55. Abboud R, Keller J, Slade M, et al. Severe cytokine-release syndrome after T-cell-replete peripheral blood haploidentical donor transplantation is associated with poor survival and anti-IL-6 therapy is safe and well-tolerated. *Biol Blood Marrow Transplant.* 2016;22(10):1851–1860. doi:10.1016/j.bbmt.2016.06.010
56. Pedersen SF, Ho YC. SARS-CoV-2: A storm is raging. *J Clin Invest.* 2020;130(5):2202–2205. doi:10.1172/JCI137647
57. Mehta P, McAuley DF, Brown M, Sanchez E, Tattersall RS, Manson JJ. COVID-19: Consider cytokine storm syndromes and immunosuppression. *Lancet.* 2020;395(10229):1033–1034. doi:10.1016/S0140-6736(20)30628-0
58. Liu Q, Zhou YH, Yang ZQ. The cytokine storm of severe influenza and development of immunomodulatory therapy. *Cell Mol Immunol.* 2016;13(1):3–10. doi:10.1038/cmi.2015.74

Comparison of the clinical differences between COVID-19, SARS, influenza, and the common cold: A systematic literature review

Jacek Czubak^{1,A,B,D}, Karolina Stolarczyk^{1,B,D}, Anna Orzeł^{2,C,D}, Marcin Frączek^{1,E,F}, Tomasz Zatoński^{1,E,F}

¹ Department and Clinic of Otolaryngology, Head and Neck Surgery, Wrocław Medical University, Poland

² Faculty of Medicine, Medical University of Lublin, Poland

A – research concept and design; B – collection and/or assembly of data; C – data analysis and interpretation; D – writing the article; E – critical revision of the article; F – final approval of the article

Advances in Clinical and Experimental Medicine, ISSN 1899–5276 (print), ISSN 2451–2680 (online)

Adv Clin Exp Med. 2021;30(1):109–114

Address for correspondence

Jacek Czubak

E-mail: jacekcz90@gmail.com

Funding sources

None declared

Conflict of interest

None declared

Received on July 16, 2020

Reviewed on August 9, 2020

Accepted on October 29, 2020

Published online on January 30, 2021

Abstract

Background. This review focuses on the frequency of symptoms in COVID-19 in comparison to SARS, influenza and common cold.

Objectives. To evaluate and compare the knowledge about the clinical features, symptoms and differences between patients with COVID-19, SARS, influenza, and common cold. The research can help ear, nose and throat specialists and other health practitioners manage patients during the COVID-19 pandemic.

Material and methods. The biomedical databases used in the study included PubMed and MEDLINE. Statistical analysis using the Z-score test assessed which symptoms were more characteristic of COVID-19 than other viral diseases.

Results. Among individuals with COVID-19, the most frequently reported symptoms were cough (70%), fever (45%), muscular pain (29%), and headache (21%), whereas sore throat (12%), and rhinorrhea (4%) were observed at lower rates. Fever was identified as most frequent in COVID-19 (74%), appearing at a higher rate in those cases than in influenza (68%) or the common cold (40%) ($p < 0.05$). In comparison to other viral diseases, sore throat was rarely reported in COVID-19 and SARS (12% and 18%, respectively) ($p < 0.05$). In influenza and common cold, a cough was identified in 93% and 80% of cases ($p < 0.05$). Headache, rhinorrhea, muscular pain, and sore throat were more common in influenza (91%, 91%, 94%, and 84%, respectively) and common cold (89%, 81%, 94%, and 84%, respectively) than in COVID-19 (21%, 4%, 29%, and 12%, respectively) and SARS (45%, 12%, 55%, and 18%, respectively) ($p < 0.05$).

Conclusions. The results of the analysis show that a greater number of general symptoms should lead to a diagnosis of influenza or common cold rather than COVID-19.

Key words: influenza, ENT, common cold, COVID-19, SARS

Cite as

Czubak J, Stolarczyk K, Orzeł A, Frączek M, Zatoński T. Comparison of the clinical differences between COVID-19, SARS, influenza, and the common cold: A systematic literature review. *Adv Clin Exp Med.* 2021;30(1):109–114. doi:10.17219/acem/129573

DOI

10.17219/acem/129573

Copyright

© 2021 by Wrocław Medical University

This is an article distributed under the terms of the Creative Commons Attribution 3.0 Unported (CC BY 3.0) (<https://creativecommons.org/licenses/by/3.0/>)

Introduction

The outbreak of the COVID-19 coronavirus epidemic in the Chinese city of Wuhan and its spread have become a global threat. Severe acute respiratory syndrome coronavirus 2 (SARS-CoV-2) is a β -coronavirus and the 7th coronavirus to be identified that causes human disease. Overall, SARS-CoV-2 was the 3rd zoonotic human coronavirus of the century.^{1,2} It is spread by human-to-human transmission via droplets over short distances (1.5 m), direct contact or (potentially) the gastrointestinal tract.^{3–5} It creates a high risk for virus transmission during ears, nose and throat (ENT) examination, especially during the direct examination of patients' respiratory tract. Moreover, recent studies indicate that ENT specialists are among the groups at a higher risk of exposure to the virus.⁶

COVID-19 is similar to the disease caused by SARS-CoV. Although SARS-CoV-2 is less virulent, it is more infectious and its rapid spread has led to the coronavirus pandemic.^{7,8} According to present clinical data about COVID-19, the symptoms of the disease may affect the upper respiratory tract, similarly to SARS, influenza and common cold. These similarities can pose a major diagnostic problem for any physician.

Every year, the world faces seasonal flu caused by influenza viruses. Three types of influenza viruses affect humans, the most common being type A and type B.⁹ Approximately 30–50% of cases of common cold are caused by rhinoviruses. The second-most common agents are human coronaviruses (HCoV-OC43, HCoV-HKU1, HCoV-229E, and HCoV-NL63), which account for 10–15% of cases of this disease. The other causes associated with the common cold are adenoviruses, human respiratory syncytial virus (orthopneumovirus), enteroviruses, and human parainfluenza viruses.¹⁰

This review focuses on the frequency of symptoms in COVID-19 in comparison to SARS, influenza and common cold. Additionally, the research assesses the incidence of upper respiratory tract symptoms and influenza-like symptoms for the abovementioned viral diseases. To the best of our knowledge, no previous reports have focused on the differential diagnosis between those infectious diseases. The data presented herein are important for ENT specialists, who are often the first-line doctors for patients with upper respiratory tract infection.

Objectives

The aim of the study was to evaluate and compare information about the clinical features, symptoms and differences between patients with COVID-19, SARS, influenza, and common cold. The research can help ENT specialists and other health practitioners around the world manage patients in the current COVID-19 pandemic.

Material and methods

The database presented in the study was built from the results of 9 studies published after March 2003.^{11–19} Only articles with data about symptoms of upper respiratory tract infection, such as fever, cough, muscular pain, headache, sore throat, and rhinorrhea, were included. Based on the search strategy, 1729 studies were found in the online database. Then, 1676 articles were excluded after the titles and abstracts were reviewed. The full texts of 53 articles were evaluated. Finally, 9 articles were included in the systematic literature review (Fig. 1).

The data was from 5400 patients with the following diseases: 1347 patients with COVID-19 (25.44%), 2470 patients with influenza (45.74%), 282 patients with SARS (5.22%), and 1274 patients with common cold (23.59%). Selected clinical presentation of patients with COVID-19, influenza, SARS, and common cold is also presented in Tables 1,2,3.

PubMed was the biomedical database used in the study. To identify the studies for potential review, the following search terms were used: “COVID-19,” “SARS,” “influenza,” “common cold,” “upper respiratory symptoms,” “influenza-like symptoms,” “otolaryngology,” “ENT,” and “otolaryngological manifestation.” The Boolean operators “NOT,” “AND” and “OR” were also used in succession to narrow and widen the search.

Only the following symptoms were taken into consideration while comparing the diseases: fever, sore throat, rhinorrhea, headache, cough, and myalgia. Our review was focused on studies about COVID-19, SARS, influenza, and common cold in which upper respiratory tract symptoms and influenza-like symptoms were considered, since they are the most common, mutual shared symptoms. Therefore, a large number of studies focusing on other symptoms (such as gastrointestinal symptoms or cardiologic symptoms) were excluded, which may have led to the omission of some important studies.

The search was limited to publications in English.

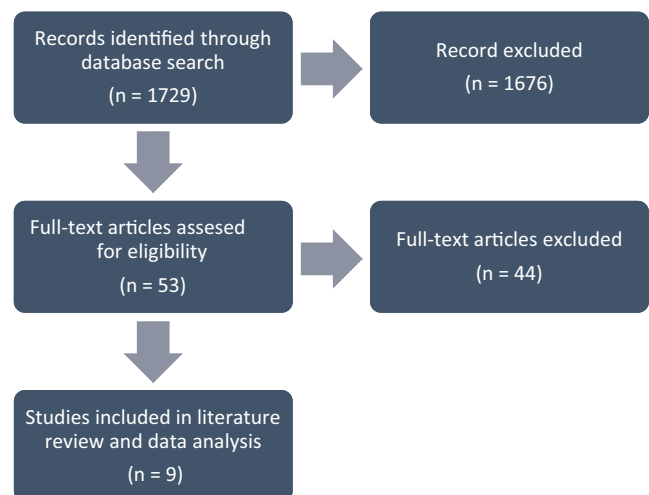


Fig. 1. A flow diagram of the inclusion criteria of studies eligible for the systematic literature review

Table 1. Selected clinical presentation of patients with COVID-19

Symptoms	Study							
	Wang et al. ¹¹ (n = 138) (%)	Chen et al. ¹² (n = 99) (%)	Huang et al. ¹³ (n = 41) (%)	Kim et al. ¹⁴ (n = 28) (%)	Jin et al. ¹⁵ (n = 74) (n = 577) no GI symptoms (n = 577) (%)	Jin et al. ¹⁵ (n = 577) (%)	Lechien et al. ¹⁶ (n = 417) (%)	Pooled data (n = 1374) (%)
Age, mean [years]	56	55.5	49	42.6	46.14	45.09	36.9	47.3
Sex								
female	63 (45.7)	32 (32)	11 (27)	13 (46.4)	37 (50)	283 (49)	263 (63)	702 (51)
male	75 (54.3)	67 (68)	30 (73)	15 (53.6)	37 (50)	294 (51)	154 (37)	672 (49)
Main symptom	fever	fever	fever	cough	fever	fever	cough	fever
Fever	136 (98.6)	82 (83)	40 (98)	7 (25.0)	63 (85.14)	482 (84)	204 (49)	1014 (74)
Sore throat	24 (17.4)	5 (5)	–	8 (28.6)	6 (8.11)	93 (16)	33 (7.93)	169 (12)
Rhinorrhea	–	4 (4)	–	2 (7.1)	2 (2.70)	35 (6)	18 (4.34)	61 (4)
Headache	9 (6.5)	8 (8)	3/38 (8)	7 (25.0)	16 (21.62)	51 (9)	196 (45)	290 (21)
Cough	82 (59.4)	81 (82)	31 (76)	8 (28.6)	53 (71.62)	382 (66)	329 (79)	966 (70)
Myalgia	48 (34.8)	11 (11)	18 (44)	7 (25.0)	10 (13.51)	61 (11)	246 (59)	401 (29)
Postnasal drip	–	–	–	–	–	–	29 (6.97)	29 (2.11)
Ear pain	–	–	–	–	–	–	13 (3.13)	13 (0.95)
Nasal obstruction	–	–	–	–	2 (2.70)	35 (6.07)	50 (12.02)	87 (6.33)
Facial pain/heaviness	–	–	–	–	–	–	54 (12.98)	54 (3.93)
Dyspnea	43 (31.2)	31 (31)	22 (55)	–	–	–	19 (4.57)	115 (8.36)
Diarrhea	14 (10.1)	2 (2)	1 (3)	3 (10.7)	53 (71.62)	–	51 (12.23)	124 (9.02)
Nausea	14 (10.1)	1 (1)	–	–	10 (13.52)	–	21 (5.03)	46 (3.34)
Vomiting	5 (3.6)	1 (1)	–	–	11 (14.86)	–	21 (5.03)	38 (2.76)
Abdominal pain	3 (2.2)	–	–	1 (3.6)	–	–	30 (7.19)	34 (2.47)
Dizziness	13 (9.4)	–	–	–	–	–	–	13 (0.95)

Table 2. Selected clinical presentation of patients with influenza and the common cold

Symptoms	Study: Monto et al. ¹⁷	
	Laboratory confirmed tested negative for influenza (n = 2470) (%)	Influenza (common cold) (n = 1274) (%)
Age, mean [years]	34.8	34.5
Sex		
female	1223 (49.5)	697 (54.7)
male	1247 (50.5)	577 (45.3)
Main symptom	myalgia	myalgia
Fever	848 (68)	510 (40)
Sore throat	2075 (84)	1070 (84)
Rhinorrhea	2248 (91)	1032 (81)
Headache	2248 (91)	1134 (89)
Cough	2298 (93)	1019 (80)
Myalgia	2321 (94)	1198 (94)
Nasal obstruction	2248 (91)	1032 (81)
Loss of appetite	2272 (92)	1096 (86)
Weakness	2321 (94)	1198 (94)

Table 3. Selected clinical presentation of patients with SARS

Symptoms	Study		
	Booth et al. ¹⁸ (n = 144) (%)	Lee et al. ¹⁹ (n = 138) (%)	Pooled data (n = 282) (%)
Age, mean [years]	45	39.3	42.15
Sex			
female	88 (61)	72 (52)	160 (57)
male	56 (39)	66 (48)	122 (43)
Main symptom	fever	fever	fever
Fever	143 (99.3)	138 (100)	281 (100)
Sore throat	18 (12.5)	32 (23.3)	50 (18)
Rhinorrhea	3 (2.1)	31 (22.5)	34 (12)
Headache	51 (35.4)	31 (22.5)	128 (45)
Cough	100 (69.4)	79 (57.3)	179 (63)
Myalgia	71 (49.3)	84 (60.9)	155 (55)
Nausea	28 (19.4)	27 (19.6)	55 (19.5)
Vomiting	28 (19.4)	27 (19.6)	55 (19.5)
Diarrhea	34 (23.6)	27 (19.6)	61 (21.6)
Dizziness	6 (4.2)	59 (42.8)	65 (23)
Dyspnea	60 (41.7)	–	60 (21.3)
Malaise	45 (31.2)	–	45 (16)
Arthralgia	15 (10.4)	–	15 (5.3)
Chest pain	15 (10.4)	–	15 (5.3)
Abdominal pain	5 (3.5)	–	5 (1.8)

Articles that did not address the selected topics, low-quality studies, case reports, and studies based on non-significant cohorts were excluded. The full texts of the remaining high-quality articles were examined and elaborated on.

The data analysis involved frequency tables with numerical and percentage values, descriptive statistics, and statistical tests. Statistical analysis was performed using IBM SPSS Statistics v. 25 software (IBM Corp., Armonk, USA). The tests involved in the data analysis were the χ^2 and Z-score tests. The non-parametric χ^2 test was used to assess the differences in the appearance of symptoms in studied diseases: COVID-19, influenza, SARS, and common cold. The level of statistical significance was set at $p = 0.05$.

The Z-score test was used to compare the results of independent studies with large sample sizes. It was used to compare patients with COVID-19 and patients with other diseases under study in pairs in terms of the frequency of symptom appearance. Such an approach can determine which symptom was more likely to be observed in COVID-19, and can possibly lead to its diagnosis. Each studied disease was compared separately with COVID-19. The level of statistical significance was set at $p = 0.05$.

Results

The data regarding the symptoms in viral diseases was analyzed and the results are presented as descriptive and percentage values (Table 4). Moreover, the statistical significance was assessed with a p -value < 0.05 . The analyzed cases of patients with viral diseases indicated that the distribution of symptoms was differentiated. Among individuals with COVID-19, the most frequently reported symptoms were fever (74%), cough (70%), muscular pain (29%), and headache (21%), whereas sore throat (12%) and rhinorrhea (4%) were observed at lower rates (Table 4). Regarding patients with influenza, all of the symptoms were identified in the majority of cases: myalgia (94%), cough (93%), rhinorrhea (91%), headache (91%), sore throat (84%), and fever (68%) (Table 4). In common cold, 94% of patients endured muscle pain, the most frequent symptom in that disease. Furthermore, 89% of the patients reported headache, 84% sore throat, 81% rhinorrhea, and 80% cough; however, a fever was reported in only 40% of cases (Table 4). When it comes to individuals with SARS, fever was the symptom observed most often (100%). A cough was

reported in 179 patients (63%), headache in 128 (45%) and rhinorrhea in 34 patients (12%). On the other hand, sore throat was identified only in 18% of patients with SARS (Table 4). These results, showing differences in the frequency of symptoms in viral diseases were found to be statistically significant ($p < 0.05$; Table 4).

The statistical analysis using the Z-score test allowed us to assess which symptoms were more characteristic of COVID-19 than of other viral diseases. Fever was identified as the most frequent symptom in COVID-19 (74%), appearing at a higher rate than in influenza (68%) or common cold (40%) ($p < 0.05$). On the other hand, 100% of patients with SARS infection reported having a fever (Table 4). In comparison to the other viral diseases, patients with COVID-19 and SARS rarely reported sore throat (12% and 18%, respectively) ($p < 0.05$). However, in influenza and in common cold, cough was identified in 93% and 80% of patients, respectively ($p < 0.05$). Headache, rhinorrhea, muscular pain, and sore throat were more common in influenza (91%, 91%, 94%, and 84%, respectively) and in common cold (89%, 81%, 94%, and 84%, respectively) than in COVID-19 (21%, 4%, 29%, and 12%, respectively) or SARS (45%, 12%, 55%, and 18%, respectively) ($p < 0.05$; Table 4). Other symptoms are also presented in Tables 1,2,3.

Discussion

To the best of our knowledge, this review is the first to compare the upper respiratory tract and influenza-like symptoms in COVID-19, SARS, influenza, and common cold. Knowledge of the frequency of upper respiratory tract symptoms and influenza-like symptoms in COVID-19, SARS, influenza, and common cold could be used in the differential diagnosis.

The clinical classification divides COVID-19 into 4 types based on the severity of the symptoms. The 1st one, the mild type, is defined as having slight clinical symptoms without pneumonia in radiography, which can be asymptomatic or imitating the common cold.^{3,13,15} The 2nd one, the moderate type, is defined as presenting with fever and/or respiratory symptoms, plus pneumonia

Table 4. Comparison of symptom frequency between the studied diseases

Variable	COVID 19	Influenza	SARS	Common cold
Number of cases	1374	2470	282	1274
Fever	1014 (74%)	848 (68%)	281 (100%)	510 (40%)
Sore throat	169 (12%)	2075 (84%)	50 (18%)	1070 (84%)
Rhinorrhea	61 (4%)	2248 (91%)	34 (12%)	1032 (81%)
Headache	290 (21%)	2248 (91%)	128 (45%)	1134 (89%)
Cough	966 (70%)	2298 (93%)	179 (63%)	1019 (80%)
Myalgia	401 (29%)	2321 (94%)	155 (55%)	1198 (94%)

$p < 0.00001$; result are significant at $p < 0.05$.

in radiography, which may resemble influenza.^{3,13} The 3rd one, the severe type, is diagnosed based on dyspnea (a respiratory rate ≥ 30 times/min), a resting finger oxygen saturation $\leq 93\%$ and an arterial PaO₂/FiO₂ ratio ≤ 300 mm Hg (1 mm Hg = 0.133 kPa). The last, the critical type, is defined as respiratory failure with shock and multiple organ failure, requiring mechanical ventilation and admission to the intensive care unit (ICU).^{3,14} The last 2 types can imitate SARS.

The analysis of clinical data in the study indicated significant similarities in the frequency of the symptoms fever and cough in infections caused by SARS-CoV (100% and 63%, respectively) and SARS-CoV2 (74% and 70%, respectively). The results show that it may not be possible to distinguish among the viral diseases under study judging only by the clinical presentation. The study reveals that general symptoms, like headache and myalgia, or non-specific upper respiratory tract inflammation symptoms, such as sore throat and rhinorrhea, are more likely to be found in patients with influenza or common cold than in patients with COVID-19. Ninety-four percent of patients with both influenza and the common cold reported myalgia, whereas in the case of COVID-19 patients, this symptom was observed in 29% of cases. The results show that an increased number of general symptoms should lead to a diagnosis of influenza rather than COVID-19. In the case of common cold, symptoms like headache, myalgia, rhinorrhea, and sore throat will appear more likely than fever. As in a study by Monto et al., comparing influenza and common cold, those factors can be used in common cold and COVID-19 for the initial differential diagnosis.¹⁷ Therefore, a lack of fever and the presence of headache, myalgia, rhinorrhea, and sore throat could suggest a diagnosis of common cold.

Anosmia and gustatory dysfunction are characteristic signs of SARS-CoV-2 infection. Recently published studies have demonstrated that anosmia and hyposmia can appear before the respiratory symptoms of COVID-19, or even as the only sign of the infection.²⁰ It should also be pointed out that anosmia and gustatory dysfunction can occur in patients who do not complain of nasal blockage or any other rhinitis symptoms.²¹ That could indicate direct damage from the virus on the olfactory and gustatory receptors. Researchers from South Korea, China, Germany, France, and Italy have found that a significant number of individuals with COVID-19 were affected by hyposmia or anosmia. For example, in a study by Lechien et al., anosmia occurred in 86% of patients and gustatory dysfunction was present in 88.8% of patients.¹⁶ Further, in a study by Klopfenstein et al., anosmia occurred in 47% of patients and was associated with dysgeusia in 85% of cases.²¹ Those smell disorders are very rare in SARS or other coronavirus infections.²² Therefore, the British Association of Otorhinolaryngology (ENT-UK) includes a loss of the sense of smell in their list of COVID-19 markers of infection.²⁰ Lechien et al. also observed that 3% of COVID-19 patients complained

of ear pain, 6.97% of postnasal drip and 13% of facial pain/heaviness. In the other articles analyzed, those symptoms were not found; therefore, these symptoms were not taken into consideration.¹⁶ However, it has to be considered that asymptomatic and mild infections of SARS-CoV-2 are frequent. That is why a physician should always treat their patients as potentially infected and follow appropriate precautions to avoid the further spread of the virus. Due to the non-specific symptoms presented in COVID-19, patients cannot be diagnosed solely by clinical presentation; only laboratory tests can confirm a diagnosis. The presence of a wide range of general symptoms (headache, rhinorrhea, myalgia, and sore throat) should lead physicians to clinically suspect influenza or common cold rather than COVID-19. This could then guide medical decisions to be made before confirmatory tests are available.


Real-time reverse transcriptase-polymerase chain reaction (RT-PCR) is a specific molecular examination for SARS-CoV-2. It is performed on specimens which are obtained mainly from nasopharyngeal swabs or oropharyngeal swabs, but also from the stool.^{23,24} Wang et al. recommend samples from the lower respiratory tract of the patients (sputum and bronchoalveolar lavage fluid), although nasopharyngeal swab is more commonly used and easier to obtain.^{24,25} Recent studies suggest that chest computed tomography (CT) is a sensitive diagnostic tool for COVID-19 diagnosis with a sensitivity of 97% in a patient with positive RT-PCR tests.^{24,26} Interestingly, even asymptomatic patients with COVID-19 had radiological changes in their lungs 1 day after exposure, which is also helpful in differential diagnostics.¹⁴ In influenza, RT-PCR and viral culturing have a sensitivity close to 100%, but the turnaround time for a viral culture is 3–10 days compared to 1–8 h for RT-PCR.⁹ In SARS, RT-PCR is the method of the first choice for detection.²⁷

Conclusions

Although further investigation is required to strengthen the observation made in the present study, our results add some evidence that could be used in the differential diagnosis of COVID-19, SARS, influenza, and common cold.


ORCID iDs

Jacek Czubałak  <https://orcid.org/0000-0003-0205-1955>

Karolina Stolarczyk  <https://orcid.org/0000-0002-4514-0387>

Anna Orzeł  <https://orcid.org/0000-0002-5908-6967>

Marcin Frączek  <https://orcid.org/0000-0003-0181-122X>

Tomasz Zatoński  <https://orcid.org/0000-0003-3043-4806>

References

1. Zhu N, Zhang D, Wang W, et al; China Novel Coronavirus Investigating and Research Team. A novel coronavirus from patients with pneumonia in China, 2019. *N Engl J Med*. 2020;382(8):727–733. doi:10.1056/NEJMoa2001017
2. Zhou M, Zhang X, Qu J. Coronavirus disease 2019 (COVID-19): A clinical update. *Front Med*. 2020;2:1–10. doi:10.1007/s11684-020-0767-8

3. Lovato A, de Filippis C. Clinical presentation of COVID-19: A systematic review focusing on upper airway symptoms. *Ear Nose Throat*. 2020;99(9):569–576. doi:10.1177/0145561320920762
4. Trilla A. One world, one health: The novel coronavirus COVID-19 epidemic. *Med Clin (Barc)*. 2020;154(5):175–177. doi:10.1016/j.medcli.2020.02.002
5. Wong SH, Lui RN, Sung JJ. Covid-19 and the digestive system. *J Gastroenterol Hepatol*. 2020;35(5):744–748. doi:10.1111/jgh.15047
6. Boccalatte LA, Larranaga JJ, Perez Raffo GM, et al. Brief guideline for the prevention of COVID-19 infection in head and neck and otolaryngology surgeons. *Am J Otolaryngol*. 2020;41(3):102484. doi:10.1016/j.amjoto.2020.102484
7. Guo YR, Cao QD, Hong ZS, et al. The origin, transmission and clinical therapies on coronavirus disease 2019 (COVID-19) outbreak: An update on the status. *Mil Med Res*. 2020;7(1):11. doi:10.1186/s40779-020-00240-0
8. Chen J, Qi T, Liu L, et al. Clinical progression of patients with COVID-19 in Shanghai, China. *J Infect*. 2020;80(5):e1–e6. doi:10.1016/j.jinf.2020.03.004
9. Paules C, Subbarao K. Influenza. *Lancet*. 2017;390(10095):697–708. doi:10.1016/S0140-6736(17)30129-0
10. Eccles R. Understanding the symptoms of the common cold and influenza. *Lancet Infect Dis*. 2005;5(11):718–725. doi:10.1016/S1473-3099(05)70270-X
11. Wang D, Hu B, Hu C, et al. Clinical characteristics of 138 hospitalized patients with 2019 novel coronavirus-infected pneumonia in Wuhan, China. *JAMA*. 2020;323(11):1061–1069. doi:10.1001/jama.2020.1585
12. Chen N, Zhou M, Dong X, et al. Epidemiological and clinical characteristics of 99 cases of 2019 novel coronavirus pneumonia in Wuhan, China: A descriptive study. *Lancet*. 2020;395(10223):507–513. doi:10.1016/S0140-6736(20)30211-7
13. Huang C, Wang Y, Li X, et al. Clinical features of patients infected with 2019 novel coronavirus in Wuhan, China. *Lancet*. 2020;395(10223):497–506. doi:10.1016/S0140-6736(20)30183-5
14. Kim ES, Chin BS, Kang CK, et al; Korea National Committee for Clinical Management of COVID-19. Clinical course and outcomes of patients with severe acute respiratory syndrome coronavirus 2 infection: A preliminary report of the first 28 patients from the Korean cohort study on COVID-19. *J Korean Med Sci*. 2020;35(13):e142. doi:10.3346/jkms.2020.35.e142
15. Jin X, Lian JS, Hu JH, et al. Epidemiological, clinical and virological characteristics of 74 cases of coronavirus-infected disease 2019 (COVID-19) with gastrointestinal symptoms. *Gut*. 2020;69(6):1002–1009. doi:10.1136/gutjnl-2020-320926
16. Lechien JR, Chiesa-Estomba CM, De Siati DR, et al. Olfactory and gustatory dysfunctions as a clinical presentation of mild-to-moderate forms of the coronavirus disease (COVID-19): A multicenter European study. *Eur Arch Otorhinolaryngol*. 2020;277(8):2251–2261. doi:10.1007/s00405-020-05965-1
17. Monto AS, Gravenstein S, Elliott M, Colopy M, Schweinle J. Clinical signs and symptoms predicting influenza infection. *Arch Intern Med*. 2000;160(21):3243–3247. doi:10.1001/archinte.160.21.3243
18. Booth CM, Matukas LM, Tomlinson GA, et al. Clinical features and short-term outcomes of 144 patients with SARS in the greater Toronto area. *JAMA*. 2003;289(21):2801–2809. doi:10.1001/jama.289.21.JOC30885
19. Lee N, Hui D, Wu A, et al. A major outbreak of severe acute respiratory syndrome in Hong Kong. *N Engl J Med*. 2003;348(20):1986–1994. doi:10.1056/NEJMoa030685
20. Pallanti S. Importance of SARs-Cov-2 anosmia: From phenomenology to neurobiology. *Compr Psychiatry*. 2020;100:152184. doi:10.1016/j.comppsy.2020.152184
21. Klopfenstein T, Kadiane-Oussou NJ, Toko L, et al. Features of anosmia in COVID-19. *Med Mal Infect*. 2020;50(5):436–439. doi:10.1016/j.medmal.2020.04.006
22. Vaira LA, Salzano G, Deiana G, De Riu G. Anosmia and ageusia: Common findings in COVID-19 patients. *Laryngoscope*. 2020;130(7):1787. doi:10.1002/lary.28692
23. Singhal T. A review of coronavirus disease-2019 (COVID-19). *Indian J Pediatr*. 2020;87(4):281–286. doi:10.1007/s12098-020-03263-6
24. Krajewska J, Krajewski W, Zub K, Zatoński T. COVID-19 in otolaryngologist practice: A review of current knowledge. *Eur Arch Otorhinolaryngol*. 2020;277(7):1885–1897. doi:10.1007/s00405-020-05968-y
25. Wang Y, Kang H, Liu X, Tong Z. Combination of RT-qPCR testing and clinical features for diagnosis of COVID-19 facilitates management of SARS-CoV-2 outbreak. *J Med Virol*. 2020;92(6):538–539. doi:10.1002/jmv.25721
26. Ai T, Yang Z, Hou H, et al. Correlation of chest CT and RT-PCR testing in coronavirus disease 2019 (COVID-19) in China: A report of 1014 cases. *Radiology*. 2020;296(2):E32–E40. doi:10.1148/radiol.2020200642
27. Noh JY, Yoon SW, Kim DJ, et al. Simultaneous detection of severe acute respiratory syndrome, Middle East respiratory syndrome, and related bat coronaviruses by real-time reverse transcription PCR. *Arch Virol*. 2017;162(6):1617–1623. doi:10.1007/s00705-017-3281-9